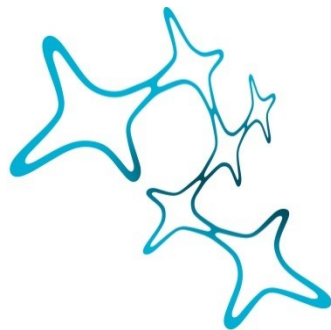


Neural oscillations underlying gait and decision making

Franz Lukas Hell



Graduate School of
Systemic Neurosciences

LMU Munich



Dissertation at the
Graduate School of Systemic Neurosciences
Ludwig-Maximilians-Universität München

November, 2018

Supervisor

<Prof. Dr. Kai Bötzel>

<Klinikum der Universität München/Department of Neurology>

<Ludwig-Maximilians Universität>

First Reviewer: <Prof. Dr. Kai Bötzel>

Second Reviewer: <Dr. Virginia Flanagan >

Date of Submission: <28.11.2018>

Date of Defense : <14.03.2019>

Contents

Abbreviations	7
Summary	9
1. Introduction	11
1.1 Parkinson's disease	12
1.1.1 Aetiology and pathophysiology	13
1.1.2 Motor and non-motor symptoms.....	14
1.1.3 Treatment.....	16
1.1.4 Neural mechanisms of PD	19
1.2 Human locomotion and locomotor control	21
1.2.1 Gait cycle and analysis	21
1.2.2 Neural mechanisms for locomotion and locomotor control.....	24
1.2.3 Electrophysiology of human locomotion	30
1.3 Decision making and inhibition	36
1.3.1 Models of inhibition: Proactive and reactive inhibitory control	37
1.3.2 Neural mechanisms underlying response inhibition during decision making under conflict.....	39
1.4 Aim of the thesis	42
2. Cumulative thesis.....	44
2.1 Subthalamic oscillatory activity and connectivity during gait in Parkinson's disease	45
2.2 Subthalamic stimulation, oscillatory activity and connectivity reveal functional role of STN and network mechanisms during decision making under conflict	46
3. Discussion	47
3.1 Subthalamic oscillatory activity during gait.....	47
3.1.1 Beta band oscillatory activity during gait.....	47
3.1.3 Modulation of oscillatory activity during gait and origin of signal	49
3.2 The functional role of STN and network mechanisms during decision making under conflict.....	52
3.3 Future directions for DBS	53
3.3.1 Improving targeting approaches for DBS surgery.....	54
3.3.2 Novel stimulation approaches in DBS	55
4. References.....	63

Appendix I	93
Appendix II.....	113
Affidavit.....	133
Author contributions	133
Acknowledgments	134
Curriculum vitae	Fehler! Textmarke nicht definiert.
Publications	135

Abbreviations

aDBS	Adaptive deep brain stimulation
AR	Akinetic-rigid
ACC	Anterior cingulate cortex
CPG	Central pattern generators
CNS	Central nervous system
CT	Computed tomography
CLR	Cerebellar locomotor region
DBS	Deep brain stimulation
DLPFC	Dorsolateral prefrontal cortex
EEG	Electroencephalography
EMG	Electromyography
ENG	Electroneurogram
fMRI	Functional magnetic resonance imaging
GPI	Internal segment of the globus pallidus
GPe	External segment of the globus pallidus
ICD	Impulse control disorders
IC	Initial contact
IPC	Inferior parietal cortex
ICOH	Imaginary part of the coherence
IFC	Inferior frontal cortex
IPL	Inferior parietal lobe
LFP	Local field potentials
LFO	Low frequency oscillations
MSA	Multiple system atrophy
MLR	Mesencephalic locomotor region

MRI	Magnetic resonance imaging
mPFC	Medial prefrontal cortex
M1	Primary motor cortex
PD	Parkinson's disease
PPN	Pedunculopontine nuclei
PSP	Progressive supranuclear palsy
Prec	Precuneus
PCC	Posterior cingulate cortex
pre-SMA	Pre-supplementary motor area
PMRF	Medullary and pontine reticular formations
RT	Reaction times
STN	Subthalamic nucleus
SLR	Subthalamic locomotor region
SNr	Substantia nigra pars reticulata
SN	Substantia nigra
SNr	Substantia nigra pars reticulata
S1	Primary somatosensory cortex
TD	Tremor-dominant
TC	Terminal contact
UPDRS	Unified Parkinson's disease rating scale
VTA	Volume of tissue activated
ViM	Ventral intermedius nucleus

Summary

Several theoretical models have been put forward to explain the coordination of different networks of the nervous system during complex tasks such as locomotion, inhibitory control and decision making and acting under conditions of uncertainty. The communication within and between brain networks is thought to be supported by numerous brain rhythms of different frequencies that allow for the temporal coordination and information exchange between different neural network nodes (Engel et al., 2010; Singer, 1993). This communication is thought to be impaired in a number of neuropsychiatric and neurological disorders such as Parkinson's disease (PD).

Neural oscillations as measured by local field potential (LFP) recordings are a cardinal way to investigate these processes (Buzsáki and Draguhn, 2004) and have become popular in the research on movement disorders. Features of local field potentials are also debated as a biomarker for adaptive closed-loop stimulation in PD (Cagnan et al., 2013; Johnson et al., 2016; Little et al., 2013; Tinkhauser et al., 2017a). It is therefore imperative to describe the functionality of neural structures and networks that are targeted by deep brain stimulation (DBS) as well as their malfunction during disease to fully understand the complexity of biomarkers and to further improve DBS therapy.

To elucidate the functional role of oscillatory activity in the subthalamic nucleus (STN), a popular target for DBS in PD, during locomotion and cognitive control, we conducted two studies in which we collected electrophysiological recordings from patients with PD. In both studies, we asked whether and how oscillatory signals are related to behaviour. In the first study, we collected STN-LFP during different gait and resting scenarios. In the second study we collected STN-LFP from a fully implanted sensing neurostimulator and parallel EEG recordings during a modified version of an Eriksen Flanker task inducing different levels of perceptual and response conflict (Van Veen and Carter, 2005).

With our first study, we show that it is feasible to record neural activity from a sensing neurostimulator in parallel with kinematic measurements in PD patients during walking and to detect gait-cycle related changes in subthalamic oscillatory power (Hell et al., 2018b). We report that high beta frequency power (20-30Hz) and bilateral oscillatory connectivity are reduced throughout the gait-cycle. Oscillatory characteristics like burst shape, burst amplitude and burst duration are affected in a similar way. We describe a reduction in overall high beta burst amplitude and burst lifetimes during gait as compared to rest. Investigating gait-cycle related oscillatory dynamics, we found that alpha, beta and gamma frequency power is modulated in time during gait, locked to the gait-cycle. We believe caution is necessary when interpreting the origin of the signal modulations during gait and argue that our results

show physiological effects as well as technical artifacts. We argue that beta suppression is most likely related to neurophysiological processes while gait-cycle specific modulations of power across frequencies are possibly related to movement induced artifacts. These issues have important implications for similar research approaches.

With our second study, we report on the functional relevance of the STN during decision making under conflict and its involvement in a larger network for cognitive control. We found that STN DBS generally decreased reaction times but did not alter conflict related processing in our task. Drift diffusion modelling hints that the decision threshold is altered by stimulation while drift rates are modulated by stimulus conflict (Hell et al., 2018c). We suggest that the STN does not implement a stimulus-conflict related inhibitory signal but rather a dynamic decision threshold. Our electrophysiological results extend previous findings concerning the roles of subcortical and cortical low frequency oscillations (2 - 6 Hz) (LFO) and alpha/beta oscillations and their functional importance during responding under conflict and provide new insights on the putative mechanisms involved in inhibitory control. We propose that subthalamic activity as well as subthalamic-cortical oscillatory connectivity reflect an inhibitory control and motor network with different oscillatory mechanisms. We further suggest that proactive as well as reactive mechanisms and putative neural structures are involved in implementing a dynamic executive control signal.

1. Introduction

Deep brain stimulation via electrodes implanted deep in the brain is an established option for the treatment of symptoms associated with several movement disorders like PD, essential tremor and dystonia. These electrodes allow for the study of neural oscillations in humans even deep in the brain and are a cardinal way to investigate neural processes underlying behaviour such as movement and inhibitory control and their dysfunction during disease.

The ability to move is essential in our daily life, which we barely recognize until problems arise. Locomotion is commonly executed with a high degree of automaticity and mostly without effort, once learned. However, many different forms of locomotion such as walking require complex and coordinated movements. The control of gait for example requires manifold interactions between different brain regions, the spinal cord and muscles. This complex network is impaired at different stages in patients with movement disorders such as Parkinson's disease (PD). The physiological as well as the pathophysiological neural processes associated with normal and abnormal movement can be investigated by local field potential recordings from implanted DBS electrodes.

Inhibitory control is a vital executive function that is needed to suppress premature actions and to block interference from irrelevant stimuli and is associated with functional imbalance between facilitation and inhibition in the fronto-striatal networks (Jahansahi and Rothwell, 2017). Part of this network is the STN, a basal ganglia nucleus in which DBS electrodes are frequently implanted for alleviating the symptoms of PD. By inhibiting the pallidial-thalamic-cortical loop via inhibitory connections to the GPi, the STN is thought to suspend responses until sufficient information has been integrated. The exact function of the STN in inhibitory control however remains debated (Bogacz and Gurney, 2007; Frank et al., 2007; Herz et al., 2017). Patients with STN-DBS offer the rare chance to investigate the contribution of the STN in inhibitory control.

Features of local field potentials are not only related to behaviour but are also linked to disease symptoms and are debated as biomarkers for adaptive closed-loop stimulation in PD (Cagnan et al., 2013; Johnson et al., 2016; Little et al., 2013; Tinkhauser et al., 2017a). In open loop DBS, which is the current standard protocol, the stimulation parameters like stimulation frequency, amplitude and pulse width are set by a clinician in a trial and error procedure and remain constant until manually updated, irrespective of disease fluctuations. A major point of interest in DBS research therefore is to develop more sophisticated strategies and automated algorithms on how to program and adjust stimulation

parameters in a precise and effective manner. In an adaptive closed loop DBS system, a sensor continuously records a feedback signal, a so-called biomarker, which should be correlated or causally linked to a clinical symptom, and alterations in the biomarker should ideally predict alterations in disease symptoms. With this information, adaptive closed loop DBS should adjust the stimulation based on the evolution of such biomarkers.

To improve DBS therapy it is important to fully understand neural feedback signals. It is therefore imperative to investigate the complex functionality of targeted neural structures and networks during behaviour as well as their malfunction during disease.

1.1 Parkinson's disease

Parkinson's disease is the second most prevalent progressive disorder of the nervous system after Alzheimer's disease and strongly affects the motor system while often also being accompanied by a spectrum of non-motor symptoms. PD has first been described by James Parkinson in 1807 and is diagnosed based mainly on motor symptoms, although non-motor problems might be preceding those years earlier (Tolosa et al., 2009). Slowing of movement (bradykinesia) and one or more of the following symptoms: postural instability, rigidity or resting tremor, are obligatory for the diagnosis (Se, 1993). A second step in the assessment of the disease is excluding other parkinsonian syndromes, such as progressive supranuclear palsy (PSP), multiple system atrophy (MSA) or others, based on behavioural assessment and neuroimaging results using dedicated tracer molecules. While PD is caused by a pathological aggregation of α -synuclein forming Lewy bodies and Lewy-neurites (Braak et al., 2004) in the nerve cells of select parts of the nervous system, MSA is linked to accumulation of α -synuclein within glial cytoplasmic inclusions. PSP on the other hand, associated with severe impairments of postural instability, is characterized by an accumulation of the tau protein within neurons and glia cells (Dickson, 2012), which can only be found after inspection of postmortal brain tissue. Furthermore, three additional criteria such as a clinically beneficial response to dopaminergic medication and induction of dyskinesias by levedopa, unilateral onset and persistent asymmetric manifestation of symptoms, support the diagnosis (Hughes et al., 1992; Poewe et al., 2017).

1.1.1 Aetiology and pathophysiology

The aetiology of PD is assumed to be multifactorial and thought to involve environmental as well as genetic factors (Schapira, 2006; Schapira and Jenner, 2011). Several environmental toxins have been shown to interfere with mitochondrial and proteasomal function, inducing oxidative stress, potentially leading to nigral dopaminergic cell death (Schapira and Jenner, 2011). Different genes have been discovered to be associated with inherited PD and genetic mutations have been found in parkin, UCHL1, DJ1, PINK1, and LRRK2. Changes in and over expression of alpha-synuclein are associated with mitochondrial defects and the formation of Lewy bodies, which are a hallmark of PD. Several altered proteins and genes are involved in protein handling, dysfunction of mitochondria and response to oxidative stress. Together they cause inflammatory processes that are thought to lead to cell dysfunction and death by apoptosis or autophagy (Schapira, 2006).

While the underlying aetiology is multifactorial, the pathology is relatively well described. The basic pathological process is the aggregation of alpha synuclein, a 14-kDa protein, in neural synapses (Spillantini and Goedert, 2017). This pathological process is spreading slowly across the whole brain (Braak et al., 2004) and causes death of nerve cells, predominantly in the substantia nigra, probably because of the high content of Fe^{+++} in this region (Levin et al., 2011). The irreversible loss of dopaminergic neurons is a hallmark of the disease (Petrucci and Dickson, 2008), while an estimated 80% of dopaminergic cells in the nigro-striatal system are lost before the onset of the major motor symptoms of PD (Cheng et al., 2010; Chung et al., 2001). Striatal dopamine depletion however is not the only pathology, many studies have also shown that additional neural structures and neurochemical systems such as the prefrontal cortex, the cerebellum as well as serotonergic, glutamatergic and cholinergic systems are affected by the disease (Bohnen et al., 2013; Fox, 2013).

Changes on a macroscopic level are visible in imaging as well as neurophysiological measurements. Neuroimaging studies report structural and functional changes in the motor system in subjects with non-manifesting PD and *Parkin* gene mutation (Eimeren and Siebner, 2006). It has been reported that different PD subtypes are associated with different structural as well as functional brain changes. Tremor-dominant (TD) and akinetic-rigid (AR) subtypes are linked to different patterns of nigrostriatal degeneration: TD is associated with less widespread pallidal and striatal dopamine depletion compared to akinetic-rigid PD patients (Eggers et al., 2012, 2011; Schilaci et al., 2011). Both subtypes also do show differences in intrinsic brain activity and functional connectivity for example in the default mode network detected in resting-state MRI studies (Karunanayaka et al., 2016; Zhang et al., 2015).

1.1.2 Motor and non-motor symptoms

PD is associated with primary and secondary motor symptoms. Primary symptoms include bradykinesia, resting tremor, muscular rigidity, postural instability and secondary symptoms, which can occur later in the course of the disease, including gait disturbance like freezing of gait (sudden inability to make a step), problems with writing (micrographia), precision grip impairments and speech problems (Kalia and Lang, 2015; Lees et al., 2009; Moustafa et al., 2016). There are three subtypes of idiopathic Parkinson's disease described in the literature, namely the akinetic-rigid type, the tremor-dominant type and the mixed type. As a fourth subtype, monosymptomatic rest tremor is discussed (Postuma et al., 2016, 2015). While patients with tremor-dominance mainly show resting tremor, subjects with an akinetic-rigid syndrome are mainly affected by bradykinesia and rigidity, causing problems during locomotion and especially during gait (Thenganatt and Jankovic, 2014). Many patients however show both tremor as well as bradykinesia/rigidity and are categorized under the label equivalent/mixed type (Eggers et al., 2012; Jankovic et al., 1990).

It has been suggested that in PD the control of habitual behaviour is more severely impaired, while the control of goal directed actions is preserved (Redgrave et al., 2010). Patients in the early stages of the disease often show impaired performance when carrying out normal automatic and habitual components of actions like fingertapping, blinking, pacing of gait or the modulation of speech (Marsden, 1982). These problems might be explained by the observation that the loss of dopamine in PD predominantly affects the posterior putamen, a region involved in the control of habitual action, while processing in the rostromedial striatum, which mediates goal directed behaviour (Gurney et al., 2001), is preserved in comparison. Behavioural problems during locomotion might therefore reflect a loss of normal automatic control (Redgrave et al., 2010).

Different studies also suggest that many primary and secondary symptoms are correlated. For example, speech and hand movement impairments are reported within the same patients (Skodda et al., 2011; Vercruyssen et al., 2012). Speech and gait impairments correlate (Cantinioux et al., 2010; Nutt et al., 2011) and micrographia and primary motor symptoms are also reported within the same patients (Wagle Shukla et al., 2012). Moreover, different symptoms such as micrographia and gait benefit both from cues such as lines (Cantinioux et al., 2010; Nutt et al., 2011). A single case study reports a patient with both micrographia and hypophonia, suggesting that the reduction in speech volume and handwriting size may have common neuronal underpinnings (Sekar et al., 2010). Confirming interdependencies between symptoms, a study found that motor blockings such as freezing of gait and stuttering correlate in PD patients, also suggesting common neural substrates (Morgante et al., 2013). It has also been reported that complex motor symptoms such as freezing of gait and speech problems are only partly responsive to

levodopa medication while motor symptoms like rigidity and bradykinesia can effectively be treated with dopaminergic medication. These correlations might be explained by the hypothesis, that complex motor behaviours underlying locomotion, speech or handwriting, are based on the integration of different elemental motor processes (Moustafa et al., 2016). Future theoretical and experimental studies will aim at clarifying how exactly the different brain regions interact to produce different basic motor commands which together yield complex locomotion and how abnormal communication between them is related to different movement disorder symptoms.

Although PD is primarily characterized as a movement disorder, it is associated with a wide range of non-motor symptoms, which lead to severe disabilities and a strong reduction in the quality of life, especially in advanced stages of the disease. Several impairments are reported to accompany PD, including worsening of verbal fluency (Højlund et al., 2017), olfactory dysfunction, dysautonomia, mood and sleep disorders (Tolosa et al., 2009), sensory dysfunction with hyposmia or pain, dementia and cognitive dysfunction, hallucinosis (Poewe, 2008) and deficits in inhibitory control. Patients most commonly affected by impulse control disorders (ICD), such as pathologic gambling and hypersexuality, are most often males who develop PD at a younger age, and those with a previous history of mood disorder, alcohol abuse, or obsessive-compulsive disorder. In particular, dopamine agonists, which are widely used to treat the dopaminergic deficit of these patients, are associated with the development of such nonmotor symptoms (Seeman, 2015; Stamey and Jankovic, 2008) and several studies could show that dopamine agonist treatment is associated with increased odds of having an ICD (Garcia-Ruiz et al., 2014; Weintraub et al., 2010). Some studies suggest that reducing medication after STN DBS may be the main factor in improving ICDs. Lees et al report that all patients who were treated with a dopamine agonist gathered significantly less information and made more irrational decisions, regardless of whether they underwent DBS treatment (Lees et al., 2013). Another group reported that ICDs were abolished 3 years after STN DBS surgery and after dopamine agonist dosages were lowered, confirming the role of dopamine in ICDs (Amami et al., 2015).

1.1.3 Treatment

Motor symptoms can be treated by dopaminergic substances, resulting in the reduction of the cardinal motor symptoms. Levodopa, a precursor of dopamine, is the most common initially used medication for PD. However, after a normally satisfying early response, medication has to be increased with disease progression, which is accompanied by reduced dopamine storage capacity. The changes in the response to the medication can induce fluctuations of mobility (on-state, off-state), involuntary movements (dyskinesias) and other motor complications. Additionally, monoamine oxidase type B inhibitors (Selegelin), catechol-O-methyltransferase inhibitors (Entacapone, Tolcapone) or the NMDA receptor antagonist amantadine and dopamine receptor agonists (Pramipexol, Rotigotin, Ropinirol) can be used to manage symptoms until non-dopamine-responsive symptoms (i.e. falls or dementia) prevail (Jankovic and Stacy, 2007).

In contrast to the classical trias of rigidity, bradykinesia and tremor, several motor as well as non-motor symptoms (falls, freezing of gait, speech problems, olfactory loss, dementia) are often only poorly responsive to treatment with dopaminergic medication (Chaudhuri et al., 2006). While dopaminergic medication can ameliorate depression or anxiety, other neuropsychiatric symptoms such as psychosis or impulse control disorders can be induced or worsened by dopaminergic agonists (Schaeffer and Berg, 2017).

When pharmacological intervention starts to become ineffective and induces side effects, neurosurgery is considered as a treatment option. Several surgical approaches have been used over the years. The first surgical approaches were brain lesioning procedures starting with undercutting motor fibres in the cervical spinal cord for alleviation of tremor (Walker, 1952). With the advent of stereotactical planning of targeting brain areas, thermocoagulation of thalamic areas to alleviate tremor was introduced by Hassler in the 50ies of the last century (Hassler and Riechert, 1955). A novel technique based on MRI-guided focused ultrasound is now being used as a “minimally-invasive” surgical technique to induce lesions and surgically treat tremor (Fasano et al., 2017). However, as lesioning introduces irreversible damages to the brain, this type of surgery has been largely replaced by deep brain stimulation surgery. DBS surgery was introduced by the neurosurgeon Benabid and the neurologist Pollak in the 90ies of the last century (Benabid et al., 1991) and has developed into an established option for the treatment of movement disorders, including essential tremor, Parkinson’s disease and dystonia and other neurological disorders like epilepsy and neuropathic pain, and is being investigated for psychiatric disorders, i.e. depression, obsessive-compulsive disorder and Tourette syndrome.

DBS surgery involves implantation of electrodes into one of several target regions and applying electrical current pulses, typically at 130 Hz, that are generated by a subcutaneous impulse generator. In comparison with lesioning approaches, DBS surgery does not or only minimally destroy brain tissue. Instead it modulates the function of the target region by applying electrical current to the area (Ashkan et al., 2017).

Electrical stimulation has been thought to introduce a virtual lesion of the specific brain area, while putatively preventing pathological circuit hypersynchrony and therefore alleviating clinical symptoms (Jenkinson and Brown, 2011). The exact mechanisms of DBS however remain debated. DBS was shown to alter beta band activity within the basal ganglia-cortical network, decreasing the amplitude of these oscillations (Oswal et al., 2016). DBS likely not only affects neuronal firing and oscillations but also neurotransmitters (Benabid et al., 2009). DBS also seems to act over multiple timescales. The effects of DBS on tremor for example are immediate, while the effects on dystonia emerge over several weeks, suggesting that not only local processing is disrupted, but that also large networks are affected (Ashkan et al., 2017). Recent reviews propose that DBS likely acts through multimodal, nonexclusive mechanisms including immediate neuromodulatory effects on local and network-wide electrical and neurochemical properties, synaptic plasticity and long-term neuronal reorganization, potentially also providing neuroprotective effects and leading to neurogenesis (Ashkan et al., 2017; Chiken and Nambu, 2015, 2014; Herrington et al., 2016).

In movement disorders like PD, the DBS electrodes are most often implanted in the basal ganglia thalamo-cortical loop, especially in the STN, globus pallidus pars interna (GPi) and thalamus (Chiken and Nambu, 2014). Other nuclei like the pedunculopontine nuclei (PPN) have been targeted in PD patients with freezing of gait (Follett and Torres-Russotto, 2012). A recent meta study however found no conclusive improvements in freezing of gait with PPN DBS, although a significant improvement in postural instability and motor symptoms of Parkinson disease are reported (Golestanirad et al., 2016). Also recently, stimulation of the substantia nigra (SN), which is located ventrally and medially to the STN, has been explored. One study reports that STN-DBS at 130 Hz in PD patients via the most distal contact of the electrode resulted in an improvement of gait and posture (Chastan et al., 2009). Subsequently, Weiss et al. used interleaving to stimulate both the STN and the substantia nigra pars reticulata (SNr) and found that freezing of gait was significantly improved compared to STN-DBS, although other axial symptoms did not significantly differ (Weiss et al., 2013).

To achieve the best clinical outcome, stimulation parameters are commonly determined empirically. Previous studies investigating the specific contribution of stimulation amplitude, frequency and pulse width found that manipulating the amplitude had the greatest effect on ameliorating PD motor signs

relative to energy-equivalent changes in frequency and pulse width. Sauleau et al. found that the mean threshold for disappearance of wrist rigidity was 0.94V (at 130 Hz stimulation frequency and 100 μ s pulse width) (Sauleau et al., 2005). Another study confirms these findings and reports that the amplitude required to ameliorate wrist rigidity with STN-DBS ranges from 0.7 to 1.7 mA (Rizzone, 2001), while in yet another study, a stimulation amplitude of 3 V and higher provided a consistent motor improvement (Moro et al., 2002).

STN-DBS with stimulation frequencies of 50Hz and 130Hz is reported to improve tremor, rigidity and bradykinesia and frequencies of less than 50Hz have been shown to have no beneficial effect on motor symptoms (Rizzone, 2001). Compared with no stimulation, very low frequencies of 5–10 Hz have been reported to worsen motor symptoms, in particular bradykinesia and to a lesser degree tremor (Miocinovic et al., 2014; Moro et al., 2002; Timmermann et al., 2004). Rizzone et al. report no significant improvement at above 185 Hz for neither target symptom, although other reports suggest that tremor tends to respond to a higher frequency (Miocinovic et al., 2014).

Pulse widths between 60 μ s and 210 μ s are reported to improve tremor control and rigidity, while bradykinesia was only significantly reduced at 60 μ s. Stimulation with high pulse widths (> 210 μ s) was in general not well tolerated (Moro et al., 2002). Decreasing the standard pulse width represents an alternative strategy for DBS programming. For example, Reich et al. investigated pulse widths of less than 60 μ s at a fixed frequency of 130 Hz and found that the therapeutic window increased by a mean of 182% with at a pulse width of 30 μ s, and decreased by 46% with a pulse width of 120 μ s compared to stimulation with 60 μ s pulse width (Reich et al., 2015). These effects are thought to be due to a more selective action of stimulation with lower pulse width on the fibre tracts that are responsible for symptom relief, while the neighbouring corticospinal and corticobulbar fibres are thought to be less affected.

Although the effects of DBS on Parkinsonian symptoms and quality of life are generally satisfying (Deuschl et al., 2013), the clinical outcome may vary between patients (Merola et al., 2011) and side effects can be induced (Højlund et al., 2017), probably also due to the stimulation of different functional pathways or nearby structures. DBS has several advantages over other surgical procedures but the setting of DBS parameters to optimize therapy is time-consuming and will likely get more complicated with new technological developments, introducing an ever increasing combination of parameters like pulse duration, stimulation frequency, stimulation contacts and so forth.

1.1.4 Neural mechanisms of PD

At the physiological level, oscillators do a great service for the brain: they coordinate or “synchronize” various operations within and across neuronal networks. Syn (meaning same) and chronos (meaning time) together make sure that everyone is up to the job and no one is left behind, the way the conductor creates temporal order among the large number of instruments in an orchestra. A close view of Seiji Ozawa at the end of a concert, sweat falling from his face, is proof that conducting an orchestra is a physically and mentally demanding job. In contrast, coupled oscillators perform the job of synchronization virtually effortlessly. This feature is built into their nature. In fact, oscillators do not do much else. They synchronize and predict. Yet, take away these features, and our brains will no longer work. Compromise them, and we will be treated for epilepsy, Parkinson’s disease, sleep disorders, and other rhythm-based cognitive maladies.

György Buzsáki, Rhythms of the Brain

Oscillatory rhythms are an essential part of normal brain function, however, when these rhythms change during disease, i.e. get exaggerated, unique oscillatory patterns can arise which are associated with specific behavioural deficits. Tremor is associated with increased LFP power in basal ganglia nuclei at individual tremor frequency (around 5 Hz) and cortical power decreases in the beta band (13-30 Hz), while STN-cortical, cortico-muscular and STN-muscle coherence is reported to be increased during tremor, specifically at tremor frequency (Hirschmann et al., 2013; Tass et al., 2010). It has also been shown that during tremor, gamma power is increased and beta power is decreased, probably reflecting movement related frequency modulations. Confirming the causal relevance of neural tremor frequency oscillations, studies found that DBS at tremor frequency induces behavioural tremor (Barnikol et al., 2008). Akinetic-rigid symptoms by contrast are reported to be correlated with beta power increases across subcortical and cortical sites in human patients (Hammond et al., 2007; Kühn et al., 2006; Mallet et al., 2008; Moran et al., 2011; Neumann et al., 2016; Sharott et al., 2005) as well as in animal models of parkinsonism (Costa et al., 2006; Mallet et al., 2008; Sharott et al., 2005). Studies in which either cortical or subcortical sites have been stimulated in the beta frequency range reportedly induced bradykinesia (Eusebio et al., 2008; Little and Brown, 2014). Beta oscillations are also reported to be attenuated by STN-DBS in a stimulation intensity dependent manner and are reduced in amplitude after levodopa intake (Kühn et al., 2008; Oswal et al., 2016; Quinn et al., 2015; Trager et al., 2016; Weiss et al., 2015). Neuronal circuit dysfunction is the origin of many symptoms of neurological disorders. Commonly, it has been assumed that bradykinetic PD symptoms are related to an imbalance between the direct and indirect pathways of the basal ganglia (Albin et al., 1989; Frank, 2005) which lead to the generation of abnormal synchronous oscillations (hypersynchrony) throughout the basal ganglia circuit (Humphries et al., 2006; Kumar et al., 2011; Lindahl and Hellgren-Kotaleski, 2016).

However, the origin of pathological oscillations and the exact relation between dopamine, beta and motor function remain debated (Beck et al., 2016; Cole et al., 2017; Lienard et al., 2017; McCarthy et al., 2011; Moran et al., 2011; Pavlides et al., 2015; Yang et al., 2014). Several hypotheses for the origin of the hypersynchronous beta-band oscillations (Jenkinson and Brown, 2011) are discussed in the literature (Humphries et al., 2018). One popular candidate is the negative feedback loop between the STN and the external globus pallidus (GPe). It has been proposed that strengthening of the input to the pallidum from D2-receptor striatal projection neurons (Gillies et al., 2002) might shift the loop from a stable to an oscillatory state. Another possible mechanisms could be that the connections between the STN and GPe are strengthened, because pre-synaptic D2 receptors, that normally prevent transmitter release in both nuclei, are no longer activated due to dopamine depletion (Humphries et al., 2006). A third hypothesis targets changes within the striatum. Damodaran, Corbit and colleagues (Corbit et al., 2016; Damodaran et al., 2015) propose that a change in the balance of D1 and D2 projection neuron activity due to dopamine depletion is compensated by changes in the behaviour of fast-spiking striatal interneurons, which in turn causes entrainment of projection neurons to interneuron output within the beta-band. Another hypothesis proposes that (aberrant) beta-band oscillations are not caused in a single loop but rather in the full cortical-basal ganglia-thalamic-cortical network, as dopamine depletion leads to an imbalance between different pathways (e.g. hyperdirect and direct pathway) (Kumaravelu et al., 2016; Leblois, 2006; Pavlides et al., 2015).

The heterogeneity of empirical results and modelling approaches to explain pathological oscillations reflects the complexity of the underlying circuit and hints at a still very basic understanding of the underlying system and the dynamics that are associated with clinical symptoms.

1.2 Human locomotion and locomotor control

Walking is a paradigmatic and clinically relevant example of complex and coordinated human locomotion. Human gait can be described as a periodic succession of symmetric and alternating movements of both legs. There are several basic processes reported to contribute to the impaired performance of patients with Parkinson's disease during locomotion. Problems during locomotion arise due to deficits to initiate, modulate and scale movements (Jackson et al., 2000; Majsak et al., 1998; Morris et al., 1994a), insufficient activation of leg extensor muscles (Dietz and Colombo, 1998), deficits in upper and lower limbs and interleg coordination. PD patients also frequently show reduced arm swings (Carpinella et al., 2007; Dietz and Michel, 2008; Plotnik et al., 2007), abnormal postural reactions and poor adaptation to environmental cues due to impaired proprioceptive feedback (Benecke et al., 1987a, 1987b; Rogers, 1996).

1.2.1 Gait cycle and analysis

Figure 1 represents the different phases and events that together describe the gait cycle. The gait cycle begins with the initial contact (IC), when the heel strikes the ground. In this phase, both feet are on the ground (double support). At the beginning of this phase, knees are fully extended and a hip flexion of about 30 degrees can be observed. Then the ankle moves from a neutral position into plantar flexion, enabled by eccentric contraction of the tibialis anterior muscle. This phase is followed by concurrent knee and heel plantar flexion increases, while the extension of the knee is driven by a contraction of the quadriceps and knee flexion by contraction of the hamstrings (Loudon et al., 2008).

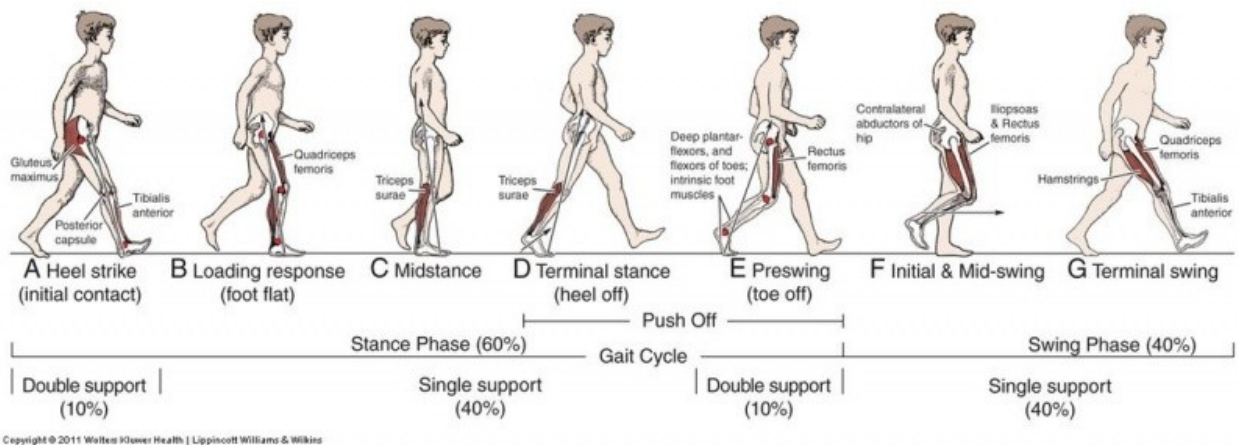


Figure 1. Illustration of the gait cycle. The gait cycle begins with the double support phase, initiated by the initial contact of the heel and ends with the terminal contact of the toes, at which time the swing phase begins, which ends with the initial contact of the same heel, completing the gait cycle for one leg. Adapted with permission from Wolters Kluwer Health, Lippincott Williams & Wilkins, 2011.

The initial contact is followed by the loading response, in which the body absorbs the impact of the initial contact by rolling into pronation, while the hip moves into extension, driven by contraction of the gluteus maximus and adductor magnus muscles. This is accompanied by increasing knee and plantar flexion up to 20 degrees and 15 degrees respectively (Shultz et al., 2005). The loading response is followed by midstance and terminal stance. During the midstance phase in which the body is only supported by one leg, the hip moves from flexion to extension via contraction of the gluteus maximus, while the knee begins to extend after reaching maximal flexion and the ankles become supinated and dorsiflexed (Loudon et al., 2008).

The stance phase ends with the terminal contact (TC), when the heel leaves the floor and concludes with the pre-swing phase, in which the toe leaves the ground. During the stance phase the hip is hyperextended, then goes into flexion and becomes less extended in the pre-swing phase. The knee becomes increasingly flexed and plantar flexion of the ankle increases throughout both phases (Loudon et al., 2008; Shultz et al., 2005). The terminal contact is followed by initial swing, midswing and finally terminal swing, completing the gait-cycle. Beginning with the initial swing phase, the hip first extends about 10 degrees, followed by flexion up to 30 degrees in the midswing phase, supported by contraction of iliopectus muscles and adductors. The knee initially flexes up to about 60 degrees, then extending about 30 degrees, while the ankle goes from about 20 degrees of plantar flexion to dorsiflexion, ending in a neutral position (Loudon et al., 2008; Shultz et al., 2005).

With small inertial sensors (accelerometers and gyroscopes) it is possible to record kinematic parameters, which can be later used to reconstruct the limb trajectory (Figure 2). To reproduce the gait cycle, events such as the initial and terminal contact of the foot (IC, TC) have to be reconstructed from the recorded kinematic signals. The IC for example causes a sharp transient in the signal of the shank accelerometers as well as a clearly recognizable trough in the gyroscope signal curve. This trough represents the initial contact as confirmed by recordings from pressure-sensitive soles (Figure 2 upper panel, left depiction). The TC can be pragmatically defined as the point midway between trough and zero-crossing before the point of peak velocity at the moment when the gyroscope trace crosses the midline, i.e. when the direction of rotation changes (Bötzel et al., 2016).

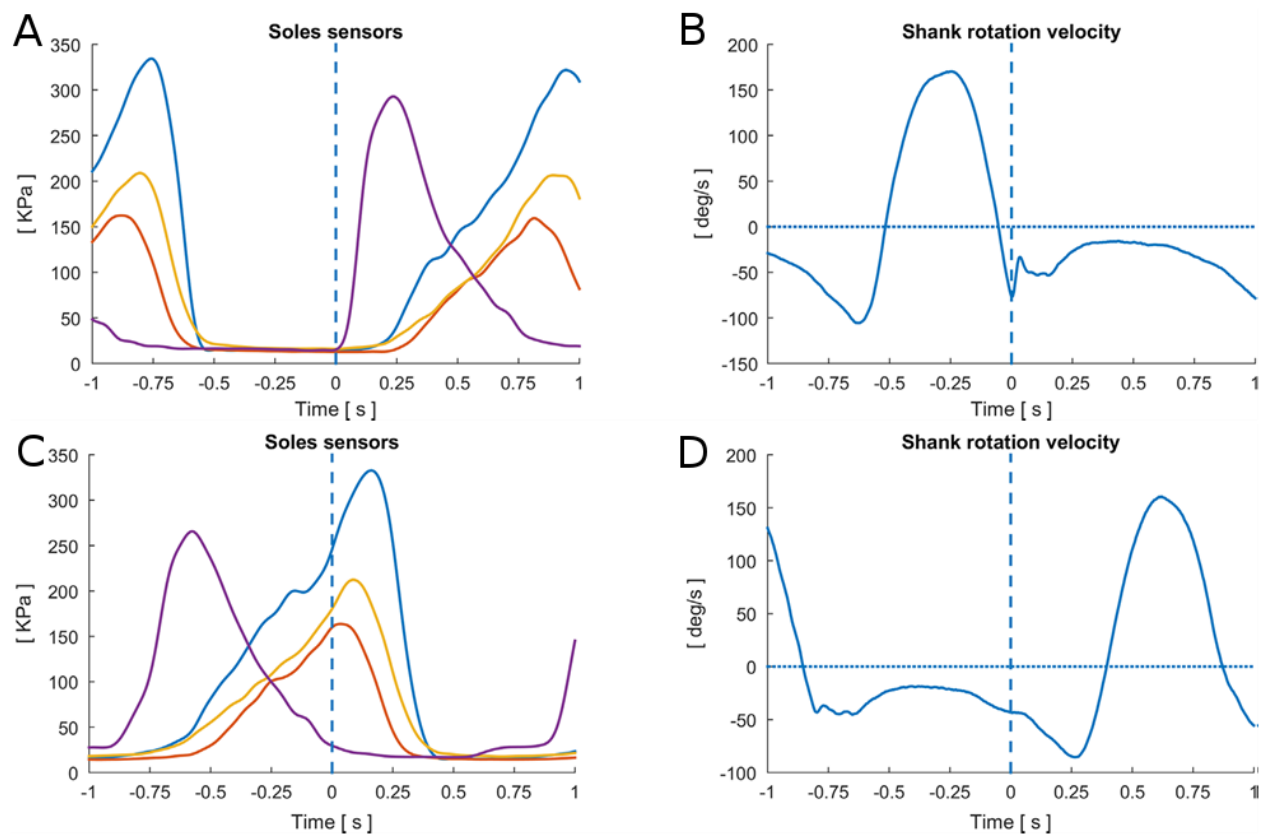


Figure 2. Illustration of kinematic measurements: Using gyroscopes and sole pressure sensors to reconstruct the gait cycle. Sole sensor pressure (A,C; the four coloured traces represent four pressure-sensitive elements in the sole; the purple trace represents the heel sensor, which is the first to signal the heel contact, the red trace represents the big toe sensor and the blue and yellow trace represent first and fifth metatarsals sensors) and shank rotation velocity (B, D) of left and right foot respectively. A & B show the determination of the initial contact in the shank rotational velocity (B), confirmed by the curves of the pressure sensitive sole (A). C & D show the determination of the terminal contact ('heel-off') point in the curves of the pressure sensitive sole (C) and shank rotational velocity (D). Adapted with permission from (Bötzel et al., 2016).

1.2.2 Neural mechanisms for locomotion and locomotor control

Movement is thought to be initiated, maintained and controlled by a complex hierarchical system (la Fougère et al., 2010; Takakusaki et al., 2004). A large body of research suggests that motor commands are initiated and controlled by a brain network consisting of forebrain regions like the motor cortex, thalamus, basal ganglia, midbrain areas like the mesencephalic locomotor region (MLR) and hindbrain regions like the cerebellum and the pons reticulospinal and sent down to spinal networks consisting of central pattern generators (CPG) (Figure 3). Each level of this hierarchy also receives and transmits peripheral sensory feedback, which in turn modifies the output at the same and upstream levels (Brown, 1912; Goulding, 2009; Koch et al., 2017; Sherrington, 1923; Tresch et al., 1999).

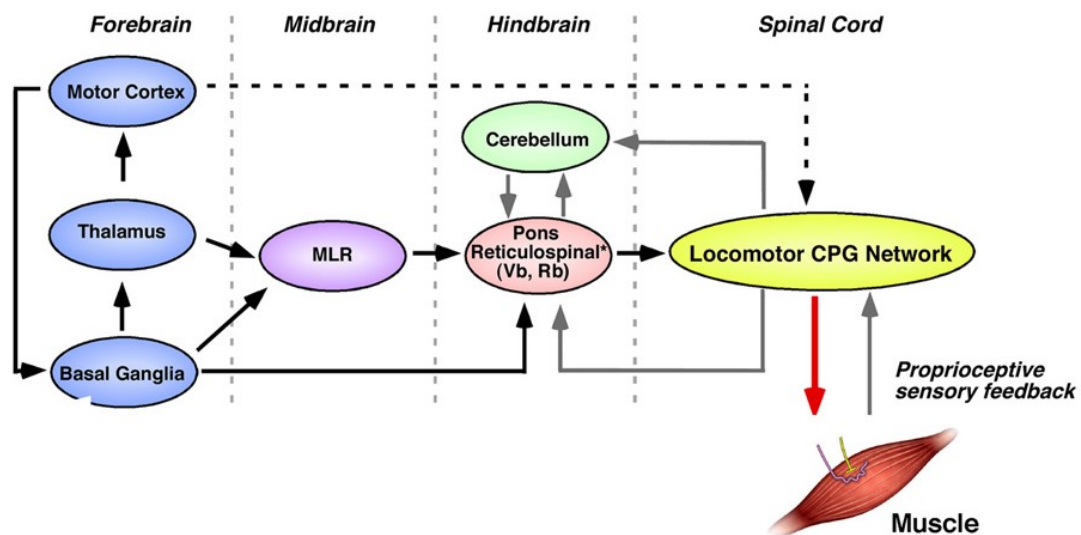


Figure 3. Organization of the locomotor system in vertebrates. Motor pathways in aquatic and terrestrial vertebrates share a similar neuroanatomical structure. Local control of muscle movements is affected by pools of motor neurons in the spinal cord that are part of a dispersed locomotor CPG network. The motor commands are modulated by proprioceptive sensory feedback via sensory afferents. Descending reticulospinal, rubrospinal and vestibulospinal pathways control the locomotor network in the spinal cord, although the reticulospinal pathway is the primary pathway for initiating locomotion. The reticulospinal pathway can be activated by the mesencephalic locomotor region (MLR), which has inputs from the basal ganglia and thalamus. The cerebellum coordinates motor behaviors by mediating sensory and internal feedback and optimizing the motor pattern to the task at hand. It also coordinates spinal motor actions with the supraspinal motor pathways. Connections from the motor cortex refine and initiate motor actions. The black lines indicate direct command pathways, the grey lines indicate feed-back pathways. VS, vestibulospinal; RbS, rubrospinal. Adapted with permission from (Goulding, 2009).

Research suggests that the coordinated and alternating movements of both legs in primates and humans during gait are at least partly driven by spinal CPG networks (Kandel et al., 2000). The CPG network can be described as coupled antagonist oscillators connected to different extensor and flexor muscles (Figure 4). This network is responsible for the generation of the rhythm that shapes the activity of motorneurons (Duysens and Van de Crommert, 1998; Grillner, 1985; Ijspeert, 2008; Marder and Bucher, 2001) and is able to produce simple and coordinated rhythmic movements like walking.

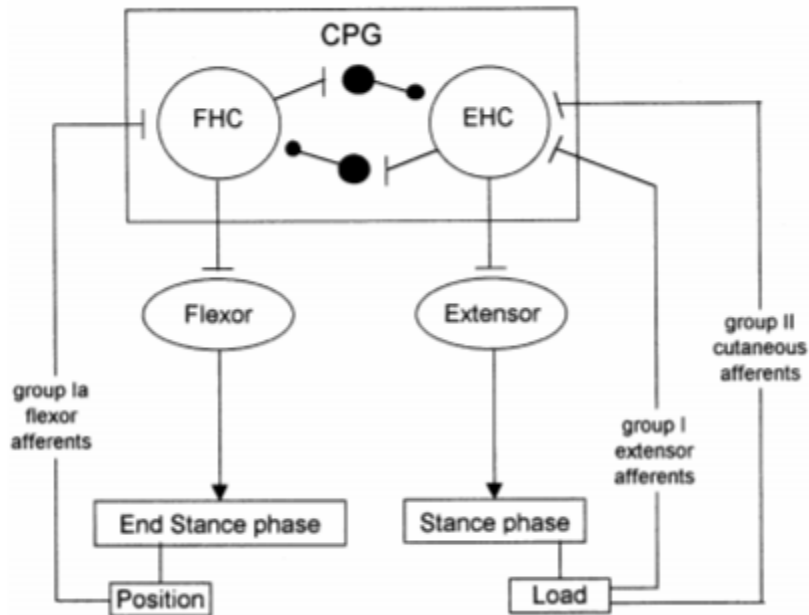


Figure 4. Model of the different pathways indicating how afferents can act on the central pattern generator (CPG) during the stance phase of locomotion. The CPG contains a mutually inhibiting extensor and flexor half-center (EHC and FHC, respectively). During the stance phase, the load of the lower limb is detected by group I extensor muscle afferents and group II (low threshold) cutaneous afferents, which activate the EHC. In this way, extensor activity is reinforced during the loading period of the stance phase. At the end of the stance phase, group Ia afferents of flexor muscles excite the FHC (which inhibits the EHC) and, thereby, initiate the onset of the swing phase. Adapted with permission from (Van de Crommert et al., 1998).

Arguments in favour of a CPG network come from various experiments with cats and primates with a complete or partial transection of the spinal cord, who show partially intact movement patterns during walking (Duysens and Van de Crommert, 1998; Nielsen, 2003). Further evidence comes from electric spinal cord stimulation experiments in various vertebrates, which could induce locomotor activity regardless of injuries to the spinal cord (Dorofeev et al., 2008; Duysens and Van de Crommert, 1998; Gerasimenko et al., 2000, 2003). Electromyography (EMG) of myotomes at different axial levels does show slow patterns of rhythmic motor activity, even in animals with isolated spinal cords (Figure 5)

(Orlovsky et al., 1999). The existence of a human CPG is supported by the observation that patients with complete and partial spinal cord injuries do show spontaneous leg movements (Calancie et al., 1994; Kuhn, 1950). Periodic leg movements have also been described during sleep, even in patients with complete spinal lesions (Coleman et al., 1980; Lugaesi et al., 1986).

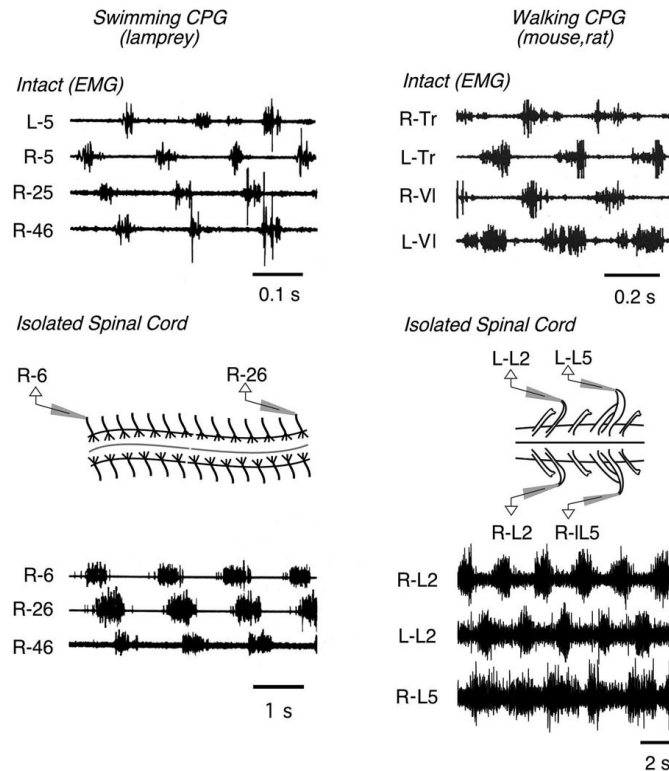


Figure 5. Rhythmic motor patterns underlying vertebrate locomotion. (a) Examples of spinal motor activity during swimming in the lamprey. (Top) Electromyograph (EMG) recordings of different myotomes at located at different axial levels. (Bottom) Ventral root recordings from the isolated spinal cord exhibit a slow pattern of rhythmic motor activity. (b) Walking motor behaviour. (Top) EMG recordings showing muscle activity in the cat hindlimb. (Bottom) Isolated mouse spinal cord preparation. Electroneurogram (ENG) recordings from L2 and L5 ventral roots following the induction of walking by NMDA and serotonin (5-HT). The ENG traces give a measure of flexor-related (L2) and extensor-related (L5) motor activity. Adapted with permission from (Orlovsky et al., 1999).

Although a feedback driven central pattern generator network provides a mechanism for the generation and maintenance of locomotion, cortical and subcortical areas play an important role in the initiation and control of human gait (Rodríguez-Oroz et al., 2009; Yang and Gorassini, 2006).

Evidence for the involvement of mid- and hindbrain structures comes from various experimental studies in animals as well as in humans. Clinical studies show, that patients with lesions at supra-spinal regions of the CNS never fully recover their walking abilities. This underlines the importance of

cerebral control of locomotion in humans. Lesion studies show that most animals lose their ability to initiate movements after spinal cord transection. Lesions at different levels of the spinal cord suggest that regions for the initiation of movement are most likely located at supra-spinal levels in the brain stem (Whelan, 1996). Shik and colleagues (Shik et al., 1966) discovered that electrically stimulating a region in the brainstem between the midbrain and hindbrain, now called the mesencephalic locomotor region, initiates rhythmic locomotion patterns. They also showed that manipulating the strength of the stimulation could induce differences in walking speed.

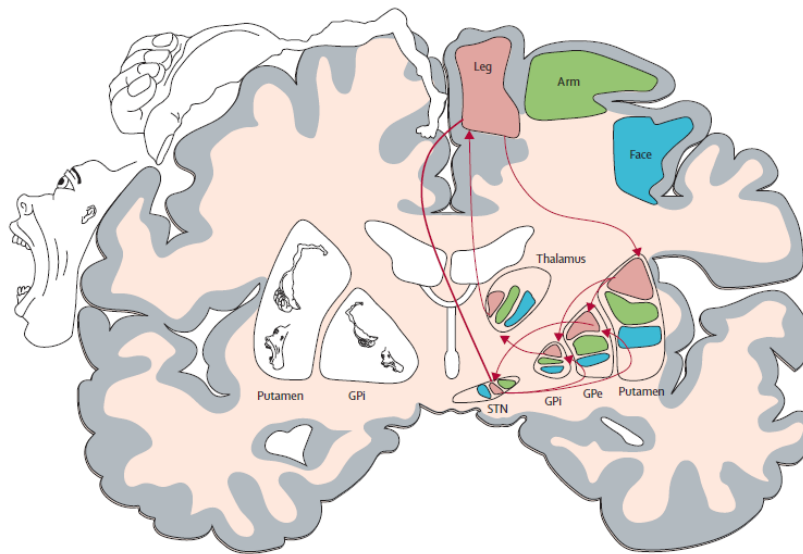


Figure 6. The motor circuit and its somatotopic organization. The motor circuit (indicated by red arrows connecting the regions that modulate leg movements) is somatotopically organised throughout the loop, with the regions representing leg movements lying dorsal and medial, those representing face movements lying ventral and lateral, and those representing arm movements lying in-between. The somatotopic arrangement of the primary motor cortex is generally maintained in the striatopallidal and subthalamic nuclei. GPe: globus pallidus pars externa. GPi: globus pallidus pars interna. STN: subthalamic nucleus. Adapted with permission from (Rodriguez-Oroz et al., 2009).

The forebrain motor circuit is thought to be somatotopically organized across the whole cortical-basal ganglia loop including motor cortices, putamen, pallidum, subthalamic nucleus and thalamus (Figure 6) (Rodriguez-Oroz et al., 2009). Experiments exploiting transcranial magnetic stimulation in humans confirm that the motor cortex is involved in activating the dorsiflexor and plantarflexor muscles during walking (Petersen et al., 2001). Functional neuroimaging studies in humans have demonstrated the existence of a supraspinal sensorimotor network for the neural control of locomotion in humans and

show that the primary motor cortex is recruited during rhythmic foot movements (Dobkin et al., 2004). Activations are also reported in the frontal cortex, cerebellum, pontomesencephalic tegmentum, parahippocampal, fusiform and occipital gyri, accompanied by deactivations in superior temporal gyrus and inferior parietal cortex (Figure 7) (la Fougère et al., 2010) during real and imagined movement.

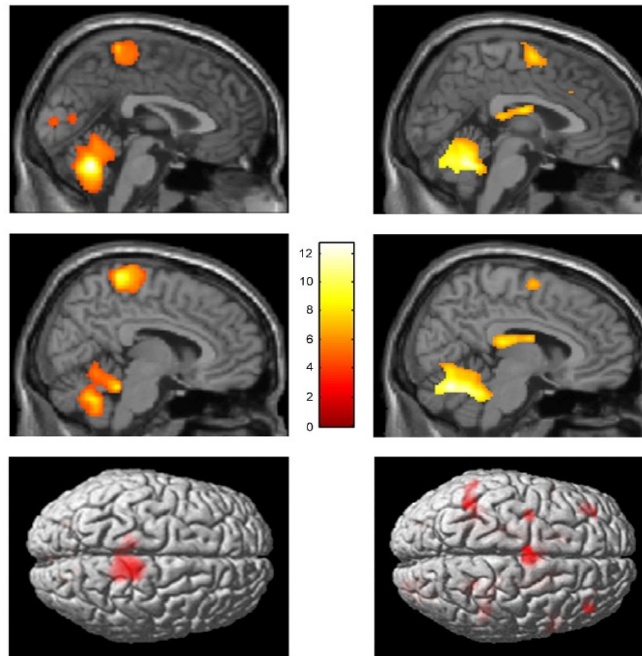


Figure 7. Comparison of real ([^{18}F]-FDG-PET) and imagined locomotion (fMRI). Sagittal midline and render views are shown. It can be seen that during real locomotion the primary motorsensory cortices (pre- and postcentral gyri) are active (left) as compared to the supplementary motor areas (superior and medial frontal gyri) in mental imagery of locomotion (right). Furthermore during imagined locomotion the basal ganglia (caudate nucleus, putamen) are active, which is not the case for real locomotion. Adapted with permission from (la Fougère et al., 2010).

When comparing real and imagined movement, researchers found activation in the primary motor cortex primarily during real locomotion, while supplementary motor areas and basal ganglia activations were found during mental imagery. It has been suggested that these differences could reflect two complementary networks. A network for the modulation and control of locomotion, including premotor and basal ganglia areas, which is activated during imagined movement, and a network responsible for the execution of continuous locomotion, including the primary motor cortex (Figure 8) (la Fougère et al., 2010). Together they are thought to be responsible for controlling e.g. gait initiation and termination,

velocity and spatial orientation while integrating information from sensory feedback (Castermans et al., 2013).

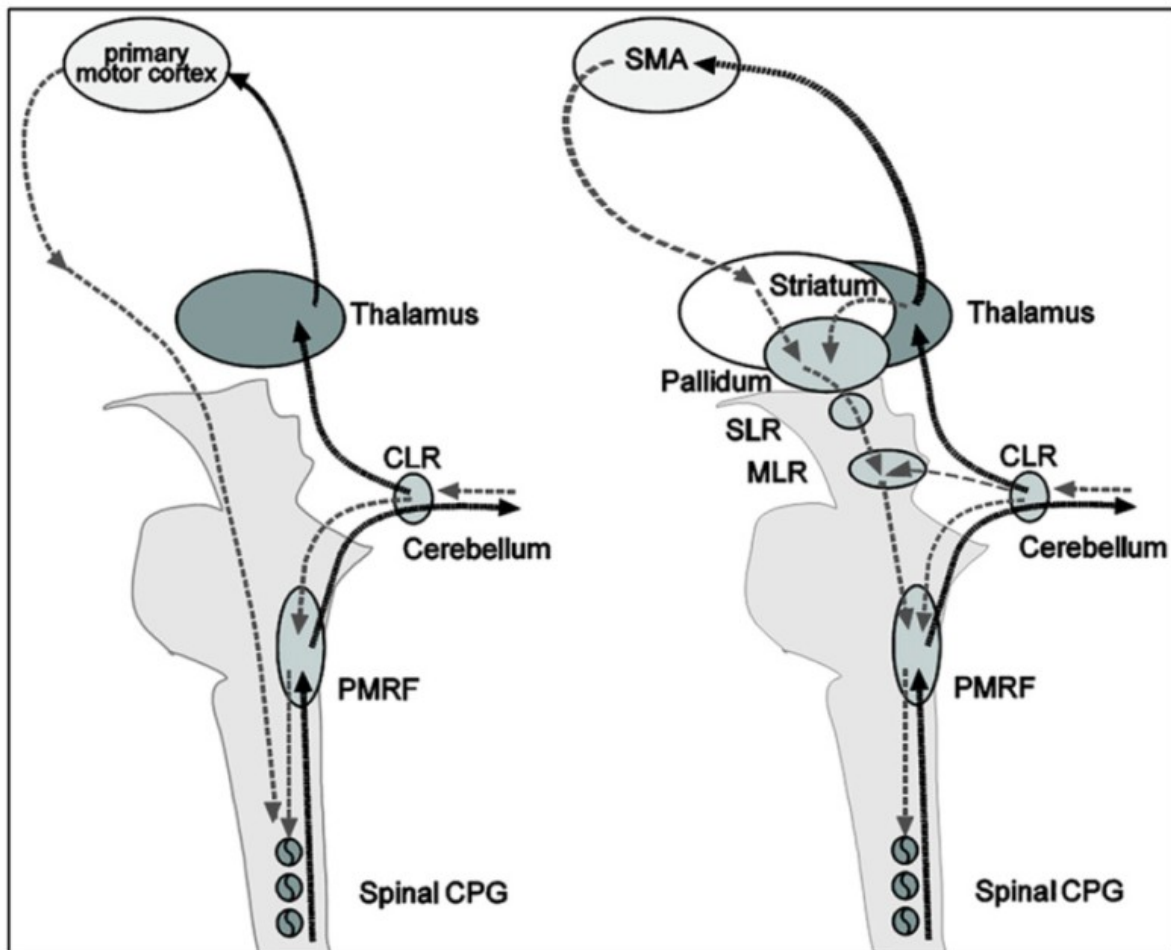


Figure 8. The “executive” (left) and “planning” (right) network of locomotion. Execution of locomotion in a non-modulatory steady state (left side) goes from the primary motor cortex areas directly to the spinal central pattern generators (CPG), thereby bypassing the basal ganglia and the brainstem locomotor centers. A feedback loop runs from the spinal cord to the cerebellum and thereby via the thalamus to the cortex. For planning and modulation of locomotion (right side) cortical locomotor signals originate in the prefrontal supplementary motor areas and are transmitted through the basal ganglia via disinhibition of the subthalamic locomotor region (SLR) and mesencephalic locomotor region (MLR) where they converge with cerebellar signals from the cerebellar locomotor region (CLR). The MLR functionally represents a crosspoint for motor information for basal ganglia and cerebellar loops. Descending anatomical projections are directed to the medullary and pontine reticular formations (PMRF) and the spinal cord, ascending projections are in the main part concentrated on the basal ganglia and the nonspecific nuclei of the thalamus (not shown for sake of clarity). The CLR also projects via the thalamus back to the cortex. Cortical signals are furthermore modulated via a thalamo-cortical-basal ganglia circuit. The schematic

drawing shows a hypothetical concept of a direct pathway of steady-state locomotion (left) and an indirect pathway of modulatory locomotion (right). Adapted with permission from (la Fougère et al., 2010).

1.2.3 Electrophysiology of human locomotion

Using scalp EEG recordings in humans, different studies report similar intra-stride changes in spectral power at electrocortical sources in the anterior cingulate, posterior-parietal, and sensorimotor cortices. In the double support phase around the terminal contact at the end of the stance phase, alpha- and beta-band spectral power was increased bilaterally in the sensorimotor and dorsal anterior cingulate cortices. High-gamma spectral power changes were observed during the swing phase in anterior cingulate, posterior parietal and sensorimotor cortex (Figure 9) (Gwin et al., 2011; Seeber et al., 2015; Severens et al., 2012; Storzer et al., 2016; Trenado, 2015; Wagner et al., 2012).

Confirming results from experiments with rats and cats (Beloozerova et al., 2010; Iosa et al., 2013; Marlinski et al., 2012; Smith, 1997), a study by Fitzsimmons (Fitzsimmons, 2009) was able to extract walking patterns, decode the phase of the gait cycle and predict future locomotion parameters from monkey primary somatosensory cortex (S1) and primary motor cortex (M1) neuronal ensemble recordings. A recent study with human subjects implanted with electrocorticographic grids over the motor cortex demonstrates that M1 is primarily responsible for high-level locomotor control (i.e. walking duration and speed). Authors show, that both subjects who took part in the study show generalized γ -band (40–200 Hz) increases and periodic gait-cycle specific γ -band modulations in M1 activity during treadmill walking. However, M1 activity during walking was neither highly predictive of lower limb trajectories nor was it overly similar to activity during individual leg muscle movements. The authors suggest that the control of human locomotion depends on the interaction between M1, responsible for high-level motor commands, and subcortical and spinal low-level motor control networks (McCrimmon et al., 2017).

Gait phase related amplitude modulations

Amplitude changes: walking vs. standing

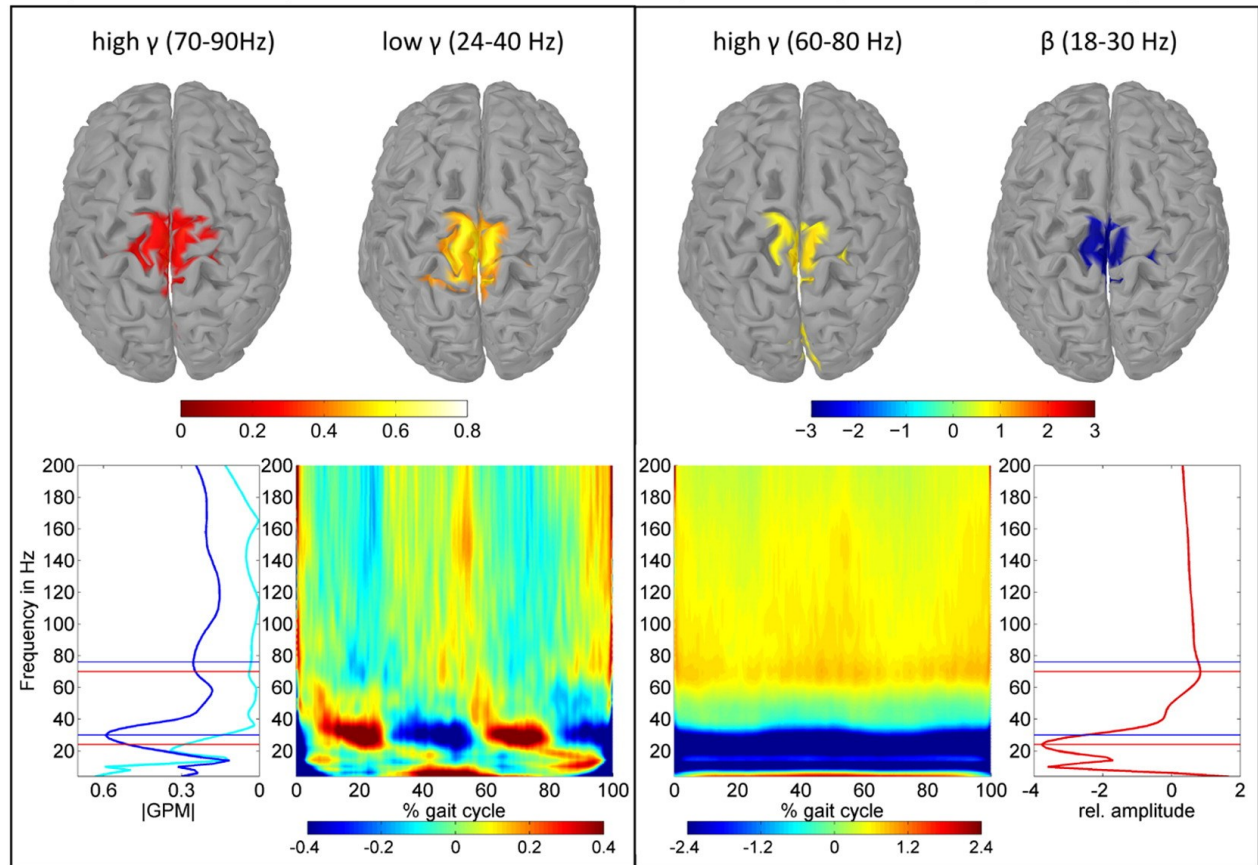


Figure 9. Left panel: Gait phase related amplitude modulations (GPM). EEG source images show significant high γ and low γ GPM (grand average) located focally in central sensorimotor areas. The temporal modulation of high γ and low γ amplitudes in the gait cycle is illustrated in the time-frequency plot (reference: walking; colors depict change in dB relative to reference) below. The spectrum of GPM magnitudes (walking in blue, standing in cyan) indicates amplitude modulation in relation to the gait cycle as a function of frequency. Right panel: Relative amplitude changes between walking and standing. Significant high γ increase and β decrease (grand average) occurred in central sensorimotor areas. The sustained high γ increase and μ and β decrease during the gait cycle is shown in the TF plot (reference: standing). The temporal mean of the relative amplitude changes (walking vs. standing) are illustrated as frequency spectrum (red). Spectra and TF plots were calculated in the central sensorimotor ROI, all amplitude changes in dB. Spectral peaks of high γ (76 Hz) and low γ (30 Hz) GPM are marked with blue lines, while the spectral peaks of high γ increase (70 Hz) and β decrease (24 Hz) are marked with red lines. Adapted with permission from (Wagner et al., 2012)

Recordings of local field potentials in the basal ganglia of patients with movement disorders have demonstrated subcortical oscillations at several frequencies, which are reactive to movement, especially prominent beta band activity around 13 to 35 Hz. Beta power has been shown to be suppressed during

movement and has also been shown to be correlated with akinetic-rigid symptoms (Hammond et al., 2007; Kühn et al., 2006; Neumann et al., 2016) in human patients as well as in animal models of parkinsonism (Costa et al., 2006; Mallet et al., 2008; Sharott et al., 2005). Confirming these findings, it has been shown that low frequency (5 and 10 Hz) and beta frequency (20 Hz) stimulation of the STN slows movement in Parkinson's disease (Chen et al., 2007; Eusebio et al., 2008).

Evidence for beta power attenuation in various cortical and subcortical structures like the basal ganglia during single movements comes from various studies (Kühn et al., 2004; Litvak et al., 2012). Reports about subcortical frequency amplitude modulations during repetitive movements and especially during gait are rare. Studies with PD patients suggest a reduction in beta frequency power in the STN during walking as compared to a resting baseline, particularly in akinetic-rigid patients (Figure 10) (Quinn et al., 2015). Singh and colleagues report that the amplitude of the alpha frequency on the contralateral side was significantly higher in ballistic fast movements compared with rest, in both STN and GPi (Singh et al., 2011b).

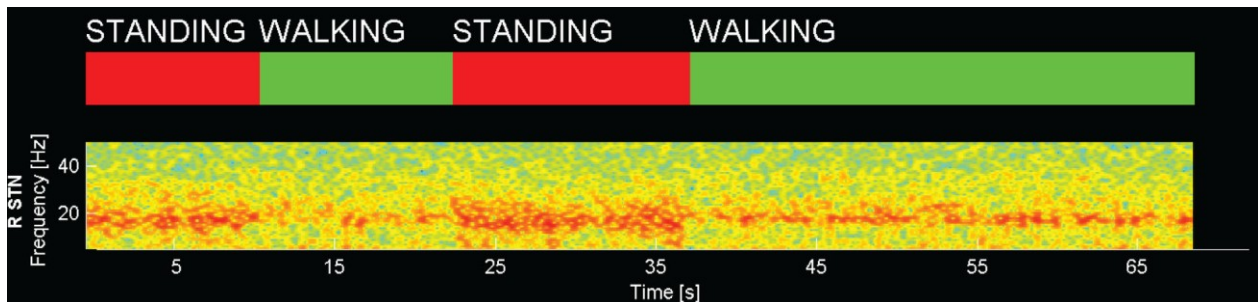


Figure 10. Continuous LFP spectrogram of subthalamic recordings from one subject during standing and forward walking. The spectrogram shows attenuation of beta frequency power during walking episodes. Colour in the spectrogram depicts power. Adapted with permission from (Quinn et al., 2015).

Studies investigating repetitive movements paint a slightly different and more complex picture. Androulidakis and colleagues show that STN LFP activity, especially oscillatory activity in the beta band, was modulated in amplitude during continuous finger tapping (similar to Figure 9, left panel) and this modulation probably failed as bradykinesia increased (Androulidakis et al., 2008). Steiner and colleagues (Steiner et al., 2017) argue that beta is attenuated during repetitive finger movement and that the attenuation of beta oscillations is reduced with increasing bradykinesia (Figure 11). Florin et al. report significantly increased activity in the low beta (12-18 Hz) and gamma (30-48 Hz) frequency ranges within the STN during fist flexion and extension and hypothesise that increases in gamma power enable repetitive fist movement despite increased beta levels (Florin et al., 2013).

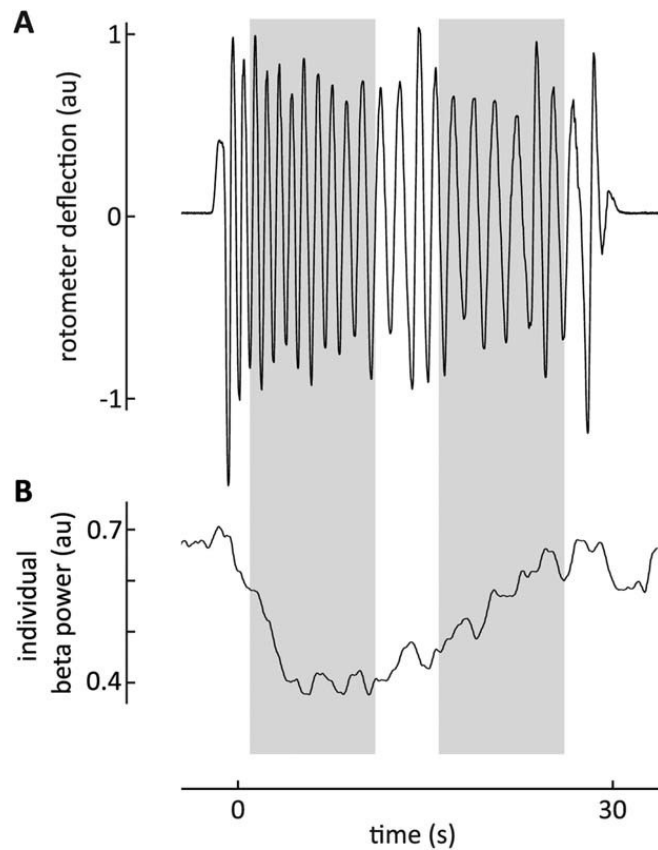


Figure 11. Example trace of beta power dynamics alongside motor impairment. Gray boxes indicate 10-second windows, the means of which were used in further analysis. (A) Movement trace of a PD patient performing continuous and alternating pronation and supination movements for 30 seconds. Raw movement trace shown was detrended to allow better assessment of movement amplitude. (B) Trace of individual beta power (patient-specific beta peak during movement performance 6.5 Hz) smoothed using an overlapping, sliding average window to capture the general trend in beta activity over time. Smoothing was applied for visualization purposes only. Unlike Figure 1, beta power is not normalized by rest power. Adapted with permission from (Steiner et al., 2017).

Local LFP recordings from DBS electrodes located in the globus pallidus internum in dystonia patients without gait impairments showed significantly higher power in the lower frequency bands (4–12 Hz) and in the gamma band (60–90 Hz) during gait as compared to during sitting or standing, while the beta band (15–25 Hz) power was significantly reduced during walking. Additionally, the authors report contralateral increases in power in the alpha range between 6 and 11 Hz during the early stance phase (Figure 13) (Singh et al., 2011a).

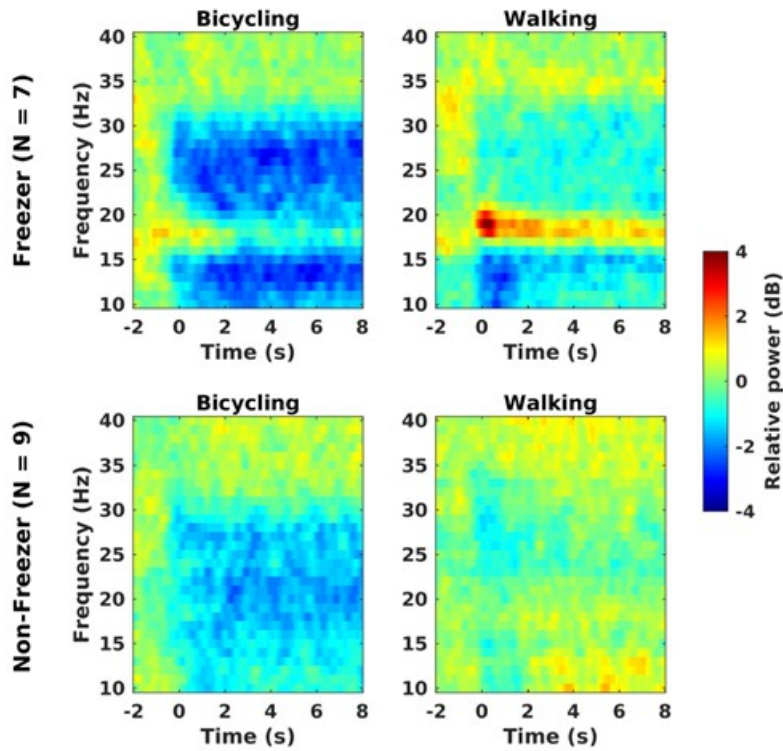


Figure 12. Beta power changes in freezers and non-freezers. Grand average time-frequency plots showing power changes locked to movement initiation ($t = 0$) in freezers (7 STNs) and non-freezers (9 STNs) for bicycling and walking, and the difference between both (non-significant differences are masked). Lower row: Beta power decreases (blue) in both conditions in non-freezers, but with a stronger beta power decrease in bicycling. Upper row: In freezers, bicycling is accompanied by a broad-band beta power decrease and briefly by a slight power increase (red) in a narrow band around 18 Hz, following movement initiation. Opposed to this, walking is accompanied by a distinctive and sustained power increase in this band. Adapted with permission from (Storzer et al., 2017).

Furthermore, recent studies suggest that PD-patients displaying freezing of gait show an additional increase in low beta (12-20Hz) power during gait (Singh et al., 2013; Storzer et al., 2017). Storzer and colleagues (Storzer et al., 2017) compared STN activity during bicycling and walking in PD patients with and without freezing of gait. While patients without freezing of gait, in both bicycling and walking conditions, showed a suppression of subthalamic beta power (13–35Hz), Freezers showed a similar pattern in general and an additional, movement-induced, narrowband power increase around 18Hz (Figure 12).

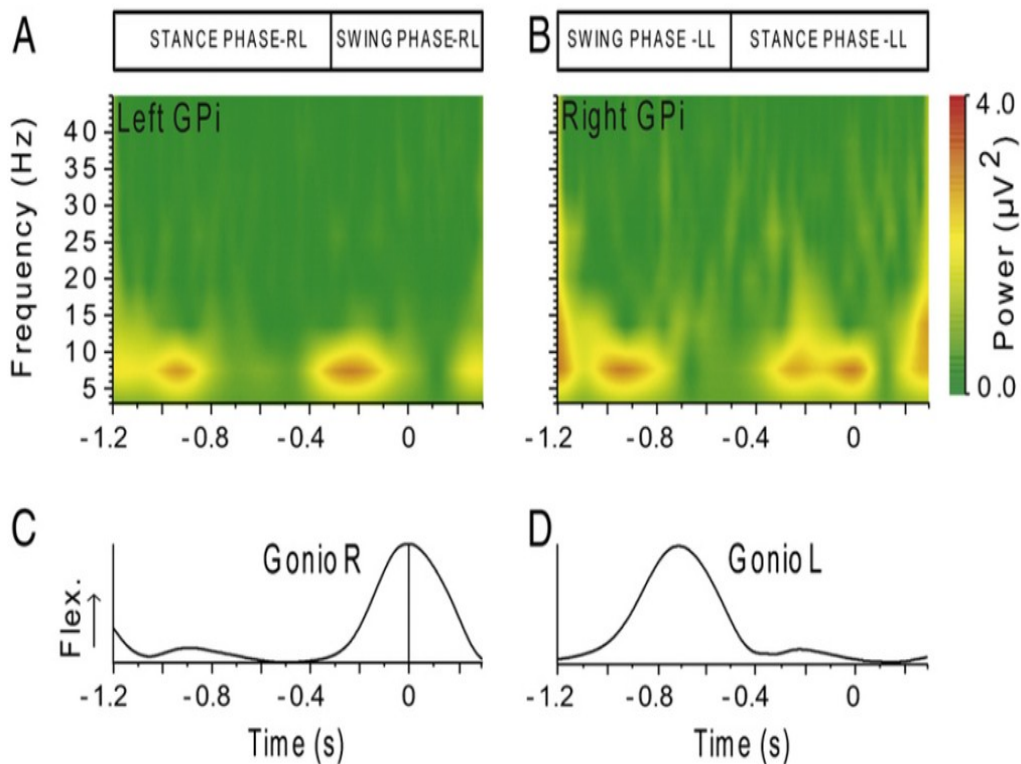


Figure 13. Time–frequency plots of LFP oscillations during gait cycle. Upper row (A and B): analyzed electrode pair. Right electrode pair is on the right side. C and D: goniometer traces. Modulation of LFPs occurs in the 6–11 Hz frequency range. In this frequency band, amplitudes are up-regulated during the early stance phase and swing phase of the contralateral leg. LL: left leg, RL: right leg, Gonio: goniometer. Flex: flexion. Adapted with permission from (Singh et al., 2011a)

Synchronization of neural activity across different parts of the brain likely plays a key role in the coordination of neural activity underlying behaviour and excessive synchronization has been linked to various movement disorders (Buzsáki and Draguhn, 2004; Chou et al., 2005; Schnitzler and Gross, 2005). Beta coherence has been shown between ipsilateral STN, GPi and cortical regions and is reported to be attenuated by movement, while patients were off levodopa. While most studies focus on within hemisphere connectivity, other reports show that even unilateral movement results in bilateral changes in the STN, probably reflecting cortical input (Alegre et al., 2005). Niketeghad et al., report motor-modulated inter-hemispheric connectivity between bilateral STN-LFP signals (Niketeghad et al., 2017). Hohlefeld and colleagues demonstrated coherence (iCOH) between bilateral STN in the beta range (10–30Hz). While iCOH in the 10–20 Hz frequency range positively correlated with the worsening of motor symptoms in the OFF medication condition, iCOH in the high beta range (21–30 Hz) was increased after levodopa administration (Hohlefeld et al., 2014).

1.3 Decision making and inhibition

Inhibitory control is an executive function that is needed to suppress premature actions and to block interference from irrelevant stimuli. According to the definition from Norman and Shallice (Norman and Shallice, 1986), executive control/inhibition is essential in unfamiliar and difficult situations that require planning or decision making under conflict and in situations in which a strong habitual ('normal') response has to be overcome. According to a prominent model for deliberate decision making, evidence is accumulated until a response threshold is reached and an action is triggered (Ratcliff and McKoon, 2008). Habitual responses are usually executed fast (Schneider and Chein, 2003) without much deliberation and the decision threshold is presumably reached faster than with unfamiliar decisions (Ratcliff, 1978; Ratcliff et al., 2016). For example, if someone approaches pedestrian lights and the lights are green, the prepotent response will be to cross the street. However, if a car is approaching the crossing, one has to decide to do the familiar and cross the road or to stay put and not risk a potentially fatal accident if the car is ignoring the lights. This scenario requires the inhibition of a strong habitual response to allow for proper decision making and a more adequate action selection. Reduced executive/inhibitory control can thus result in premature actions as well as socially unacceptable behaviour.

Inhibitory control is impaired in a number of neuropsychiatric and neurological disorders and is associated with disrupted neural activity in the cortico-striatal circuitry, including the STN (Antonelli et al., 2011; Lipszyc and Schachar, 2010; Richardson, 2008; Zamboni et al., 2008). However, the influence of STN DBS on impulse control is debated. In general, studies show an improvement of automatic (habitual) response activation when DBS is turned on, while DBS also increases the susceptibility to impulsive responses (Plessow et al., 2014), which is in favour of reduced inhibition caused by STN stimulation.

Models propose that the behavioural disinhibition following STN-DBS is caused by the failure of executive control over prepotent responses (Frank et al., 2007). Various studies have reported that stimulation of the STN can be associated with impulsive action. For example, STN-DBS has been shown to result in fast, but erroneous decisions in a variety of tasks that require response selection under conflict and inhibition of prepotent responses, such as the Go/No-Go task, the Stroop, or the Simon task Simon effect (Jahanshahi et al., 2015a). It must be noted, however, that different studies report conflicting results (Ray et al., 2011), while some report that response inhibition worsens during DBS, others state that it is unaffected, while others again show improvements (Ballanger et al., 2009; Jahanshahi, 2013; Obeso et al., 2011). One reason for this discrepancy could be that the STN consist of at least 3 subregions

(motor/associative/limbic) and DBS of different subdivisions of this nucleus may have different effects on inhibitory control (Hershey et al., 2010). When STN DBS does not only selectively target the motor subregion, stimulation might induce behavioural disinhibitions similar to those caused by lesions to the STN. Such lesions have been induced in a small number of PD patients for therapeutic reasons and it was reported that these patients show increased behavioural impulsivity, especially during responses with the hand contralateral to the lesion (Frank, 2006; Jahanshahi et al., 2015a; Obeso et al., 2011).

1.3.1 Models of inhibition: Proactive and reactive inhibitory control

Several cortical regions, especially the anterior cingulate cortex (ACC), the dorsolateral prefrontal cortex (DLPFC), the medial prefrontal cortex (mPFC), the inferior parietal cortex (IPC) and the precuneus/posterior cingulate cortex (Prec/PCC), are reported to be involved in inhibitory processes (Botvinick et al., 2004; Cohen and Ridderinkhof, 2013; Liston et al., 2006; Zavala et al., 2016). Computational models as well as experimental studies in humans and primates also highlight the role of several subcortical structures including the basal ganglia and especially the STN in inhibitory control (Aron et al., 2007; Benis et al., 2014; Cavanagh et al., 2011; Frank, 2006; Zaghoul et al., 2012).

There are two major theoretical mechanisms discussed for response inhibition: proactive and reactive inhibitory control (Figure 14) (Martínez-Selva et al., 2006). In the reactive model established by Frank et al. (Frank, 2006), response inhibition is implemented as response selection processes evolve. The global inhibitory signal is described as reactive in nature and is triggered by the stimulus conflict (Aron et al., 2007). In contrast, the “proactive inhibition” theory assumes that inhibition is the default mode of an executive control network responsible for basic preparatory processes, which prevents automatic responses to irrelevant signals by maintaining tonic inhibition over response processes until uncertainty is resolved (Jaffard et al., 2008).

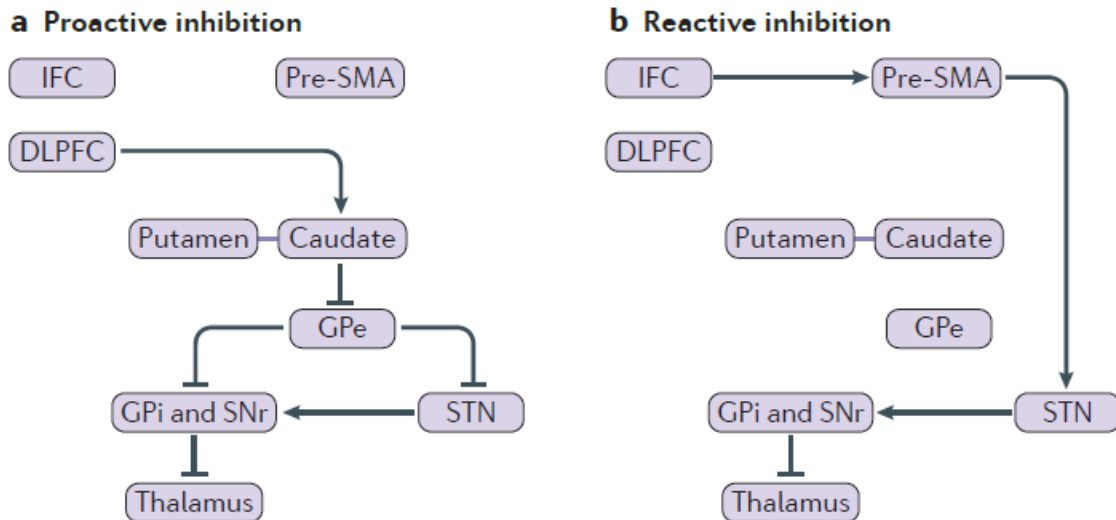


Figure 14. The fronto–basal ganglia pathways mediating proactive and reactive inhibitory control. a. Proactive inhibition is prospective and serves goal attainment - for example, when intentionally suppressing the desire to eat high-calorie foods in order to proactively meet the goal of weight control. The indirect fronto–striato–pallido–thalamo–cortical pathway could mediate such proactive inhibition. b. Stimulus-driven reactive inhibition, which is built up through learning and experience and is more automatic and habitual — for example, when a pedestrian stops at a red traffic light — is proposed to be mediated by the hyperdirect cortico–subthalamic–pallidal–thalamo–cortical pathway. For clarity, some connections are not shown. DLPFC: dorsolateral prefrontal cortex; GPe: external segment of the globus pallidus; GPi: internal segment of the globus pallidus; IFC: inferior frontal cortex; pre-SMA: pre-supplementary motor area; SNr: substantia nigra pars reticulata; STN: subthalamic nucleus. Adapted with permission from (Jahanshahi et al., 2015b)

Both theories assume a global modulatory signal suppressing all responses, rather than modulating the execution of any particular response and postulate attenuation of thalamocortical activity, with different cortical structures involved. The reactive model claims specific changes in primary motor cortex (PMC), pre-supplementary motor area (pre-SMA), the anterior cingulate cortex (ACC), and the inferior frontal cortex (Frank, 2006). The “proactive inhibition” hypothesis is linked to possible activation changes in medial prefrontal cortex (mPFC), precuneus, posterior cingulate cortex (PCC), inferior parietal cortex (IPC) and dorsolateral prefrontal cortex (DLPFC) (Ballanger et al., 2009; Boulinguez et al., 2009; Jaffard et al., 2008; Jahanshahi et al., 2015b). Hence, while both models claim frontal structures to be involved, only the proactive model invokes posterior structures, which have been shown to be important for movement initiation and planning (Mattingley et al., 1998; Scherberger et al., 2005).

In both models, the STN plays a major role. Optimal action selection in conflict situations with competing or uncertain stimulus and response relations is proposed to rely on an intact hyperdirect pathway and STN (for an overview of cortico-basal ganglia-thalamo-cortical pathways and structures, see (Jahanshahi

et al., 2015b)). By inhibiting the pallidial-thalamic-cortical loop via inhibitory connections to the GPi, the STN is thought to suspend responses until sufficient information has been integrated and uncertainty is resolved (Bogacz and Gurney, 2007; Frank et al., 2007; Herz et al., 2017).

1.3.2 Neural mechanisms underlying response inhibition during decision making under conflict

Different neuronal processes play an important role during inhibition and decision making tasks. Like locomotion, cognitive processes underlying goal-directed behaviour also require a dynamic interaction of information from spatially distant brain regions (Buzsáki and Draguhn, 2004; Hipp et al., 2011; Siegel et al., 2012; Varela et al., 2001). This integration and coordination is in part enabled by coherent neuronal oscillations at different frequencies. A number of studies report conflict-related modulations in subthalamic oscillatory power in the theta frequency band (Cavanagh et al., 2011; Zavala et al., 2013), which has also been observed in cortical structures involved in response inhibition (Zavala et al., 2015a). Increases in delta and theta power during cognitive motor tasks have been mainly observed at frontal midline areas that mediate response inhibition (Cavanagh et al., 2011; Cavanagh and Frank, 2014), for example over the PFC and the IFG, which are connected to the STN via the hyperdirect and indirect pathway (Alexander et al., 1986; Forstmann et al., 2010; Monakow et al., 1978; Swann et al., 2012).

Decision making is not only a covert process but is often accompanied by an overt reaction, especially in investigational studies. It has been suggested that beta-band de/resynchronization accompanies motor planning and responding (Chung et al., 2017; Te Woerd et al., 2015). Beta oscillatory activity reduction during an overt response followed by a rebound after movement has been reported by a number of studies, especially over motor cortical areas (Espenhahn et al., 2017; Gross et al., 2005; Pfurtscheller et al., 1996; Salmelin and Hari, 1994) but also other areas, e.g. parietal cortex (Chung et al., 2017). There are also several reports (Alegre et al., 2013; Bastin et al., 2014; Benis et al., 2014; Joundi et al., 2013; Kühn et al., 2004; Leventhal et al., 2012; Zavala et al., 2015a) of the involvement of subthalamic beta oscillations in response inhibition during conflict. These and other studies (Espenhahn et al., 2017; Gross et al., 2005; Meirovitch et al., 2015; Pfurtscheller et al., 1996) show that cortical beta-band desynchronization precedes motor output and that the duration of suppression correlates with the amount of conflict present in the task (Alegre et al., 2013; Bastin et al., 2014; Benis et al., 2014; Brittain et al., 2012; Kühn et al., 2004; Leventhal et al., 2012; Ray et al., 2012).

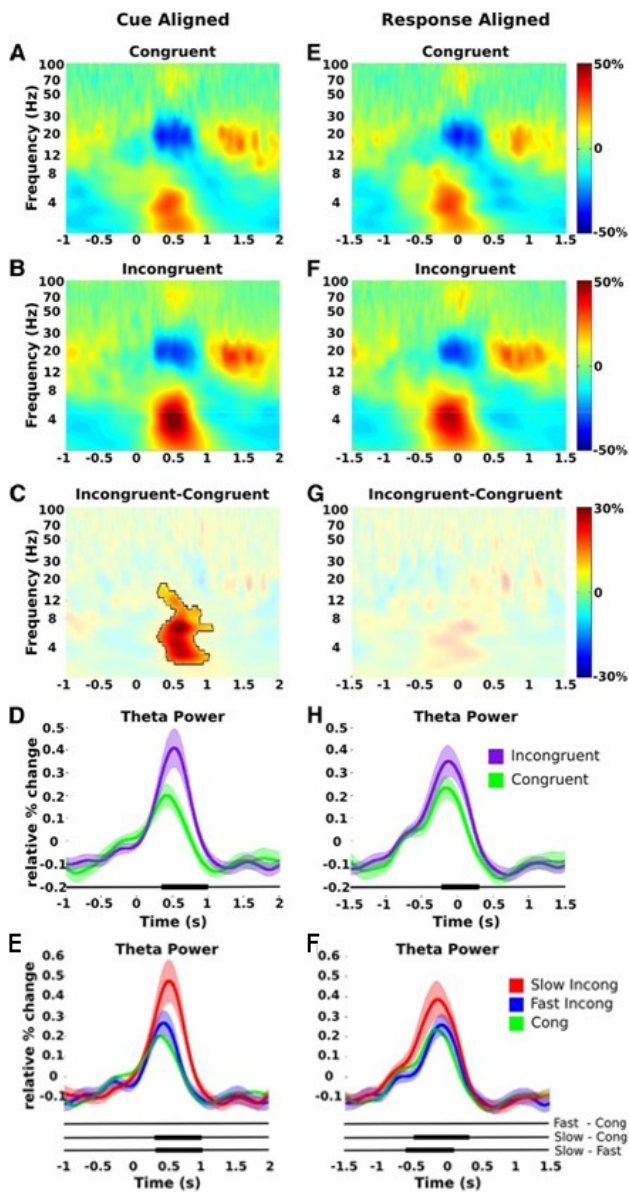


Figure 15. Effects of congruency on LFP across all subjects.

A–D, Imperative cue-aligned ($t = 0$) averages of induced spectral change. Both congruent (A) and incongruent (B) trials showed an increase in cue-aligned theta power, a decrease in beta power followed by a postresponse rebound, and an increase in gamma power. C, Difference between trial types masked at a 0.05 significance level corrected for multiple comparisons, showing the theta band difference. D, Cue-aligned theta (3–8 Hz) band average time series (mean \pm SEM) for congruent (green) and incongruent (purple) trials. Significant difference between the two conditions is marked by black bar ($p < 0.05$ corrected for multiple comparisons). E–H, Same as A–D but aligned to the response. Theta difference is weaker and only significant in the theta band average time series (H). Note that here and in ensuing time–frequency plots that frequency is given on a log axis. E, F, Theta (3–8 Hz) band average time series for slow-incongruent (red), fast-incongruent (blue), and congruent (green) trials locked to the cue and response respectively. Note that mean \pm SEM values are shown except for congruent trials (where \pm SEM values were shown in Fig. 2). Significant difference between trial types is marked by horizontal bars ($p < 0.05$, corrected for multiple comparisons). Modified with permission from (Zavala et al., 2013)

The interpretation of the functional role of frequency specific activity however is complicated. A few studies compare „Go“ and „No-Go“ trials, which implement either the execution or the inhibition of a response (Kühn et al., 2004). While many studies interpret STN activity as related to conflict processing (Frank et al., 2007; Zavala et al., 2015a), Zavala and colleagues found no power differences between the fast-incongruent trials and congruent trials with similar RTs (Figure 15) (Zavala et al., 2013).

Theory and experimental studies suggest that coherent oscillations could reflect the coordination of neural activities between different structures and the basal ganglia during response inhibition (Alegre et al., 2013; Zavala et al., 2014). Combined recordings of LFP and cortical EEG/MEG show conflict and error related activity in and coherence between frontal regions and STN in the delta/theta band and beta frequency band (Zavala, 2016; Herz et al., 2017). Previous studies reported stimulus as well as response

locked low frequency connectivity between electrodes placed at frontal midline and the STN to be correlated with conflict (Zavala et al., 2016, 2013, 2014). Zavala and colleagues report coherence increases between subthalamic LFP and frontal EEG recordings during high conflict situations (Figure 16) (Zavala et al., 2014). Herz and colleagues (Herz et al., 2017) report that STN low frequency oscillations are coupled to activity at prefrontal electrode Fz and are related to decision thresholds and that STN beta activity (13–30 Hz) is coupled to electrodes C3/C4 close to motor cortex (Herz et al., 2017; Tan et al., 2014).

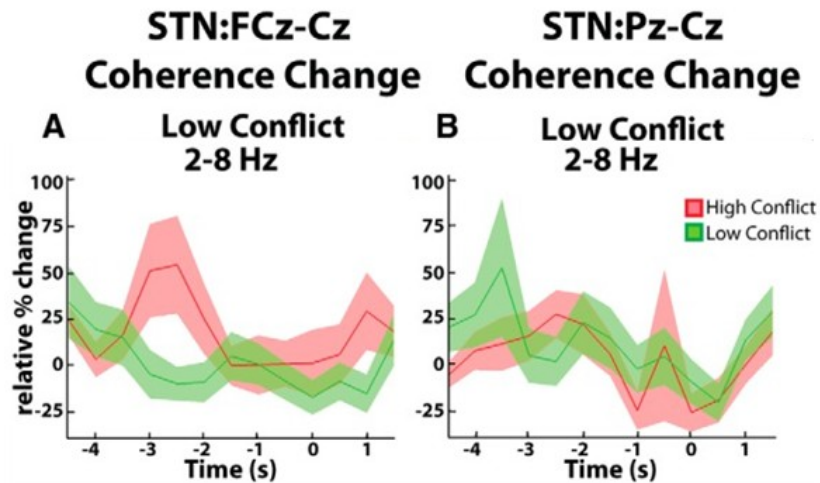


Figure 16. Group average normalized changes in EEG-STN LFP coherence. *A*, High conflict trials showed a relative increase in response locked STN-frontal (FCz-Cz) cortex coherence compared with low-conflict trials. *B*, There were no conflict-related changes in STN-parietal (Pz-Cz) cortex coupling. $T = 0$ corresponds to response onset. Shaded areas depict 95% confidence intervals. Adapted with permission from (Zavala et al., 2014)

Recently it has been described that the dorsal motor area in the STN showing the highest beta activity projected predominantly to motor and premotor cortical regions (Accolla et al., 2016). Fronto-parietal dynamics then are important for accurate motor performance (Chung et al., 2017; Cohen and Ridderinkhof, 2013). Previous studies neglected the posterior sensorimotor network that is involved in the initiation of motor programs and which supports proactive inhibitory control (Booth et al., 2005; Boulinguez et al., 2009; Jaffard et al., 2008; Lavalley et al., 2014; Menon et al., 2001). Neglect patients with right inferior parietal lobe (IPL) lesions show specific difficulties in initiating leftward movements towards visual targets on the left side of space, while this motor impairment was not found in neglect patients with frontal lesions (Mattingley et al., 1998), suggesting that the IPL operates as a sensorimotor interface (Fransson and Marrelec, 2008), rather than subserving only perceptual functions.

Together, these observations hint that a large network of cortical and subcortical regions is involved in the integration of information, the resolution of conflict and the execution of responses and that the STN likely plays an important role in response inhibition. In fact, a recent perspective by Wessel et al. (Wessel et al., 2017) is that both the cortical network, involved in proactive inhibition, as well as the cortical-basal ganglia loop, including the STN, form a global network involved in response inhibition. To this date however, it is still debated which exact functional role the STN plays during decision making under conflict, as argued above, as it has been related to various variables such as stimulus conflict, reaction times and decision thresholds (Herz et al., 2016; Williams et al., 2005; Zavala et al., 2015b).

1.4 Aim of the thesis

Electric brain potential recordings offer the possibility to investigate neural processes (Buzsáki and Draguhn, 2004) underlying behaviour and have become popular in the research on movement disorders and decision making, as it is possible to record local field potentials from electrodes implanted deeply in the brain. Several descriptors of local field potential oscillations such as beta oscillations and network connectivity measures such as M1-STN phase amplitude coupling were suggested as feedback signals for adaptive closed-loop deep brain stimulation in PD (de Hemptinne et al., 2013; Little et al., 2013; Meidahl et al., 2017).

In order to improve DBS therapy, it is imperative to understand the complex functionality of involved neural structures and networks during behaviour as well as the effect of stimulation on symptoms and behaviour. To elucidate the functional role of oscillatory activity in the STN and network activity during locomotion and cognitive control, we conducted two studies in which we collected electrophysiological recordings from patients with Parkinson's disease. In both studies, we asked whether and how oscillatory signals reflect the functionality of the underlying structures and networks and how they are related to behaviour, while also manipulating behaviour and neural structures via deep brain stimulation.

With our first study, we investigated the involvement of the STN during normal walking by analyzing STN-LFP we collected during different gait and resting scenarios in patients with PD undergoing DBS surgery. Depth recordings from the STN of PD patients have revealed LFP activity in specific frequency bands during movements like fingertapping, however, a clear characterization of the involvement of the STN during gait has been missing from the literature. We asked how the subthalamic oscillatory activity and bilateral subthalamic connectivity changes during gait as compared to rest as well as how oscillatory

activity and connectivity are modulated during the gait-cycle. As the weak amplitude of EEG/LFP signals makes them susceptible to electronic noise and artifacts, arising from e.g. recording cable movement, the analysis of oscillatory signals during human locomotion is especially complicated. Therefore, we devote part of our investigation to describing possible movement related artifacts in the signal.

With our second study, we investigated the functional relevance of the STN during decision making under conflict and its involvement in a larger network as well as the impact of DBS on decision making behaviour. As part of a fronto-striatal network (Jahanshahi and Rothwell, 2017), the STN plays a crucial role in inhibitory control. By inhibiting the pallidial-thalamic-cortical loop via inhibitory connections to the GPi, the STN is thought to suspend responses until sufficient information has been integrated. The exact function of the STN in decision making however remains debated (Bogacz and Gurney, 2007; Frank et al., 2007; Herz et al., 2017; Williams et al., 2005). To investigate this issue, we collected STN-LFP from a fully implanted sensing neurostimulator and parallel EEG recordings during a modified version of an Eriksen Flanker task inducing different levels of conflict (Van Veen and Carter, 2005) and analyzed subthalamic oscillatory activity as well as subthalamic cortical connectivity.

2. Cumulative thesis

The cumulative thesis is based on 2 publications. The abstracts of both publications and the contribution of the author to the relevant publication are listed in this part, followed by a discussion and future directions. The full articles are included in the appendix section of this thesis.

2.1 Subthalamic oscillatory activity and connectivity during gait in Parkinson's disease

Hell, F., Plate, A., Mehrkens, J., Bötzel, K. (2018). Subthalamic oscillatory activity and connectivity during gait in Parkinson's disease. *NeuroImage: Clinical*. <https://doi.org/10.1016/j.nicl.2018.05.001>

Abstract

Local field potentials (LFP) of the subthalamic nucleus (STN) recorded during walking may provide clues for determining the function of the STN during gait and also, may be used as biomarker to steer adaptive brain stimulation devices. Here, we present LFP recordings from an implanted sensing neurostimulator (Medtronic Activa PC+S) during walking and rest in 10 patients with Parkinson's disease and electrodes placed bilaterally in the STN. We also present recordings from two of these patients recorded with externalized leads. We analyzed changes in overall frequency power, bilateral connectivity, high beta frequency oscillatory characteristics and gait-cycle related oscillatory activity. We report that high beta frequency power (20-30Hz) and bilateral oscillatory connectivity are reduced during gait. Oscillatory characteristics are affected in a similar way. We describe a reduction in overall high beta burst amplitude and burst lifetimes during gait as compared to rest. Investigating gait cycle related oscillatory dynamics, we found that alpha, beta and gamma frequency power is modulated in time during gait, locked to the gait cycle. We argue that these changes are related to movement induced artifacts and that these issues have important implications for similar research.

The author contributed to this work by running the experiment, recording LFP and kinematic measurements, devising and programming the analysis, analyzing the data and writing the manuscript.

2.2 Subthalamic stimulation, oscillatory activity and connectivity reveal functional role of STN and network mechanisms during decision making under conflict

Hell, F., Taylor, P., Mehrkens, J., Bötzel, K. (2018). Subthalamic stimulation, oscillatory activity and connectivity reveal functional role of STN and network mechanisms during decision making under conflict. *NeuroImage* 171. 222–233. <https://doi.org/10.1016/j.neuroimage.2018.01.001>

Abstract

Inhibitory control is an important executive function that is necessary to suppress premature actions and to block interference from irrelevant stimuli. Current experimental studies and models highlight proactive and reactive mechanisms and claim several cortical and subcortical structures to be involved in response inhibition. However, the involved structures, network mechanisms and the behavioural relevance of the underlying neural activity remain debated. We report cortical EEG and invasive subthalamic local field potential recordings from a fully implanted sensing neurostimulator in Parkinson's patients during a stimulus- and response conflict task with and without deep brain stimulation (DBS). DBS made reaction times faster overall while leaving the effects of conflict intact: this lack of any effect on conflict may have been inherent to our task encouraging a high level of proactive inhibition. Drift diffusion modelling hints that DBS influences decision thresholds and drift rates are modulated by stimulus conflict. Both cortical EEG and subthalamic (STN) LFP oscillations reflected reaction times (RT). With these results, we provide a different interpretation of previously conflict-related oscillations in the STN and suggest that the STN implements a general task-specific decision threshold. The timecourse and topography of subthalamic-cortical oscillatory connectivity suggest the involvement of motor, frontal midline and posterior regions in a larger network with complementary functionality, oscillatory mechanisms and structures. While beta oscillations are functionally associated with motor cortical-subthalamic connectivity, low frequency oscillations reveal a subthalamic-frontal-posterior network. With our results, we suggest that proactive as well as reactive mechanisms and structures are involved in implementing a task-related dynamic inhibitory signal. We propose that motor and executive control networks with complementary oscillatory mechanisms are tonically active, react to stimuli and release inhibition at the response when uncertainty is resolved and return to their default state afterwards.

The author contributed to this work by devising the research question, designing and programming the experiment, setting up the recording and experimental equipment, running the experiment and recording EEG, LFP and behavioural data, programming the analysis, analyzing the data and writing the manuscript.

3. Discussion

To elucidate the functional role of oscillatory activity in the STN during locomotion and cognitive control, we discuss the two studies in which we collected electrophysiological recordings in patients with PD during different gait and resting scenarios and during a conflict decision making task. We conclude this discussion with an outlook on the future directions of DBS.

3.1 Subthalamic oscillatory activity during gait

Recently, several studies utilizing invasive and non-invasive EEG recordings to characterize the neurophysiology of locomotion have been published, reporting varying and contradictive results (Do et al., 2011; Fischer et al., 2018; Gwin et al., 2011; Petersen et al., 2012; Presacco et al., 2011; Quinn et al., 2015; Raethjen et al., 2008; Severens et al., 2012; Singh et al., 2013, 2011b; Storzer et al., 2017; Wagner et al., 2012; Wieser et al., 2010). Major points of interest in these studies are the characteristics of beta oscillations during gait. In contrary to most studies before, which were mostly conducted in patients right after DBS surgery within a limited range of motion and with externalized leads, we were able to investigate gait in freely moving patients with a fully implanted sensing system months after initial surgery.

3.1.2 Beta band oscillatory activity during gait

Our spectral analysis showed a significant attenuation of subthalamic high beta frequency power throughout the gait cycle in patients with PD off medication. Reports about beta power attenuation in the cortex and basal ganglia during single movements come from multiple studies (Kühn et al., 2004; Litvak et al., 2012; Tan et al., 2016). For example, Tan et al. recently described that oscillatory activity in the STN, particularly the beta (13-30 Hz) and gamma (55-90 Hz) band of the contralateral STN were most useful for decoding ipsilateral movement force during single movements. Earlier studies recording STN LFP during walking suggest a reduction in beta frequency power during walking, particularly in akinetic-rigid, but not tremor dominant and freezing patients (Quinn et al., 2015; Singh et al., 2013; Storzer et al., 2017). Contradicting these results, another study described that beta power attenuation was even stronger in patients displaying freezing of gait (Syrkin-Nikolau et al., 2017).

A few factors might influence consistency of findings in the literature. A reason for the lack of consistent reports might be that these studies are conducted in PD patients and group sizes are often very small. It is known that patients with PD show different degrees of movement impairment and are therefore a heterogeneous group. It is also known that these patients show elevated beta levels, correlating with disease severity (Hammond et al., 2007). Also, the development of bradykinesia during locomotion might be associated with a failure of beta attenuation, i.e. after initial suppression of beta, beta may re-emerge during prolonged gait. Confirming earlier reports, Steiner et al. showed that activity in the beta band was reduced during initial repetitive finger tapping, but re-occurred simultaneously with the re-emergence of bradykinesia during prolonged tapping (Kühn et al., 2006; Steiner et al., 2017).

Another reason for the inconsistency between reports might be movement related artefacts. Tan et al. report that decoding gripping force was only successful in part of the recordings in which beta suppression was visible, but not in a second cluster, in which no significant gripping movement related modulation was observed in either the beta or gamma band. The mean frequency spectrum of the second group showed increased activity at low frequencies, extending to 25 Hz and sometimes to even higher frequencies, particularly during the force onset phase. They argue that movement related artifacts are a possible cause for their observation of frequency spanning power increases at the time of movement onset, which also contaminated the beta band (Tan et al., 2016). It is conceivable that movement related artifacts during gait possibly also influence higher frequencies including beta and gamma and induce increases that obliterate physiological effects, therefore making it hard to detect such decreases.

As a second finding, we also report a reduction in bilateral high beta amplitude-amplitude correlations during gait, extending previous reports about reduction in bilateral connectivity during limb movements. It has been reported, that beta coherence between ipsilateral STN, GPi and cortical regions is attenuated by limb movement without dopaminergic medication. Studies investigating interhemispheric connectivity report that even unilateral movement results in bilateral changes in the STN, probably reflecting cortical input (Alegre et al., 2005). Niketeghad et al., report locomotion related modulation of inter-hemispheric connectivity between bilateral STN LFP signals (Niketeghad et al., 2017). With medication however, beta levels are generally attenuated and power within the STN and coherence between the STN, GPi and cortical EEG is reported to be dominated by gamma band activity (70-85 Hz), increasing with movement (Cassidy et al., 2002; Lalo et al., 2008; Little et al., 2013).

Additionally, we showed that high beta burst amplitude and width is reduced during gait. Life-times of high beta bursts are reduced while waiting-times are increased, as indicated by significantly reduced life-waiting-time ratio (LWR) during gait. Recently, it has been proposed to use pathological long beta bursts

as a feedback signal for adaptive DBS (Meidahl et al., 2017; Tinkhauser et al., 2017a). The same group described that overall beta burst amplitude and duration in the STN are reduced by dopaminergic medication, while beta bursts with a long duration are decreased and short duration low amplitude bursts are increased (Tinkhauser et al., 2017b). Our findings indicate that burst strength and duration are not only modified by medication but also are reactive to the behavioural state.

3.1.3 Modulation of oscillatory activity during gait and origin of signal

Our analysis of gait cycle related oscillatory dynamics suggests that power in alpha, beta and gamma frequencies is increased before and around the point of terminal contact of the foot contralateral to the respective STN. Although our results overlap in part with previous reports, we argue that while the reported beta power attenuation during gait is genuinely of neuronal origin, the gait cycle locked signal increases we report here, although resembling patterns in the literature (Fischer et al., 2018), are possibly driven by movement-related artifacts. Fischer et al. describe that subthalamic oscillatory activity in the beta band is attenuated after ipsilateral heel strikes during stepping in place, when raising the contralateral foot, and appears again after contralateral heel strikes, when the contralateral foot is resting on the floor (Fischer et al., 2018).

A main problem in the investigation of movement-related EEG signals are the different sources that together make up the signal. While the EEG signal recorded at different cortical and subcortical locations most likely contains information about descending commands sent from the motor cortex as well as from ascending sensory feedback, it is also possible that recordings are influenced by technical artifacts. For example those induced by body movement, which in turn causes movements of the recording cables (within surrounding electric fields), inducing electric currents in the cables. Various previous invasive studies claim that movement related artifacts are restricted to low frequencies below 10 Hz (Figure 17) (McCrimmon et al., 2017; Singh et al., 2011b; Storz et al., 2017). However, it has been previously shown that the influences of movement artifacts in electrophysiological signals on the frequency spectrum are not restricted to low frequency oscillations, but could indeed span several frequency ranges and are possibly time-locked to the gait cycle, using scalp EEG recordings (Castermans et al., 2013, 2012; Kline et al., 2015). Rhythmic movement of different body parts can cause slow swings of the electrode cables, movements of the shoulder and head region can cause sharp, spike-like artifacts in the data (Figure 18 B). Frequency spanning activity and possibly movement artifact related activity has been previously reported in single movements (Tan et al., 2016). Movement artifacts can severely alter the signal to noise ratio of the data and might not only introduce general increases in low frequencies and

harmonics (Figure 17), but also induce movement cycle locked artifacts at different frequencies (Castermans et al., 2011; Kline et al., 2015; Report et al., 2009; Singh et al., 2011b).

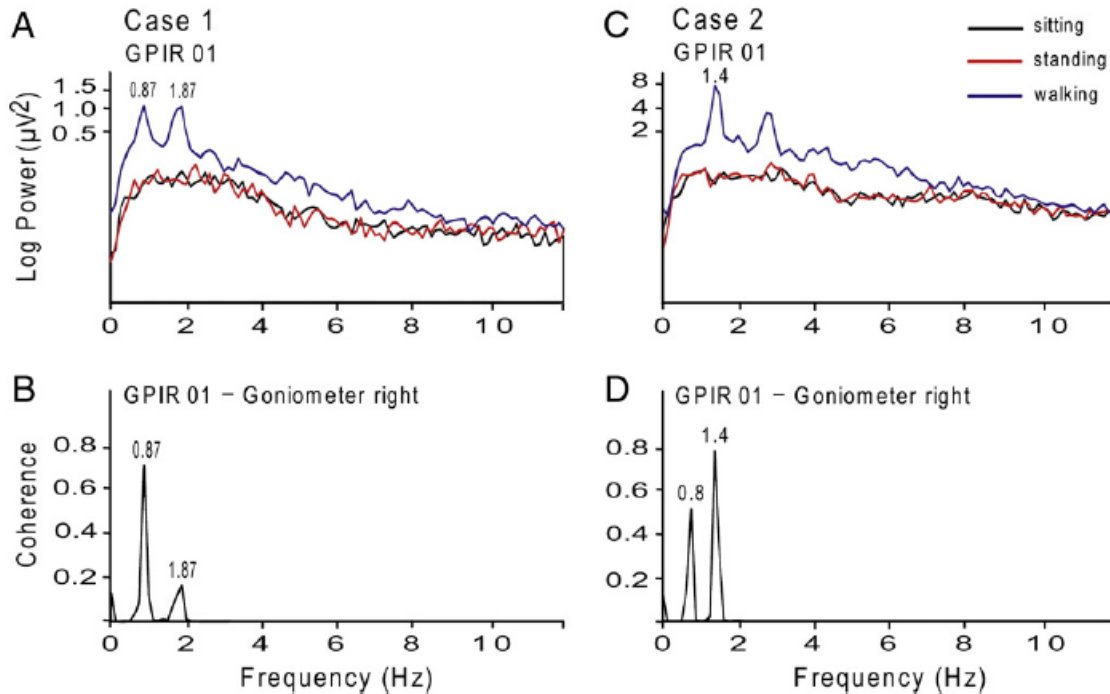


Figure 17. Spectra of LFPs and coherence with the goniometer trace exemplified in two cases. In the frequency range between 1 and 2 Hz distinct peaks in the LFP spectrum show high coherence with the goniometer trace and can thus be judged as artifacts. Increment of the LFP spectrum in lower frequency bands during gait can clearly be seen (blue traces) and shows no correlation with goniometer data. Adapted with permission from (Singh et al., 2011a)

We report that artifacts are possibly contained in recordings with externalized cables connected to implanted electrodes with considerable electrode movement possibilities as well as in recordings with internal sensing equipment (Hell et al., 2018b). We argue that the exact pattern of movement related signal alterations in time in the raw recordings due to upper body movement – which is arguably coordinated in time to the gait cycle (Romkes and Bracht-Schweizer, 2017), lead jitters, slow or sudden cable movements, influence the raw signal shape and resulting time-frequency decomposition (Hell et al., 2018b). Also, with limited cable movement possibilities in implanted sensing equipment, triboelectric effects might induce signal changes, as certain materials like electrode cables can become electrically charged after they come into frictional contact with a different material, like different parts of tissue inside the body. Depending on the exact shape of the artifacts in time, low frequency as well as frequency spanning and high frequency power can be induced (Smith, 2002).

Storzer et al. report that PD patients showing the freezing of gait phenomenon showed a movement-induced, narrowband power increase around 18Hz time-locked to the onset of gait, reflecting earlier reports by Singh et al. (Singh et al., 2013; Storzer et al., 2017). Similar to the results, Figure 18 shows gait-cycle related modulations of frequency power in a subject with freezing from the cohort used by Singh et al. (Singh et al., 2013). The pattern of movement related artifacts in time shape the raw LFP (Figure 18 B) and are arguable locked to the gait cycle (Figure 18 A). This can influence time-frequency profiles, for example in the low beta band (Figure 18 C). It is conceivable that movement related artifacts together with putative physiological effects like beta band suppression during locomotion can lead to artificial alterations of specific frequency bands – e.g. increases around 18 Hz, when comparing recordings made during gait to those made during rest (Figure 18 D). These issues might induce severe group biases, especially with small group sizes used in invasive studies.

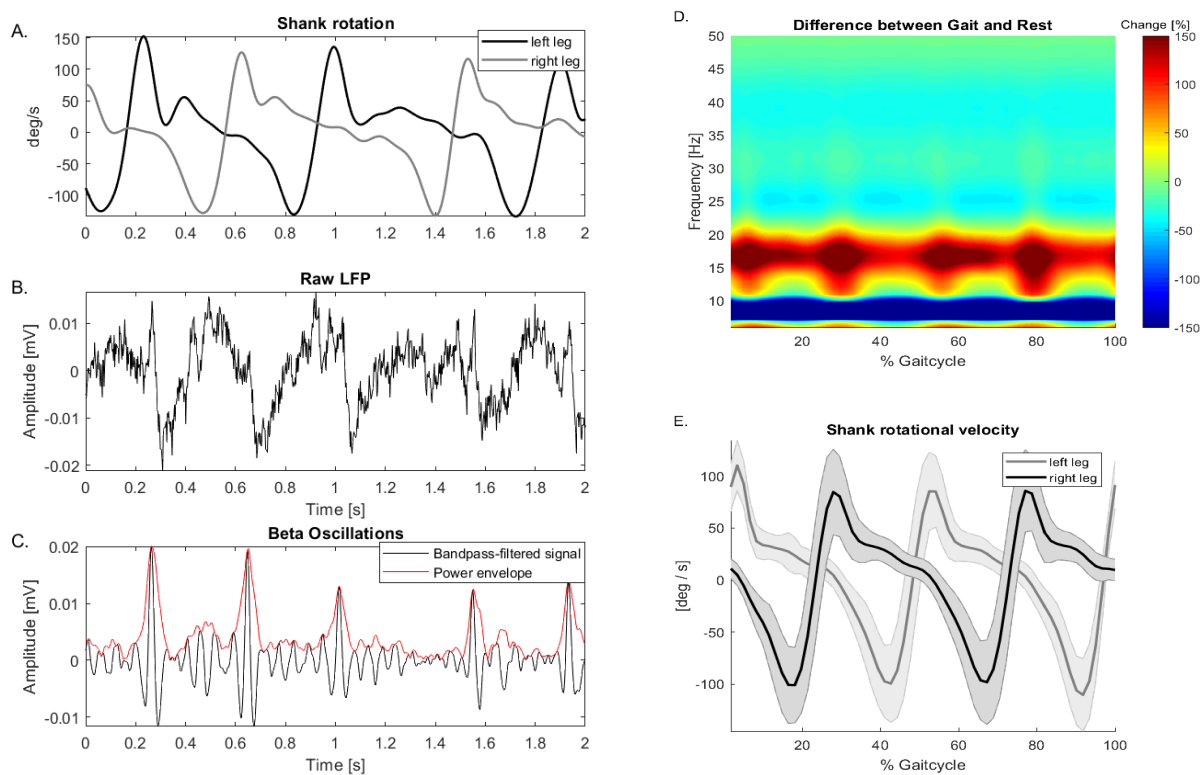


Figure 18. Shank rotation velocity, raw LFP recordings and gait cycle time-frequency power analysis and average gait-cycle related time-frequency power modulation. A, B. Angular position of a goniometer measuring knee angle of patients during walking and raw LFP trace from bilateral STN recordings with externalized leads. (B). Example externalized raw STN LFP recordings showing slow swing artifacts and high-frequency dirac-pulse like artifacts timelocked to the gait cycle and across hemispheres, inducing frequency spanning artifacts. C. Beta oscillations showing gait-cycle locked increases at the time of potential movement artifacts in the raw LFP. D. Average gait

cycle related frequency power modulation reveals timelocked and frequency spanning nature of movement related artifact (colors depict change in % from rest to gait). E. Shank rotation velocity averaged across multiple epochs, displaying the same epochs used in the time-frequency average (D). We report that internal sensing equipment is also prone to pick up similar artifacts, possibly induced by jerk-like movements or tribo-electric effects (Hell et al., 2018b). We could demonstrate that artifact induced oscillatory activity is not restricted to low frequencies, but could indeed span several frequency ranges. The above analysis shows a re-evaluation of data previously published by Singh et al. (Singh et al., 2013).

Disentangling possible physiological effects from artifacts is therefore a main challenge in the analysis of locomotion related electrophysiological signals, especially when signals resemble a modulatory pattern, that has been previously associated with physiological processes. The possibility of artifact induced activity in higher frequency bands has implications for the interpretation of previous publications and for the evaluation of future studies, which have to consider that such signal modulations could be related to movement artifacts.

3.2 The functional role of STN and network mechanisms during decision making under conflict

In this study, we found that STN DBS generally decreased reaction times but did not alter conflict related processing in our task. Drift diffusion modelling hints that the decision threshold is altered by stimulation, while drift rates are modulated by stimulus conflict. Between stimulus presentation and response, the STN low frequency activity was most strongly coherent with frontal midline electrodes (Fz/FCz), likely reflecting a tonic (not conflict-related) inhibitory signal. Oscillations in the alpha/beta range were coherent with those in motor cortical structures during that same period, consistent with tonic hyperdirect pathway connectivity (Accolla et al., 2016). Behaviourally relevant induced low frequency STN-cortical coherence changes between target and response included not only frontal but also parietal and occipital areas, possibly reflecting a reactive mechanism. Alpha/beta oscillations were reduced in amplitude and decorrelated globally, consistent with functionally relevant motor processing. It is difficult to determine the exact functionality of the STN and the importance of the respective oscillatory mechanisms and to entangle conflict from reaction times, as trials with higher conflict generally show slower reaction times (Cohen and Nigbur, 2013; Nachev et al., 2007; Scherbaum and Dshemuchadse, 2013; Yeung et al., 2011). While many studies interpret STN activity as related to conflict processing (Zavala et al., 2015a), a study by Williams et al. (Williams et al., 2005) did show a significant

relationship between oscillatory activity in the beta band and reaction times in the parkinsonian STN after “Go” cues. Indeed, Zavala and colleagues found no power differences between the fast-incongruent trials and congruent trials with similar reaction times (Figure 16) (Zavala et al., 2013).

Our results extend previous findings concerning the roles of subcortical and cortical low frequency and alpha/beta oscillations and their functional importance during responding under conflict (Cavanagh et al., 2011; Herz et al., 2017; Zavala et al., 2013) and provide new insights on the putative mechanisms involved in inhibitory control. Our findings suggest that the STN does not implement a stimulus-conflict related inhibitory signal but rather a dynamic decision threshold. We suggest that subthalamic activity as well as subthalamic-cortical oscillatory connectivity reflect an inhibitory control and motor network with different oscillatory mechanisms and propose that proactive as well as reactive mechanisms and putative neural structures are involved in implementing a dynamic executive control signal. Functionally relevant and coherent low frequency oscillations could reflect the communication within an executive control network with subcortical, frontal and posterior nodes and alpha/beta oscillations might reflect the coordination of a motor network with subcortical and motor cortical structures. These networks may be tonically and coherently active, are reactive to stimulus presentation, functionally linked to response preparation and execution and return to their default and possibly proactive state afterwards.

3.3 Future directions for DBS

DBS has been used successfully in movement disorders for over 25 years; however, the standard stimulation schemes have not changed substantially. So far, surgical planning is commonly done based on basic structural MR images and programming of stimulation parameters is still dependent on trial and error. For the further development of DBS, two major points of interest are target-structures and novel adaptive stimulation algorithms integrating feedback signals. In this regard, we could show that the most discussed feedback signals, namely beta frequency oscillations, do not only correlate with disease symptoms and medication (Kühn et al., 2008; Williams et al., 2005), but are also functionally relevant during cognition and movement. It will be imperative to further understand the functional importance of different target areas as well as their structural connectivity and involvement in the genesis of clinical symptoms to further improve DBS therapy and targeting.

3.3.1 Improving targeting approaches for DBS surgery

There are currently a handful of FDA approved targets, including the internal segment of the globus pallidus, nucleus ventralis intermedius (ViM), subthalamic nucleus as well as several other investigational targets used for DBS in movement and other neurological disorders, often more than one for a specific symptom (Johnson et al., 2008).

Contemporary research in humans highlights different network structures connected to individual DBS targets and explores structural networks (Accolla et al., 2016) involved in the generation of disease symptoms. New programming approaches such as current steering (Timmermann et al., 2015) are able to manipulate the volume of tissue activated (VTA) (Butson et al., 2007) and therefore a more precise stimulation of neural structures. New software now allows for a patient-specific reconstruction of DBS leads based on MRI and postoperative CT imaging, the reconstruction of nuclei and fibre tracts adjacent to stimulation sites and the mapping of intra- and perioperative electrophysiological recordings (Duchin et al., 2018; Horn and Kühn, 2015). Improving the targeting of specific (sub)-structures and fibres involved in the generation of pathological neural activity and avoiding others will be crucial for improving the clinical DBS effect and limiting side-effects.

While some studies suggest that PD patients show similar improvement in motor function after pallidal as well as subthalamic stimulation (Follett et al., 2010), others state that STN DBS is superior in improving off-drug phase motor symptoms (Odekerken et al., 2016). Therefore, the STN is often the favoured target to treat Parkinsonian symptoms such as bradykinesia, tremor and rigidity. Accolla et al. used STN LFP recordings from PD patients to investigate the relation between oscillatory activity and subthalamic fibre connectivity. The dorso-lateral portion of the STN, which shows the highest beta power in the STN, predominantly projected to motor, premotor, but also to limbic and associative areas. Ventral areas are associated with connectivity to medial temporal regions, like amygdala and hippocampus (Accolla et al., 2016). Various research groups (Caire et al., 2011; Coenen et al., 2008; Horn et al., 2017; Vertinsky et al., 2009; Welter et al., 2014) suggest that the posterior lateral subthalamic area next to the nucleus ruber might be a sweet spot to guide DBS electrode placement.

There is an ongoing debate about the real parcellation of the STN, its connectivity and functional relevance of different subsystems (Lambert et al., 2015). The STN is reported to be grouped into a posterolateral motor and a gradually overlapping central associative area, while the limbic area is reported in the anteromedial part of the nucleus (Jahanshahi et al., 2015b; Lambert et al., 2012; Plantinga et al., 2016). Several groups report that DBS of the medial and limbic STN can result in the stimulation of the medial forebrain bundle and can induce side effects like hypomania (Coenen et al.,

2009; Welter et al., 2014). Similar can be said, to a degree, for every major DBS target (Cheung et al., 2014; Follett and Torres-Russotto, 2012).

Advancements in structural imaging methods such as ultra-high field MRI and novel data analysis algorithms, inspired by machine learning approaches such as deep learning (Amoroso et al., 2017; Horn and Kühn, 2015; Milletari et al., 2016; Shen et al., 2017; Stephan et al., 2017) will ultimately refine our understanding and conception of different neural structures and their wiring in health and disease and could provide a novel way to find and elaborate target structures, individualizing DBS surgery. The study of network dynamics (Grosse-Wentrup et al., 2016; Weichwald et al., 2015) in humans and animal models during behaviour and their relation to the pathophysiology of the disorder as well as the manipulation of neural circuits with methods such as electric or optogenetic stimulation will provide further insights into the neural mechanisms, potential target structures and effects of DBS.

3.3.2 Novel stimulation approaches in DBS

DBS systems available today provide stimulation in an open-loop manner, which means that stimulation settings are pre-programmed and do not automatically respond to changes in the patient's clinical symptoms or in the underlying physiological activity. Although open-loop stimulation paradigms remain state of the art, limitations like overall efficiency, reduction of efficiency over time or side-effects have become more evident as clinical experience grows. DBS therapy adjustment also remains time-consuming, requiring physicians to evaluate countless combinations of stimulation parameters to achieve the optimal outcome. DBS practice currently requires patients to follow-up for months postoperatively to optimize the clinical effect of DBS. Ideally, patient and disease specific biomarkers could help optimize and individualize therapy and help finding the optimal parameters for stimulation.

Looking forward, feedback signals will ideally be integrated into adaptive closed-loop stimulation systems that rapidly respond to real-time patient needs and obviate the need for human programming. Local field potentials and network connectivity measures based on electrophysiological signals with their high temporal resolution can easily be measured with DBS electrodes or other implanted neural sensors and hold great promise as such biomarkers. New miniature implants (Seo et al., 2016) with names like Neural dust (Neely et al., 2018), Neurograins or Neural lace will push the boundary of signal collection even further and ultimately promise to provide read and stimulation capabilities with a far greater spatial and temporal detail than available at present. There now are several companies actively pursuing brain computer interface technology by developing new neural implants, ranging from traditional medical device producer like Medtronic, St. Jude Medical or Boston Scientific to tech start-ups like

Neuralink, Kernel or Cortera, which in part work in close cooperation with several research institutes and are driven by funding from the DARPA program. Efforts to create a brain-computer interface are not limited to invasive approaches. Alternative stimulation techniques like deep brain stimulation via temporally interfering electric fields (Grossman et al., 2017) promise new non-invasive ways to manipulate the brain, even in deep structures. Facebook is currently pioneering an approach to read brain signals via optical imaging and aims to sample neural activity at a greater spatial and temporal resolution as compared to current optical approaches like functional near-infrared spectroscopy, which is only able to measure a blood oxygen level dependent signal, and therefore is limited in its temporal resolution.

Initial approaches incorporating LFP as feedback signals into adaptive DBS using beta frequency amplitude as a mechanism to trigger stimulation (Little et al., 2013) could show clinical improvement of symptoms compared to standard DBS (Figure 19 B). Several oscillatory patterns in different structures like aberrant subcortical tremor and beta-frequency activity (Kühn et al., 2006; Steiner et al., 2017; Tinkhauser et al., 2017b; Wang et al., 2006), pathological cross-frequency coupling (de Hemptinne et al., 2015; van Wijk et al., 2016) or pathological coherence of neural activity between cortical and subcortical structures (Cole et al., 2016) have been reported to be correlated with clinical symptoms and are discussed as potential feedback signals, among others. A new approach by Meidahl et al. targets potentially pathological beta bursts with long duration (Figure 19 C) sparing presumably functionally relevant short beta bursts (Meidahl et al., 2017; Tinkhauser et al., 2017a).

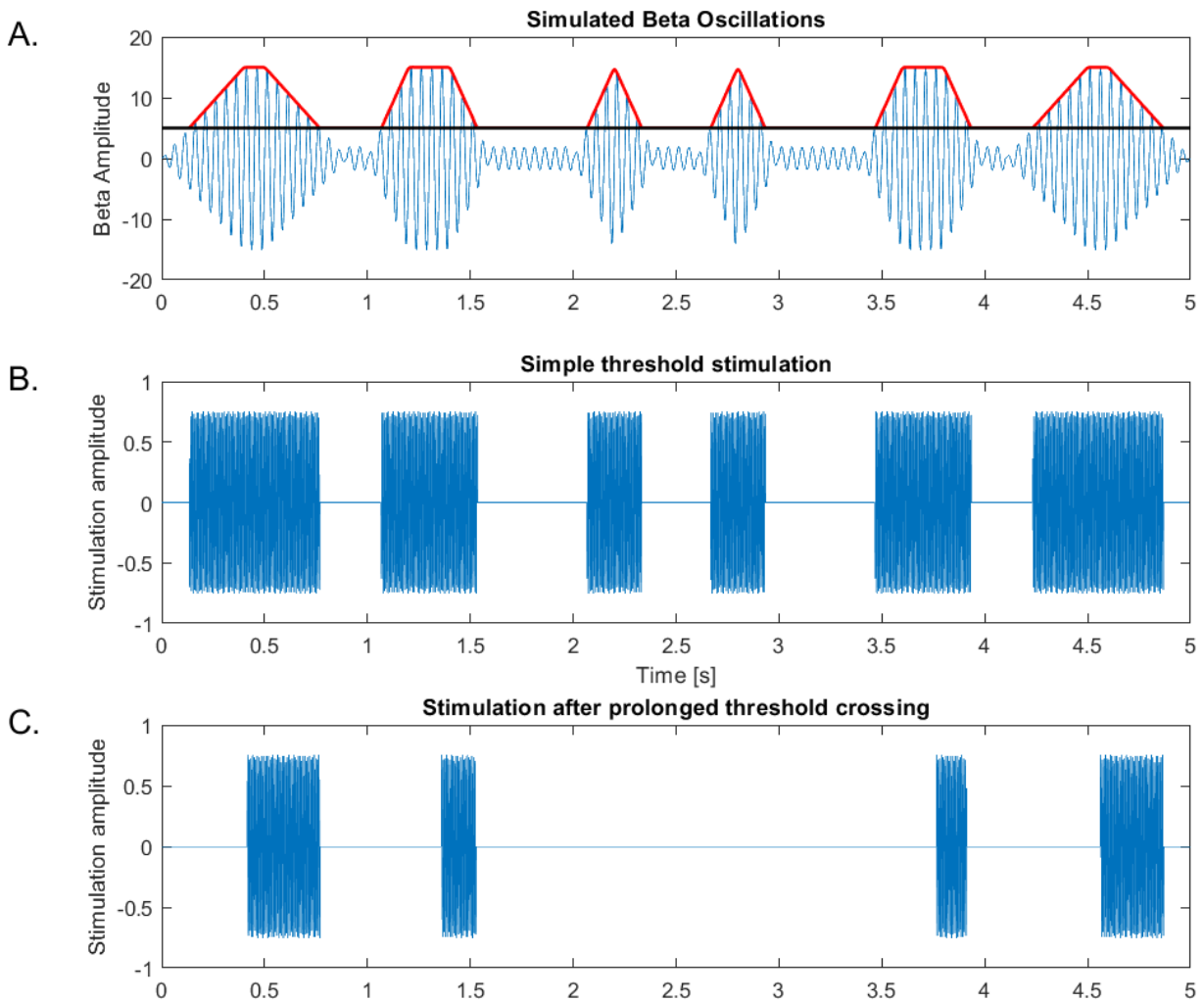


Figure 19. Schematic depiction of adaptive DBS stimulation paradigms based on beta frequency activity. A. Simulated beta frequency oscillations (blue) and amplitude envelope (red) with bursts of different duration and an arbitrary threshold (black). B. Adaptive stimulation pattern for threshold triggered stimulation. C. The stimulation pattern when targeting only long beta bursts. Adapted with permission from (Hell et al., 2018a).

Despite early success, challenges have yet to be overcome. Beta power in the STN for example correlates with rigidity and bradykinesia, but not with tremor (Lenka et al., 2016; Little and Brown, 2012), which is linked to low frequency activity at tremor frequency. As PD patients for example often show multiple symptoms, a single one-dimensional biomarker might therefore be only partly useful. Most neural biomarkers like beta frequency oscillations are not only correlated with disease symptoms, but are also reactive to medication (Kühn et al., 2008; Williams et al., 2005), are functionally relevant and modulated during normal behaviour like movement or cognition (Foffani et al., 2005; Herz et al., 2016). Although

biomarkers like beta activity seem to be stable months after DBS surgery (Staub et al., 2016), it is also conceivable that they evolve with disease progression.

Body measurements using electromyography or kinematic sensors allowing for the assessment of behaviour and symptom severity could be a promising alternative or additional feedback signal for use in adaptive DBS. Kinematic parameters for example can be computed from signals collected by inertial sensor units and then be used to quantify clinical symptoms like tremor, rigidity or bradykinesia (Cagnan et al., 2013; Hell et al., 2018b; Niazmand et al., 2011; Singh et al., 2012). Cagnan and colleagues stimulated patients with essential tremor and thalamic electrodes, while recording tremor amplitude and phase with inertial sensor units. They report that the amplitude of the tremor was modulated depending on the phase relative to the tremor cycle, at which stimulation pulses were delivered. While stimuli in one half of the tremor cycle lead to a reduction of tremor amplitude, those in the opposite half of the tremor cycle similarly increased tremor amplitude. Tremor suppression reached 27% at optimal phase alignment (Cagnan et al., 2013).

As a future direction, parameters derived from different signal sources could be used in parallel to establish a feedback driven stimulation algorithm based on the analysis of behavioural and physiological data and a suitable control mechanism. By integrating features derived from electrophysiological recordings, kinematic measurements and other sensor like electromyography, the state of the patient and the severity of disease symptoms and related neural activity might be ultimately learned and classified end to end (Schirrmester et al., 2017), using machine learning algorithms. To establish a real-time link between behavioural and neural measurements, however, a data analysis model has to be able to extract features from all sources and reliably decode clinical symptom severity as well as find predictors for changes in behaviour in physiological measurements in real time. Large scale datasets with both behavioural and neural measurements could provide the means to establish and validate such models and could ultimately help establishing adaptive DBS paradigms.

When thinking about closed loop adaptive DBS, however, a distinction has to be made between biomarkers or feedback signals and mechanisms of control. A biomarker can only describe a correlative/predictive or causal relation to a clinical symptom. Adaptive control mechanisms then outline how to adjust stimulation based on the evolution of biomarkers. The most basic mechanism is threshold targeting, as briefly discussed above: when the amplitude of a biomarker, for example β -band oscillations, exceeds a defined threshold for a specific time period, stimulation is turned on, while it is idle the rest of the time (Little et al., 2013; Meidahl et al., 2017). As discussed above, one problem of this approach is that beta oscillatory characteristics are not only related to symptom severity, but also to medication and behaviour. Stimulation on demand has been introduced by Herron et al. who used

cortical electrodes to sense β -band desynchronization in essential tremor patients when a movement started, which then triggered the stimulation, while stimulation was switched off otherwise (Herron et al., 2017; Malekmohammadi et al., 2016). A way to improve this approach would be if one is able to predict movement before it occurs, as tremor at the beginning of a movement could not be prevented. Another possible control mechanism was introduced by Cagnan et al., who suggest a method akin to noise cancelling used in headphones. As described above, they detect the patient's tremor with an accelerometer attached to the affected hand and switch on the thalamus stimulation in specific phases of the essential tremor (Cagnan et al., 2013). In PD patients with tremor, the principle of noise cancellation has also already been used to target cortical oscillations within the tremor network with non-invasive transcranial alternating current stimulation, which has been shown to reduce the amplitude of resting tremor by 50% (Brittain et al., 2013). Phase targeting might potentially achieve tremor control with far greater specificity and less power demand than current stimulation approaches. However, the effects achieved up to date are less than generally achieved with continuous high-frequency deep brain stimulation. Yet another alternative stimulation protocol is the temporal stimulation pattern termed coordinated reset stimulation, which exploits plasticity mechanisms in the brain (Wang et al., 2016; Zeitler and Tass, 2015). In coordinated reset stimulation, brief high-frequency pulse trains are delivered through different stimulation contacts of the DBS lead at random times to introduce desynchronization of neural activity and reset abnormal synchronization (Ebert et al., 2014). It has been shown that coordinated reset stimulation is able to decrease abnormal synchronous oscillations in basal ganglia structures such as the GPe and STN, improving rigidity and bradykinesia (Adamchic et al., 2014). Appropriate randomized controlled trial studies investigating coordinated reset stimulation in a larger cohort are needed and could ultimately confirm the encouraging preliminary results shown in this study. Given physiological and behavioural features that describe the neural and clinical state of the patient can be reliably decoded and ideally predicted from measurements, reinforcement learning could be another option to learn and control stimulation paradigms and optimize the clinical state (Figure 20 depicts a schematic for a general adaptive DBS system based on feature and reinforcement learning). In reinforcement learning, an agent, in this case the DBS stimulation controller interacts with an uncertain environment, namely stimulating the brain of a patient at a specific time with specific parameters, with the goal to maximize a numerical long-term reward, in this case the (long term) clinical state of the patient. Through the learned policy the controller ideally knows the right stimulation action in every state (Sutton and Barto, 1998).

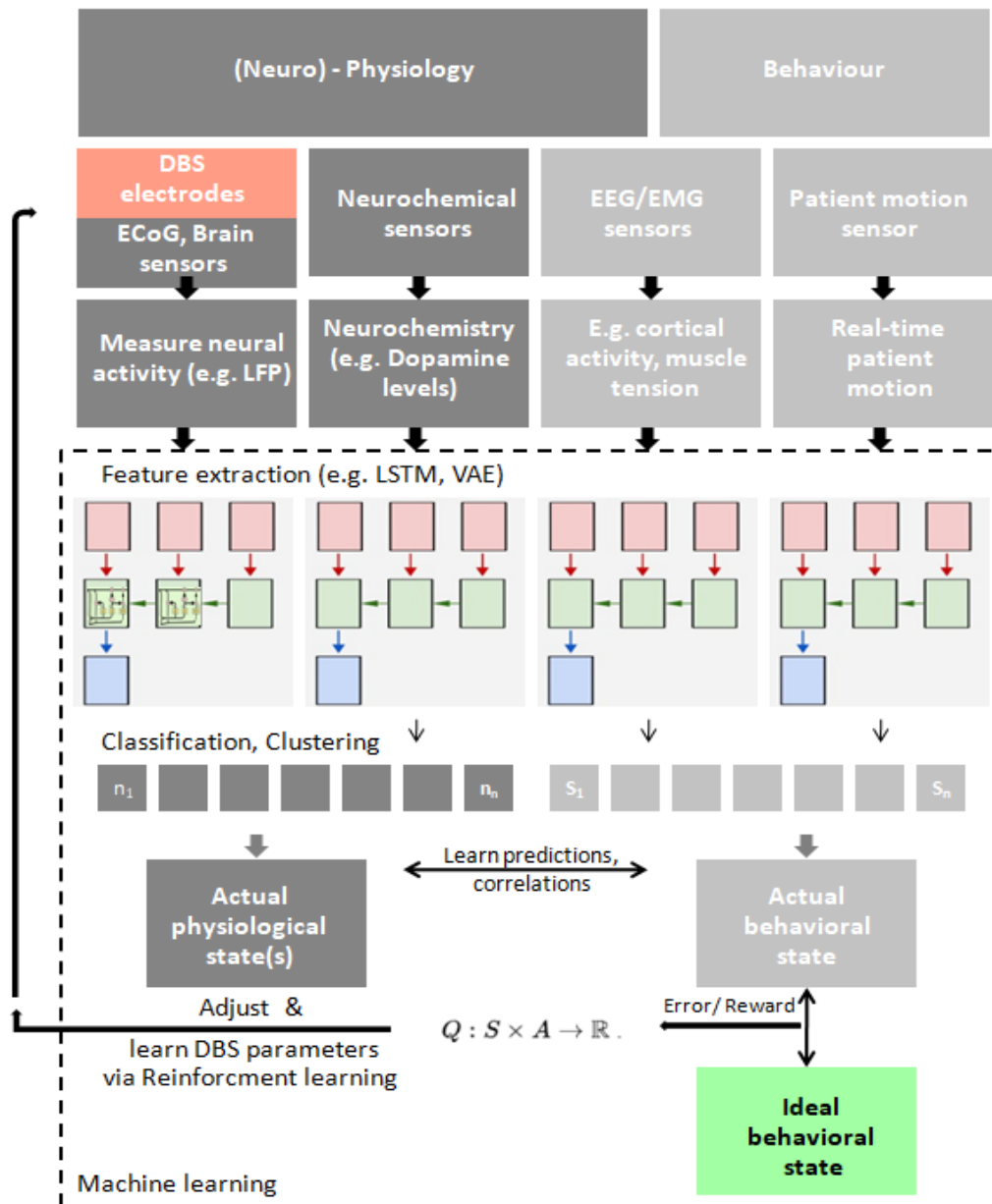


Figure 20. Schematic of general adaptive closed loop DBS for adaptive adjustment of deep brain stimulation (DBS) parameters based upon real time patient measurements, such as electrophysiological signals (LFP, M/EEG, EMG), neurochemical parameters and behavioural measurements and machine learning. First, features from different possible signal sources are learned (e.g. beta frequency amplitude) using deep learning approaches to classify between different behavioural (clinical) states (e.g. bradykinesia) and corresponding neural states. Then, actual states are compared with ideal states and stimulation parameters are adjusted and finally learned via reinforcement learning. In this closed-loop paradigm, the stimulation parameters are adjusted within clinical limits based upon the difference between actual neural/behavioural and desired neural/behavioural state.

A simple version of this idea could be realised in patients with tremor dominant PD. The amplitude of the tremor can be measured with kinematic sensors and then be used to describe the clinical state of the patient, possibly also providing labels for supervised learning of neural parameters that are associated with and predictive of each state. It is conceivable that deep neural nets then learn to extract features from neural recordings such as aberrant tremor or beta frequency activity and relate them to kinematic parameters describing tremor, bradykinesia or rigidity, augmenting the control signal for adaptive DBS. Such a signal could then also serve as a reward signal for reinforcement learning, with the reward simply being the difference between optimal clinical state (no tremor amplitude) and actual clinical state (actual tremor amplitude). With such an approach, the optimal stimulation action could ultimately be learned and adjusted based on feedback signals, when needed, closing the loop. Alternative stimulation protocols and parameters like stimulation amplitude, frequency or pulse width, temporal stimulation patterns like coordinated reset, timing of stimulation relative to neural and behavioural activity and stimulated contacts could be tested within clinical limits.

However, the vast number of free parameters in DBS programming introduces a potentially very large search space to evaluate during reinforcement learning. Algorithms for reinforcement learning are commonly either model-free or model-based. While in model-free learning, the agent simply relies on trial-and-error experience to learn a policy that optimizes immediate and future reward, in model-based learning, the agent exploits previously learned lessons (Huys et al., 2014). Although model-free deep reinforcement learning algorithms are suited for learning a wide range of applications, they often require millions of training iterations to achieve good performance (Schulman et al., 2017, 2015), rendering this approach inappropriate for adaptive DBS trials in humans. In model-based reinforcement learning, experience is used to construct a model of the world, describing the transitions between states and associated outcomes, while suitable actions are chosen by searching or planning in this world model (Dayan and Niv, 2008). Using transfer learning could then help to personalize such a model, which has been used before in personalized brain computer interfaces for motor rehabilitation (Jayaram et al., 2016; Mastakouri et al., 2017). To learn such models in the first place, however, a large number of training trials would also likely be required. Possibly animal models could help pioneering such an approach (Temel, 2013).

Ultimately, only interventional studies can prove causal relationships and in this case the effects of adaptive deep brain stimulation on the clinical and overall state of the patient. However, applying countless experimental perturbations, which are necessary to gather enough observational data to learn from, can be costly and time consuming, even when done in animal models. Inferring the causal structure of brain networks from neuroimaging data is an important goal in neuroscience (Grosse-

Wentrup et al., 2016; Smith et al., 2011) and various methods such as Granger causality (Granger, 1969; Gregoriou et al., 2009), dynamic causal modelling (Friston et al., 2003; Daunizeau et al., 2011), structural equation modelling (Atlas et al., 2010; McIntosh and Gonzalez-Lima, 1994) and causal Bayesian networks (Grosse-Wentrup et al., 2011; Weichwald et al., 2015) have been developed to infer causal relations from brain imaging data. Recently, van Wijk et al. applied dynamic causal modelling to explore the cortical-basal ganglia-thalamus loop in patients with PD and to study pathways that contribute to the suppression of beta oscillations induced by dopaminergic medication (van Wijk et al., 2018). Also recently, Bogacz et al. described a coupled oscillator model to predict the effects of deep brain stimulation (Weerasinghe et al., 2018). Ideally, causal inference methods based on i.e. causal Bayesian networks could also help give testable predictions on the effects of external manipulations (Pearl, 2011), such as the effects of deep brain stimulation. In this way, different adaptive approaches could be explored or learned in silico and the number of interventional studies, that are required to establish an approach, could be reduced substantially (Maathuis et al., 2010).

4. References

- Accolla, E.A., Herrojo Ruiz, M., Horn, A., Schneider, G.-H., Schmitz-Hübsch, T., Draganski, B., Kühn, A.A., 2016. Brain networks modulated by subthalamic nucleus deep brain stimulation. *Brain* 139, 2503–2515. doi:10.1093/brain/aww182
- Adamchic, I., Hauptmann, C., Barnikol, U.B., Pawelczyk, N., Popovych, O., Barnikol, T.T., Silchenko, A., Volkmann, J., Deuschl, G., Meissner, W.G., Maarouf, M., Sturm, V., Freund, H.J., Tass, P.A., 2014. Coordinated reset neuromodulation for Parkinson's disease: Proof-of-concept study. *Mov. Disord.* 29, 1679–1684. doi:10.1002/mds.25923
- Albin, R.L., Young, A.B., Penney, J.B., 1989. The functional anatomy of basal ganglia disorders. *Trends Neurosci.* 12, 366–375. doi:10.1016/0166-2236(89)90074-X
- Alegre, M., Alonso-Frech, F., Rodríguez-Oroz, M.C., Guridi, J., Zamarbide, I., Valencia, M., Manrique, M., Obeso, J.A., Artieda, J., 2005. Movement-related changes in oscillatory activity in the human subthalamic nucleus: Ipsilateral vs. contralateral movements. *Eur. J. Neurosci.* 22, 2315–2324. doi:10.1111/j.1460-9568.2005.04409.x
- Alegre, M., Lopez-Azcarate, J., Obeso, I., Wilkinson, L., Rodriguez-Oroz, M.C., Valencia, M., Garcia-Garcia, D., Guridi, J., Artieda, J., Jahanshahi, M., Obeso, J.A., 2013. The subthalamic nucleus is involved in successful inhibition in the stop-signal task: A local field potential study in Parkinson's disease. *Exp. Neurol.* 239, 1–12. doi:10.1016/j.expneurol.2012.08.027
- Alexander, G.E., DeLong, M.R., Strick, P.L., 1986. Parallel Organization of Functionally Segregated Circuits Linking Basal Ganglia and Cortex. *Annu. Rev. Neurosci.* 9, 357–381. doi:10.1146/annurev.ne.09.030186.002041
- Amami, P., Dekker, I., Piacentini, S., Ferré, F., Romito, L.M., Franzini, A., Foncke, E.M.J., Albanese, A., 2015. Impulse control behaviours in patients with Parkinson's disease after subthalamic deep brain stimulation: de novo cases and 3-year follow-up. *J. Neurol. Neurosurg. Psychiatry* 86, 562–564. doi:10.1136/jnnp-2013-307214
- Amoroso, N., La Rocca, M., Bruno, S., Maggipinto, T., Monaco, A., Bellotti, R., Tangaro, S., 2017. Brain structural connectivity atrophy in Alzheimer's disease. arXiv:1709.02369v2 [physics.med-ph] 1–16.
- Androulidakis, A.G., Brücke, C., Kempf, F., Kupsch, A., Aziz, T., Ashkan, K., Kühn, A.A., Brown, P., 2008. Amplitude modulation of oscillatory activity in the subthalamic nucleus during movement. *Eur. J. Neurosci.* 27, 1277–1284. doi:10.1111/j.1460-9568.2008.06085.x
- Antonelli, F., Ray, N., Strafella, A.P., 2011. Impulsivity and Parkinson's disease: More than just disinhibition. *J. Neurol. Sci.* 310, 202–207. doi:10.1016/j.jns.2011.06.006

- Aron, A.R., Behrens, T.E., Smith, S., Frank, M.J., Poldrack, R.A., 2007. Triangulating a Cognitive Control Network Using Diffusion-Weighted Magnetic Resonance Imaging (MRI) and Functional MRI. *J. Neurosci.* 27, 3743–3752. doi:10.1523/JNEUROSCI.0519-07.2007
- Ashkan, K., Rogers, P., Bergman, H., Ughratdar, I., 2017. Insights into the mechanisms of deep brain stimulation. *Nat. Rev. Neurol.* doi:10.1038/nrneurol.2017.105
- Atlas, L.Y., Bolger, N., Lindquist, M.A., Wager, T.D., 2010. Brain Mediators of Predictive Cue Effects on Perceived Pain. *J. Neurosci.* 30, 12964–12977. doi:10.1523/JNEUROSCI.0057-10.2010
- Ballanger, B., van Eimeren, T., Moro, E., Lozano, A.M., Hamani, C., Boulinguez, P., Pellecchia, G., Houle, S., Poon, Y.Y., Lang, A.E., Strafella, A.P., 2009. Stimulation of the subthalamic nucleus and impulsivity: release your horses. *Ann. Neurol.* 66, 817–24. doi:10.1002/ana.21795
- Barnikol, U.B., Popovych, O. V, Hauptmann, C., Sturm, V., Freund, H.-J., Tass, P.A., 2008. Tremor entrainment by patterned low-frequency stimulation. *Philos. Trans. R. Soc. A Math. Phys. Eng. Sci.* 366, 3545–3573. doi:10.1098/rsta.2008.0104
- Bastin, J., Polosan, M., Benis, D., Goetz, L., Bhattacharjee, M., Piallat, B., Krainik, A., Bougerol, T., Chabardès, S., David, O., 2014. Inhibitory control and error monitoring by human subthalamic neurons. *Transl. Psychiatry* 4, e439. doi:10.1038/tp.2014.73
- Beck, M.H., Haumesser, J.K., Kühn, J., Altschüler, J., Kühn, A.A., van Riesen, C., 2016. Short- and long-term dopamine depletion causes enhanced beta oscillations in the cortico-basal ganglia loop of parkinsonian rats. *Exp. Neurol.* 286, 124–136. doi:10.1016/j.expneurol.2016.10.005
- Beloozerova, I.N., Farrell, B.J., Sirota, M.G., Prilutsky, B.I., 2010. Differences in Movement Mechanics, Electromyographic, and Motor Cortex Activity Between Accurate and Nonaccurate Stepping. *J. Neurophysiol.* 103, 2285–2300. doi:10.1152/jn.00360.2009
- Benabid, A.L., Chabardès, S., Mitrofanis, J., Pollak, P., 2009. Deep brain stimulation of the subthalamic nucleus for the treatment of Parkinson's disease. *Lancet Neurol.* doi:10.1016/S1474-4422(08)70291-6
- Benabid, A.L., Pollak, P., Hoffmann, D., Gervason, C., Hommel, M., Perret, J.E., de Rougemont, J., Gao, D.M., 1991. Long-term suppression of tremor by chronic stimulation of the ventral intermediate thalamic nucleus. *Lancet* 337, 403–406. doi:10.1016/0140-6736(91)91175-T
- Benecke, R., Rothwell, J.C., Dick, J.P., Day, B.L., Marsden, C.D., 1987a. Simple and complex movements off and on treatment in patients with Parkinson's disease. *J. Neurol. Neurosurg. Psychiatry* 50, 296–303.
- Benecke, R., Rothwell, J.C., Dick, J.P., Day, B.L., Marsden, C.D., 1987b. Disturbance of sequential movements in patients with Parkinson's disease. *Brain* 110 (Pt 2, 361–379.

- Benis, D., David, O., Lachaux, J.-P., Seigneuret, E., Krack, P., Fraix, V., Chabardès, S., Bastin, J., 2014. Subthalamic nucleus activity dissociates proactive and reactive inhibition in patients with Parkinson's disease. *Neuroimage* 91, 273–281. doi:10.1016/j.neuroimage.2013.10.070
- Bogacz, R., Gurney, K., 2007. The basal ganglia and cortex implement optimal decision making between alternative actions. *Neural Comput.* 19, 442–477. doi:10.1162/neco.2007.19.2.442
- Bohnen, N.I., Frey, K.A., Studenski, S., Kotagal, V., Koeppe, R.A., Scott, P.J.H., Albin, R.L., Müller, M.L.T.M., 2013. Gait speed in Parkinson disease correlates with cholinergic degeneration. *Neurology* 81, 1611–1616. doi:10.1212/WNL.0b013e3182a9f558
- Booth, J.R., Burman, D.D., Meyer, J.R., Lei, Z., Trommer, B.L., Davenport, N.D., Li, W., Parrish, T.B., Gitelman, D.R., Marsel Mesulam, M., 2005. Larger deficits in brain networks for response inhibition than for visual selective attention in attention deficit hyperactivity disorder (ADHD). *J. Child Psychol. Psychiatry* 46, 94–111. doi:10.1111/j.1469-7610.2004.00337.x
- Botvinick, M.M., Cohen, J.D., Carter, C.S., 2004. Conflict monitoring and anterior cingulate cortex: An update. *Trends Cogn. Sci.* 8, 539–546. doi:10.1016/j.tics.2004.10.003
- Bötzel, K., Marti, F.M., Rodríguez, M.Á.C., Plate, A., Vicente, A.O., 2016. Gait recording with inertial sensors – How to determine initial and terminal contact. *J. Biomech.* 49, 332–337. doi:10.1016/j.jbiomech.2015.12.035
- Boulinguez, P., Ballanger, B., Granjon, L., Benraiss, A., 2009. The paradoxical effect of warning on reaction time: Demonstrating proactive response inhibition with event-related potentials. *Clin. Neurophysiol.* 120, 730–737. doi:10.1016/j.clinph.2009.02.167
- Braak, H., Ghebremedhin, E., Rüb, U., Bratzke, H., Del Tredici, K., 2004. Stages in the development of Parkinson's disease-related pathology. *Cell Tissue Res.* doi:10.1007/s00441-004-0956-9
- Brittain, J.-S., Watkins, K.E., Joundi, R.A., Ray, N.J., Holland, P., Green, A.L., Aziz, T.Z., Jenkinson, N., 2012. A Role for the Subthalamic Nucleus in Response Inhibition during Conflict. *J. Neurosci.* 32.
- Brittain, J.S., Probert-Smith, P., Aziz, T.Z., Brown, P., 2013. Tremor suppression by rhythmic transcranial current stimulation. *Curr. Biol.* 23, 436–440. doi:10.1016/j.cub.2013.01.068
- Brown, T.G., 1912. The Factors in Rhythmic Activity of the Nervous System. *R. Soc. Publ.* 85, 278–289. doi:Doi 10.1098/Rspb.1912.0051
- Butson, C.R., Cooper, S.E., Henderson, J.M., McIntyre, C.C., 2007. Patient-specific analysis of the volume of tissue activated during deep brain stimulation. *Neuroimage* 34, 661–70. doi:10.1016/j.neuroimage.2006.09.034
- Buzsáki, G., Draguhn, A., 2004. Neuronal oscillations in cortical networks. *Science* 304, 1926–9. doi:10.1126/science.1099745

- Cagnan, H., Brittain, J.-S., Little, S., Foltynie, T., Limousin, P., Zrinzo, L., Hariz, M., Joint, C., Fitzgerald, J., Green, A.L., Aziz, T., Brown, P., 2013. Phase dependent modulation of tremor amplitude in essential tremor through thalamic stimulation. *Brain* 136, 3062–3075. doi:10.1093/brain/awt239
- Caire, F., Maubon, A., Moreau, J.J., Cuny, E., 2011. The mamillothalamic tract is a good landmark for the anterior border of the subthalamic nucleus on axial MR images. *Stereotact. Funct. Neurosurg.* 89, 286–290. doi:10.1159/000329356
- Calancie, B., Needham-shropshire, B., Jacobs, P., Willer, K., Zych, G., Green, B.A., 1994. Involuntary stepping after chronic spinal cord injury: Evidence for a central rhythm generator for locomotion in man. *Brain* 117, 1143–1159. doi:10.1093/brain/117.5.1143
- Cantiniiaux, S., Vaugoyeau, M., Robert, D., Horrelou-Pitek, C., Mancini, J., Witjas, T., Azulay, J.-P., 2010. Comparative analysis of gait and speech in Parkinson's disease: hypokinetic or dysrhythmic disorders? *J. Neurol. Neurosurg. Psychiatry* 81, 177–184. doi:10.1136/jnnp.2009.174375
- Carpinella, I., Crenna, P., Marzegan, A., Rabuffetti, M., Rizzone, M., Lopiano, L., Ferrarin, M., 2007. Effect of L-dopa and subthalamic nucleus stimulation on arm and leg swing during gait in parkinson's disease, in: *Annual International Conference of the IEEE Engineering in Medicine and Biology - Proceedings*. pp. 6664–6667. doi:10.1109/IEMBS.2007.4353888
- Cassidy, M., Mazzone, P., Oliviero, A., Insola, A., Tonali, P., Di Lazzaro, V., Brown, P., 2002. Movement-related changes in synchronization in the human basal ganglia. *Brain* 125, 1235–1246. doi:10.1093/brain/awf135
- Castermans, T., Duvinage, M., Cheron, G., Dutoit, T., 2013. Towards Effective Non-Invasive Brain-Computer Interfaces Dedicated to Gait Rehabilitation Systems. *Brain Sci.* 4, 1–48. doi:10.3390/brainsci4010001
- Castermans, T., Duvinage, M., Cheron, G., Dutoit, T., 2012. EEG and human locomotion: Descending Commands and Sensory Feedback Should be Disentangled From Artifacts Thanks to New Experimental Protocols Position Paper, in: *Proceedings of the International Conference on Bio-Inspired Systems and Signal Processing*. pp. 309–314. doi:10.5220/0003871403090314
- Castermans, T., Duvinage, M., Petieau, M., Hoellinger, T., Saedeleer, C. De, Seetharaman, K., Bengoetxea, A., Cheron, G., Dutoit, T., 2011. Optimizing the performances of a P300-based brain-computer interface in ambulatory conditions. *IEEE J. Emerg. Sel. Top. Circuits Syst.* 1, 566–577. doi:10.1109/JETCAS.2011.2179421
- Cavanagh, J.F., Frank, M.J., 2014. Frontal theta as a mechanism for cognitive control. *Trends Cogn. Sci.* 18, 414–421. doi:10.1016/j.tics.2014.04.012
- Cavanagh, J.F., Wiecki, T. V, Cohen, M.X., Figueroa, C.M., Samanta, J., Sherman, S.J., Frank, M.J., 2011.

- Subthalamic nucleus stimulation reverses mediofrontal influence over decision threshold. *Nat. Neurosci.* 14, 1462–1467. doi:10.1038/nn.2925
- Chastan, N., Westby, G.W.M., Yelnik, J., Bardinet, E., Do, M.C., Agid, Y., Welter, M.L., 2009. Effects of nigral stimulation on locomotion and postural stability in patients with Parkinson's disease. *Brain* 132, 172–184. doi:10.1093/brain/awn294
- Chaudhuri, K.R., Healy, D.G., Schapira, A.H., 2006. Non-motor symptoms of Parkinson's disease: diagnosis and management. *Lancet Neurol.* 5, 235–245. doi:10.1016/S1474-4422(06)70373-8
- Chen, C.C., Litvak, V., Gilbertson, T., Kühn, A., Lu, C.S., Lee, S.T., Tsai, C.H., Tisch, S., Limousin, P., Hariz, M., Brown, P., 2007. Excessive synchronization of basal ganglia neurons at 20 Hz slows movement in Parkinson's disease. *Exp. Neurol.* 205, 214–221. doi:10.1016/j.expneurol.2007.01.027
- Cheng, H.C., Ulane, C., Burke, R., 2010. Clinical progression in Parkinson's disease and the neurobiology of Axons. *Ann. Neurol.* 67, 715–725. doi:10.1002/ana.21995.Clinical
- Cheung, T., Noecker, A.M., Alterman, R.L., McIntyre, C.C., Tagliati, M., 2014. Defining a therapeutic target for pallidal deep brain stimulation for dystonia. *Ann. Neurol.* 76, 22–30. doi:10.1002/ana.24187
- Chiken, S., Nambu, A., 2015. Mechanism of Deep Brain Stimulation: Inhibition, Excitation, or Disruption? *Neuroscientist.* doi:10.1177/1073858415581986
- Chiken, S., Nambu, A., 2014. Disrupting neuronal transmission: mechanism of DBS? *Front. Syst. Neurosci.* 8. doi:10.3389/fnsys.2014.00033
- Chou, K.L., Hurtig, H.I., Jaggi, J.L., Baltuch, G.H., 2005. Bilateral subthalamic nucleus deep brain stimulation in a patient with cervical dystonia and essential tremor. *Mov. Disord.* 20, 377–380. doi:10.1002/mds.20341
- Chung, J.W., Ofori, E., Misra, G., Hess, C.W., Vaillancourt, D.E., 2017. Beta-band activity and connectivity in sensorimotor and parietal cortex are important for accurate motor performance. *Neuroimage* 144, 164–173. doi:10.1016/j.neuroimage.2016.10.008
- Chung, K.K.K., Zhang, Y., Lim, K.L., Tanaka, Y., Huang, H., Gao, J., Ross, C.A., Dawson, V.L., Dawson, T.M., 2001. Parkin ubiquitinates the α -synuclein-interacting protein, synphilin-1: Implications for Lewy-body formation in Parkinson disease. *Nat. Med.* 7, 1144–1150. doi:10.1038/nm1001-1144
- Coenen, V.A., Honey, C.R., Hurwitz, T., Rahman, A.A., McMaster, J., Bürgel, U., Mädler, B., 2009. Medial forebrain bundle stimulation as a pathophysiological mechanism for hypomania in subthalamic nucleus deep brain stimulation for Parkinson's disease. *Neurosurgery* 64, 1106–1114. doi:10.1227/01.NEU.0000345631.54446.06
- Coenen, V.A., Prescher, A., Schmidt, T., Picozzi, P., Gielen, F.L.H., 2008. What is dorso-lateral in the subthalamic Nucleus (STN)? - A topographic and anatomical consideration on the ambiguous

- description of today's primary target for deep brain stimulation (DBS) surgery. *Acta Neurochir. (Wien)*. 150, 1163–1165. doi:10.1007/s00701-008-0136-x
- Cohen, M.X., Nigbur, R., 2013. Reply to "Higher response time increases theta energy, conflict increases response time." *Clin. Neurophysiol.* 124, 1479–1481. doi:10.1016/j.clinph.2013.03.013
- Cohen, M.X., Ridderinkhof, K.R., 2013. EEG Source Reconstruction Reveals Frontal-Parietal Dynamics of Spatial Conflict Processing. *PLoS One* 8, e57293. doi:10.1371/journal.pone.0057293
- Cole, S.R., Peterson, E.J., van der Meij, R., de Hemptinne, C., Starr, P.A., Voytek, B., 2016. Nonsinusoidal oscillations underlie pathological phase-amplitude coupling in the motor cortex in Parkinson's disease. *bioRxiv* 049304. doi:10.1101/049304
- Cole, S.R., van der Meij, R., Peterson, E.J., de Hemptinne, C., Starr, P.A., Voytek, B., 2017. Nonsinusoidal Beta Oscillations Reflect Cortical Pathophysiology in Parkinson's Disease. *J. Neurosci.* 37, 4830–4840. doi:10.1523/JNEUROSCI.2208-16.2017
- Coleman, R.M., Pollak, C.P., Weitzman, E.D., 1980. Periodic movements in sleep (nocturnal myoclonus): Relation to sleep disorders. *Ann. Neurol.* 8, 416–421. doi:10.1002/ana.410080413
- Collomb-Clerc, A., Welter, M.-L., 2015. Effects of deep brain stimulation on balance and gait in patients with Parkinson's disease: A systematic neurophysiological review. *Neurophysiol. Clin. Neurophysiol.* 45, 371–388. doi:10.1016/j.neucli.2015.07.001
- Corbit, V.L., Whalen, T.C., Zitelli, K.T., Crilly, S.Y., Rubin, J.E., Gittis, A.H., 2016. Pallidostriatal Projections Promote Oscillations in a Dopamine-Depleted Biophysical Network Model. *J. Neurosci.* 36, 5556–5571. doi:10.1523/JNEUROSCI.0339-16.2016
- Costa, R.M., Lin, S.C., Sotnikova, T.D., Cyr, M., Gainetdinov, R.R., Caron, M.G., Nicolelis, M.A.L., 2006. Rapid Alterations in Corticostriatal Ensemble Coordination during Acute Dopamine-Dependent Motor Dysfunction. *Neuron* 52, 359–369. doi:10.1016/j.neuron.2006.07.030
- Damodaran, S., Cressman, J.R., Jedrzejewski-Szmek, Z., Blackwell, K.T., 2015. Desynchronization of Fast-Spiking Interneurons Reduces β -Band Oscillations and Imbalance in Firing in the Dopamine-Depleted Striatum. *J. Neurosci.* 35, 1149–1159. doi:10.1523/JNEUROSCI.3490-14.2015
- Dayan, P., Niv, Y., 2008. Reinforcement learning: The Good, The Bad and The Ugly. *Curr. Opin. Neurobiol.* doi:10.1016/j.conb.2008.08.003
- de Hemptinne, C., Ryapolova-Webb, E.S., Air, E.L., Garcia, P.A., Miller, K.J., Ojemann, J.G., Ostrem, J.L., Galifianakis, N.B., Starr, P.A., 2013. Exaggerated phase-amplitude coupling in the primary motor cortex in Parkinson disease. *Proc. Natl. Acad. Sci.* 110, 4780–4785. doi:10.1073/pnas.1214546110
- de Hemptinne, C., Swann, N.C., Ostrem, J.L., Ryapolova-Webb, E.S., San Luciano, M., Galifianakis, N.B., Starr, P.A., 2015. Therapeutic deep brain stimulation reduces cortical phase-amplitude coupling in

- Parkinson's disease. *Nat. Neurosci.* 18, 779–786. doi:10.1038/nn.3997
- Deuschl, G., Paschen, S., Witt, K., 2013. Chapter 10 – Clinical outcome of deep brain stimulation for Parkinson's disease. *Handb. Clin. Neurol.* 116, 107–128. doi:10.1016/B978-0-444-53497-2.00010-3
- Dickson, D.W., 2012. Parkinson's disease and parkinsonism: Neuropathology. *Cold Spring Harb. Perspect. Med.* 2. doi:10.1101/cshperspect.a009258
- Dietz, V., Colombo, G., 1998. Influence of body load on the gait pattern in Parkinson's disease. *Mov. Disord.* 13, 255–261. doi:10.1002/mds.870130210
- Dietz, V., Michel, J., 2008. Locomotion in Parkinson's disease: Neuronal coupling of upper and lower limbs. *Brain* 131, 3421–3431. doi:10.1093/brain/awn263
- Do, A.H., Wang, P.T., King, C.E., Abiri, A., Nenadic, Z., 2011. Brain-Computer Interface Controlled Functional Electrical Stimulation System for Ankle Movement. *J. Neuroeng. Rehabil.* 8, 49. doi:10.1186/1743-0003-8-49
- Dobkin, B.H., Firestine, A., West, M., Saremi, K., Woods, R., 2004. Ankle dorsiflexion as an fMRI paradigm to assay motor control for walking during rehabilitation. *Neuroimage* 23, 370–381. doi:10.1016/j.neuroimage.2004.06.008
- Dorofeev, I.Y., Avelev, V.D., Shcherbakova, N.A., Gerasimenko, Y.P., 2008. The role of cutaneous afferents in controlling locomotion evoked by epidural stimulation of the spinal cord in decerebrate cats. *Neurosci. Behav. Physiol.* 38, 695–701. doi:10.1007/s11055-008-9034-1
- Duchin, Y., Shamir, R.R., Patriat, R., Kim, J., Vitek, J.L., Sapiro, G., Harel, N., 2018. Patient-specific Anatomical Model for Deep Brain Stimulation based on 7 Tesla MRI. *Under Revis.* 13, 1–23. doi:10.1371/journal.pone.0201469
- Duysens, J., Van de Crommert, H.W., 1998. Neural control of locomotion; The central pattern generator from cats to humans. *Gait Posture* 7, 131–141. doi:10.1016/S0966-6362(97)00042-8
- Ebert, M., Hauptmann, C., Tass, P.A., 2014. Coordinated reset stimulation in a large-scale model of the STN-GPe circuit. *Front. Comput. Neurosci.* doi:10.3389/fncom.2014.00154
- Eggers, C., Kahraman, D., Fink, G.R., Schmidt, M., Timmermann, L., 2011. Akinetic-rigid and tremor-dominant Parkinson's disease patients show different patterns of FP-CIT single photon emission computed tomography. *Mov. Disord.* 26, 416–23. doi:10.1002/mds.23468
- Eggers, C., Pedrosa, D.J., Kahraman, D., Maier, F., Lewis, C.J., Fink, G.R., Schmidt, M., Timmermann, L., 2012. Parkinson Subtypes Progress Differently in Clinical Course and Imaging Pattern. *PLoS One* 7. doi:10.1371/journal.pone.0046813
- Eimeren, T. Van, Siebner, H.R., 2006. An update on functional neuroimaging of parkinsonism and dystonia. *Curr. Opin. Neurol.* doi:10.1097/01.wco.0000236623.68625.54

- Engel, A., Friston, K., Kelso, J., König, P., 2010. Coordination in Behavior and Cognition, Dynamic Coordination in the Brain: from Neurons to Mind. doi:10.7551/mitpress/9780262014717.001.0001
- Espenhahn, S., de Berker, A.O., van Wijk, B.C.M., Rossiter, H.E., Ward, N.S., 2017. Movement-related beta oscillations show high intra-individual reliability. *Neuroimage* 147, 175–185. doi:10.1016/j.neuroimage.2016.12.025
- Eusebio, A., Chen, C.C., Lu, C.S., Lee, S.T., Tsai, C.H., Limousin, P., Hariz, M., Brown, P., 2008. Effects of low-frequency stimulation of the subthalamic nucleus on movement in Parkinson's disease. *Exp. Neurol.* 209, 125–130. doi:10.1016/j.expneurol.2007.09.007
- Fasano, A., Lozano, A.M., Cubo, E., 2017. New neurosurgical approaches for tremor and Parkinson's disease. *Curr. Opin. Neurol.* doi:10.1097/WCO.0000000000000465
- Fischer, P., Chen, C.C., Chang, Y.-J., Yeh, C.-H., Pogosyan, A., Herz, D.M., Cheeran, B., Green, A.L., Aziz, T.Z., Hyam, J., Little, S., Foltynie, T., Limousin, P., Zrinzo, L., Hasegawa, H., Samuel, M., Ashkan, K., Brown, P., Tan, H., 2018. Alternating Modulation of Subthalamic Nucleus Beta Oscillations during Stepping. *J. Neurosci.* 38, 5111–5121. doi:10.1523/JNEUROSCI.3596-17.2018
- Fitzsimmons, N.A., 2009. Extracting kinematic parameters for monkey bipedal walking from cortical neuronal ensemble activity. *Front. Integr. Neurosci.* 3. doi:10.3389/neuro.07.003.2009
- Florin, E., Erasmí, R., Reck, C., Maarouf, M., Schnitzler, A., Fink, G.R., Timmermann, L., 2013. Does increased gamma activity in patients suffering from Parkinson's disease counteract the movement inhibiting beta activity? *Neuroscience* 237, 42–50. doi:10.1016/j.neuroscience.2013.01.051
- Foffani, G., Bianchi, A.M., Baselli, G., Priori, A., 2005. Movement-related frequency modulation of beta oscillatory activity in the human subthalamic nucleus. *J. Physiol.* 568, 699–711. doi:10.1113/jphysiol.2005.089722
- Follett, K.A., Torres-Russotto, D., 2012. Deep brain stimulation of globus pallidus interna, subthalamic nucleus, and pedunculo pontine nucleus for Parkinson's disease: Which target? *Parkinsonism Relat. Disord.* 18, S165–S167. doi:10.1016/S1353-8020(11)70051-7
- Follett, K.A., Weaver, F.M., Stern, M., Hur, K., Harris, C.L., Luo, P., Marks, W.J., Rothlind, J., Sagher, O., Moy, C., Pahwa, R., Burchiel, K., Hogarth, P., Lai, E.C., Duda, J.E., Holloway, K., Samii, A., Horn, S., Bronstein, J.M., Stoner, G., Starr, P.A., Simpson, R., Baltuch, G., De Salles, A., Huang, G.D., Reda, D.J., 2010. Pallidal versus Subthalamic Deep-Brain Stimulation for Parkinson's Disease. *N. Engl. J. Med.* 362, 2077–2091. doi:10.1056/NEJMoa0907083
- Forstmann, B.U., Anwander, A., Schafer, A., Neumann, J., Brown, S., Wagenmakers, E.-J., Bogacz, R., Turner, R., 2010. Cortico-striatal connections predict control over speed and accuracy in perceptual decision making. *Proc. Natl. Acad. Sci.* 107, 15916–15920. doi:10.1073/pnas.1004932107

- Fox, S.H., 2013. Non-dopaminergic treatments for motor control in Parkinson's disease. *Drugs*. doi:10.1007/s40265-013-0105-4
- Frank, M.J., 2006. Hold your horses: A dynamic computational role for the subthalamic nucleus in decision making. *Neural Networks* 19, 1120–1136. doi:10.1016/j.neunet.2006.03.006
- Frank, M.J., 2005. Dynamic Dopamine Modulation in the Basal Ganglia: A Neurocomputational Account of Cognitive Deficits in Medicated and Nonmedicated Parkinsonism. *J. Cogn. Neurosci.* 17, 51–72. doi:10.1162/0898929052880093
- Frank, M.J., Samanta, J., Moustafa, A.A., Sherman, S.J., 2007. Hold Your Horses: Impulsivity, Deep Brain Stimulation, and Medication in Parkinsonism. *Science* (80-.). 318, 1309–1312. doi:10.1126/science.1146157
- Fransson, P., Marrelec, G., 2008. The precuneus/posterior cingulate cortex plays a pivotal role in the default mode network: Evidence from a partial correlation network analysis. *Neuroimage* 42, 1178–1184. doi:10.1016/j.neuroimage.2008.05.059
- Garcia-Ruiz, P.J., Martinez Castrillo, J.C., Alonso-Canovas, A., Herranz Barcenas, A., Vela, L., Sanchez Alonso, P., Mata, M., Olmedilla Gonzalez, N., Mahillo Fernandez, I., 2014. Impulse control disorder in patients with Parkinson's disease under dopamine agonist therapy: A multicentre study. *J. Neurol. Neurosurg. Psychiatry* 85, 841–845. doi:10.1136/jnnp-2013-306787
- Gerasimenko, A., Makarovski, N., Nikitin, O., 2000. Control of the human and animal locomotor activity in the absence of supraspinal effects. *Russ Fiziol Zh Im I M Sechenova* 86, 1502–1511. doi:10.1023/a:1015836428932
- Gerasimenko, Y.P., Avelev, V.D., Nikitin, O.A., Lavrov, I.A., 2003. Initiation of locomotor activity in spinal cats by epidural stimulation of the spinal cord. *Neurosci. Behav. Physiol.* 33, 247–254. doi:10.1023/A:1022199214515
- Gillies, A., Willshaw, D., Li, Z., 2002. Subthalamic–pallidal interactions are critical in determining normal and abnormal functioning of the basal ganglia. *Proc. R. Soc. London B Biol. Sci.* 269, 545–551. doi:10.1098/rspb.2001.1817
- Golestanirad, L., Elahi, B., Graham, S.J., Das, S., Wald, L.L., 2016. Efficacy and Safety of Pedunclopontine Nuclei (PPN) Deep Brain Stimulation in the Treatment of Gait Disorders: A Meta-Analysis of Clinical Studies. *Can. J. Neurol. Sci. / J. Can. des Sci. Neurol.* doi:10.1017/cjn.2015.318
- Goulding, M., 2009. Circuits controlling vertebrate locomotion: Moving in a new direction. *Nat. Rev. Neurosci.* doi:10.1038/nrn2608
- Granger, C.W.J., 1969. Investigating Causal Relations by Econometric Models and Cross-spectral Methods. *Econometrica* 37, 424. doi:10.2307/1912791

- Gregoriou, G.G., Gotts, S.J., Zhou, H., Desimone, R., 2009. High-Frequency, long-range coupling between prefrontal and visual cortex during attention. *Science* (80-). 324, 1207–1210.
doi:10.1126/science.1171402
- Grillner, S., 1985. Neurobiological bases of rhythmic motor acts in vertebrates. *Science* (80-). 228, 143–149. doi:10.1126/science.3975635
- Gross, J., Pollok, B., Dirks, M., Timmermann, L., Butz, M., Schnitzler, A., 2005. Task-dependent oscillations during unimanual and bimanual movements in the human primary motor cortex and SMA studied with magnetoencephalography. *Neuroimage* 26, 91–98. doi:10.1016/j.neuroimage.2005.01.025
- Grosse-Wentrup, M., Janzing, D., Siegel, M., Schölkopf, B., 2016. Identification of causal relations in neuroimaging data with latent confounders: An instrumental variable approach. *Neuroimage* 125, 825–833. doi:10.1016/j.neuroimage.2015.10.062
- Grosse-Wentrup, M., Schölkopf, B., Hill, J., 2011. Causal influence of gamma oscillations on the sensorimotor rhythm. *Neuroimage* 56, 837–842. doi:10.1016/j.neuroimage.2010.04.265
- Grossman, N., Bono, D., Dedic, N., Kodandaramaiah, S.B., Rudenko, A., Suk, H.-J., Cassara, A.M., Neufeld, E., Kuster, N., Tsai, L.-H., Pascual-Leone, A., Boyden, E.S., 2017. Noninvasive Deep Brain Stimulation via Temporally Interfering Electric Fields. *Cell* 169, 1029–1041.e16. doi:10.1016/j.cell.2017.05.024
- Gurney, K., Prescott, T.J., Redgrave, P., 2001. A computational model of action selection in the basal ganglia. II. Analysis and simulation of behaviour. *Biol. Cybern.* 84, 411–423.
doi:10.1007/PL00007985
- Gwin, J.T., Gramann, K., Makeig, S., Ferris, D.P., 2011. Electrocortical activity is coupled to gait cycle phase during treadmill walking. *Neuroimage* 54, 1289–1296.
doi:10.1016/j.neuroimage.2010.08.066
- Hammond, C., Bergman, H., Brown, P., 2007. Pathological synchronization in Parkinson's disease: networks, models and treatments. *Trends Neurosci.* doi:10.1016/j.tins.2007.05.004
- Hassler, R., Riechert, T., 1955. A Special Method of Stereotactic Brain Operation. *Proc. R. Soc. Med.* 48, 469–470.
- Hausdorff, J.M., 2009. Gait dynamics in Parkinson's disease: Common and distinct behavior among stride length, gait variability, and fractal-like scaling. *Chaos* 19. doi:10.1063/1.3147408
- Hell, F., H. Mehrkens, J., Bötzel, K., 2018a. Auf dem Weg zur adaptiven Hirnstimulation, Das Neurophysiologie-Labor. doi:10.1016/j.neulab.2018.02.001
- Hell, F., Plate, A., Mehrkens, J.H., Bötzel, K., 2018b. Subthalamic oscillatory activity and connectivity during gait in Parkinson's disease. *NeuroImage Clin.* 19, 396–405.
doi:https://doi.org/10.1016/j.nicl.2018.05.001

- Hell, F., Taylor, P.C.J., Mehrkens, J.H., Bötzel, K., 2018c. Subthalamic stimulation, oscillatory activity and connectivity reveal functional role of STN and network mechanisms during decision making under conflict. *Neuroimage*. doi:10.1016/j.neuroimage.2018.01.001
- Herrington, T.M., Cheng, J.J., Eskandar, E.N., 2016. Mechanisms of deep brain stimulation. *J. Neurophysiol.* 115, 19–38. doi:10.1152/jn.00281.2015
- Herron, J.A., Thompson, M.C., Brown, T., Chizeck, H.J., Ojemann, J.G., Ko, A.L., 2017. Cortical Brain-Computer Interface for Closed-Loop Deep Brain Stimulation. *IEEE Trans. Neural Syst. Rehabil. Eng.* 25, 2180–2187. doi:10.1109/TNSRE.2017.2705661
- Hershey, T., Campbell, M.C., Videen, T.O., Lugar, H.M., Weaver, P.M., Hartlein, J., Karimi, M., Tabbal, S.D., Perlmutter, J.S., 2010. Mapping Go-No-Go performance within the subthalamic nucleus region. *Brain* 133, 3625–3634. doi:10.1093/brain/awq256
- Herz, D.M., Tan, H., Brittain, J.-S., Fischer, P., Cheeran, B., Green, A.L., FitzGerald, J., Aziz, T.Z., Ashkan, K., Little, S., Foltynie, T., Limousin, P., Zrinzo, L., Bogacz, R., Brown, P., 2017. Distinct mechanisms mediate speed-accuracy adjustments in cortico-subthalamic networks. *Elife* 6. doi:10.7554/eLife.21481
- Herz, D.M., Zavala, B.A., Bogacz, R., Brown, P., 2016. Neural Correlates of Decision Thresholds in the Human Subthalamic Nucleus. *Curr. Biol.* 26, 916–920. doi:10.1016/j.cub.2016.01.051
- Hipp, J.F., Engel, A.K., Siegel, M., 2011. Oscillatory synchronization in large-scale cortical networks predicts perception. *Neuron* 69, 387–396. doi:10.1016/j.neuron.2010.12.027
- Hirschmann, J., Hartmann, C.J., Butz, M., Hoogenboom, N., Özkurt, T.E., Elben, S., Vesper, J., Wojtecki, L., Schnitzler, A., 2013. A direct relationship between oscillatory subthalamic nucleus-cortex coupling and rest tremor in Parkinson’s disease. *Brain* 136, 3659–3670. doi:10.1093/brain/awt271
- Hohlefeld, F.U., Huchzermeyer, C., Huebl, J., Schneider, G.H., Brücke, C., Schönecker, T., Kühn, A.A., Curio, G., Nikulin, V. V., 2014. Interhemispheric functional interactions between the subthalamic nuclei of patients with Parkinson’s disease. *Eur. J. Neurosci.* 40, 3273–3283. doi:10.1111/ejn.12686
- Højlund, A., Petersen, M. V., Sridharan, K.S., Østergaard, K., 2017. Worsening of Verbal Fluency After Deep Brain Stimulation in Parkinson’s Disease: A Focused Review. *Comput. Struct. Biotechnol. J.* doi:10.1016/j.csbj.2016.11.003
- Horn, A., Kühn, A.A., 2015. Lead-DBS: A toolbox for deep brain stimulation electrode localizations and visualizations. *Neuroimage* 107, 127–135. doi:10.1016/j.neuroimage.2014.12.002
- Horn, A., Neumann, W.-J., Degen, K., Schneider, G.-H., Kühn, A.A., 2017. Toward an electrophysiological “sweet spot” for deep brain stimulation in the subthalamic nucleus. *Hum. Brain Mapp.* doi:10.1002/hbm.23594

- Hughes, A.J., Daniel, S.E., Kilford, L., Lees, A.J., 1992. Accuracy of clinical diagnosis of idiopathic Parkinson's disease: a clinico-pathological study of 100 cases. *J. Neurol. Neurosurg. Psychiatry* 55, 181–4. doi:10.1136/jnnp.55.3.181
- Humphries, M.D., Obeso, J.A., Dreyer, J.K., 2018. Insights into Parkinson's disease from computational models of the basal ganglia. *J. Neurol. Neurosurg. Psychiatry*. doi:10.1136/jnnp-2017-315922
- Humphries, M.D., Stewart, R.D., Gurney, K.N., 2006. A Physiologically Plausible Model of Action Selection and Oscillatory Activity in the Basal Ganglia. *J. Neurosci.* 26, 12921–12942. doi:10.1523/JNEUROSCI.3486-06.2006
- Huys, Q.J.M., Cruickshank, A., Seriès, P., 2014. Reward-Based Learning, Model-Based and Model-Free, in: Jaeger, D., Jung, R. (Eds.), *Encyclopedia of Computational Neuroscience*. Springer New York, New York, NY, pp. 1–10. doi:10.1007/978-1-4614-7320-6_674-1
- Ijspeert, A.J., 2008. Central pattern generators for locomotion control in animals and robots: A review. *Neural Networks* 21, 642–653. doi:10.1016/j.neunet.2008.03.014
- Iosa, M., Fusco, A., Marchetti, F., Morone, G., Caltagirone, C., Paolucci, S., Peppe, A., 2013. The golden ratio of gait harmony: Repetitive proportions of repetitive gait phases. *Biomed Res. Int.* 2013. doi:10.1155/2013/918642
- Jackson, G.M., Jackson, S.R., Hindle, J. V., 2000. The control of bimanual reach-to-grasp movements in hemiparkinsonian patients. *Exp. Brain Res.* 132, 390–398. doi:10.1007/s002210000354
- Jaffard, M., Longcamp, M., Velay, J.L., Anton, J.L., Roth, M., Nazarian, B., Boulinguez, P., 2008. Proactive inhibitory control of movement assessed by event-related fMRI. *Neuroimage* 42, 1196–1206. doi:10.1016/j.neuroimage.2008.05.041
- Jahanshahi, M., 2013. Effects of deep brain stimulation of the subthalamic nucleus on inhibitory and executive control over prepotent responses in Parkinson's disease. *Front. Syst. Neurosci.* 7. doi:10.3389/fnsys.2013.00118
- Jahanshahi, M., Obeso, I., Baunez, C., Alegre, M., Krack, P., 2015a. Parkinson's disease, the subthalamic nucleus, inhibition, and impulsivity. *Mov. Disord.* doi:10.1002/mds.26049
- Jahanshahi, M., Obeso, I., Rothwell, J.C., Obeso, J.A., 2015b. A fronto–striato–subthalamic–pallidal network for goal-directed and habitual inhibition. *Nat. Rev. Neurosci.* 16, 719–732. doi:10.1038/nrn4038
- Jahanshahi, M., Rothwell, J.C., 2017. Inhibitory dysfunction contributes to some of the motor and non-motor symptoms of movement disorders and psychiatric disorders. *Philos. Trans. R. Soc. B Biol. Sci.* 372, 20160198. doi:10.1098/rstb.2016.0198
- Jankovic, J., McDermott, M., Carter, J., Gauthier, S., Goetz, C., Golbe, L., Huber, S., Koller, W., Olanow, C.,

- Shoulson, I., Stern, M., Tanner, C., Weiner, W., Group, P.S., 1990. Variable expression of Parkinson's disease: a base-line analysis of the DATATOP cohort. The Parkinson Study Group. *Neurology* 40, 1529–34. doi:10.1212/WNL.40.10.1529
- Jankovic, J., Stacy, M., 2007. Medical management of levodopa-associated motor complications in patients with Parkinson's disease. *CNS Drugs*. doi:10.2165/00023210-200721080-00005
- Jayaram, V., Alamgir, M., Altun, Y., Scholkopf, B., Grosse-Wentrup, M., 2016. Transfer Learning in Brain-Computer Interfaces. *IEEE Comput. Intell. Mag.* doi:10.1109/MCI.2015.2501545
- Jenkinson, N., Brown, P., 2011. New insights into the relationship between dopamine, beta oscillations and motor function. *Trends Neurosci.* doi:10.1016/j.tins.2011.09.003
- Johnson, L.A., Nebeck, S.D., Muralidharan, A., Johnson, M.D., Baker, K.B., Vitek, J.L., 2016. Closed-Loop Deep Brain Stimulation Effects on Parkinsonian Motor Symptoms in a Non-Human Primate. Is Beta Enough? *Brain Stimul.* 9. doi:10.1016/j.brs.2016.06.051
- Johnson, M.D., Miocinovic, S., McIntyre, C.C., Vitek, J.L., 2008. Mechanisms and Targets of Deep Brain Stimulation in Movement Disorders. *Neurotherapeutics* 5, 294–308. doi:10.1016/j.nurt.2008.01.010
- Joundi, R.A., Brittain, J.S., Green, A.L., Aziz, T.Z., Brown, P., Jenkinson, N., 2013. Persistent suppression of subthalamic beta-band activity during rhythmic finger tapping in Parkinson's disease. *Clin. Neurophysiol.* 124, 565–573. doi:10.1016/j.clinph.2012.07.029
- Kalia, L. V., Lang, A.E., 2015. Parkinson's disease. *Lancet* 386, 896–912. doi:10.1016/S0140-6736(14)61393-3
- Kandel, E.R., Schwartz, J.H., Jessell, T.M., 2000. *Principles of Neural Science, Neurology.* doi:10.1036/0838577016
- Karunanayaka, P.R., Lee, E.Y., Lewis, M.M., Sen, S., Eslinger, P.J., Yang, Q.X., Huang, X., 2016. Default mode network differences between rigidity- and tremor-predominant Parkinson's disease. *Cortex* 81, 239–250. doi:10.1016/j.cortex.2016.04.021
- Kline, J.E., Huang, H.J., Snyder, K.L., Ferris, D.P., 2015. Isolating gait-related movement artifacts in electroencephalography during human walking. *J. Neural Eng.* 12, 046022. doi:10.1088/1741-2560/12/4/046022
- Koch, S.C., Del Barrio, M.G., Dalet, A., Gatto, G., Günther, T., Zhang, J., Seidler, B., Saur, D., Schüle, R., Goulding, M., 2017. ROR β Spinal Interneurons Gate Sensory Transmission during Locomotion to Secure a Fluid Walking Gait. *Neuron* 96, 1419–1431.e5. doi:10.1016/j.neuron.2017.11.011
- Kryptos, A.-M., Beckers, T., Kindt, M., Wagenmakers, E.-J., 2015. A Bayesian hierarchical diffusion model decomposition of performance in Approach–Avoidance Tasks. *Cogn. Emot.* 29, 1424–1444.

doi:10.1080/02699931.2014.985635

- Kühn, A.A., Kempf, F., Brücke, C., Gaynor Doyle, L., Martinez-Torres, I., Pogosyan, A., Trottenberg, T., Kupsch, A., Schneider, G.-H., Hariz, M.I., Vandenberghe, W., Nuttin, B., Brown, P., 2008. High-frequency stimulation of the subthalamic nucleus suppresses oscillatory beta activity in patients with Parkinson's disease in parallel with improvement in motor performance. *J. Neurosci.* 28, 6165–6173. doi:10.1523/JNEUROSCI.0282-08.2008
- Kühn, A.A., Kupsch, A., Schneider, G.H., Brown, P., 2006. Reduction in subthalamic 8-35 Hz oscillatory activity correlates with clinical improvement in Parkinson's disease. *Eur. J. Neurosci.* 23, 1956–1960. doi:10.1111/j.1460-9568.2006.04717.x
- Kühn, A.A., Williams, D., Kupsch, A., Limousin, P., Hariz, M., Schneider, G.H., Yarrow, K., Brown, P., 2004. Event-related beta desynchronization in human subthalamic nucleus correlates with motor performance. *Brain* 127, 735–746. doi:10.1093/brain/awh106
- Kuhn, R.A., 1950. Functional capacity of the isolated human spinal cord. *Brain* 73, 1–51. doi:10.1093/brain/73.1.1
- Kumar, A., Cardanobile, S., Rotter, S., Aertsen, A., 2011. The Role of Inhibition in Generating and Controlling Parkinson's Disease Oscillations in the Basal Ganglia. *Front. Syst. Neurosci.*
- Kumaravelu, K., Brocker, D.T., Grill, W.M., 2016. A biophysical model of the cortex-basal ganglia-thalamus network in the 6-OHDA lesioned rat model of Parkinson's disease. *J. Comput. Neurosci.* 40, 207–229. doi:10.1007/s10827-016-0593-9
- la Fougère, C., Zwergal, A., Rominger, A., Förster, S., Fesl, G., Dieterich, M., Brandt, T., Strupp, M., Bartenstein, P., Jahn, K., 2010. Real versus imagined locomotion: A [18F]-FDG PET-fMRI comparison. *Neuroimage* 50, 1589–1598. doi:10.1016/j.neuroimage.2009.12.060
- Lalo, E., Thobois, S., Sharott, A., Polo, G., Mertens, P., Pogosyan, A., Brown, P., 2008. Patterns of Bidirectional Communication between Cortex and Basal Ganglia during Movement in Patients with Parkinson Disease. *J. Neurosci.* 28, 3008–3016. doi:10.1523/JNEUROSCI.5295-07.2008
- Lambert, C., Zrinzo, L., Nagy, Z., Lutti, A., Hariz, M., Foltynie, T., Draganski, B., Ashburner, J., Frackowiak, R., 2015. Do we need to revise the tripartite subdivision hypothesis of the human subthalamic nucleus (STN)? Response to Alkemade and Forstmann. *Neuroimage.* doi:10.1016/j.neuroimage.2015.01.038
- Lambert, C., Zrinzo, L., Nagy, Z., Lutti, A., Hariz, M., Foltynie, T., Draganski, B., Ashburner, J., Frackowiak, R., 2012. Confirmation of functional zones within the human subthalamic nucleus: Patterns of connectivity and sub-parcellation using diffusion weighted imaging. *Neuroimage* 60, 83–94. doi:10.1016/j.neuroimage.2011.11.082

- Lavallee, C.F., Meemken, M.T., Herrmann, C.S., Huster, R.J., 2014. When holding your horses meets the deer in the headlights: time-frequency characteristics of global and selective stopping under conditions of proactive and reactive control. *Front. Hum. Neurosci.* 8, 994. doi:10.3389/fnhum.2014.00994
- Leblois, A., 2006. Competition between Feedback Loops Underlies Normal and Pathological Dynamics in the Basal Ganglia. *J. Neurosci.* 26, 3567–3583. doi:10.1523/JNEUROSCI.5050-05.2006
- Lees, A.J., Djamshidian, A., O’Sullivan, S.S., Foltynie, T., Aviles-Olmos, I., Limousin, P., Noyce, A., Zrinzo, L., 2013. Dopamine agonists rather than deep brain stimulation cause reflection impulsivity in Parkinson’s disease. *J. Parkinsons. Dis.* 3, 139–144. doi:10.3233/JPD-130178
- Lees, A.J., Hardy, J., Revesz, T., 2009. Parkinson’s disease. *Lancet.* doi:10.1016/S0140-6736(09)60492-X
- Lenka, A., Hegde, S., Jhunjhunwala, K.R., Pal, P.K., 2016. Interactions of visual hallucinations, rapid eye movement sleep behavior disorder and cognitive impairment in Parkinson’s disease: A review. *Parkinsonism Relat. Disord.* 22, 1–8. doi:10.1016/j.parkreldis.2015.11.018
- Leventhal, D.K., Gage, G.J., Schmidt, R., Pettibone, J.R., Case, A.C., Berke, J.D., 2012. Basal ganglia beta oscillations accompany cue utilization. *Neuron* 73, 523–536. doi:10.1016/j.neuron.2011.11.032
- Levin, J., Högen, T., Hillmer, A.S., Bader, B., Schmidt, F., Kamp, F., Kretzschmar, H.A., Bötzel, K., Giese, A., 2011. Generation of ferric iron links oxidative stress to α -synuclein oligomer formation. *J. Parkinsons. Dis.* 1, 205–216. doi:10.3233/JPD-2011-11040
- Lienard, J.F., Cos, I., Girard, B., 2017. Beta-Band Oscillations without Pathways: the opposing Roles of D2 and D5 Receptors. *Doi.Org* 161661. doi:10.1101/161661
- Lindahl, M., Hellgren-Kotaleski, J., 2016. Untangling Basal Ganglia Network Dynamics and Function: Role of Dopamine Depletion and Inhibition Investigated in a Spiking Network Model. *Eneuro* 3, ENEURO.0156-16.2016. doi:10.1523/ENEURO.0156-16.2016
- Lipszyc, J., Schachar, R., 2010. Inhibitory control and psychopathology: A meta-analysis of studies using the stop signal task. *J. Int. Neuropsychol. Soc.* 16, 1064–1076. doi:10.1017/S1355617710000895
- Liston, C., Matalon, S., Hare, T.A., Davidson, M.C., Casey, B.J., 2006. Anterior Cingulate and Posterior Parietal Cortices Are Sensitive to Dissociable Forms of Conflict in a Task-Switching Paradigm. *Neuron* 50, 643–653. doi:10.1016/j.neuron.2006.04.015
- Little, S., Brown, P., 2014. The functional role of beta oscillations in Parkinson’s disease. *Park. Relat. Disord.* 20. doi:10.1016/S1353-8020(13)70013-0
- Little, S., Brown, P., 2012. What brain signals are suitable for feedback control of deep brain stimulation in Parkinson’s disease? *Ann. N. Y. Acad. Sci.* 1265, 9–24. doi:10.1111/j.1749-6632.2012.06650.x
- Little, S., Pogosyan, A., Neal, S., Zavala, B., Zrinzo, L., Hariz, M., Foltynie, T., Limousin, P., Ashkan, K.,

- Fitzgerald, J., Green, A.L., Aziz, T.Z., Brown, P., 2013. Adaptive deep brain stimulation in advanced Parkinson disease. *Ann. Neurol.* 74, n/a-n/a. doi:10.1002/ana.23951
- Litvak, V., Eusebio, A., Jha, A., Oostenveld, R., Barnes, G., Foltynie, T., Limousin, P., Zrinzo, L., Hariz, M.I., Friston, K., Brown, P., 2012. Movement-related changes in local and long-range synchronization in Parkinson's disease revealed by simultaneous magnetoencephalography and intracranial recordings. *J. Neurosci.* 32, 10541–53. doi:10.1523/JNEUROSCI.0767-12.2012
- Loudon, J.K., Swift, M., Bell, S., 2008. The clinical orthopedic assessment guide. SciTech B. News.
- Lugaresi, E., Cirignotta, F., Coccagna, G., Montagna, P., 1986. Nocturnal myoclonus and restless legs syndrome. *Adv. Neurol.* 43, 295–307.
- Maathuis, M.H., Colombo, D., Kalisch, M., Bühlmann, P., 2010. Predicting causal effects in large-scale systems from observational data. *Nat. Methods.* doi:10.1038/nmeth0410-247
- Majsak, M.J., Kaminski, T., Gentile, A.M., Flanagan, J.R., 1998. The reaching movements of patients with Parkinson's disease under self-determined maximal speed and visually cued conditions. *Brain* 121, 755–766. doi:10.1093/brain/121.4.755
- Malekmohammadi, M., Herron, J., Velisar, A., Blumenfeld, Z., Trager, M.H., Chizeck, H.J., Bronte-Stewart, H., 2016. Kinematic Adaptive Deep Brain Stimulation for Resting Tremor in Parkinson's Disease. *Mov. Disord.* doi:10.1002/mds.26482
- Mallet, N., Pogosyan, A., Marton, L.F., Bolam, J.P., Brown, P., Magill, P.J., 2008. Parkinsonian Beta Oscillations in the External Globus Pallidus and Their Relationship with Subthalamic Nucleus Activity. *J. Neurosci.* 28, 14245–14258. doi:10.1523/JNEUROSCI.4199-08.2008
- Marder, E., Bucher, D., 2001. Central pattern generators and the control of rhythmic movements. *Curr. Biol.* doi:10.1016/S0960-9822(01)00581-4
- Marlinski, V., Nilaweera, W.U., Zelenin, P. V., Sirota, M.G., Beloozerova, I.N., 2012. Signals from the ventrolateral thalamus to the motor cortex during locomotion. *J. Neurophysiol.* 107, 455–472. doi:10.1152/jn.01113.2010
- Marsden, C.D., 1982. The mysterious motor function of the basal ganglia: The Robert Wartenberg lecture. *Neurology* 32, 514–539. doi:10.1212/WNL.32.5.514
- Martínez-Selva, J.M., Sánchez-Navarro, J.P., Bechara, A., Román, F., 2006. Mecanismos cerebrales de la toma de decisiones. *Rev. Neurol.* 42, 411–418. doi:10.1016/j.biopsych.2010.07.024
- Mastakouri, A.A., Weichwald, S., Ozdenizciy, O., Meyer, T., Scholkopf, B., Grosse-Wentrup, M., 2017. Personalized brain-computer interface models for motor rehabilitation, in: 2017 IEEE International Conference on Systems, Man, and Cybernetics, SMC 2017. pp. 3024–3029. doi:10.1109/SMC.2017.8123089

- Mattingley, J.B., Husain, M., Rorden, C., Kennard, C., Driver, J., 1998. Motor role of human inferior parietal lobe revealed in unilateral neglect patients. *Nature* 392, 179–182. doi:10.1038/32413
- McCarthy, M.M., Moore-Kochlacs, C., Gu, X., Boyden, E.S., Han, X., Kopell, N., 2011. Striatal origin of the pathologic beta oscillations in Parkinson’s disease. *Proc. Natl. Acad. Sci.* 108, 11620–11625. doi:10.1073/pnas.1107748108
- McCrimmon, C.M., Wang, P.T., Heydari, P., Nguyen, A., Shaw, S.J., Gong, H., Chui, L.A., Liu, C.Y., Nenadic, Z., Do, A.H., 2017. Electrocorticographic Encoding of Human Gait in the Leg Primary Motor Cortex. *Cereb. Cortex* 1–11. doi:10.1093/cercor/bhx155
- McIntosh, A.R., Gonzalez-Lima, F., 1994. Structural equation modeling and its application to network analysis in functional brain imaging. *Hum. Brain Mapp.* 2, 2–22. doi:10.1002/hbm.460020104
- Meidahl, A.C., Tinkhauser, G., Herz, D.M., Cagnan, H., Debarros, J., Brown, P., 2017. Adaptive Deep Brain Stimulation for Movement Disorders: The Long Road to Clinical Therapy. *Mov. Disord.* 32, 810–819. doi:10.1002/mds.27022
- Meirovitch, Y., Harris, H., Dayan, E., Arieli, A., Flash, T., 2015. Alpha and Beta Band Event-Related Desynchronization Reflects Kinematic Regularities. *J. Neurosci.* 35, 1627–1637. doi:10.1523/JNEUROSCI.5371-13.2015
- Menon, V., Adelman, N.E., White, C.D., Glover, G.H., Reiss, A.L., 2001. Error-related brain activation during a Go/NoGo response inhibition task. *Hum. Brain Mapp.* 12, 131–143. doi:10.1002/1097-0193(200103)12:3<131::AID-HBM1010>3.0.CO;2-C
- Merola, A., Zibetti, M., Angrisano, S., Rizzi, L., Ricchi, V., Artusi, C.A., Lanotte, M., Rizzone, M.G., Lopiano, L., 2011. Parkinson’s disease progression at 30 years: A study of subthalamic deep brain-stimulated patients. *Brain A J. Neurol.* 134, 2074–2084. doi:10.1093/brain/awr121
- Milletari, F., Navab, N., Ahmadi, S.A., 2016. V-Net: Fully convolutional neural networks for volumetric medical image segmentation, in: *Proceedings - 2016 4th International Conference on 3D Vision, 3DV 2016*. pp. 565–571. doi:10.1109/3DV.2016.79
- Miocinovic, S., Khemani, P., Whiddon, R., Zeilman, P., Martinez-Ramirez, D., Okun, M.S., Chitnis, S., 2014. Outcomes, management, and potential mechanisms of interleaving deep brain stimulation settings. *Park. Relat. Disord.* 20, 1434–1437. doi:10.1016/j.parkreldis.2014.10.011
- Monakow, K., Akert, K., Künzle, H., 1978. Projections of the precentral motor cortex and other cortical areas of the frontal lobe to the subthalamic nucleus in the monkey. *Exp. Brain Res.* 33, 395–403. doi:10.1007/BF00235561
- Moran, R.J., Mallet, N., Litvak, V., Dolan, R.J., Magill, P.J., Friston, K.J., Brown, P., 2011. Alterations in brain connectivity underlying beta oscillations in parkinsonism. *PLoS Comput. Biol.* 7.

doi:10.1371/journal.pcbi.1002124

Morgante, F., Barbuto, M., Ricciardi, L., Sorbera, C., Graziosi, A., Girlanda, P., Ebreo, M., Morgante, L., 2013. Stuttering speech disorder is related to freezing of gait in Parkinson's disease. *Mov. Disord.* 28, S306.

Moro, E., Esselink, R.J.A., Xie, J., Hommel, M., Benabid, A.L., Pollak, P., 2002. The impact on Parkinson's disease of electrical parameter settings in STN stimulation. *Neurology* 59, 706–713.

doi:10.1212/WNL.59.5.706

Morris, M.E., Iansek, R., Matyas, T.A., Summers, J.J., 1994a. Ability to modulate walking cadence remains intact in Parkinson's disease. *J. Neurol. Neurosurg. Psychiatry* 57, 1532–1534.

doi:10.1136/jnnp.57.12.1532

Morris, M.E., Iansek, R., Matyas, T.A., Summers, J.J., 1994b. The pathogenesis of gait hypokinesia in parkinson's disease. *Brain* 117, 1169–1181. doi:10.1093/brain/117.5.1169

Moustafa, A.A., Chakravarthy, S., Phillips, J.R., Gupta, A., Keri, S., Polner, B., Frank, M.J., Jahanshahi, M., 2016. Motor symptoms in Parkinson's disease: A unified framework. *Neurosci. Biobehav. Rev.* 68, 727–740. doi:10.1016/j.neubiorev.2016.07.010

Nachev, P., Wydell, H., O'Neill, K., Husain, M., Kennard, C., 2007. The role of the pre-supplementary motor area in the control of action. *Neuroimage* 36 Suppl 2, T155-63.

doi:10.1016/j.neuroimage.2007.03.034

Neely, R.M., Piech, D.K., Santacruz, S.R., Maharbiz, M.M., Carmena, J.M., 2018. Recent advances in neural dust: towards a neural interface platform. *Curr. Opin. Neurobiol.*

doi:10.1016/j.conb.2017.12.010

Neumann, W.J., Staub, F., Horn, A., Schanda, J., Mueller, J., Schneider, G.H., Brown, P., Kühn, A.A., 2016. Deep brain recordings using an implanted pulse generator in Parkinson's disease. *Neuromodulation* 19, 20–23. doi:10.1111/ner.12348

Niazmand, K., Tonn, K., Kalaras, A., Fietzek, U.M., Mehrkens, J.H., Lueth, T.C., 2011. Quantitative evaluation of Parkinson's disease using sensor based smart glove, in: *Proceedings - IEEE Symposium on Computer-Based Medical Systems*. doi:10.1109/CBMS.2011.5999113

Nielsen, J.B., 2003. How we walk: central control of muscle activity during human walking. *Neuroscientist* 9, 195–204. doi:10.1177/1073858403251978

Niketeghad, S., Hebb, A.O., Nedrud, J., Hanrahan, S.J., Mahoor, M.H., 2017. Motor Task Detection from Human STN using Interhemispheric Connectivity. *IEEE Trans. Neural Syst. Rehabil. Eng.*

doi:10.1109/TNSRE.2017.2754879

Nilsson, H., Rieskamp, J., Wagenmakers, E.J., 2011. Hierarchical Bayesian parameter estimation for

- cumulative prospect theory. *J. Math. Psychol.* 55, 84–93. doi:10.1016/j.jmp.2010.08.006
- Norman, D.A., Shallice, T., 1986. Attention to action: willed and automatic control of behavior., in: *Consciousness and Self-Regulation: Advances in Research and Theory*. pp. 1–18.
- Nutt, J.G., Bloem, B.R., Giladi, N., Hallett, M., Horak, F.B., Nieuwboer, A., 2011. Freezing of gait: Moving forward on a mysterious clinical phenomenon. *Lancet Neurol.* doi:10.1016/S1474-4422(11)70143-0
- O’Callaghan, C., Hall, J., Tomassini, A., Muller, A., Walpola, I., Moustafa, A., Shine, J., Lewis, S., 2017. Accumulation of sensory evidence is impaired in Parkinson’s disease with visual hallucinations. doi.org 111278. doi:10.1101/111278
- Obeso, I., Wilkinson, L., Casabona, E., Bringas, M.L., Álvarez, M., Álvarez, L., Pavón, N., Rodríguez-Oroz, M.C., Macías, R., Obeso, J.A., Jahanshahi, M., 2011. Deficits in inhibitory control and conflict resolution on cognitive and motor tasks in Parkinson’s disease. *Exp. Brain Res.* 212, 371–384. doi:10.1007/s00221-011-2736-6
- Odekerken, V.J.J., Boel, J.A., Schmand, B.A., de Haan, R.J., Figeer, M., van den Munckhof, P., Schuurman, P.R., de Bie, R.M.A., NSTAPS study group, 2016. GPi vs STN deep brain stimulation for Parkinson disease: Three-year follow-up. *Neurology* 86, 755–61. doi:10.1212/WNL.0000000000002401
- Orlovsky, G.N., Deliagina, T.G., Grillner, S., 1999. *Neuronal Control of Locomotion: From Mollusc to Man*, Oxford University Press. doi:10.2460/ajvr.75.1.4
- Oswal, A., Beudel, M., Zrinzo, L., Limousin, P., Hariz, M., Foltynie, T., Litvak, V., Brown, P., 2016. Deep brain stimulation modulates synchrony within spatially and spectrally distinct resting state networks in Parkinson’s disease. *Brain* 139, 1482–1496. doi:10.1093/brain/aww048
- Pavlidis, A., Hogan, S.J., Bogacz, R., 2015. Computational Models Describing Possible Mechanisms for Generation of Excessive Beta Oscillations in Parkinson’s Disease. *PLoS Comput. Biol.* 11. doi:10.1371/journal.pcbi.1004609
- Pearl, J., 2011. *Causality: Models, reasoning, and inference*, second edition, *Causality: Models, Reasoning, and Inference, Second Edition*. doi:10.1017/CBO9780511803161
- Petersen, N.T., Butler, J.E., Marchand-Pauvert, V., Fisher, R., Ledebt, A., Pyndt, H.S., Hansen, N.L., Nielsen, J.B., 2001. Suppression of EMG activity by transcranial magnetic stimulation in human subjects during walking. *J. Physiol.* 537, 651–6. doi:PHY_13122 [pii]
- Petersen, T.H., Willerslev-Olsen, M., Conway, B.A., Nielsen, J.B., 2012. The motor cortex drives the muscles during walking in human subjects. *J. Physiol.* 590, 2443–2452. doi:10.1113/jphysiol.2012.227397
- Petrucelli, L., Dickson, D.W., 2008. Neuropathology of Parkinson’s Disease. In: *Parkinson’s Disease: molecular and therapeutic insights from model systems*. Acad. Press 1, 35–48.

doi:<http://dx.doi.org/10.1016/B978-0-12-374028-1.00003-8>

- Pfurtscheller, G., Stancák, A., Neuper, C., 1996. Post-movement beta synchronization. A correlate of an idling motor area? *Electroencephalogr. Clin. Neurophysiol.* 98, 281–293. doi:10.1016/0013-4694(95)00258-8
- Plantinga, B.R., Temel, Y., Duchin, Y., Roebroek, A., Kuijf, M., Jahanshahi, A., ter Haar Romenij, B., Vitek, J., Harel, N., 2016. Individualized parcellation of the subthalamic nucleus in patients with Parkinson’s disease with 7T MRI. *Neuroimage*. doi:10.1016/j.neuroimage.2016.09.023
- Plessow, F., Fischer, R., Volkmann, J., Schubert, T., 2014. Subthalamic deep brain stimulation restores automatic response activation and increases susceptibility to impulsive behavior in patients with Parkinson’s disease. *Brain Cogn.* 87, 16–21. doi:10.1016/j.bandc.2014.02.009
- Plotnik, M., Giladi, N., Hausdorff, J.M., 2007. A new measure for quantifying the bilateral coordination of human gait: Effects of aging and Parkinson’s disease. *Exp. Brain Res.* 181, 561–570. doi:10.1007/s00221-007-0955-7
- Plummer, M., 2008. Penalized loss functions for Bayesian model comparison. *Biostatistics* 9, 523–539. doi:10.1093/biostatistics/kxm049
- Poewe, W., 2008. Non-motor symptoms in Parkinson’s disease. *Eur. J. Neurol.* doi:10.1111/j.1468-1331.2008.02056.x
- Poewe, W., Seppi, K., Tanner, C.M., Halliday, G.M., Brundin, P., Volkmann, J., Schrag, A.E., Lang, A.E., 2017. Parkinson disease. *Nat. Rev. Dis. Prim.* 3, 1–21. doi:10.1038/nrdp.2017.13
- Postuma, R.B., Berg, D., Adler, C.H., Bloem, B.R., Chan, P., Deuschl, G., Gasser, T., Goetz, C.G., Halliday, G., Joseph, L., Lang, A.E., Liepelt-Scarfone, I., Litvan, I., Marek, K., Oertel, W., Olanow, C.W., Poewe, W., Stern, M., 2016. The new definition and diagnostic criteria of Parkinson’s disease. *Lancet Neurol.* doi:10.1016/S1474-4422(16)00116-2
- Postuma, R.B., Berg, D., Stern, M., Poewe, W., Olanow, C.W., Oertel, W., Obeso, J., Marek, K., Litvan, I., Lang, A.E., Halliday, G., Goetz, C.G., Gasser, T., Dubois, B., Chan, P., Bloem, B.R., Adler, C.H., Deuschl, G., 2015. MDS clinical diagnostic criteria for Parkinson’s disease. *Mov. Disord.* doi:10.1002/mds.26424
- Pote, I., Torkamani, M., Kefalopoulou, Z.-M., Zrinzo, L., Limousin-Dowsey, P., Foltynie, T., Speekenbrink, M., Jahanshahi, M., 2016. Subthalamic nucleus deep brain stimulation induces impulsive action when patients with Parkinson’s disease act under speed pressure. *Exp. Brain Res.* 234, 1837–48. doi:10.1007/s00221-016-4577-9
- Presacco, A., Goodman, R., Forrester, L., Contreras-Vidal, J.L., 2011. Neural decoding of treadmill walking from noninvasive electroencephalographic signals. *J. Neurophysiol.* 106, 1875–1887.

doi:10.1152/jn.00104.2011

- Quinn, E.J., Blumenfeld, Z., Velisar, A., Koop, M.M., Shreve, L.A., Trager, M.H., Hill, B.C., Kilbane, C., Henderson, J.M., Bronte-Stewart, H., 2015. Beta oscillations in freely moving Parkinson's subjects are attenuated during deep brain stimulation. *Mov. Disord.* 30, 1750–1758. doi:10.1002/mds.26376
- Raethjen, J., Govindan, R.B., Binder, S., Zeuner, K.E., Deuschl, G., Stolze, H., 2008. Cortical representation of rhythmic foot movements. *Brain Res.* 1236, 79–84. doi:10.1016/j.brainres.2008.07.046
- Ratcliff, R., 1978. A theory of memory retrieval. *Psychol. Rev.* 85, 59–108. doi:10.1037/0033-295X.85.2.59
- Ratcliff, R., McKoon, G., 2008. The diffusion decision model: theory and data for two-choice decision tasks. *Neural Comput.* 20, 873–922. doi:10.1162/neco.2008.12-06-420
- Ratcliff, R., Smith, P.L., Brown, S.D., McKoon, G., 2016. Diffusion Decision Model: Current Issues and History. *Trends Cogn. Sci.* 20, 260–281. doi:10.1016/j.tics.2016.01.007
- Ray, N., Antonelli, F., Strafella, A.P., 2011. Imaging Impulsivity in Parkinson's Disease and the Contribution of the Subthalamic Nucleus. *Parkinsons. Dis.* 2011, 1–5. doi:10.4061/2011/594860
- Ray, N.J., Brittain, J.S., Holland, P., Joundi, R.A., Stein, J.F., Aziz, T.Z., Jenkinson, N., 2012. The role of the subthalamic nucleus in response inhibition: Evidence from local field potential recordings in the human subthalamic nucleus. *Neuroimage* 60, 271–278. doi:10.1016/j.neuroimage.2011.12.035
- Redgrave, P., Rodriguez, M., Smith, Y., Rodriguez-Oroz, M.C., Lehericy, S., Bergman, H., Agid, Y., Delong, M.R., Obeso, J.A., 2010. Goal-directed and habitual control in the basal ganglia: Implications for Parkinson's disease. *Nat. Rev. Neurosci.* doi:10.1038/nrn2915
- Reich, M.M., Steigerwald, F., Sawalhe, A.D., Reese, R., Gunalan, K., Johannes, S., Nickl, R., Matthies, C., McIntyre, C.C., Volkmann, J., 2015. Short pulse width widens the therapeutic window of subthalamic neurostimulation. *Ann. Clin. Transl. Neurol.* 2, 427–432. doi:10.1002/acn3.168
- Report, T., Kerick, S., States, U., Oie, K.S., Mcdowell, K., Soldier, A., View, T., Oie, K.S., 2009. Assessment of EEG Signal Quality in Motion Environments Assessment of EEG Signal Quality in Motion Environments, Army Research Laboratory.
- Richardson, T.H., 2008. Inhibitory Control in Psychiatric Disorders — A Review of Neuropsychological and Neuroimaging Research. *Undergrad. Res. J. Hum. Sci.* 7.
- Rizzone, M., 2001. Deep brain stimulation of the subthalamic nucleus in Parkinson's disease: effects of variation in stimulation parameters. *J. Neurol. Neurosurg. Psychiatry* 71, 215–219. doi:10.1136/jnnp.71.2.215
- Rodriguez-Oroz, M.C., Jahansahi, M., Krack, P., Litvan, I., Macias, R., Bezard, E., Obeso, J.A., 2009. Initial clinical manifestations of Parkinson's disease: features and pathophysiological mechanisms. *Lancet*

- Neurol. doi:10.1016/S1474-4422(09)70293-5
- Rogers, M.W., 1996. Disorders of posture, balance, and gait in Parkinson's disease. *Clin. Geriatr. Med.* 12, 825–45.
- Romkes, J., Bracht-Schweizer, K., 2017. The effects of walking speed on upper body kinematics during gait in healthy subjects. *Gait Posture* 54, 304–310. doi:10.1016/j.gaitpost.2017.03.025
- Roper, J.A., Kang, N., Ben, J., Cauraugh, J.H., Okun, M.S., Hass, C.J., 2016. Deep brain stimulation improves gait velocity in Parkinson's disease: a systematic review and meta-analysis. *J. Neurol.* 263, 1195–1203. doi:10.1007/s00415-016-8129-9
- Salmelin, R., Hari, R., 1994. Spatiotemporal characteristics of sensorimotor neuromagnetic rhythms related to thumb movement. *Neuroscience* 60, 537–50.
- Sauleau, P., Raoul, S., Lallement, F., Rivier, I., Drapier, S., Lajat, Y., Verin, M., 2005. Motor and non motor effects during intraoperative subthalamic stimulation for Parkinson's disease. *J. Neurol.* 252, 457–464. doi:10.1007/s00415-005-0675-5
- Schaeffer, E., Berg, D., 2017. Dopaminergic Therapies for Non-motor Symptoms in Parkinson's Disease. *CNS Drugs*. doi:10.1007/s40263-017-0450-z
- Schapira, A.H., 2006. Etiology of Parkinson's disease. *Neurology* 66, S10-23. doi:66/10_suppl_4/S10 [pii]
- Schapira, A.H., Jenner, P., 2011. Etiology and pathogenesis of Parkinson's disease. *Mov. Disord.* doi:10.1002/mds.23732
- Scherbaum, S., Dshemuchadse, M., 2013. Higher response time increases theta energy, conflict increases response time. *Clin. Neurophysiol.* 124, 1477–1479. doi:10.1016/j.clinph.2012.12.007
- Scherberger, H., Jarvis, M.R., Andersen, R.A., 2005. Cortical local field potential encodes movement intentions in the posterior parietal cortex. *Neuron* 46, 347–354. doi:10.1016/j.neuron.2005.03.004
- Schilaci, O., Chiaravaloti, A., Pierantozzi, M., Di Pietro, B., Koch, G., Bruni, C., Stanzione, P., Stefani, A., 2011. Different patterns of nigrostriatal degeneration in tremor type versus the akinetic-rigid and mixed types of Parkinson's disease at the early stages: Molecular imaging with 123I-FP-CIT SPECT. *Int. J. Mol. Med.* 28, 881–886. doi:10.3892/ijmm.2011.764
- Schirrneister, R.T., Springenberg, J.T., Fiederer, L.D.J., Glasstetter, M., Eggensperger, K., Tangermann, M., Hutter, F., Burgard, W., Ball, T., 2017. Deep learning with convolutional neural networks for EEG decoding and visualization. *Hum. Brain Mapp.* doi:10.1002/hbm.23730
- Schneider, W., Chein, J.M., 2003. Controlled & automatic processing: Behavior, theory, and biological mechanisms. *Cogn. Sci.* doi:10.1016/S0364-0213(03)00011-9
- Schnitzler, A., Gross, J., 2005. Normal and pathological oscillatory communication in the brain. *Nat. Rev. Neurosci.* 6, 285–96. doi:10.1038/nrn1650

- Schulman, J., Levine, S., Moritz, P., Jordan, M.I., Abbeel, P., 2015. Trust Region Policy Optimization. CoRR abs/1502.0. doi:10.1063/1.4927398
- Schulman, J., Wolski, F., Dhariwal, P., Radford, A., Klimov, O., 2017. Proximal Policy Optimization Algorithms. CoRR abs/1707.0.
- Se, D., 1993. Parkinson's Disease Society Brain Bank, London: overview and research. *J Neural Transm Suppl* 39, 165–72.
- Seeber, M., Scherer, R., Wagner, J., Solis-Escalante, T., Müller-Putz, G.R., 2015. High and low gamma EEG oscillations in central sensorimotor areas are conversely modulated during the human gait cycle. *Neuroimage* 112, 318–326. doi:10.1016/j.neuroimage.2015.03.045
- Seeman, P., 2015. Parkinson's disease treatment may cause impulse-control disorder via dopamine D3 receptors. *Synapse* 69, 183–189. doi:10.1002/syn.21805
- Sekar, M.K., Arcelus, J., Palmer, R.L., 2010. Micrographia and hypophonia in anorexia nervosa. *Int. J. Eat. Disord.* 43, 762–765. doi:10.1002/eat.20768
- Seo, D., Neely, R.M., Shen, K., Singhal, U., Alon, E., Rabaey, J.M., Carmena, J.M., Maharbiz, M.M., 2016. Wireless Recording in the Peripheral Nervous System with Ultrasonic Neural Dust. *Neuron* 91, 529–539. doi:10.1016/j.neuron.2016.06.034
- Severens, M., Nienhuis, B., Desain, P., Duysens, J., 2012. Feasibility of measuring event Related Desynchronization with electroencephalography during walking, in: *Proceedings of the Annual International Conference of the IEEE Engineering in Medicine and Biology Society, EMBS.* pp. 2764–2767. doi:10.1109/EMBC.2012.6346537
- Sharott, A., Magill, P.J., Harnack, D., Kupsch, A., Meissner, W., Brown, P., 2005. Dopamine depletion increases the power and coherence of beta-oscillations in the cerebral cortex and subthalamic nucleus of the awake rat. *Eur. J. Neurosci.* 21, 1413–1422. doi:10.1111/j.1460-9568.2005.03973.x
- Shen, D., Wu, G., Suk, H.-I., 2017. Deep Learning in Medical Image Analysis. *Annu. Rev. Biomed. Eng.* 19, 221–248. doi:10.1146/annurev-bioeng-071516-044442
- Sherrington, C.S., 1923. The Integrative Action of the Nervous System. *J. Nerv. Ment. Dis.* 57, 589. doi:10.1097/00005053-192306000-00038
- Shiffrin, R.M., Lee, M.D., Kim, W., Wagenmakers, E.-J., 2008. A survey of model evaluation approaches with a tutorial on hierarchical bayesian methods. *Cogn. Sci.* 32, 1248–84. doi:10.1080/03640210802414826
- Shik, M.L., Severin, F. V., Orlovskii, G.N., 1966. Control of walking and running by means of electrical stimulation of the mid-brain. *Biophysics (Oxf).* 11, 756–765.
- Shultz, S.J., Houglum Peggy A., 1948-, Perrin David H., 1954-, Shultz Sandra J., 1961-. Assessment of

- athletic injuries, 2005. Examination of musculoskeletal injuries, 2nd ed. ed. Champaign, Ill. ; Leeds : Human Kinetics.
- Siegel, M., Donner, T.H., Engel, A.K., 2012. Spectral fingerprints of large-scale neuronal interactions. *Nat. Rev. Neurosci.* doi:10.1038/nrn3137
- Singer, W., 1993. Synchronization of cortical activity and its putative role in information processing and learning. *Annu. Rev. Physiol.* 55, 349–374. doi:10.1146/annurev.ph.55.030193.002025
- Singh, A., Kammermeier, S., Mehrkens, J.H., Bötzel, K., 2012. Movement kinematic after deep brain stimulation associated microlesions. *J. Neurol. Neurosurg. Psychiatry* 83, 1022–1026. doi:10.1136/jnnp-2012-302309
- Singh, A., Kammermeier, S., Plate, A., Mehrkens, J.H., Ilmberger, J., Bötzel, K., 2011a. Pattern of local field potential activity in the globus pallidus internum of dystonic patients during walking on a treadmill. *Exp. Neurol.* 232, 162–167. doi:10.1016/j.expneurol.2011.08.019
- Singh, A., Levin, J., Mehrkens, J.H., Bötzel, K., 2011b. Alpha frequency modulation in the human basal ganglia is dependent on motor task. *Eur. J. Neurosci.* 33, 960–967. doi:10.1111/j.1460-9568.2010.07577.x
- Singh, A., Plate, A., Kammermeier, S., Mehrkens, J.H., Ilmberger, J., Bötzel, K., 2013. Freezing of gait-related oscillatory activity in the human subthalamic nucleus. *Basal Ganglia* 3, 25–32. doi:10.1016/j.baga.2012.10.002
- Skodda, S., Visser, W., Schlegel, U., 2011. Acoustical analysis of speech in progressive supranuclear palsy. *J. Voice* 25, 725–31. doi:10.1016/j.jvoice.2010.01.002
- Smith, S., 2002. *Digital Signal Processing: A Practical Guide for Engineers and Scientists*, Demystifying technology series.
- Smith, S.M., Miller, K.L., Salimi-Khorshidi, G., Webster, M., Beckmann, C.F., Nichols, T.E., Ramsey, J.D., Woolrich, M.W., 2011. Network modelling methods for FMRI. *Neuroimage* 54, 875–891. doi:10.1016/j.neuroimage.2010.08.063
- Smith, S.S., 1997. Step cycle-related oscillatory properties of inferior olivary neurons recorded in ensembles. *Neuroscience* 82, 69–81. doi:10.1016/S0306-4522(97)00213-3
- Spiegelhalter, D.J., Best, N.G., Carlin, B.P., van der Linde, A., 2002. Bayesian measures of model complexity and fit. *J. R. Stat. Soc.* 64, 583–639. doi:10.1111/1467-9868.00353
- Spillantini, M.G., Goedert, M., 2017. Neurodegeneration and the ordered assembly of α -synuclein. *Cell Tissue Res.* 1–12. doi:10.1007/s00441-017-2706-9
- Stamey, W., Jankovic, J., 2008. Impulse control disorders and pathological gambling in patients with Parkinson disease. *Neurologist* 14, 89–99. doi:10.1097/NRL.0b013e31816606a7

- Staub, F., Neumann, W.-J., Horn, A., Schanda, J., Schneider, G.-H., Brown, P., Kühn, A., 2016. EP 4. Long term recordings of deep brain activity from the subthalamic nucleus in PD patients using PC+S. *Clin. Neurophysiol.* 127. doi:10.1016/j.clinph.2016.05.199
- Steiner, L.A., Neumann, W.J., Staub-Bartelt, F., Herz, D.M., Tan, H., Pogosyan, A., Kuhn, A.A., Brown, P., 2017. Subthalamic beta dynamics mirror Parkinsonian bradykinesia months after neurostimulator implantation. *Mov. Disord.* 32, 1183–1190. doi:10.1002/mds.27068
- Stephan, K.E., Schlagenhauf, F., Huys, Q.J.M., Raman, S., Aponte, E.A., Brodersen, K.H., Rigoux, L., Moran, R.J., Daunizeau, J., Dolan, R.J., Friston, K.J., Heinz, A., 2017. Computational neuroimaging strategies for single patient predictions. *Neuroimage* 145, 180–199. doi:10.1016/j.neuroimage.2016.06.038
- Storzer, L., Butz, M., Hirschmann, J., Abbasi, O., Gratkowski, M., Saupe, D., Schnitzler, A., Dalal, S.S., 2016. Bicycling and Walking are Associated with Different Cortical Oscillatory Dynamics. *Front. Hum. Neurosci.* 10. doi:10.3389/fnhum.2016.00061
- Storzer, L., Butz, M., Hirschmann, J., Abbasi, O., Gratkowski, M., Saupe, D., Vesper, J., Dalal, S.S., Schnitzler, A., 2017. Bicycling suppresses abnormal beta synchrony in the Parkinsonian basal ganglia. *Ann. Neurol.* doi:10.1002/ana.25047
- Sutton, R.S., Barto, A.G., 1998. Reinforcement Learning: An Introduction. *IEEE Trans. Neural Networks* 9, 1054–1054. doi:10.1109/TNN.1998.712192
- Swann, N.C., Cai, W., Conner, C.R., Pieters, T.A., Claffey, M.P., George, J.S., Aron, A.R., Tandon, N., 2012. Roles for the pre-supplementary motor area and the right inferior frontal gyrus in stopping action: Electrophysiological responses and functional and structural connectivity. *Neuroimage* 59, 2860–2870. doi:10.1016/j.neuroimage.2011.09.049
- Syrkin-Nikolau, J., Koop, M.M., Prieto, T., Anidi, C., Afzal, M.F., Velisar, A., Blumenfeld, Z., Martin, T., Trager, M., Bronte-Stewart, H., 2017. Subthalamic neural entropy is a feature of freezing of gait in freely moving people with Parkinson's disease. *Neurobiol. Dis.* 108, 288–297. doi:10.1016/j.nbd.2017.09.002
- Takakusaki, K., Saitoh, K., Harada, H., Kashiwayanagi, M., 2004. Role of basal ganglia-brainstem pathways in the control of motor behaviors. *Neurosci. Res.* doi:10.1016/j.neures.2004.06.015
- Tan, H., Jenkinson, N., Brown, P., 2014. Dynamic neural correlates of motor error monitoring and adaptation during trial-to-trial learning. *J. Neurosci.* 34, 5678–88. doi:10.1523/JNEUROSCI.4739-13.2014
- Tan, H., Pogosyan, A., Ashkan, K., Green, A.L., Aziz, T., Foltynie, T., Limousin, P., Zrinzo, L., Hariz, M., Brown, P., 2016. Decoding gripping force based on local field potentials recorded from subthalamic nucleus in humans. *Elife* 5. doi:10.7554/eLife.19089

- Tass, P., Smirnov, D., Karavaev, A., Barnikol, U., Barnikol, T., Adamchic, I., Hauptmann, C., Pawelczyk, N., Maarouf, M., Sturm, V., Freund, H.J., Bezruchko, B., 2010. The causal relationship between subcortical local field potential oscillations and Parkinsonian resting tremor. *J. Neural Eng.* 7. doi:10.1088/1741-2560/7/1/016009
- Te Woerd, E.S., Oostenveld, R., Bloem, B.R., De Lange, F.P., Praamstra, P., 2015. Effects of rhythmic stimulus presentation on oscillatory brain activity: The physiology of cueing in Parkinson's disease. *NeuroImage Clin.* 9, 300–309. doi:10.1016/j.nicl.2015.08.018
- Temel, Y., 2013. Deep brain stimulation in animal models. *Handb. Clin. Neurol.* doi:10.1016/B978-0-444-53497-2.00002-4
- Thenganatt, M.A., Jankovic, J., 2014. Parkinson disease subtypes. *JAMA Neurol.* doi:10.1001/jamaneurol.2013.6233
- Timmermann, L., Jain, R., Chen, L., Maarouf, M., Barbe, M.T., Allert, N., Brücke, T., Kaiser, I., Beirer, S., Sejio, F., Suarez, E., Lozano, B., Haegelen, C., Vérin, M., Porta, M., Servello, D., Gill, S., Whone, A., Van Dyck, N., Alesch, F., 2015. Multiple-source current steering in subthalamic nucleus deep brain stimulation for Parkinson's disease (the VANTAGE study): A non-randomised, prospective, multicentre, open-label study. *Lancet Neurol.* 14, 693–701. doi:10.1016/S1474-4422(15)00087-3
- Timmermann, L., Wojtecki, L., Gross, J., Lehrke, R., Voges, J., Maarouf, M., Treuer, H., Sturm, V., Schnitzler, A., 2004. Ten-hertz stimulation of subthalamic nucleus deteriorates motor symptoms in Parkinson's disease. *Mov. Disord.* 19, 1328–1333. doi:10.1002/mds.20198
- Tinkhauser, G., Pogosyan, A., Little, S., Beudel, M., Herz, D.M., Tan, H., Brown, P., 2017a. The modulatory effect of adaptive deep brain stimulation on beta bursts in Parkinson's disease. *Brain* 140, 1053–1067. doi:10.1093/brain/awx010
- Tinkhauser, G., Pogosyan, A., Tan, H., Herz, D.M., Kühn, A.A., Brown, P., 2017b. Beta burst dynamics in Parkinson's disease OFF and ON dopaminergic medication. *Brain.* doi:10.1093/brain/awx252
- Tolosa, E., Gaig, C., Santamaría, J., Compta, Y., 2009. Diagnosis and the premotor phase of Parkinson disease. *Neurology.* doi:10.1212/WNL.0b013e318198db11
- Trager, M.H., Koop, M.M., Velisar, A., Blumenfeld, Z., Nikolau, J.S., Quinn, E.J., Martin, T., Bronte-Stewart, H., 2016. Subthalamic beta oscillations are attenuated after withdrawal of chronic high frequency neurostimulation in Parkinson's disease. *Neurobiol. Dis.* 96, 22–30. doi:10.1016/j.nbd.2016.08.003
- Trenado, C., 2015. Commentary: EEG beta suppression and low gamma modulation are different elements of human upright walking. *Front. Hum. Neurosci.* 9. doi:10.3389/fnhum.2015.00380
- Tresch, M.C., Saltiel, P., Bizzi, E., 1999. The construction of movement by the spinal cord. *Nat. Neurosci.* 2, 162–167. doi:10.1038/5721

- Van de Crommert, H.W., Mulder, T., Duysens, J., 1998. Neural control of locomotion: sensory control of the central pattern generator and its relation to treadmill training. *Gait Posture* 7, 251–263. doi:10.1016/S0966-6362(98)00010-1
- Van Veen, V., Carter, C.S., 2005. Separating semantic conflict and response conflict in the Stroop task: A functional MRI study. *Neuroimage* 27, 497–504. doi:10.1016/j.neuroimage.2005.04.042
- van Wijk, B.C.M., Beudel, M., Jha, A., Oswal, A., Foltynie, T., Hariz, M.I., Limousin, P., Zrinzo, L., Aziz, T.Z., Green, A.L., Brown, P., Litvak, V., 2016. Subthalamic nucleus phase–amplitude coupling correlates with motor impairment in Parkinson’s disease. *Clin. Neurophysiol.* 127, 2010–2019. doi:10.1016/j.clinph.2016.01.015
- van Wijk, B.C.M., Cagnan, H., Litvak, V., Kühn, A.A., Friston, K.J., 2018. Generic dynamic causal modelling: An illustrative application to Parkinson’s disease. *Neuroimage*. doi:10.1016/j.neuroimage.2018.08.039
- Varela, F., Lachaux, J.P., Rodriguez, E., Martinerie, J., 2001. The brainweb: Phase synchronization and large-scale integration. *Nat. Rev. Neurosci.* 2, 229–239. doi:10.1038/35067550
- Vercruyse, S., Spildooren, J., Heremans, E., Vandenbossche, J., Wenderoth, N., Swinnen, S.P., Vandenberghe, W., Nieuwboer, A., 2012. Abnormalities and Cue Dependence of Rhythmical Upper-Limb Movements in Parkinson Patients With Freezing of Gait. *Neurorehabil. Neural Repair* 26, 636–645. doi:10.1177/1545968311431964
- Vertinsky, A.T., Coenen, V.A., Lang, D.J., Kolind, S., Honey, C.R., Li, D., Rauscher, A., 2009. Localization of the subthalamic nucleus: Optimization with susceptibility-weighted phase MR imaging. *Am. J. Neuroradiol.* 30, 1717–1724. doi:10.3174/ajnr.A1669
- Wagenmakers, E.-J., 2009. Methodological and empirical developments for the Ratcliff diffusion model of response times and accuracy. *Eur. J. Cogn. Psychol.* 21, 641–671. doi:10.1080/09541440802205067
- Wagle Shukla, A., Ounpraseuth, S., Okun, M.S., Gray, V., Schwankhaus, J., Metzer, W.S., 2012. Micrographia and related deficits in Parkinson’s disease: a cross-sectional study. *BMJ Open* 2, e000628–e000628. doi:10.1136/bmjopen-2011-000628
- Wagner, J., Solis-Escalante, T., Grieshofer, P., Neuper, C., Müller-Putz, G., Scherer, R., 2012. Level of participation in robotic-assisted treadmill walking modulates midline sensorimotor EEG rhythms in able-bodied subjects. *Neuroimage* 63, 1203–1211. doi:10.1016/j.neuroimage.2012.08.019
- Walker, A.E., 1952. Cerebral pedunculotomy for the relief of involuntary movements: II. Parkinsonian tremor. *J. Nerv. Ment. Dis.* 116, 766–775. doi:10.1097/00005053-195212000-00027
- Wang, J., Nebeck, S., Muralidharan, A., Johnson, M.D., Vitek, J.L., Baker, K.B., 2016. Coordinated Reset

- Deep Brain Stimulation of Subthalamic Nucleus Produces Long-Lasting, Dose-Dependent Motor Improvements in the 1-Methyl-4-phenyl-1,2,3,6-tetrahydropyridine Non-Human Primate Model of Parkinsonism. *Brain Stimul.* 9, 609–617. doi:10.1016/j.brs.2016.03.014
- Wang, S., Aziz, T.Z., Stein, J.F., Bain, P.G., Liu, X., 2006. Physiological and harmonic components in neural and muscular coherence in Parkinsonian tremor. *Clin. Neurophysiol.* 117, 1487–1498. doi:10.1016/j.clinph.2006.03.027
- Weerasinghe, G., Duchet, B., Cagnan, H., Brown, P., Bick, C., Bogacz, R., 2018. Predicting the effects of deep brain stimulation using a reduced coupled oscillator model. *bioRxiv*. doi:10.1101/448290
- Weichwald, S., Meyer, T., Özdenizci, O., Schölkopf, B., Ball, T., Grosse-Wentrup, M., 2015. Causal interpretation rules for encoding and decoding models in neuroimaging. *Neuroimage* 110, 48–59. doi:10.1016/j.neuroimage.2015.01.036
- Weintraub, D., Koester, J., Potenza, M.N., Siderowf, A.D., Stacy, M., Voon, V., Whetteckey, J., Wunderlich, G.R., Lang, A.E., 2010. Impulse control disorders in Parkinson disease: A cross-sectional study of 3090 patients. *Arch. Neurol.* 67, 589–595. doi:10.1001/archneurol.2010.65
- Weiss, D., Klotz, R., Govindan, R.B., Scholten, M., Naros, G., Ramos-Murguialday, A., Bunjes, F., Meisner, C., Plewnia, C., Kruger, R., Gharabaghi, A., 2015. Subthalamic stimulation modulates cortical motor network activity and synchronization in Parkinson's disease. *Brain* 138, 679–693. doi:10.1093/brain/awu380
- Weiss, D., Walach, M., Meisner, C., Fritz, M., Scholten, M., Breit, S., Plewnia, C., Bender, B., Gharabaghi, A., Wächter, T., Krüger, R., 2013. Nigral stimulation for resistant axial motor impairment in Parkinson's disease? A randomized controlled trial. *Brain* 136, 2098–2108. doi:10.1093/brain/awt122
- Welter, M.-L., Schüpbach, M., Czernecki, V., Karachi, C., Fernandez-Vidal, S., Golmard, J.-L., Serra, G., Navarro, S., Welaratne, A., Hartmann, A., Mesnage, V., Pineau, F., Cornu, P., Pidoux, B., Worbe, Y., Zikos, P., Grabli, D., Galanaud, D., Bonnet, A.-M., Belaid, H., Dormont, D., Vidailhet, M., Mallet, L., Houeto, J.-L., Bardinet, E., Yelnik, J., Agid, Y., 2014. Optimal target localization for subthalamic stimulation in patients with Parkinson disease. *Neurology* 82, 1352–61. doi:10.1212/WNL.0000000000000315
- Wessel, J.R., Aron, A.R., Brown, P., Anderson, S.J., Yoshida, Y., Kawato, M., Butman, J.A., Horwitz, B., Cohen, L.G., Stein, J.S., Aziz, T.Z., 2017. On the Globality of Motor Suppression: Unexpected Events and Their Influence on Behavior and Cognition. *Neuron* 93, 259–280. doi:10.1016/j.neuron.2016.12.013
- Whelan, P.J., 1996. Control of locomotion in the decerebrate cat. *Prog. Neurobiol.* 49, 481–515.

doi:10.1016/0301-0082(96)00028-7

- Wiecki, T. V., Sofer, I., Frank, M.J., 2013. HDDM: Hierarchical Bayesian estimation of the Drift-Diffusion Model in Python. *Front. Neuroinform.* 7, 14. doi:10.3389/fninf.2013.00014
- Wieser, M., Haefeli, J., Bütler, L., Jäncke, L., Riener, R., Koeneke, S., 2010. Temporal and spatial patterns of cortical activation during assisted lower limb movement. *Exp. Brain Res.* 203, 181–191. doi:10.1007/s00221-010-2223-5
- Williams, D., Kühn, A., Kupsch, A., Tijssen, M., Van Bruggen, G., Speelman, H., Hotton, G., Loukas, C., Brown, P., 2005. The relationship between oscillatory activity and motor reaction time in the parkinsonian subthalamic nucleus. *Eur. J. Neurosci.* 21, 249–258. doi:10.1111/j.1460-9568.2004.03817.x
- Yang, A.I., Vanegas, N., Lungu, C., Zaghoul, K.A., 2014. Beta-Coupled High-Frequency Activity and Beta-Locked Neuronal Spiking in the Subthalamic Nucleus of Parkinson's Disease. *J. Neurosci.* 34, 12816–12827. doi:10.1523/JNEUROSCI.1895-14.2014
- Yang, J.F., Gorassini, M., 2006. Spinal and Brain Control of Human Walking: Implications for Retraining of Walking. *Neurosci.* 12, 379–389. doi:10.1177/1073858406292151
- Yeung, N., Cohen, J.D., Botvinick, M.M., 2011. Errors of interpretation and modeling: A reply to Grinband et al. *Neuroimage* 57, 316–319. doi:10.1016/j.neuroimage.2011.04.029
- Zaghoul, K.A., Weidemann, C.T., Lega, B.C., Jaggi, J.L., Baltuch, G.H., Kahana, M.J., 2012. Neuronal Activity in the Human Subthalamic Nucleus Encodes Decision Conflict during Action Selection. *J. Neurosci.* 32, 2453–2460. doi:10.1523/JNEUROSCI.5815-11.2012
- Zamboni, G., Huey, E.D., Krueger, F., Nichelli, P.F., Grafman, J., 2008. Apathy and disinhibition in frontotemporal dementia: Insights into their neural correlates. *Neurology* 71, 736–742. doi:10.1212/01.wnl.0000324920.96835.95
- Zavala, B., Brittain, J.-S., Jenkinson, N., Ashkan, K., Foltynie, T., Limousin, P., Zrinzo, L., Green, A.L., Aziz, T., Zaghoul, K., Brown, P., 2013. Subthalamic Nucleus Local Field Potential Activity during the Eriksen Flanker Task Reveals a Novel Role for Theta Phase during Conflict Monitoring. *J. Neurosci.* 33, 14758–14766. doi:10.1523/JNEUROSCI.1036-13.2013
- Zavala, B., Damera, S., Dong, J.W., Lungu, C., Brown, P., Zaghoul, K.A., 2015a. Human subthalamic nucleus theta and beta oscillations entrain neuronal firing during sensorimotor conflict. *Cereb. Cortex* 27, 496–508. doi:10.1093/cercor/bhv244
- Zavala, B., Tan, H., Ashkan, K., Foltynie, T., Limousin, P., Zrinzo, L., Zaghoul, K., Brown, P., 2016. Human subthalamic nucleus-medial frontal cortex theta phase coherence is involved in conflict and error related cortical monitoring. *Neuroimage* 137, 178–187. doi:10.1016/j.neuroimage.2016.05.031

- Zavala, B., Zaghoul, K., Brown, P., 2015b. The subthalamic nucleus, oscillations, and conflict. *Mov. Disord.* 30, 328–38. doi:10.1002/mds.26072
- Zavala, B.A., Tan, H., Little, S., Ashkan, K., Hariz, M., Foltynie, T., Zrinzo, L., Zaghoul, K.A., Brown, P., 2014. Midline Frontal Cortex Low-Frequency Activity Drives Subthalamic Nucleus Oscillations during Conflict. *J. Neurosci.* 34, 7322–7333. doi:10.1523/JNEUROSCI.1169-14.2014
- Zeitler, M., Tass, P.A., 2015. Augmented brain function by coordinated reset stimulation with slowly varying sequences. *Front. Syst. Neurosci.* 9, 49. doi:10.3389/fnsys.2015.00049
- Zhang, J., Rowe, J.B., 2014. Dissociable mechanisms of speed-accuracy tradeoff during visual perceptual learning are revealed by a hierarchical drift-diffusion model. *Front. Neurosci.* 8. doi:10.3389/fnins.2014.00069
- Zhang, J., Wei, L., Hu, X., Xie, B., Zhang, Y., Wu, G.-R., Wang, J., 2015. Akinetic-rigid and tremor-dominant Parkinson's disease patients show different patterns of intrinsic brain activity. *Parkinsonism Relat. Disord.* 21, 23–30. doi:10.1016/j.parkreldis.2014.10.017

Appendix I

NeuroImage: Clinical 19 (2018) 396–405



Contents lists available at ScienceDirect

NeuroImage: Clinical

journal homepage: www.elsevier.com/locate/ynicl

Subthalamic oscillatory activity and connectivity during gait in Parkinson's disease

Franz Hell^{a,b,c,*}, Annika Plate^{a,c}, Jan H. Mehrkens^b, Kai Bötzel^{a,c}^a Department of Neurology, Ludwig-Maximilians-Universität München, Marchioninistr. 15, D-81377 Munich, Germany^b Department of Neurosurgery, Ludwig-Maximilians-Universität München, Marchioninistr. 15, D-81377 Munich, Germany^c Graduate School of Systemic Neurosciences, GSN, Ludwig-Maximilians-Universität München, Grosshadernerstr. 2, D-82152 Martinsried, Germany

ARTICLE INFO

Keywords:

Deep brain stimulation
Subthalamic nucleus
Gait
Oscillations
Beta rhythm

ABSTRACT

Local field potentials (LFP) of the subthalamic nucleus (STN) recorded during walking may provide clues for determining the function of the STN during gait and also, may be used as biomarker to steer adaptive brain stimulation devices. Here, we present LFP recordings from an implanted sensing neurostimulator (Medtronic Activa PC + S) during walking and rest with and without stimulation in 10 patients with Parkinson's disease and electrodes placed bilaterally in the STN. We also present recordings from two of these patients recorded with externalized leads. We analyzed changes in overall frequency power, bilateral connectivity, high beta frequency oscillatory characteristics and gait-cycle related oscillatory activity. We report that deep brain stimulation improves gait parameters. High beta frequency power (20–30 Hz) and bilateral oscillatory connectivity are reduced during gait, while the attenuation of high beta power is absent during stimulation. Oscillatory characteristics are affected in a similar way. We describe a reduction in overall high beta burst amplitude and burst lifetimes during gait as compared to rest off stimulation. Investigating gait cycle related oscillatory dynamics, we found that alpha, beta and gamma frequency power is modulated in time during gait, locked to the gait cycle. We argue that these changes are related to movement induced artifacts and that these issues have important implications for similar research.

1. Introduction

Recordings of local field potentials (LFP) in the basal ganglia of patients with Parkinson's disease (PD) have demonstrated oscillations at several frequencies, of which the beta band has gained most attention (Stein and Bar-Gad, 2013). Although the functional and pathological role of (beta) oscillations are still debated (Espenhahn et al., 2017; Eusebio and Brown, 2009; Gross et al., 2005; Pfurtscheller et al., 1996; Raz et al., 1996), beta power has been shown to be correlated with akinetic-rigid symptoms (Hammond et al., 2007; Kühn et al., 2006b; Neumann et al., 2016) in human patients as well as in animal models of parkinsonism (Costa et al., 2006; Mallet et al., 2008; Sharott et al., 2005). Beta oscillations are also reported to be reduced in amplitude after levodopa intake and are attenuated by STN deep brain stimulation (DBS) in a stimulation intensity dependent manner (Kühn et al., 2008a, 2008b; Oswal et al., 2016; Quinn et al., 2015; Trager et al., 2016; Weiss et al., 2015).

Local field potentials are investigated as biomarkers for adaptive closed-loop stimulation in PD (Cagnan et al., 2013; Johnson et al., 2016; Little et al., 2013a; Piña-Fuentes et al., 2017; Tinkhauser et al.,

2017a). When considering oscillatory activity as a feedback signal, it is important to understand its functional role as well as its contributions to the genesis of clinical symptoms. Cortical as well as subcortical beta has been shown to be involved in a series of neural processes underlying cognitive functioning and motor behavior (Frank, 2006; Frank et al., 2007; Herz et al., 2017a; Meijer et al., 2016; Tan et al., 2014a, 2014b; Te Woerd et al., 2015; Williams et al., 2005; Zavala et al., 2013). Beta modulations are reported to be correlated with decision thresholds and reaction times as well as with grip force (Hell et al., 2018; Herz et al., 2017b; Tan et al., 2016). Beta is decreased in amplitude during motor imagery (Kühn et al., 2006a; Marceglia et al., 2009) and movements (Joundi et al., 2013; Kühn et al., 2004; Litvak et al., 2012), while this mechanism probably fails as bradykinesia increases (Steiner et al., 2017). While beta power is attenuated prior, during and shortly after movements followed by a rebound after movement termination, low frequencies in the theta range and gamma frequencies exhibit increases at movement onset (Cassidy et al., 2002; Chung et al., 2001; Foffani et al., 2005, 2003; Fogelson et al., 2005; Kane et al., 2009; Özkurt et al., 2011; Priori et al., 2002; Tan et al., 2014a, 2014b).

Reports of beta band suppression during movement are ubiquitous,

* Corresponding author at: Department of Neurology, Ludwig-Maximilians-University, Marchioninistrasse 15, D-81377 Munich, Germany.
E-mail address: Franz.Hell@med.uni-muenchen.de (F. Hell).

<https://doi.org/10.1016/j.nicl.2018.05.001>

Received 28 February 2018; Received in revised form 24 April 2018; Accepted 1 May 2018
Available online 03 May 2018

2213-1582/ © 2018 The Authors. Published by Elsevier Inc. This is an open access article under the CC BY-NC-ND license (<http://creativecommons.org/licenses/by-nc-nd/4.0/>).

but investigations of the modulation of beta during gait are rare and conflicting (Quinn et al., 2015; Singh et al., 2013; Storz et al., 2017). Quinn et al. report that subthalamic beta power was relatively similar during lying, sitting, standing, and during forward walking and that akinetic-rigid PD subjects tended to exhibit decreased beta power when walking, while tremor dominant subjects did not. Storz et al. report, that patients without freezing of gait show a suppression of beta power in both bicycling and walking, while this suppression was stronger for bicycling. Both Singh and Storz report a movement-induced, narrowband power increase in the low beta band during walking in patients with freezing of gait, time-locked to the onset of gait.

In this study, we used a sensing neurostimulator (Activa PC + S[®], Medtronic, plc.) connected to electrodes implanted bilaterally in the STN's of 10 patients with PD as well as recordings from externalized leads in two of the same patients. We investigated subthalamic oscillatory activity during continuous gait, while also comparing neural activity during gait and sitting and standing rest. Recordings were made off stimulation, with stimulation at half the clinical most beneficiary amplitude and stimulation with full amplitude. Kinematic parameters were recorded with inertial sensor units and subsequently analyzed in parallel to the electrophysiological activity to reconstruct gait-cycle related oscillatory activity. Our main aim was to discuss whether and how subthalamic frequency content changes during walking across the gait cycle as compared to rest.

2. Material and methods

2.1. Patients, surgery, electrode localization

Ten participants with a mean age of 61.7 years (SEM \pm 2.1), including 9 males and one female patient with Parkinson's disease (PD) took part in this study and gave their written informed consent. The protocol was approved by the Ethics Committee of the medical faculty of the University of Munich. Clinical details of all participants are provided in Table 1. All patients underwent implantation of DBS leads (model 3389; Medtronic Neurological Division, MN, USA) with 4 ring electrodes in the left and right STN for the treatment of advanced Parkinsonism at the Department of Neurosurgery at the hospital of the University of Munich. Initial stereotactic coordinates were 12 mm lateral, 3 mm posterior and 4 mm below the midpoint of the AC-PC line. Coordinates were adjusted by direct visualization of the STN in individual pre-operative T2-weighted MRI scans. Intraoperative single cell recordings and macrostimulation guided the final placement of the electrode leads. The exact position of the DBS electrodes in relation to the subthalamic target structures were determined based on the pre-operative T2-weighted MRI and postoperative CT scans, using the Lead DBS toolbox (Horn and Kühn, 2015) and 3DSlicer software (www.

slicer.org). MRT and CT were aligned manually using 3DSlicer software, co-registered using a two-stage linear registration (rigid followed by affine) as implemented in Advanced Normalization Tools (Avants et al., 2008) and normalized to MNI space (MNI ICBM Nonlinear 2009b template), (Fonov et al., 2011). To visualize the STN, we used an atlas to outline the STN and its putative subdivisions, the motor, the associative and the limbic area (Accolla et al., 2014).

2.2. LFP recordings and kinematic measurements

In all patients, the leads were connected to the implanted sensing neurostimulator (Activa PC + S[®], Medtronic, plc.) to record LFPs bipolarly from the electrode contact above and below the single negative stimulation contact, colored in light red (Fig. 1). The stimulation contact was chosen according to best clinical outcome. All LFP data were sampled at 422 Hz. We additionally recorded LFP data from externalized leads during the same conditions in two of these patients before implantation of the neurostimulator. Here, subthalamic LFP were recorded from the four contacts of the implanted stimulation electrodes in bipolar fashion using Brain Vision Recorder software and Brainamp amplifiers (Brain Products GmbH, Gilching, Germany). The bipolar pair containing the later stimulation electrode was chosen for evaluation. The experiments with externalized recording were performed two days after the initial surgery and the experiments with internal sensing equipment were performed at least 2 months after initial programming on the same or on consecutive days within the first year after implantation. We had to exclude recordings from one subject, as the LFP's were severely contaminated with ECG artifacts.

Movement parameters were recorded using inertial sensor units. We used a research prototype measurement and recording system with one analog gyroscope (IDG500, Invensense, Sunnyvale, CA, USA) and two analog accelerometers (ADXL335, Analog devices, Norwood, MA, USA) on each shank and each thigh to record kinematic profiles. Data were collected by a microprocessor (ATXMEGA 128, Atmel, San Jose, CA, USA) with 16 analog-digital converters (12-bit) connected to an SD-card for data storage. Data from the sensors were collected at 200 Hz. Synchronization of gait and LFP data was achieved by a transcutaneous electric nerve stimulator (TENS) device which was triggered at the beginning and before the end of the recording by the gait recording processor and delivered electric impulses between right mastoid and left shoulder which were recorded by the neurostimulator.

2.3. Task design

LFPs were recorded during sitting (2 min), standing rest (2 min) and free walking (approx. 125 m) along a hallway. Experiments were recorded following overnight withdrawal of dopaminergic medication

Table 1

Clinical details.

Ten patients with Parkinson's disease (1 female, mean age 61.7 \pm 2.1 years; disease duration 9.8 \pm 0.9 years) were studied 1 month – 1 year after DBS surgery.

Case	Age	Gender	Disease duration	Main symptoms	UPDRS-III ON/OFF	Tremor ON/OFF	Rigor ON/OFF	Gait ON/OFF	Lateralization Right/left
1	66	m	9	Equivalent	51/78	0/5	5/10	2/3	25/20
2	64	m	16	AR	23/73	0/0	3/9	1/3	23/20
3	61	m	8	TD	17/44	11/24	1/5	1/2	16/10
4	54	f	8	Equivalent	10/27	3/6	1/5	1/1	13/6
5	71	m	12	Equivalent	22/38	9/10	4/5	1/1	11/14
6	53	m	12	Equivalent	4/27	0/6	0/5	1/1	13/6
7	70	m	8	AR	23/40	0/0	7/11	1/2	15/15
8	55	m	7	Equivalent	15/33	4/10	3/8	1/2	3/12
9	66	m	11	Equivalent	26/75	6/18	1/12	2/2	7/11
10	57	m	7	AR	30/53	0/0	5/13	1/1	10/9

Evaluation was performed OFF medication after overnight withdrawal from dopaminergic medication in random order (ON/OFF DBS); Tremor score reflects the total score on all ratings in items 15–18 in the UPDRS III, rigor score reflects all ratings on item 3 and gait item 10, lateralization score reflects all scores that allow for the assessment of lateralization of Parkinsonian symptoms, including item 3–8, 15–17.

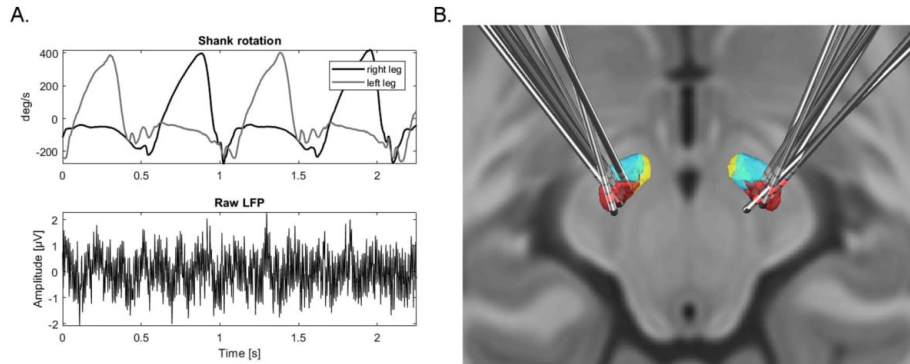


Fig. 1. Shank rotation measurements, raw LFP recordings and electrode localization. A. Shank rotation velocity of two different goniometer sensors setups mounted at right and left leg of one patient during walking and raw LFP trace from a single STN recording with Activa PC + S sensing. B. Posterior dorsal view of DBS-electrode localizations in left and right STN. The motor region of the STN is depicted in dark red, the associative subregion in light blue and limbic subregion in yellow. The contact used for stimulation is colored in light red (see text for details). (For interpretation of the references to color in this figure, the reader is referred to the web version of this article.)

and with and without DBS. DBS state (on/half/off) was changed approximately 30 min before each recording session. We conducted experiments without stimulation and with two different stimulation intensities: stimulation at the clinical optimal amplitude and half that amplitude. Stimulation frequency was 140 Hz and pulse duration was 60 μ s for all recordings. Participants were asked to walk along a corridor with slow and normal speed, turn at the end and walk back. The turn was excluded from further analysis.

3. Analysis

3.1. Analysis of kinematic measurements

First, kinematic signals were re-sampled off-line to 422 Hz to match the LFP sampling frequency. Then, rotational positions of shank and thigh were computed by Kalman filtering and the trajectory of the feet were reconstructed using a 4-segment leg model with inverse kinematics. Terminal contact (TC), peak and initial contact (IC) were defined in the shank rotational velocity signal as described previously (Bötzel et al., 2016). We used the shank rotational velocity signal to visualize the gait cycle and calculated the parameters stride length, gait velocity and foot clearing to describe the gait cycle (Bötzel et al., 2018). For statistical evaluation we computed a Wilcoxon signed rank test to test for differences between conditions. We corrected the resulting p-values with False Discovery Rate (FDR) correction for multiple comparisons (Benjamini and Yekutieli, 2005; Groppe et al., 2011). Kinematic parameters with and without stimulation during slow and normal gait are reported in Supplementary materials.

3.2. Analysis of spectral power during gait and rest

We only included recordings from Activa PC + S in the analysis, except time frequency single subject analysis. All continuous recordings were divided into equal epochs with durations of 2 s. The epochs were visually inspected for artifacts; epochs containing artifacts were discarded if they exceeded an amplitude threshold set manually for each STN recording, determined from the rest recordings. We then calculated the frequency power spectrum using fast Fourier-transform-based methods (Matlab function `fft`) and subsequently averaged over across all epochs for each nucleus. In order to control for between nucleus differences in frequency power, which can be influenced by proximity of the electrode to the LFP source and the local electrical properties of the surrounding tissue (Neumann et al., 2016), we calculated the

relative power spectrum for each recording separately. To calculate the relative spectrum, we normalized each recording by its own overall mean power across frequencies, excluding low frequencies (up to 10 Hz) and other frequencies with possible technical artifact contamination related to the sensing equipment (33–37 Hz, 48–52 Hz, 90+ Hz) (Neumann et al., 2016; Singh et al., 2013; Storz et al., 2017). To assess the effect of gait on the frequency spectrum, we conducted a one-way ANOVA with the factors gait and rest to test for differences between the average relative power in the high beta frequency band (20–30 Hz) in each nucleus, followed by a Wilcoxon signed rank test. We applied the same procedure to the factors slow gait and standing rest. To confirm this analysis, we also investigated the change of average absolute high beta power (20–30 Hz) during normal gait in % relative to sitting rest baseline across subjects, averaged across bilateral nuclei. For statistical evaluation we computed a one-sample t-test.

3.3. Instantaneous amplitude extraction

The following analyses use the instantaneous amplitude (amplitude envelope) of frequency specific activity. We used a butterworth band-pass filters (Matlab function `butter`, filter order 5, zero-phase filtering) and the Hilbert transform to extract the instantaneous amplitude (amplitude envelope) and power across time at frequencies from 3 until 100 Hz with steps of 1 Hz.

3.4. Bilateral STN amplitude-amplitude correlations

For amplitude-amplitude correlations, we computed Pearson's correlation coefficients (R) (Arnulfo et al., 2015) between bilateral STN amplitude envelope time series across frequencies, while excluding time periods with possible artifact contamination. The correlation coefficient ranges from -1 to 1 , with 0 indexing absence of correlation to 1 for perfect linear relationship and -1 for perfect anticorrelation. Correlation measures were computed separately for each subject and each resting and walking condition. To assess the modulatory effect of gait on the high beta amplitude-amplitude correlations across subjects, we conducted a one-way ANOVA to test for differences between the average correlations in the high beta frequency band (20–30 Hz) during normal gait and sitting rest without stimulation, followed by a Wilcoxon signed rank test. We applied the same procedure for testing slow gait against standing rest.

3.5. Life- and waiting-times analysis of high beta oscillation bursts

To analyze characteristics of oscillatory bursts, for each frequency and nucleus, we determined bursts based on a common median amplitude threshold across sitting rest and gait recordings, similar to recent research (Tinkhauser et al., 2017b). The epoch in which the amplitude envelope is above this threshold is considered the lifetime of a burst and the epochs below are termed waiting-times. The procedure to extract life- and waiting-times has been previously described by Montez et al. (2009). A life-/waiting-time ratio (LWR) over 1 indicates that oscillatory bursts above the threshold are longer in duration than the time-periods in which the amplitude does not cross the threshold. To evaluate the modulatory effect of gait on the high beta LWR across nuclei, we conducted a one-way ANOVA to test for differences between the average LWR in the high beta frequency band (20–30 Hz) during normal gait and sitting rest, followed by a Wilcoxon signed rank test.

3.6. High beta burst-shape analysis

To further investigate the nature of oscillatory bursts during gait as compared to rest, we studied the average shape of high beta bursts (Feingold et al., 2015). To find bursts, we marked each peak of the average high beta amplitude envelope (Matlab function `findpeaks`) and averaged across all bursts from each nucleus and condition using the timeframe of ± 30 ms around the peak. For statistical testing we used the average amplitudes across the whole epoch from each nucleus and condition for comparison. To test for differences between normal gait and sitting rest, we used a Friedman test followed by a Wilcoxon signed rank test, as data was not normally distributed (Kolmogorow-Smirnow-Test).

3.7. Gait-cycle related time-frequency power analysis

To reconstruct gait-cycle related oscillatory activity, we time-warped the shank rotational signal and the squared amplitude time course at each frequency from each gait cycle epoch, pragmatically defined as the epoch between two succeeding peaks of the rotational signal of one leg (Fig. 3A, Supplementary Fig. 3E, F). All epochs were re-sampled to a common timeframe of 100 samples, and averaged across epochs. To construct a sitting baseline, we used the same method, replacing the recordings made during gait with those during rest. For each nucleus we then calculated the mean percentage change between the gait time-frequency decomposition and the average baseline during sitting rest and gait across time for all frequencies and time points. For group analysis we then averaged across nuclei and then across subjects. For epochs starting and ending with the left leg mid-swing peak (e.g. Supplementary Fig. 3E), we used the time-frequency decomposition of the LFP from the right STN (e.g. Supplementary Fig. 3A) and vice versa (“contralateral averaging”).

To assess group differences in oscillatory activity between gait and rest across the gait cycle statistically, we first calculated the z-statistics for each time-frequency point separately (using Matlab function `signrank`) using individual time-frequency power averages across left and right nuclei. We considered the true z-value significant if it surpassed the 95% percentile of the z-statistic distribution established by testing 10,000 surrogate datasets, generated by shuffling between gait and rest averages across participants, for differences. We only considered clusters with > 20 adjacent time-frequency samples significant (Maris et al., 2007; Maris and Oostenveld, 2007).

To investigate lateralization of oscillatory activity during gait, we repeated the epoching and averaging procedure, this time using the LFP from the ipsilateral STN for the respective epochs (“ipsilateral averaging”). To compare and evaluate results, we also analyzed single subject data from recordings with externalized leads in the same fashion. We did not add these data to the group analysis.

4. Results

4.1. Patient details and localization of DBS leads

We could confirm stimulation and recording sites for all but two patients (Fig. 1). We had to exclude two subjects from localization; one subject only had a post-operative MRI image which did not allow proper electrode localization, while proper registration of MRI and post-operative CT wasn't possible in another subject because of a deformed CT scan. All but two of the analyzed stimulation contacts were placed within the motor STN (with distances between each contact center and nearest atlas voxel center below 0.5 mm). The other two had a distance of 0.9 mm and 0.54 mm and were located behind the posterior part of the STN. Overall, a mean distance of 0.19 mm (SEM ± 0.02) between each stimulation contact center and nearest atlas voxel center in the motor STN was found.

Confirming the electrode localizations, stimulation amplitudes were within normal ranges. In the condition full amplitude stimulation, which resembles clinical optimal voltage intensity, a mean constant voltage of 2.71 (± 0.15 mV) was observed on the group level. Furthermore, our cohort benefitted from stimulation as evidenced by significantly lower UPDRS-III scores with stimulation as compared to without stimulation (Wilcoxon signed rank test, $p = 0.002$, see Table 1 for clinical details) and a betterment in gait parameters (see Supplementary Fig. 1, results and discussion) with stimulation. Although patients showed minor gait impairments with varying degrees (see Table 1 for UPDRS-III scores), all patients were able to walk regularly without problems for extended periods of time.

4.2. High beta band oscillatory activity is attenuated during gait

The power-spectrum shows a significant effect in the high beta frequency range (20–30 Hz) (Fig. 2A). The average relative power in this band is reduced in amplitude during all walking conditions as compared to all resting conditions. An ANOVA with the factor task (sitting rest/normal gait) showed a significant main effect of task ($F(1, 36) = 12.38$, $p = 0.001$) on high beta band power across nuclei. A follow up Wilcoxon signed rank test confirmed significant differences ($p < 0.0001$). This difference was also significant between standing rest and slow gait ($F(1, 36) = 4.91$, $p = 0.03$; Wilcoxon signed rank test: $p < 0.0001$). No significant change was found in other frequency ranges. To supplement the relative power analysis approach and confirm results across subjects, we calculated the percent change in oscillatory power from normal gait to sitting rest in the high beta frequency range for each participant, averaging over left and right STN beforehand. Group mean percentage change from normal gait to sitting rest showed a significant attenuation of spectral power during gait as compared to rest in the high beta frequency range without stimulation (one sample t-test; $t(9) = -6.5$, $p = 0.0001$; mean = $-39.2\% \pm 6\%$).

4.3. High beta band bilateral amplitude correlations are reduced during gait

To evaluate gait-related changes in oscillatory connectivity, we compared bilateral subthalamic amplitude envelope correlations across frequencies between rest and gait (Fig. 2B). The amplitude-correlation spectrum shows a distinct effect in the high beta frequency range (20–30 Hz). Correlations are reduced in strength during walking as compared to rest. An ANOVA with the factor task (sitting rest/normal gait) showed a significant main effect of task ($F(1, 18) = 6.72$, $p = 0.02$) on average amplitude-amplitude correlations in the high beta band (20–30 Hz) across all remaining 9 participants with bilateral recordings without ECG. A follow-up Wilcoxon signed rank test confirmed significant differences ($p < 0.01$). We also evaluated differences in amplitude correlations during slow gait and standing rest. An ANOVA with the factor task (standing rest/slow gait) confirmed results with a significant main effect of task ($F(1, 18) = 6.72$, $p = 0.02$ Wilcoxon

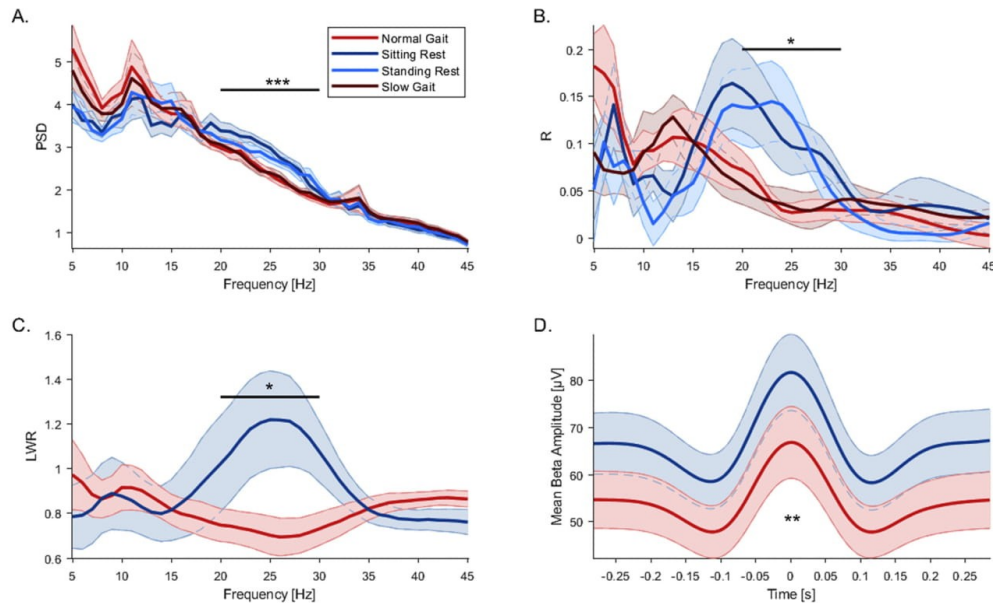


Fig. 2. Oscillatory bilateral STN frequency power, connectivity and burst analysis. A. Group relative power spectrum showing a significant difference in the high beta band 20–30 Hz. High beta power during sitting and standing rest is comparable and is attenuated during normal and slow gait. B. Group amplitude envelope correlations across frequencies between left and right STN showing significant differences between rest and gait in the high beta band. C. LWR of oscillatory bursts across frequencies during gait and sitting rest showing significant differences in the high beta band. Lifetimes of beta bursts are prolonged during rest and waiting-times are shortened as compared to gait. D. Shape of high beta bursts during rest and gait showing higher peak amplitudes and narrow in regard to burst width during rest as compared to gait. Shaded error bars indicate SEM.

signed rank test: $p = 0.02$).

4.4. High beta band burst life-times are decreased during gait

To characterize gait-related changes in high beta band burst behavior, we compared life- and waiting-times across frequencies between gait and rest (Fig. 2C). The LWR is significantly reduced in the high beta band, while during rest, life-times of high beta bursts are longer, and waiting-times are reduced as compared to gait. An ANOVA with the factor task (rest/gait) showed a significant main effect of task ($F(1, 36) = 10.88$, $p = 0.002$) on LWR in the high beta band (20–30 Hz) across all 18 nuclei. A follow up Wilcoxon signed rank test confirmed significant differences ($p = 0.01$).

4.5. High beta band burst overall amplitude is decreased during gait

To investigate high beta band burst shape, we compared the average burst amplitude in the epoch around the burst peak across patients between gait and rest (Fig. 2D). We describe that overall amplitude as well as burst width are decreased during gait. We tested overall high beta burst amplitude across the whole epoch around the burst peaks and report a significant reduction during gait ($\chi^2(2) = 9$, $p = 0.002$, Wilcoxon signed rank test: $p = 0.005$).

4.6. Time-frequency power modulation during gait

Time-frequency group analysis of gait-cycle related oscillatory activity in the STN in relation to average resting baseline shows modulation at several frequencies (Fig. 3B). While low frequencies seem increased across the whole gait cycle, alpha (8–13 Hz) and low beta (13–20 Hz) oscillations show gait-cycle locked modulations relative to the resting baseline. However, these differences are not significant on a

group level. Only high beta frequencies (20–30 Hz) show significant decreases ($p < 0.05$) across the whole gait-cycle (Fig. 3C) when compared to rest, confirming power spectral analysis results.

In relation to average gait baseline, gait-related time-frequency analysis displays a modulation pattern with alpha, beta and gamma frequency power being increased before and around the point of terminal contact of the foot contralateral to the respective STN. This lateralized modulation pattern is especially obvious when comparing contralateral and ipsilateral averaging results (Fig. 4).

This group average lateralized modulation pattern is a result of individual time-frequency modulations (see Supplementary material, Supplementary Figs. 3 and 4). Supplementary analysis shows that that signal modulations in both leads in the example subjects actually happen at the same time, regardless of laterality.

5. Discussion

This study shows that it is feasible to record neural activity from a sensing neurostimulator (Activa PC + S[®], Medtronic, plc.) in parallel with kinematic measurements in freely moving PD patients and to detect gait cycle related changes in oscillatory power. We believe caution is necessary when interpreting the origin of the signal modulations during gait and argue that our results show physiological effects as well as technical artifacts.

5.1. High beta band oscillatory activity is attenuated during gait

To investigate the function of the STN during continuous walking, we describe changes of relative spectral power and percentage change of absolute power between gait and rest. Our power spectral analysis shows a significant attenuation of subthalamic high beta frequency power on the group level (Fig. 2A) and time-frequency analysis confirm

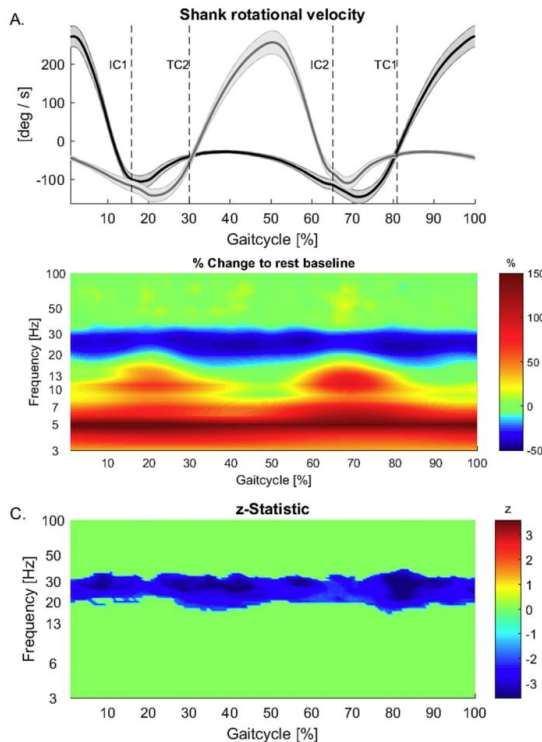


Fig. 3. A. Group shank rotation velocity. Gait cycle is epoched between the peak of the shank rotational velocity of one leg and the following peak of the same leg. Average contains epochs starting with left (e.g. Supplementary Fig. 3E) and right legs (e.g. Supplementary Fig. 3F). B, C. Time-frequency group analysis showing gait cycle locked modulation in relation to average resting using “contralateral averaging”. While high beta frequency power is attenuated across the gait cycle, low frequencies show increases. Frequencies between 8 and 20 Hz do show increases in power in the double support periods of the gait cycle. C. Group z-statistics for comparison between gait and rest showing significant decreases in power during gait in the high beta range (20–30 Hz) across the whole gait-cycle. Non significant z-values are zeroed out.

attenuation throughout the gait cycle (Fig. 3B, C). Evidence for beta power attenuation and gamma band increases in the cortex and basal ganglia during single movements come from various studies (Kühn et al., 2004; Litvak et al., 2012; Tan et al., 2016). Tan et al. described that oscillatory activity in the STN, particularly the gamma (55–90 Hz) and beta (13–30 Hz) band of the contralateral STN were most useful for decoding ipsilateral movement force during single movements. Earlier studies recording STN LFP during continuous movement suggest a reduction in beta frequency power during walking, particularly in akinetic-rigid, but not tremor dominant and freezing patients (Quinn et al., 2015; Singh et al., 2013; Storz et al., 2017).

A few factors might influence inconsistency of findings in the literature. Tan et al. report that decoding was only successful in part of the recordings in which such a pattern was visible, but not in a second cluster, in which no significant movement-related modulation was observed in either the beta or gamma band. The mean frequency spectrum of the second group showed increased activity at low frequencies, extending to 25 Hz, particularly during the force onset phase. They argue that movement related artifacts are a possible cause for their observation of low frequency power increases at the time of movement onset, which also contaminated the beta band (Tan et al., 2016). It is

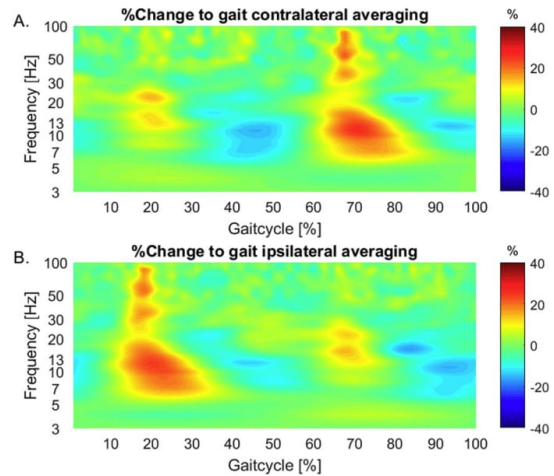


Fig. 4. A, B. Time-frequency group analysis showing gait cycle locked amplitude envelope modulation in relation to average gait baseline in alpha, beta and gamma frequencies using contralateral and ipsilateral averaging methods. For the average difference in A. signals from the left STN are used in epochs locked to right leg shank rotation peaks and right STN LFP in epochs beginning with the left foot (contralateral averaging). In B., the same analysis is presented, but using right STN LFPs for epochs which begin with right leg movement and vice versa (ipsilateral averaging).

conceivable that movement related artifacts (Fig. 4, Supplementary Figs. 3 and 4) during gait possibly also influence higher frequencies including beta and gamma and induce increases that obliterate physiological effects, therefore making it hard to detect such decreases. Another reason for the lack of consistent reports might be that these studies are conducted in PD patients, which are known to show elevated beta levels (Hammond et al., 2007). It has been shown, that excessive synchronization induced by low-frequency stimulation of subthalamic neurons at 20 Hz slows down movement in Parkinson's disease (Chen et al., 2007; Eusebio et al., 2008). Also, the development of bradykinesia during locomotion might be associated with a failure of beta attenuation. Confirming earlier reports, Steiner et al. showed that activity in the beta band was reduced during repetitive finger tapping, but re-occurred with the re-emergence of bradykinesia during prolonged tapping (Kühn et al., 2006b; Steiner et al., 2017).

5.2. High beta band bilateral connectivity is reduced during gait

With the investigation of differences in bilateral amplitude-amplitude correlations, we wanted to assess gait related changes in bilateral subthalamic oscillatory connectivity. Here, we report a reduction in bilateral amplitude-amplitude correlations in the high beta band during gait (Fig. 2B), confirming reports about movement-induced reduction in bilateral connectivity. Beta coherence between ipsilateral STN, globus pallidus internus and cortical regions has been reported to be attenuated by movement without dopaminergic medication. With medication however, beta levels are generally attenuated and power within the STN and coherence between the STN, globus pallidus internus and EEG was dominated by gamma band activity (70–85 Hz), increasing with movement (Cassidy et al., 2002; Lalo et al., 2008; Little et al., 2013b). While most studies focus on within hemisphere connectivity, other reports show that even unilateral movement results in bilateral changes in the STN, probably reflecting cortical input (Alegre et al., 2005). Niketeghad et al., report motor-modulated inter-hemispheric connectivity between bilateral STN LFP signals (Niketeghad et al., 2017). Hohlefeld and colleagues demonstrated coherence (iCOH)

between bilateral STN in the beta range (10–30 Hz). While iCOH in the 10–20 Hz frequency range positively correlated with the worsening of motor symptoms in the OFF medication condition, iCOH in the high beta range (21–30 Hz) was increased after levodopa administration (Hohlefeld et al., 2014). Hohlefeld et al. do not report on changes in oscillatory power. While this findings suggest a dissociation of low and high beta oscillations and relates only low beta oscillations to motor symptoms, our finding suggest that high beta oscillations are related to gait. The finding from Hohlefeld et al. stands in contrast with Little et al. (2013b), who also investigated the effects of levodopa medication on oscillatory power and interhemispheric connectivity in PD patients. Conversely, they report decreases in spectral power as well as decreases in standard coherence in the 13–20 Hz frequency band, but no significant changes in the high beta band. An ensuing question here is, if low and high beta band are indeed dissociable and have different functional relevance or other factors like interindividual variance (Haegens et al., 2014), small sample sizes or electrode location (Hohlefeld et al., 2014), contribute to the inconsistency and heterogeneity across reports.

5.3. High beta band burst life-times and burst amplitude are decreased during gait

Recently, it has been proposed to use pathological long beta bursts as a feedback signal for adaptive DBS (Meidahl et al., 2017; Tinkhauser et al., 2017a). The same group described that overall beta burst amplitude and duration in the STN are reduced by dopaminergic medication, while beta bursts with a long duration are decreased and short duration low amplitude bursts are increased (Tinkhauser et al., 2017b). We report that oscillatory characteristics are similarly affected during gait. We showed that the high beta burst amplitude and width is reduced during gait (Fig. 2D). Life-times of high beta bursts are reduced while waiting-times are increased, as indicated by significantly reduced LWR during gait (Fig. 2C). Together these findings indicate a reduction in burst strength and duration, mirroring differences found in recordings on and off dopaminergic medication.

5.4. Frequency modulation during gait

Here, we discuss the gait-cycle specific and seemingly lateralized modulation pattern (Fig. 4) of alpha, low beta and gamma frequencies that is time-locked to the gait-cycle. Power in alpha, beta and gamma frequencies is increased before and around the point of terminal contact of the foot contralateral to the respective STN.

Invasive electrophysiological studies reporting frequency amplitude modulations during movement and especially during gait are rare and conflicting. Androulidakis and colleagues showed that subthalamic oscillatory activity in the beta band was modulated in amplitude by finger tapping and this modulation probably failed as bradykinesia increased (Androulidakis et al., 2008). Florin et al. report increased activity in the low beta (12–18 Hz) and gamma (30–48 Hz) frequency ranges within the STN during fist flexion and extension and hypothesize that increases in gamma power enable repetitive fist movement despite increased beta levels (Florin et al., 2013). Storz et al. report gait-cycle related STN power modulations in the 24–40 Hz range, which was correlated with EMG activity (Storz et al., 2016). The same group also compared STN activity during bicycling and walking in PD patients with and without freezing of gait, affirming earlier reports. Patients without freezing of gait, in both bicycling and walking conditions, showed a suppression of subthalamic beta power (13–35 Hz). Freezers showed a similar pattern in general and an additional, movement-induced, narrowband power increase around 18 Hz time-locked to the onset of gait, reflecting earlier reports (Singh et al., 2013; Storz et al., 2017). They argue that these results indicate that bicycling facilitates overall suppression of beta power and that specifically in patients susceptible to freezing, walking leads to exaggerated synchronization in

the low beta band.

Our reported average group-level frequency dynamics seem to show a paradigmatic modulation pattern, partly overlapping with earlier studies on movement related frequency alterations. We want to argue that we are skeptical about the origin of the frequency power increases in our data and think that these considerations are relevant for similar research approaches. Previous invasive studies claim that movement related artifacts are restricted to low frequencies below 10 Hz (McCrimmon et al., 2017; Singh et al., 2011; Storz et al., 2017). However, it has been previously shown that the influences of movement artifacts in electrophysiological signals on the frequency spectrum are not restricted to low frequency oscillations, but could indeed span several frequency ranges and are possibly time-locked to the gait cycle, using scalp EEG recordings (Castermans et al., 2013, 2012; Kline et al., 2015).

The lateralized modulation pattern visible in the group average (Fig. 4) is arguably driven by differences in artifact contamination across left and right STNs in individual subjects, as evidenced by stronger modulations in both the right STN in both example subjects (see Supplementary results and discussion). We think that movement artifact related noise influences electrophysiological recordings across setups – internal or external – that involve cables that can move or can be affected by tribo-electric effects and are extremely difficult to avoid completely. Together with putative physiological signal modulations (e.g. beta-power suppression), movement artifacts can induce frequency specific biases and lead to false positive results on a group level, especially with small group sizes. Various approaches, ranging from template subtraction to independent component analysis have been used to clean recordings from movement-related artifacts, but neither could conclusively show to disentangle physiological signals from technical noise (Castermans et al., 2013; Gwin et al., 2011, 2010; Snyder et al., 2015).

5.5. Beta oscillations as input for adaptive DBS

Our results do question if a threshold based on beta band oscillations alone is appropriate to use as a feedback mechanism in closed-loop DBS (Little et al., 2013a; Meidahl et al., 2017). Beta band oscillations are not only related to symptom severity, but also to medication (Kühn et al., 2008a, 2008b; Williams et al., 2005), cognition and movement (Foffani et al., 2005; Hell et al., 2018; Herz et al., 2016). Also, PD patients for example often show multiple symptoms, a single one-dimensional biomarker might therefore be only partly useful. Beta power in the STN correlates with rigidity and bradykinesia, but not with tremor (Lenka et al., 2016; Little and Brown, 2012), which is linked to low frequency activity at tremor frequency. Moreover, movement related noise can induce tonic changes in beta levels, furthermore complicating the use of oscillatory signals for adaptive deep brain stimulation. In addition to neuronal signals, kinematic measurements that might allow for the description of movement kinematics (for an analysis of movement parameters with and without DBS, see Supplementary material) and symptom severity could be a promising alternative or additional feedback signal for use in adaptive DBS. Inertial sensor measurements have already been successfully used for adaptive stimulation in essential tremor. While recording tremor amplitude and phase with inertial sensor units, Cagnan and colleagues stimulated patients with essential tremor and thalamic electrodes at specific phases of the tremor movement, successfully reducing tremor amplitude in a subset of patients (Cagnan et al., 2013).

By integrating features from electrophysiological recordings and kinematic measurements and other sensors like electromyography, the clinical state of the patient, the severity of disease symptoms and related neural activity might be ultimately learned and related to each other, using machine learning algorithms (Schirmer et al., 2017) and causal modelling approaches (Rubenstein et al., 2017). Stimulation parameters could be varied within clinical limits and those parameters

that are associated with optimal clinical state and neural parameters could then be learned via reinforcement learning.

5.6. Study limitations

This study was conducted in patients with Parkinson's disease which are known to show aberrant subthalamic oscillatory activity (Hammond et al., 2007) and problems during walking. Although patients were investigated after overnight withdrawal of medication, they were able to walk continuously without major impairments. We could show that our leads were placed in the posterior dorsal region and putative motor part of the STN (Accolla et al., 2016). It is still debated whether the subthalamic nucleus has distinct subregions, where exactly the motor subregion resides and what oscillatory mechanisms possibly reflect different subregions, networks and processes (Coenen et al., 2009; Greenhouse et al., 2011; Groppa et al., 2014; Horn et al., 2017; Jahanshahi et al., 2015; Lambert et al., 2012; Lanciego et al., 2012; Mallet et al., 2007; Plantinga et al., 2016).

6. Conclusion

The present study provides insight into subthalamic oscillatory dynamics during walking without and with stimulation and discusses the origin of the described signal modulations. We report persistent gait related attenuation of high beta frequency oscillations throughout the gait cycle, which is absent during stimulation (see Supplementary material). High beta band power and bilateral high beta connectivity are reduced during gait and oscillatory characteristics such as high beta burst amplitude and LWR follow the same pattern. Our analysis of gait cycle related oscillatory dynamics suggest that power in alpha, beta and gamma frequencies is increased before and around the point of terminal contact of the foot contralateral to the respective STN. Although our results overlap in part with previous reports, we argue that gait cycle locked signal increases we report here are driven by movement-related artifacts.

Conflict of interest

The authors declare no competing financial interests. The Activa PC + S devices used in this study were provided by Medtronic Europe.

Acknowledgements

We thank the patients for participating in this study. We also thank Ayse Bovet, Julia Cramer and Scott Stanslaski for their help in carefully proofreading the manuscript. F.H. was supported by the Lüneburg heritage.

Appendix A. Supplementary data

Supplementary data to this article can be found online at <https://doi.org/10.1016/j.nicl.2018.05.001>.

References

Accolla, E.A., Dukart, J., Helms, G., Weiskopf, N., Kherif, F., Lutti, A., Chowdhury, R., Hetzer, S., Haynes, J.-D., Kühn, A.A., Draganski, B., 2014. Brain tissue properties differentiate between motor and limbic basal ganglia circuits. *Hum. Brain Mapp.* 35, 5083–5092. <http://dx.doi.org/10.1002/hbm.22533>.

Accolla, E.A., Herrojo Ruiz, M., Horn, A., Schneider, G.-H., Schmitz-Hübsch, T., Draganski, B., Kühn, A.A., 2016. Brain networks modulated by subthalamic nucleus deep brain stimulation. *Brain* 139, 2503–2515. <http://dx.doi.org/10.1093/brain/aww182>.

Alegre, M., Alonso-Frech, F., Rodríguez-Oroz, M.C., Guridi, J., Zamarbide, I., Valencia, M., Manrique, M., Obeso, J.A., Artieda, J., 2005. Movement-related changes in oscillatory activity in the human subthalamic nucleus: ipsilateral vs. contralateral movements. *Eur. J. Neurosci.* 22, 2315–2324. <http://dx.doi.org/10.1111/j.1460-9568.2005.04409.x>.

Androulidakis, A.G., Brücke, C., Kempf, F., Kupsch, A., Aziz, T., Ashkan, K., Kühn, A.A.,

Brown, P., 2008. Amplitude modulation of oscillatory activity in the subthalamic nucleus during movement. *Eur. J. Neurosci.* 27, 1277–1284. <http://dx.doi.org/10.1111/j.1460-9568.2008.06085.x>.

Arnulfo, G., Hirvonen, J., Nobili, L., Palva, S., Palva, J.M., 2015. Phase and amplitude correlations in resting-state activity in human stereotactical EEG recordings. *NeuroImage* 112, 114–127. <http://dx.doi.org/10.1016/j.neuroimage.2015.02.031>.

Avants, B.B., Epstein, C.L., Grossman, M., Gee, J.C., 2008. Symmetric diffeomorphic image registration with cross-correlation: evaluating automated labeling of elderly and neurodegenerative brain. *Med. Image Anal.* 12, 26–41. <http://dx.doi.org/10.1016/j.media.2007.06.004>.

Benjamini, Y., Yekutieli, D., 2005. False discovery rate-adjusted multiple confidence intervals for selected parameters. *J. Am. Stat. Assoc.* 100, 71–81. <http://dx.doi.org/10.1198/016214504000001907>.

Bötzel, K., Marti, F.M., Rodríguez, M.Á.C., Plate, A., Vicente, A.O., 2016. Gait recording with inertial sensors - how to determine initial and terminal contact. *J. Biomech.* 49, 332–337. <http://dx.doi.org/10.1016/j.jbiomech.2015.12.035>.

Bötzel, K., Olivares, A., Paulo Cunha, J., Manuel Górriz Sáez, J., Weiss, R., Plate, A., 2018. Quantification of gait parameters with inertial sensors and inverse kinematics. *J. Biomech.* <http://dx.doi.org/10.1016/j.jbiomech.2018.03.012>.

Cagnan, H., Brittain, J.-S., Little, S., Poltynie, T., Limousin, P., Zrinzo, L., Hariz, M., Joint, C., Fitzgerald, J., Green, A.L., Aziz, T., Brown, P., 2013. Phase dependent modulation of tremor amplitude in essential tremor through thalamic stimulation. *Brain* 136, 3062–3075. <http://dx.doi.org/10.1093/brain/awt239>.

Cassidy, M., Mazzone, P., Oliviero, A., Insola, A., Tonali, P., Di Lazzaro, V., Brown, P., 2002. Movement-related changes in synchronization in the human basal ganglia. *Brain* 125, 1235–1246. <http://dx.doi.org/10.1093/brain/awf135>.

Castermans, T., Duvinage, M., Cheron, G., Dutoit, T., 2012. EEG AND HUMAN LOCOMOTION descending commands and sensory feedback should be disentangled from artifacts thanks to new experimental protocols position paper. In: Proceedings of the International Conference on Bio-inspired Systems and Signal Processing, pp. 309–314. <http://dx.doi.org/10.5220/0003871403090314>.

Castermans, T., Duvinage, M., Cheron, G., Dutoit, T., 2013. Towards effective non-invasive brain-computer interfaces dedicated to gait rehabilitation systems. *Brain Sci.* 4, 1–48. <http://dx.doi.org/10.3390/brainsci4010001>.

Chen, C.C., Litvak, V., Gilbertson, T., Kühn, A., Lu, C.S., Lee, S.T., Tsai, C.H., Tisch, S., Limousin, P., Hariz, M., Brown, P., 2007. Excessive synchronization of basal ganglia neurons at 20 Hz slows movement in Parkinson's disease. *Exp. Neurol.* 205, 214–221. <http://dx.doi.org/10.1016/j.expneurol.2007.01.027>.

Chung, K.K.K., Zhang, Y., Lim, K.L., Tanaka, Y., Huang, H., Gao, J., Ross, C.A., Dawson, V.L., Dawson, T.M., 2001. Parkin ubiquitinates the α -synuclein-interacting protein, synphilin-1: implications for Lewy-body formation in Parkinson disease. *Nat. Med.* 7, 1144–1150. <http://dx.doi.org/10.1038/nm1001-1144>.

Coenen, V.A., Honey, C.R., Hurwitz, T., Rahman, A.A., McMaster, J., Bürgel, U., Mädlar, B., 2009. Medial forebrain bundle stimulation as a pathophysiological mechanism for hypomania in subthalamic nucleus deep brain stimulation for Parkinson's disease. *Neurosurgery* 64, 1106–1114. <http://dx.doi.org/10.1227/01.NEU.0000345631.54446.06>.

Costa, R.M., Lin, S.C., Sotnikova, T.D., Cyr, M., Gainetdinov, R.R., Caron, M.G., Nicoletis, M.A.L., 2006. Rapid alterations in corticostriatal ensemble coordination during acute dopamine-dependent motor dysfunction. *Neuron* 52, 359–369. <http://dx.doi.org/10.1016/j.neuron.2006.07.030>.

Espenhahn, S., de Berker, A.O., van Wijk, B.C.M., Rossiter, H.E., Ward, N.S., 2017. Movement-related beta oscillations show high intra-individual reliability. *NeuroImage* 147, 175–185. <http://dx.doi.org/10.1016/j.neuroimage.2016.12.025>.

Eusebio, A., Brown, P., 2009. Synchronisation in the beta frequency-band - the bad boy of parkinsonism or an innocent bystander? *Exp. Neurol.* 217, 1–3. <http://dx.doi.org/10.1016/j.expneurol.2009.02.003>.

Eusebio, A., Chen, C.C., Lu, C.S., Lee, S.T., Tsai, C.H., Limousin, P., Hariz, M., Brown, P., 2008. Effects of low-frequency stimulation of the subthalamic nucleus on movement in Parkinson's disease. *Exp. Neurol.* 209, 125–130. <http://dx.doi.org/10.1016/j.expneurol.2007.09.007>.

Feingold, J., Gibson, D.J., DePasquale, B., Graybiel, A.M., 2015. Bursts of beta oscillation differentiate postperformance activity in the striatum and motor cortex of monkeys performing movement tasks. *Proc. Natl. Acad. Sci.* 112, 13687–13692. <http://dx.doi.org/10.1073/pnas.1517629112>.

Florin, E., Erasmí, R., Reck, C., Maarouf, M., Schnitzler, A., Fink, G.R., Timmermann, L., 2013. Does increased gamma activity in patients suffering from Parkinson's disease counteract the movement inhibiting beta activity? *Neuroscience* 237, 42–50. <http://dx.doi.org/10.1016/j.neuroscience.2013.01.051>.

Foffani, G., Priori, A., Egidí, M., Rampini, P., Tamma, F., Caputo, E., Moxon, K.A., Cerutti, S., Barbieri, S., 2003. 300-Hz subthalamic oscillations in Parkinson's disease. *Brain* 126, 2153–2163. <http://dx.doi.org/10.1093/brain/awg229>.

Foffani, G., Bianchi, A.M., Baselli, G., Priori, A., 2005. Movement-related frequency modulation of beta oscillatory activity in the human subthalamic nucleus. *J. Physiol.* 568, 699–711. <http://dx.doi.org/10.1113/jphysiol.2005.089722>.

Fogelson, N., Pogoyan, A., Kühn, A.A., Kupsch, A., Van Bruggen, G., Speelman, H., Tijssen, M., Quararone, A., Insola, A., Mazzone, P., Di Lazzaro, V., Limousin, P., Brown, P., 2005. Reciprocal interactions between oscillatory activities of different frequencies in the subthalamic region of patients with Parkinson's disease. *Eur. J. Neurosci.* 22, 257–266. <http://dx.doi.org/10.1111/j.1460-9568.2005.04179.x>.

Fonov, V., Evans, A.C., Botteron, K., Almli, C.R., McKinstry, R.C., Collins, D.L., 2011. Unbiased average age-appropriate atlases for pediatric studies. *NeuroImage* 54, 313–327. <http://dx.doi.org/10.1016/j.neuroimage.2010.07.033>.

Frank, M.J., 2006. Hold your horses: a dynamic computational role for the subthalamic nucleus in decision making. *Neural Netw.* 19, 1120–1136. <http://dx.doi.org/10.1016/j.neunet.2006.03.006>.

- Frank, M.J., Samanta, J., Moustafa, A.A., Sherman, S.J., 2007. Hold your horses: impulsivity, deep brain stimulation, and medication in Parkinsonism. *Science* 318 (80), 1309–1312. <http://dx.doi.org/10.1126/science.1146157>.
- Greenhouse, I., Gould, S., Houser, M., Hicks, G., Gross, J., Aron, A.R., 2011. Stimulation at dorsal and ventral electrode contacts targeted at the subthalamic nucleus has different effects on motor and emotion functions in Parkinson's disease. *Neuropsychologia* 49, 528–534. <http://dx.doi.org/10.1016/j.neuropsychologia.2010.12.030>.
- Groppa, S., Herzog, J., Falk, D., Riedel, C., Deuschl, G., Volkmann, J., 2014. Physiological and anatomical decomposition of subthalamic neurostimulation effects in essential tremor. *Brain* 137, 109–121. <http://dx.doi.org/10.1093/brain/awt304>.
- Groppe, D.M., Urbach, T.P., Kutas, M., 2011. Mass univariate analysis of event-related brain potentials/fields I: a critical tutorial review. *Psychophysiology* 48, 1711–1725. <http://dx.doi.org/10.1111/j.1469-8986.2011.01273.x>.
- Gross, J., Pollok, B., Dirks, M., Timmermann, L., Butz, M., Schnitzler, A., 2005. Task-dependent oscillations during unimanual and bimanual movements in the human primary motor cortex and SMA studied with magnetoencephalography. *NeuroImage* 26, 91–98. <http://dx.doi.org/10.1016/j.neuroimage.2005.01.025>.
- Gwin, J.T., Gramann, K., Makeig, S., Ferris, D.P., 2010. Removal of movement artifact from high-density EEG recorded during walking and running. *J. Neurophysiol.* 103, 3526–3534. <http://dx.doi.org/10.1152/jn.00105.2010>.
- Gwin, J.T., Gramann, K., Makeig, S., Ferris, D.P., 2011. Electroocortical activity is coupled to gait cycle phase during treadmill walking. *NeuroImage* 54, 1289–1296. <http://dx.doi.org/10.1016/j.neuroimage.2010.08.066>.
- Haegens, S., Coussin, H., Wallis, G., Harrison, P.J., Nobre, A.C., 2014. Inter- and intra-individual variability in alpha peak frequency. *NeuroImage* 92, 46–55. <http://dx.doi.org/10.1016/j.neuroimage.2014.01.049>.
- Hammond, C., Bergman, H., Brown, P., 2007. Pathological synchronization in Parkinson's disease: networks, models and treatments. *Trends Neurosci.* <http://dx.doi.org/10.1016/j.tins.2007.05.004>.
- Hell, F., Taylor, P.C.J., Mehrkens, J.H., Bötzel, K., 2018. Subthalamic stimulation, oscillatory activity and connectivity reveal functional role of STN and network mechanisms during decision making under conflict. *NeuroImage*. <http://dx.doi.org/10.1016/j.neuroimage.2018.01.001>.
- Herz, D.M., Zavala, B.A., Bogacz, R., Brown, P., 2016. Neural correlates of decision thresholds in the human subthalamic nucleus. *Curr. Biol.* 26, 916–920. <http://dx.doi.org/10.1016/j.cub.2016.01.051>.
- Herz, D.M., Tan, H., Brittain, J.-S., Fischer, P., Cheeran, B., Green, A.L., FitzGerald, J., Aziz, T.Z., Ashkan, K., Little, S., Foltynie, T., Limousin, P., Zrinzo, L., Bogacz, R., Brown, P., 2017a. Distinct mechanisms mediate speed-accuracy adjustments in cortico-subthalamic networks. *elife* 6. <http://dx.doi.org/10.7554/eLife.21481>.
- Herz, D.M., Tan, H., Brittain, J.-S., Fischer, P., Cheeran, B., Green, A.L., FitzGerald, J., Aziz, T.Z., Ashkan, K., Little, S., Foltynie, T., Limousin, P., Zrinzo, L., Bogacz, R., Brown, P., 2017b. Distinct mechanisms mediate speed-accuracy adjustments in cortico-subthalamic networks. *elife* 6. <http://dx.doi.org/10.7554/eLife.21481>.
- Hohlefeld, F.U., Huchzermeyer, C., Huebl, J., Schneider, G.H., Brücke, C., Schönecker, T., Kühn, A.A., Curio, G., Nikulin, V.V., 2014. Interhemispheric functional interactions between the subthalamic nuclei of patients with Parkinson's disease. *Eur. J. Neurosci.* 40, 3273–3283. <http://dx.doi.org/10.1111/ejn.12686>.
- Horn, A., Kühn, A.A., 2015. Lead-DBS: a toolbox for deep brain stimulation electrode localizations and visualizations. *NeuroImage* 107, 127–135. <http://dx.doi.org/10.1016/j.neuroimage.2014.12.002>.
- Horn, A., Neumann, W.-J., Degen, K., Schneider, G.-H., Kühn, A.A., 2017. Toward an electrophysiological "sweet spot" for deep brain stimulation in the subthalamic nucleus. *Hum. Brain Mapp.* <http://dx.doi.org/10.1002/hbm.23594>.
- Jahanshahi, M., Obeso, I., Rothwell, J.C., Obeso, J.A., 2015. A fronto-subthalamic-pallidal network for goal-directed and habitual inhibition. *Nat. Rev. Neurosci.* 16, 719–732. <http://dx.doi.org/10.1038/nrn4038>.
- Johnson, L.A., Nebeck, S.D., Muralidharan, A., Johnson, M.D., Baker, K.B., Vitek, J.L., 2016. Closed-loop deep brain stimulation effects on Parkinsonian motor symptoms in a non-human primate. Is beta enough? *Brain Stimul.* 9. <http://dx.doi.org/10.1016/j.brs.2016.06.051>.
- Joundi, R.A., Brittain, J.S., Green, A.L., Aziz, T.Z., Brown, P., Jenkinson, N., 2013. Persistent suppression of subthalamic beta-band activity during rhythmic finger tapping in Parkinson's disease. *Clin. Neurophysiol.* 124, 565–573. <http://dx.doi.org/10.1016/j.clinph.2012.07.029>.
- Kane, A., Hutchison, W.D., Hodiae, M., Lozano, A.M., Dostrovsky, J.O., 2009. Dopamine-dependent high-frequency oscillatory activity in thalamus and subthalamic nucleus of patients with Parkinson's disease. *Neuroreport* 20, 1549–1553. <http://dx.doi.org/10.1097/WNR.0b013e3283282c8>.
- Kline, J.E., Huang, H.J., Snyder, K.L., Ferris, D.P., 2015. Isolating gait-related movement artifacts in electroencephalography during human walking. *J. Neural Eng.* 12, 046022. <http://dx.doi.org/10.1088/1741-2560/12/4/046022>.
- Kühn, A.A., Williams, D., Kupsch, A., Limousin, P., Hariz, M., Schneider, G.H., Yarrow, K., Brown, P., 2004. Event-related beta desynchronization in human subthalamic nucleus correlates with motor performance. *Brain* 127, 735–746. <http://dx.doi.org/10.1093/brain/awh106>.
- Kühn, A.A., Doyle, L., Pogosyan, A., Yarrow, K., Kupsch, A., Schneider, G., Hariz, M.I., Trottenberg, T., Brown, P., 2006a. Modulation of beta oscillations in the subthalamic area during motor imagery in Parkinson's disease. *Brain* 695–706. <http://dx.doi.org/10.1093/brain/awh715>.
- Kühn, A.A., Kupsch, A., Schneider, G.H., Brown, P., 2006b. Reduction in subthalamic 8–35 Hz oscillatory activity correlates with clinical improvement in Parkinson's disease. *Eur. J. Neurosci.* 23, 1956–1960. <http://dx.doi.org/10.1111/j.1460-9568.2006.04717.x>.
- Kühn, A.A., Brücke, C., Schneider, G.H., Trottenberg, T., Kivi, A., Kupsch, A., Capelle, H.H., Krauss, J.K., Brown, P., 2008a. Increased beta activity in dystonia patients after drug-induced dopamine deficiency. *Exp. Neurol.* 214, 140–143. <http://dx.doi.org/10.1016/j.expneurol.2008.07.023>.
- Kühn, A.A., Kempf, F., Brücke, C., Gaynor Doyle, L., Martinez-Torres, I., Pogosyan, A., Trottenberg, T., Kupsch, A., Schneider, G.-H., Hariz, M.I., Vandenbergh, W., Nuttin, B., Brown, P., 2008b. High-frequency stimulation of the subthalamic nucleus suppresses oscillatory beta activity in patients with Parkinson's disease in parallel with improvement in motor performance. *J. Neurosci.* 28, 6165–6173. <http://dx.doi.org/10.1523/JNEUROSCI.0282-08.2008>.
- Lalo, E., Thobois, S., Sharott, A., Polo, G., Mertens, P., Pogosyan, A., Brown, P., 2008. Patterns of bidirectional communication between cortex and basal ganglia during movement in patients with Parkinson disease. *J. Neurosci.* 28, 3008–3016. <http://dx.doi.org/10.1523/JNEUROSCI.5295-07.2008>.
- Lambert, C., Zrinzo, L., Nagy, Z., Lutti, A., Hariz, M., Foltynie, T., Draganski, B., Ashburner, J., Frackowiak, R., 2012. Confirmation of functional zones within the human subthalamic nucleus: patterns of connectivity and sub-parcellation using diffusion weighted imaging. *NeuroImage* 60, 83–94. <http://dx.doi.org/10.1016/j.neuroimage.2011.11.082>.
- Lanciego, J.L., Luquin, N., Obeso, J.A., 2012. Functional neuroanatomy of the basal ganglia. *Cold Spring Harb. Perspect. Med.* 2, a009621. <http://dx.doi.org/10.1101/cshperspect.a009621>.
- Lenka, A., Hegde, S., Jhunjhunwala, K.R., Pal, P.K., 2016. Interactions of visual hallucinations, rapid eye movement sleep behavior disorder and cognitive impairment in Parkinson's disease: a review. *Parkinsonism Relat. Disord.* 22, 1–8. <http://dx.doi.org/10.1016/j.parkrelidis.2015.11.018>.
- Little, S., Brown, P., 2012. What brain signals are suitable for feedback control of deep brain stimulation in Parkinson's disease? *Ann. N. Y. Acad. Sci.* 1265, 9–24. <http://dx.doi.org/10.1111/j.1749-6632.2012.06650.x>.
- Little, S., Pogosyan, A., Neal, S., Zavala, B., Zrinzo, L., Hariz, M., Foltynie, T., Limousin, P., Ashkan, K., Fitzgerald, J., Green, A.L., Aziz, T.Z., Brown, P., 2013a. Adaptive deep brain stimulation in advanced Parkinson disease. *Ann. Neurol.* 74. <http://dx.doi.org/10.1002/ana.23951>. (n/a-n/a).
- Little, S., Tan, H., Anzak, A., Pogosyan, A., Kühn, A., Brown, P., 2013b. Bilateral functional connectivity of the basal ganglia in patients with Parkinson's disease and its modulation by dopaminergic treatment. *PLoS One* 8, e82762. <http://dx.doi.org/10.1371/journal.pone.0082762>.
- Litvak, V., Eusebio, A., Jha, A., Oostenveld, R., Barnes, G., Foltynie, T., Limousin, P., Zrinzo, L., Hariz, M.I., Friston, K., Brown, P., 2012. Movement-related changes in local and long-range synchronization in Parkinson's disease revealed by simultaneous magnetoencephalography and intracranial recordings. *J. Neurosci.* 32, 10541–10553. <http://dx.doi.org/10.1523/JNEUROSCI.0767-12.2012>.
- Mallet, L., Schupbach, M., N'Diaye, K., Remy, P., Bardinet, E., Czernecki, V., Welter, M.-L., Pelissolo, A., Ruberg, M., Agid, Y., Yelnik, J., 2007. Stimulation of subterritories of the subthalamic nucleus reveals its role in the integration of the emotional and motor aspects of behavior. *Proc. Natl. Acad. Sci.* 104, 10661–10666. <http://dx.doi.org/10.1073/pnas.0610849104>.
- Mallet, N., Pogosyan, A., Márton, L.F., Bolam, J.P., Brown, P., Magill, P.J., 2008. Parkinsonian beta oscillations in the external globus pallidus and their relationship with subthalamic nucleus activity. *J. Neurosci.* 28, 14245–14258. <http://dx.doi.org/10.1523/JNEUROSCI.4199-08.2008>.
- Marceglia, S., Fiorio, M., Foffani, G., Mrakic-Sposta, S., Tiriticco, M., Locatelli, M., Caputo, E., Tinazzi, M., Priori, A., 2009. Modulation of beta oscillations in the subthalamic area during action observation in Parkinson's disease. *Neuroscience* 161, 1027–1036. <http://dx.doi.org/10.1016/j.neuroscience.2009.04.018>.
- Maris, E., Oostenveld, R., 2007. Nonparametric statistical testing of EEG- and MEG-data. *J. Neurosci. Methods* 164, 177–190. <http://dx.doi.org/10.1016/j.jneumeth.2007.03.024>.
- Maris, E., Schoffelen, J.M., Fries, P., 2007. Nonparametric statistical testing of coherence differences. *J. Neurosci. Methods* 163, 161–175. <http://dx.doi.org/10.1016/j.jneumeth.2007.02.011>.
- McCrinmon, C.M., Wang, P.T., Heydari, P., Nguyen, A., Shaw, S.J., Gong, H., Chui, L.A., Liu, C.Y., Nenadic, Z., Do, A.H., 2017. Electrooculographic encoding of human gait in the leg primary motor cortex. *Cereb. Cortex* 1–11. <http://dx.doi.org/10.1093/cercor/bhx155>.
- Meidahl, A.C., Tinkhauser, G., Herz, D.M., Cagnan, H., Debarros, J., Brown, P., 2017. Adaptive deep brain stimulation for movement disorders: the long road to clinical therapy. *Mov. Disord.* 32, 810–819. <http://dx.doi.org/10.1002/mds.27022>.
- Meijer, D., te Woerd, E., Praamstra, P., 2016. Timing of beta oscillatory synchronization and temporal prediction of upcoming stimuli. *NeuroImage* 138, 233–241. <http://dx.doi.org/10.1016/j.neuroimage.2016.05.071>.
- Montez, T., Poil, S.-S., Jones, B.F., Manshanden, I., Verbunt, J.P.A., van Dijk, B.W., Brussaard, A.B., van Ooyen, A., Stam, C.J., Scheltens, P., Linkenkaer-Hansen, K., 2009. Altered temporal correlations in parietal alpha and prefrontal theta oscillations in early-stage Alzheimer disease. *Proc. Natl. Acad. Sci. U. S. A.* 106, 1614–1619. <http://dx.doi.org/10.1073/pnas.0811699106>.
- Neumann, W.J., Staub, F., Horn, A., Schanda, J., Mueller, J., Schneider, G.H., Brown, P., Kühn, A.A., 2016. Deep brain recordings using an implanted pulse generator in Parkinson's disease. *NeuroImage* 19, 20–23. <http://dx.doi.org/10.1111/ner.12348>.
- Niketeghad, S., Hebb, A.O., Nedrud, J., Hanrahan, S.J., Mahoor, M.H., 2017. Motor task detection from human STN using interhemispheric connectivity. *IEEE Trans. Neural Syst. Rehabil. Eng.* <http://dx.doi.org/10.1109/TNSRE.2017.2754879>.
- Oswal, A., Beudel, M., Zrinzo, L., Limousin, P., Hariz, M., Foltynie, T., Litvak, V., Brown, P., 2016. Deep brain stimulation modulates synchrony within spatially and spectrally distinct resting state networks in Parkinson's disease. *Brain* 139, 1482–1496. <http://dx.doi.org/10.1093/brain/aww048>.

- Özkurt, T.E., Butz, M., Homburger, M., Elben, S., Vesper, J., Wojtecki, L., Schnitzler, A., 2011. High frequency oscillations in the subthalamic nucleus: a neurophysiological marker of the motor state in Parkinson's disease. *Exp. Neurol.* 229, 324–331. <http://dx.doi.org/10.1016/j.expneurol.2011.02.015>.
- Pfurtscheller, G., Stancák, A., Neuper, C., 1996. Post-movement beta synchronization. A correlate of an idling motor area? *Electroencephalogr. Clin. Neurophysiol.* 98, 281–293. [http://dx.doi.org/10.1016/0013-4694\(95\)00258-8](http://dx.doi.org/10.1016/0013-4694(95)00258-8).
- Piña-Fuentes, D., Little, S., Oerdoom, M., Neal, S., Pogoyan, A., Tijssen, M.A.J., van Laar, T., Brown, P., van Dijk, J.M.C., Beudel, M., 2017. Adaptive DBS in a Parkinson's patient with chronically implanted DBS: a proof of principle. *Mov. Disord.* <http://dx.doi.org/10.1002/mds.26959>.
- Plantinga, B.R., Temel, Y., Duchin, Y., Roebroek, A., Kuijf, M., Jahanshahi, A., ter Haar Romenij, B., Vitek, J., Harel, N., 2016. Individualized parcellation of the subthalamic nucleus in patients with Parkinson's disease with 7T MRI. *NeuroImage*. <http://dx.doi.org/10.1016/j.neuroimage.2016.09.023>.
- Priori, A., Foffani, G., Pesenti, A., Bianchi, A., Chiesa, V., Baselli, G., Caputo, E., Tamma, F., Rampini, P., Egidio, M., Locatelli, M., Barbieri, S., Scarlato, G., 2002. Movement-related modulation of neural activity in human basal ganglia and its L-DOPA dependency: recordings from deep brain stimulation electrodes in patients with Parkinson's disease. *Neurosci. Lett.* 323, s101–s102. <http://dx.doi.org/10.1007/s100720200089>.
- Quinn, E.J., Blumenfeld, Z., Velisar, A., Koop, M.M., Shreve, L.A., Trager, M.H., Hill, B.C., Kilbane, C., Henderson, J.M., Bronte-Stewart, H., 2015. Beta oscillations in freely moving Parkinson's subjects are attenuated during deep brain stimulation. *Mov. Disord.* 30, 1750–1758. <http://dx.doi.org/10.1002/mds.26376>.
- Raz, A., Feingold, A., Zelanskaya, V., Vaadia, E., 1996. Neuronal synchronization of tonically active neurons in the striatum of normal and Parkinsonian primates. *J. Neurophysiol.* 76, 2083–2088.
- Rubenstein, P.K., Weichwald, S., Bongers, S., Mooij, J.M., Janzing, D., Grosse-Wentrup, M., Schölkopf, B., 2017. Causal Consistency of Structural Equation Models.
- Schirmmeister, R.T., Springenberg, J.T., Fiederer, L.D.J., Glasstetter, M., Eggensperger, K., Tangermann, M., Hutter, F., Burgard, W., Ball, T., 2017. Deep learning with convolutional neural networks for EEG decoding and visualization. *Hum. Brain Mapp.* <http://dx.doi.org/10.1002/hbm.23730>.
- Sharott, A., Magill, P.J., Harnack, D., Kupsch, A., Meissner, W., Brown, P., 2005. Dopamine depletion increases the power and coherence of beta-oscillations in the cerebral cortex and subthalamic nucleus of the awake rat. *Eur. J. Neurosci.* 21, 1413–1422. <http://dx.doi.org/10.1111/j.1460-9568.2005.03973.x>.
- Singh, A., Levin, J., Mehrkens, J.H., Bötzel, K., 2011. Alpha frequency modulation in the human basal ganglia is dependent on motor task. *Eur. J. Neurosci.* 33, 960–967. <http://dx.doi.org/10.1111/j.1460-9568.2010.07577.x>.
- Singh, A., Plate, A., Kammermeier, S., Mehrkens, J.H., Ilmberger, J., Bötzel, K., 2013. Freezing of gait-related oscillatory activity in the human subthalamic nucleus. *Basal Ganglia* 3, 25–32. <http://dx.doi.org/10.1016/j.baga.2012.10.002>.
- Snyder, K.L., Kline, J.E., Huang, H.J., Ferris, D.P., 2015. Independent component analysis of gait-related movement artifact recorded using EEG electrodes during treadmill walking. *Front. Hum. Neurosci.* 9. <http://dx.doi.org/10.3389/fnhum.2015.00639>.
- Stein, E., Bar-Gad, I., 2013. Beta oscillations in the cortico-basal ganglia loop during parkinsonism. *Exp. Neurol.* <http://dx.doi.org/10.1016/j.expneurol.2012.07.023>.
- Steiner, L.A., Neumann, W.J., Staub-Bartelt, F., Herz, D.M., Tan, H., Pogoyan, A., Kuhn, A.A., Brown, P., 2017. Subthalamic beta dynamics mirror Parkinsonian bradykinesia months after neurostimulator implantation. *Mov. Disord.* 32, 1183–1190. <http://dx.doi.org/10.1002/mds.27068>.
- Storzer, L., Butz, M., Hirschmann, J., Abbasi, O., Gratkowski, M., Saupé, D., Schnitzler, A., Dalal, S.S., 2016. Bicycling and walking are associated with different cortical oscillatory dynamics. *Front. Hum. Neurosci.* 10. <http://dx.doi.org/10.3389/fnhum.2016.00061>.
- Storzer, L., Butz, M., Hirschmann, J., Abbasi, O., Gratkowski, M., Saupé, D., Vesper, J., Dalal, S.S., Schnitzler, A., 2017. Bicycling suppresses abnormal beta synchrony in the Parkinsonian basal ganglia. *Ann. Neurol.* <http://dx.doi.org/10.1002/ana.25047>.
- Tan, H., Jenkinson, N., Brown, P., 2014a. Dynamic neural correlates of motor error monitoring and adaptation during trial-to-trial learning. *J. Neurosci.* 34, 5678–5688. <http://dx.doi.org/10.1523/JNEUROSCI.4739-13.2014>.
- Tan, H., Zavala, B., Pogoyan, A., Ashkan, K., Zrinzo, L., Foltynic, T., Limousin, P., Brown, P., 2014b. Human subthalamic nucleus in movement error detection and its evaluation during visuomotor adaptation. *J. Neurosci.* 34, 16744–16754. <http://dx.doi.org/10.1523/JNEUROSCI.3414-14.2014>.
- Tan, H., Pogoyan, A., Ashkan, K., Green, A.L., Aziz, T., Foltynic, T., Limousin, P., Zrinzo, L., Hariz, M., Brown, P., 2016. Decoding gripping force based on local field potentials recorded from subthalamic nucleus in humans. *elife* 5. <http://dx.doi.org/10.7554/eLife.19089>.
- Te Woerd, E.S., Oostenveld, R., Bloem, B.R., De Lange, F.P., Praamstra, P., 2015. Effects of rhythmic stimulus presentation on oscillatory brain activity: the physiology of cueing in Parkinson's disease. *NeuroImage: Clin.* 9, 300–309. <http://dx.doi.org/10.1016/j.nicl.2015.08.018>.
- Tinkhauser, G., Pogoyan, A., Little, S., Beudel, M., Herz, D.M., Tan, H., Brown, P., 2017a. The modulatory effect of adaptive deep brain stimulation on beta bursts in Parkinson's disease. *Brain* 140, 1053–1067. <http://dx.doi.org/10.1093/brain/awx010>.
- Tinkhauser, G., Pogoyan, A., Tan, H., Herz, D.M., Kühn, A.A., Brown, P., 2017b. Beta burst dynamics in Parkinson's disease OFF and ON dopaminergic medication. *Brain*. <http://dx.doi.org/10.1093/brain/awx252>.
- Trager, M.H., Koop, M.M., Velisar, A., Blumenfeld, Z., Nikolau, J.S., Quinn, E.J., Martin, T., Bronte-Stewart, H., 2016. Subthalamic beta oscillations are attenuated after withdrawal of chronic high frequency neurostimulation in Parkinson's disease. *Neurobiol. Dis.* 96, 22–30. <http://dx.doi.org/10.1016/j.nbd.2016.08.003>.
- Weiss, D., Klotz, R., Govindan, R.B., Scholten, M., Naros, G., Ramos-Murguialday, A., Bunjes, F., Meissner, C., Plewnia, C., Kruger, R., Gharabaghi, A., 2015. Subthalamic stimulation modulates cortical motor network activity and synchronization in Parkinson's disease. *Brain* 138, 679–693. <http://dx.doi.org/10.1093/brain/awu380>.
- Williams, D., Kühn, A., Kupsch, A., Tijssen, M., Van Bruggen, G., Speelman, H., Hotton, G., Loukas, C., Brown, P., 2005. The relationship between oscillatory activity and motor reaction time in the Parkinsonian subthalamic nucleus. *Eur. J. Neurosci.* 21, 249–258. <http://dx.doi.org/10.1111/j.1460-9568.2004.03817.x>.
- Zavala, B., Brittain, J.-S., Jenkinson, N., Ashkan, K., Foltynic, T., Limousin, P., Zrinzo, L., Green, A.L., Aziz, T., Zaghoul, K., Brown, P., 2013. Subthalamic nucleus local field potential activity during the Eriksen flanker task reveals a novel role for Theta phase during conflict monitoring. *J. Neurosci.* 33, 14758–14766. <http://dx.doi.org/10.1523/JNEUROSCI.1036-13.2013>.

Supplementary Material

Subthalamic oscillatory activity and connectivity during gait in Parkinson's disease

Franz Hell^{1,3}, Annika Plate^{1,3}, Jan H. Mehrkens², MD, Kai Bötzel^{1,3}, MD

¹ Department of Neurology, Ludwig-Maximilians-Universität München, Marchioninstr. 15, D-81377 Munich, Germany

² Department of Neurosurgery, Ludwig-Maximilians-Universität München, Marchioninstr. 15, D-81377 Munich, Germany

³ Graduate School of Systemic Neurosciences, GSN, Ludwig-Maximilians-Universität München, Grosshadernerstr. 2, D-82152 Martinsried, Germany

Corresponding author: Franz Hell

Department of Neurology,

Ludwig-Maximilians-University, Marchioninstrasse 15, D-81377 Munich / Germany

E-Mail: Franz.Hell@med.uni-muenchen.de

Corresponding author: Franz Hell

Department of Neurology,

Ludwig-Maximilians-University of Munich, Marchioninstrasse 15, D-81377 Munich / Germany

E-Mail: Franz.Hell@med.uni-muenchen.de

Supplementary Methods

The effect of stimulation on oscillatory activity in the STN

To assess the effect of stimulation, we compared normalized power spectra during rest recorded without, with stimulation at half amplitude and with stimulation at full clinical beneficiary amplitude. Similar to the approach used by Neumann et al. (Neumann et al., 2016), we normalized individual power spectra to average of total power over the 10-32 Hz, 38-45 Hz, 55-87 Hz and 73-95 Hz ranges for each contact-pair. We omitted the frequency ranges between 0-10 Hz, 46-54 Hz, 33-37 Hz and 68-72 Hz ranges to avoid contamination by mains noise, movement artefacts, artefacts in the sub-harmonic range of 140 Hz DBS and low frequency noise due to an interaction of the sampling rate of 422 Hz and stimulation frequency (Neumann et al., 2016). To assess the effect of stimulation on beta power (13-30 Hz) on a group level, we conducted a one-way ANOVA, followed by a Wilcoxon signed rank test to confirm differences between stimulation states. Multiple comparisons were corrected using FDR correction.

To investigate the effect of stimulation on gait related high beta band attenuation, we computed the change of raw power in percent for each subject from gait to rest in the high beta frequency range (20-30) Hz for each stimulation setting and averaged across subjects. To assess the effect of stimulation on the gait-related high beta frequency modulation statistically, we conducted a one-way ANOVA, followed by a Wilcoxon signed rank test to confirm differences between stimulation states. Multiple comparisons were corrected using FDR correction.

Supplementary Results

Kinematic parameters during slow and normal walking with and without stimulation

We report that the kinematic parameters stride length, gait velocity and foot clearing are affected by DBS treatment (Figure 1). Stride length during slow as well as normal walking is significantly higher during stimulation on as compared to stimulation off. A Wilcoxon signed rank test confirmed significant differences for slow ($p < 0.03$) and normal gait ($p < 0.03$). Gait velocity during slow as well as normal walking is slightly higher with as compared to without stimulation, however, a Wilcoxon signed rank test did not show significant differences for slow ($p = 0.2$) and normal gait ($p = 0.12$). Foot clearing during slow as well as normal walking is significantly higher with stimulation, a Wilcoxon signed rank test confirmed significant differences for slow ($p = 0.04$) and normal gait ($p = 0.02$). Stride length ($p < 0.03$, $p < 0.003$) and gait velocity ($p < 0.003$, $p <$

0.003) are significantly higher during normal walking as compared to slow walking in both stimulation conditions.

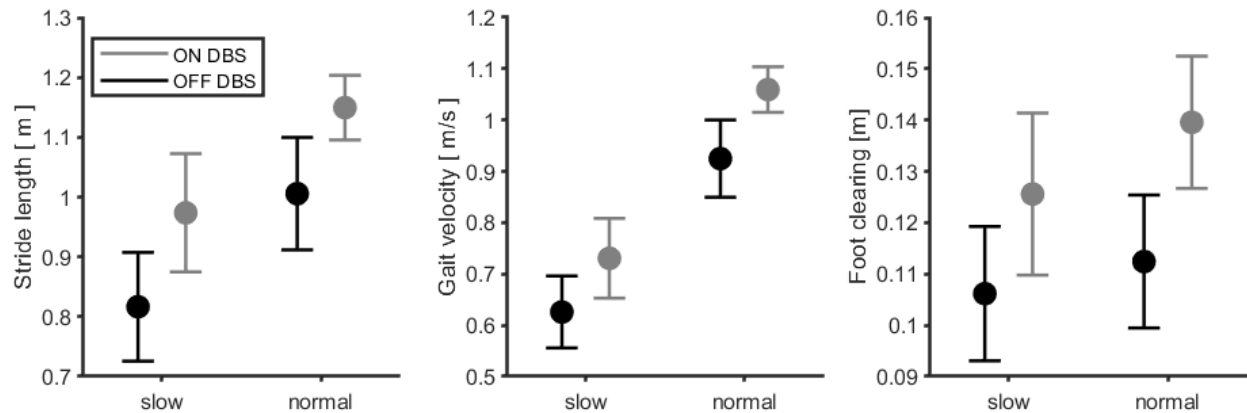


Figure 1. Kinematic parameters during slow and normal walking with and without DBS. Stride length, gait velocity and foot clearing are reduced during slow and normal gait without stimulation as compared to stimulation. Gait velocity was lower during slow as compared to normal walking across stimulation states. Error bars indicate 95% confidence intervals.

The effect of stimulation on oscillatory activity in the STN

A comparison of relative frequency power between different stimulation states in our recordings shows that beta band power (13 – 30 Hz) gets diminished in a voltage dependent manner with stimulation (Figure 2 A). There was a statistically significant main effect of stimulation on beta band power as determined by one-way ANOVA ($F(2,57) = 17.18$, $p < .000002$) across nuclei. Comparing the effect between all three stimulation conditions using a Wilcoxon signed rank test, a significant reduction from no stimulation to half-amplitude stimulation ($p = 0.002$) and a significant reduction from no stimulation to full stimulation ($p = 0.001$) and half stimulation and full stimulation ($p = 0.003$) can be observed.

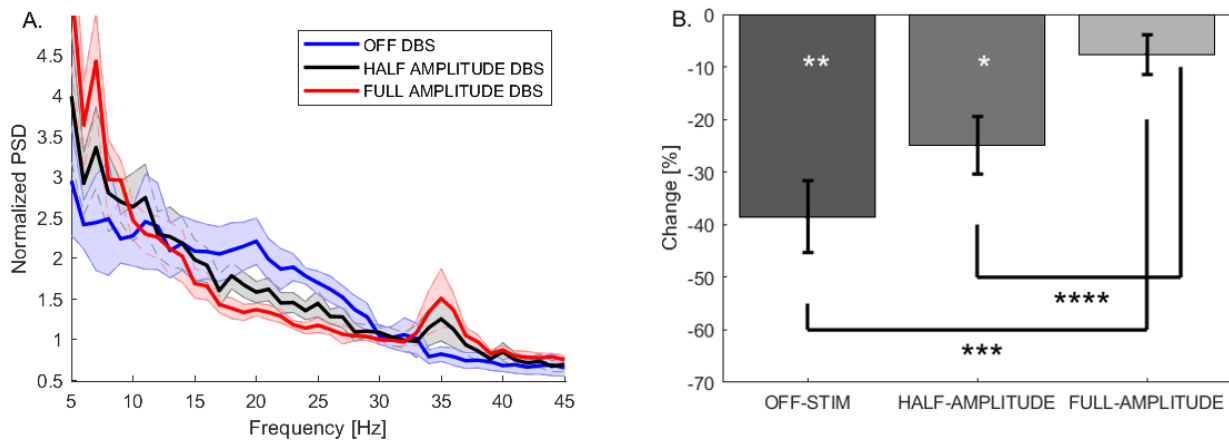


Figure 2. The effect of stimulation on oscillatory activity in the STN during rest and gait. A. Normalized STN power spectrum during rest without, with half and full clinical beneficiary stimulation amplitudes. Beta power (13 - 30 Hz) is attenuated in a voltage dependent manner. B. Gait related attenuation of high beta band power vanishes in a voltage-dependent manner. While the high beta frequency band between 20 and 30 Hz is attenuated during gait as compared to rest without and with stimulation with half amplitude, this difference is absent during stimulation with the full clinical beneficiary amplitude. Error intervals and bars indicate 95% confidence intervals.

To investigate the attenuating effect of gait on high beta band oscillations, we evaluated the high beta frequency range between 20 and 30Hz between stimulation conditions in terms of percentage change (see Figure 2 B). There was a statistically significant difference in the gait-related high beta band attenuation between stimulation conditions as determined by one-way ANOVA ($F(2,57) = 21.1$, $p < .00004$). Comparing the effect between all three stimulation conditions using a Wilcoxon signed rank test, a slight reduction from no stimulation (mean = $-39.2\% \pm 5.9\%$) to half-amplitude stimulation (mean = $-24.8\% \pm 5.2\%$; $p = 0.05$) of $\sim 14\%$ and a strong significant difference between no stimulation and full stimulation (mean = $-7.5\% \pm 4\%$) of $\sim 32\%$ ($p = 0.005$) and half stimulation and full stimulation of 17% ($p = 0.02$) can be observed (see Figure 2).

Time-Frequency power modulation during gait – origin of signal

The group average lateralized modulation pattern (Figure 4) is a result of individual time-frequency modulations (Supplementary Figure 4). Note that signal modulations in both leads in the example subjects actually happen at the same time, regardless of laterality.

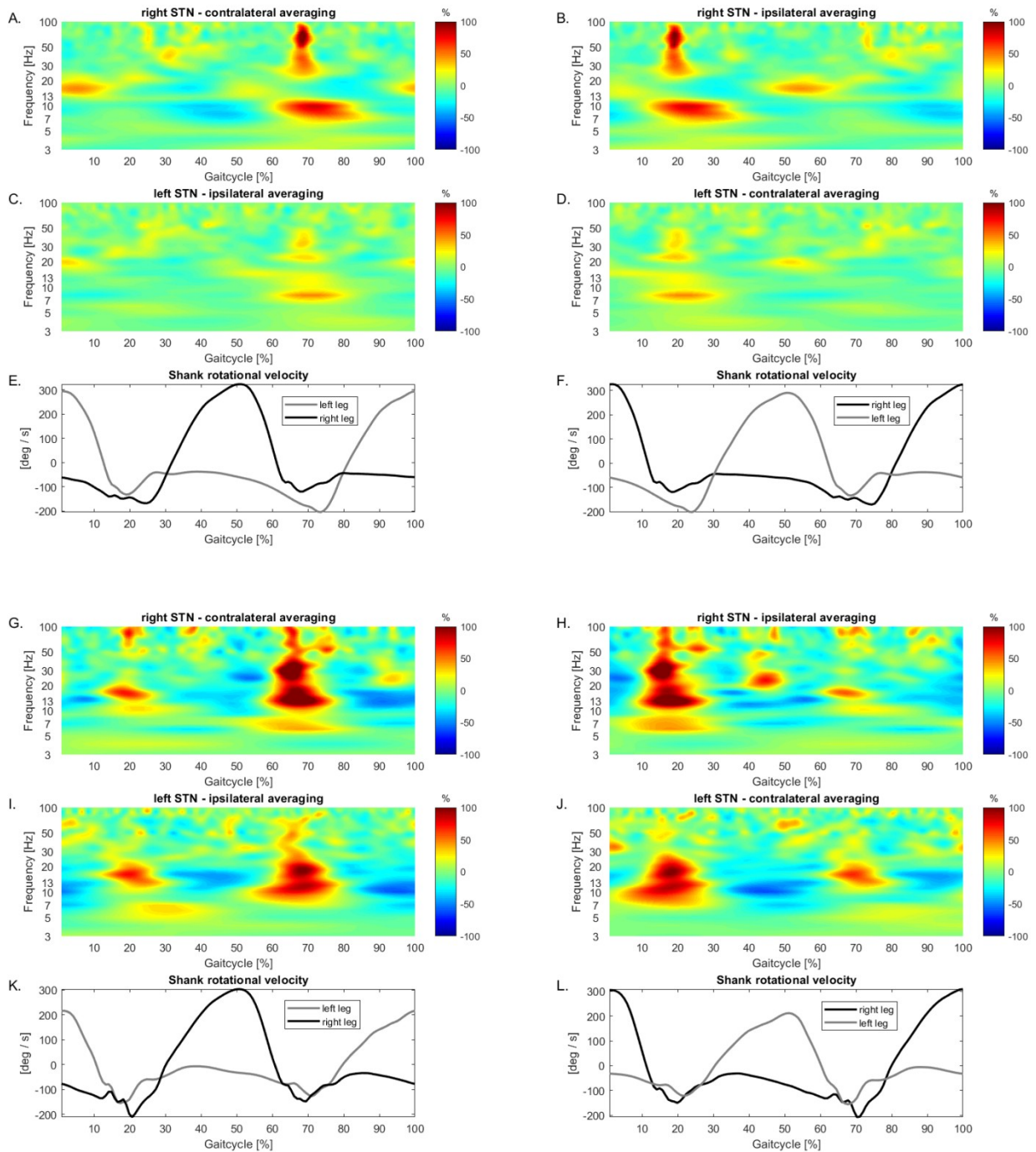


Figure 3. A-L. Modulations of left and right subthalamic time-frequency power in two paradigmatic single subjects during gait cycle recorded with Activa PC + S. A & B, G & H: Time-frequency analysis showing average gait cycle

locked modulation in relation to average baseline during gait across time for the right STN time-locked to epochs beginning with left (contralateral averaging) and right leg (ipsilateral averaging) movement. C & D, I & J showing the same for the left STNs averaged to epochs beginning with the left leg (ipsilateral averaging) and right leg (contralateral averaging). A & C and B & D as well as G & I and H & J represent averages using the same epochs, while A & B, C & D, G & H and I & J are on step off in time. Note that signal modulations happen at the same time, regardless of laterality. E & F and K & L are showing the average shank rotational velocity of both legs across epochs of the gait cycle used for averaging in the two time-frequency plots right above these plots.

When comparing activity in the left STN averaged to the gait-cycle beginning with the right leg to activity in the right STN locked to the same epochs (e.g. Supplementary Figure 3/4 B & D, H & J), it is apparent that both STN do show amplitude increases across frequencies at the same time. The laterality modulation pattern visible in the group average (Figure 4) is arguably driven by differences in the modulation strength across left and right STNs in individual subjects, as evidenced by stronger modulations in both the right STN in both example subjects, resulting in an average lateralized modulation pattern. While some subjects show modulations in one or both leads, others show gait-cycle locked signal modulations in none of the leads, together driving the lateralized group average. We found that 7 out of 20 leads recorded with Activa PC+S did show such a paradigmatic modulation pattern. To compare the signal modulations recorded with internal and externalized sensing equipment, we also present results from two subjects recorded with externalized leads after surgery (Supplementary Figure 3). Signal increases with both recording setups appear at the same time during the gait cycle and are similar in frequency content (Supplementary Figure 3 and 4). Comparing signal modulations within one subject recorded with both setups we describe that although signal modulations appear at the same time, they are similar but not completely matching in frequency content and are arguably greater in terms of the size of the change with externalized sensing equipment (Supplementary Figure 3 A – F and Supplementary Figure 4 A – F). We find a similar pattern in the majority of externalized recordings during gait including previously published recordings ((Singh et al., 2013); results not reported).

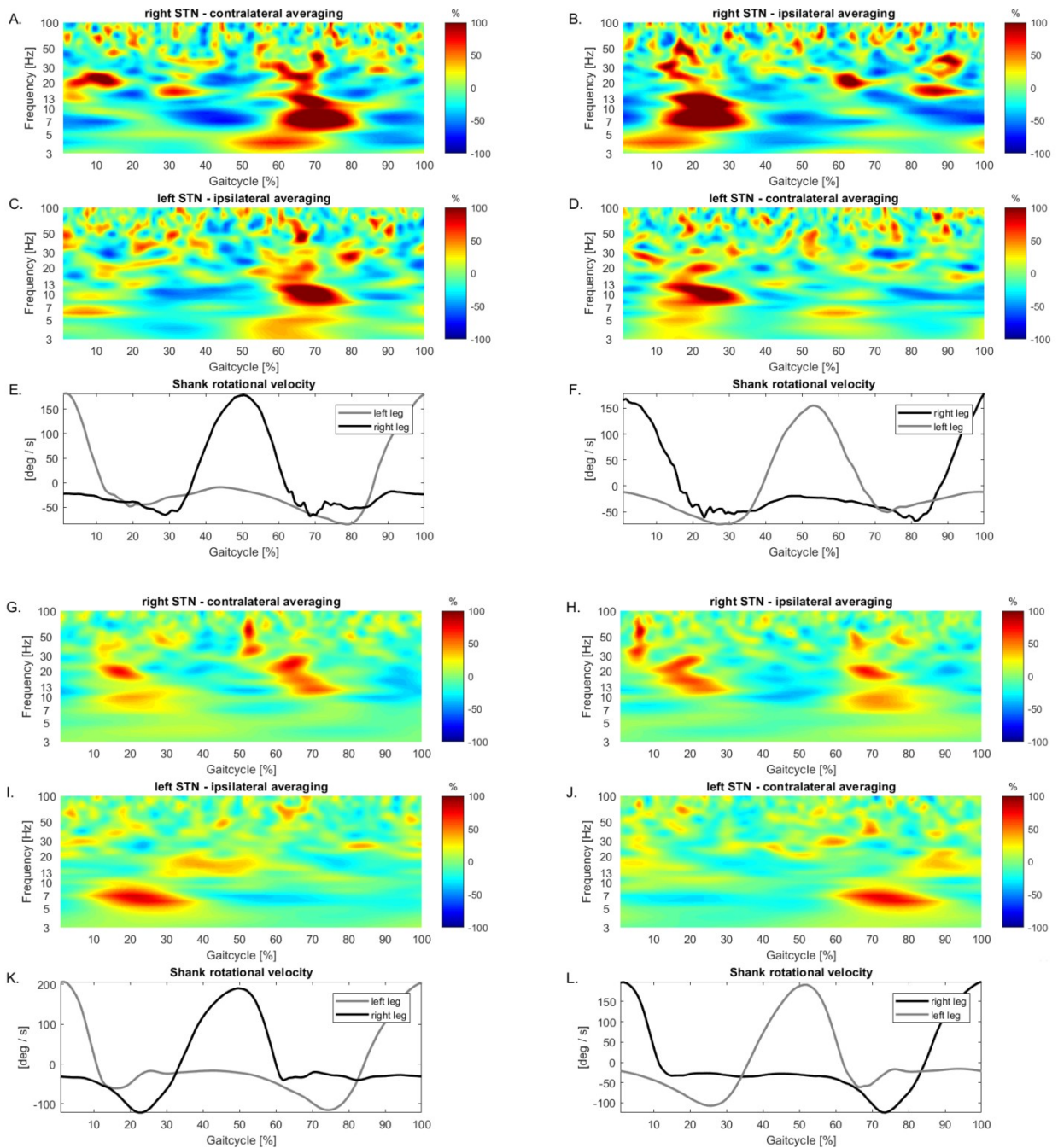


Figure 4. A-F. Modulations of left and right subthalamic time-frequency power in two single subjects during gait cycle recorded with externalized leads. A & B, G & H: Time-frequency analysis showing average gait cycle locked modulation in relation to average baseline during gait across time for the right STN time-locked to epochs beginning with left (contralateral averaging) and right leg (ipsilateral averaging) movement. C & D, I & J showing the same for the left STNs averaged to epochs beginning with the left leg (ipsilateral averaging) and right leg (contralateral averaging). A & C and B & D as well as G & I and H & J represent averages using the same epochs, while A & B, C & D, G & H and I & J are on step off in time. Note that signal modulations happen at the same time, regardless of laterality. E & F and K & L are showing the average shank rotational velocity of both legs across epochs of the gait cycle used for averaging in the two time-frequency plots right above these plots. A-F represents the same subject shown in A – F in Figure 3.

Supplementary Discussion

Kinematic parameters during slow and normal walking with and without stimulation

We report that DBS improves stride length and increases gait velocity, although the latter finding did not reach significance in our small group. We add that foot clearing is improved by DBS. Generally, PD patients show significantly slower gait velocity, with smaller stride lengths and less foot clearance as compared to healthy controls (Hausdorff, 2009; Morris et al., 1994b). Overall, DBS improves balance control and gait parameters such as stride length and gait velocity (Collomb-Clerc and Welter, 2015). Roper and colleagues report that DBS improves gait velocity, regardless of whether the patients were tested in the on or off medication state (Roper et al., 2016).

DBS suppresses beta oscillations and gait related high beta band suppression is absent during stimulation

By comparing rest and gait recordings under different stimulation settings, we want to assess the effect of stimulation on oscillatory activity in the STN and if the gait related attenuation of high beta band activity is preserved during stimulation.

It has been demonstrated with recordings from externalized leads as well as with implanted sensing neurostimulators, that high frequency STN DBS attenuates STN beta frequency power in a voltage-dependent manner (Kühn et al., 2008; Neumann et al., 2016) with a concurrent improvement of motor impairment. Here we confirm the finding that beta oscillations are reduced during stimulation and show that it is possible to detect gait related activity even during stimulation, provided the intensity of the stimulation hasn't reached its full therapeutic amplitude. With full amplitude, however, there seems to be no attenuation of beta frequency.

Our findings do speak indirectly for the hypothesis that diminishing beta band synchrony by means of DBS high frequency stimulation improves Parkinsonian symptoms. All of our patients did profit from DBS therapy indexed by significant improvement of UPDRS-III scores with stimulation and showed improved gait parameters. It can be argued, that during stimulation, the need to suppress pathological beta oscillations might be gone, as they are diminished by stimulation. However, it could also be that the noise level of the signals that are recorded during stimulation due to stimulation artifacts, signal saturation and other technical issues challenge the assessment of physiological effects.

Time-Frequency power modulation during gait – origin of signal

In our analysis, the average modulation pattern visible in the group average is most likely a result of individual time-frequency modulations caused by movement induced artifacts. We describe that signal increases actually happen at the same time in the gait cycle and are visible in left and right STN at the same exact time (Supplementary Figure 3 & 4) with internal as well as with external recording equipment. We argue that the exact pattern of movement related signal alterations in time in the raw recordings due to upper body movement – which is arguably coordinated in time to the gait cycle (Romkes and Bracht-Schweizer, 2017), lead jitters, slow or sudden cable movements or tribo-electric effects influence the raw signal shape and resulting time-frequency decomposition. Depending on the exact shape of the artifacts in time, low frequency as well as frequency spanning and high frequency power can be induced (Smith, 2002).

Supplementary References

- Collomb-Clerc, A., Welter, M.-L., 2015. Effects of deep brain stimulation on balance and gait in patients with Parkinson's disease: A systematic neurophysiological review. *Neurophysiol. Clin. Neurophysiol.* 45, 371–388. doi:10.1016/j.neucli.2015.07.001
- Hausdorff, J.M., 2009. Gait dynamics in Parkinson's disease: Common and distinct behavior among stride length, gait variability, and fractal-like scaling. *Chaos* 19. doi:10.1063/1.3147408
- Kühn, A. a, Kempf, F., Brücke, C., Gaynor Doyle, L., Martinez-Torres, I., Pogosyan, A., Trottenberg, T., Kupsch, A., Schneider, G.-H., Hariz, M.I., Vandenberghe, W., Nuttin, B., Brown, P., 2008. High-frequency stimulation of the subthalamic nucleus suppresses oscillatory beta activity in patients with Parkinson's disease in parallel with improvement in motor performance. *J. Neurosci.* 28, 6165–6173. doi:10.1523/JNEUROSCI.0282-08.2008
- Morris, M.E., Iansek, R., Matyas, T.A., Summers, J.J., 1994. The pathogenesis of gait hypokinesia in parkinson's disease. *Brain* 117, 1169–1181. doi:10.1093/brain/117.5.1169
- Neumann, W.J., Staub, F., Horn, A., Schanda, J., Mueller, J., Schneider, G.H., Brown, P., Kühn, A.A., 2016. Deep brain recordings using an implanted pulse generator in Parkinson's disease. *Neuromodulation* 19, 20–23. doi:10.1111/ner.12348
- Romkes, J., Bracht-Schweizer, K., 2017. The effects of walking speed on upper body kinematics during gait in healthy subjects. *Gait Posture* 54, 304–310. doi:10.1016/j.gaitpost.2017.03.025
- Roper, J.A., Kang, N., Ben, J., Cauraugh, J.H., Okun, M.S., Hass, C.J., 2016. Deep brain stimulation improves gait velocity in Parkinson's disease: a systematic review and meta-analysis. *J. Neurol.* 263, 1195–1203. doi:10.1007/s00415-016-8129-9
- Singh, A., Plate, A., Kammermeier, S., Mehrkens, J.H., Ilmberger, J., Bötzel, K., 2013. Freezing of gait-related oscillatory activity in the human subthalamic nucleus. *Basal Ganglia* 3, 25–32. doi:10.1016/j.baga.2012.10.002
- Smith, S.W., 2003. *Digital Signal Processing: A Practical Guide for Engineers and Scientists*, IEEE Signal Processing Magazine.

Appendix II

NeuroImage 171 (2018) 222–233



Contents lists available at ScienceDirect

NeuroImage

journal homepage: www.elsevier.com/locate/neuroimage

Subthalamic stimulation, oscillatory activity and connectivity reveal functional role of STN and network mechanisms during decision making under conflict



Franz Hell^{a,c,*}, Paul C.J. Taylor^{a,c,d}, Jan H. Mehrkens^b, Kai Bötzel^{a,c}

^a Department of Neurology, Ludwig-Maximilians-Universität München, Marchioninistr. 15, D-81377 Munich, Germany

^b Department of Neurosurgery, Ludwig-Maximilians-Universität München, Marchioninistr. 15, D-81377 Munich, Germany

^c Graduate School of Systemic Neurosciences, GSN, Ludwig-Maximilians-Universität München, Grosshadernerstr. 2, D-82152 Martinsried, Germany

^d German Center for Vertigo and Balance Disorders, Ludwig-Maximilians-Universität München, Marchioninistr. 15, D-81377 Munich, Germany

ARTICLE INFO

Keywords:

Conflict
Inhibition
Deep brain stimulation
Oscillations
Connectivity

ABSTRACT

Inhibitory control is an important executive function that is necessary to suppress premature actions and to block interference from irrelevant stimuli. Current experimental studies and models highlight proactive and reactive mechanisms and claim several cortical and subcortical structures to be involved in response inhibition. However, the involved structures, network mechanisms and the behavioral relevance of the underlying neural activity remain debated. We report cortical EEG and invasive subthalamic local field potential recordings from a fully implanted sensing neurostimulator in Parkinson's patients during a stimulus- and response conflict task with and without deep brain stimulation (DBS). DBS made reaction times faster overall while leaving the effects of conflict intact: this lack of any effect on conflict may have been inherent to our task encouraging a high level of proactive inhibition. Drift diffusion modelling hints that DBS influences decision thresholds and drift rates are modulated by stimulus conflict. Both cortical EEG and subthalamic (STN) LFP oscillations reflected reaction times (RT). With these results, we provide a different interpretation of previously conflict-related oscillations in the STN and suggest that the STN implements a general task-specific decision threshold. The timecourse and topography of subthalamic-cortical oscillatory connectivity suggest the involvement of motor, frontal midline and posterior regions in a larger network with complementary functionality, oscillatory mechanisms and structures. While beta oscillations are functionally associated with motor cortical-subthalamic connectivity, low frequency oscillations reveal a subthalamic-frontal-posterior network. With our results, we suggest that proactive as well as reactive mechanisms and structures are involved in implementing a task-related dynamic inhibitory signal. We propose that motor and executive control networks with complementary oscillatory mechanisms are tonically active, react to stimuli and release inhibition at the response when uncertainty is resolved and return to their default state afterwards.

Introduction

Inhibitory control is a vital executive function that is needed to suppress premature actions and to block interference from irrelevant stimuli. Inhibitory control is impaired in a number of neuropsychiatric and neurological disorders and is associated with disrupted neural activity in the cortico-striatal circuitry (Antonelli et al., 2011; Lipszyc and Schachar, 2010; Richardson, 2008; Zamboni et al., 2008). Computational models as well as experimental studies in humans and primates highlight several cortical regions, particularly frontal and parietal cortices (Botvinick et

al., 2004; Cohen and Ridderinkhof, 2013; Liston et al., 2006; Zavala et al., 2016) and subcortical structures, especially the basal ganglia, in inhibitory control (Aron et al., 2007; Benis et al., 2014; Cavanagh et al., 2011; Frank, 2006; Zaghoul et al., 2012). Optimal action selection in conflict situations with competing or uncertain stimulus and response relations is proposed to rely on an intact hyperdirect pathway and STN (for an overview of cortico-basal ganglia-thalamo-cortical pathways and structures, see (Jahanshahi et al., 2015)). By inhibiting the pallidum-thalamic-cortical loop, the STN is thought to suspend responses until sufficient information has been integrated and uncertainty is

* Corresponding author. Department of Neurology, Ludwig-Maximilians-University, Marchioninistrasse 15, D-81377 Munich, Germany.
E-mail address: Franz.Hell@med.uni-muenchen.de (F. Hell).

<https://doi.org/10.1016/j.neuroimage.2018.01.001>

Received 12 September 2017; Received in revised form 27 November 2017; Accepted 1 January 2018

Available online 4 January 2018

1053-8119/© 2018 Elsevier Inc. All rights reserved.

resolved (Bogacz and Gurney, 2007; Frank et al., 2007; Herz et al., 2017).

Electrophysiological recordings during inhibitory processes have demonstrated conflict and inhibition related oscillatory activity and connectivity within cortical and subcortical networks involved in reactive as well as proactive inhibition (Benis et al., 2014; Martínez-Selva et al., 2006; Zavala et al., 2015a, 2015b, 2014). Increases in cortical and subthalamic low frequency oscillations including delta and theta frequencies (2–8 Hz) and decreases in alpha/beta frequency (10–30 Hz) power have been shown to be involved in inhibitory processes and are reported to be correlated with conflict (Bastin et al., 2014; Boulinguez et al., 2009; Cavanagh and Frank, 2014; Kühn et al., 2004; Leventhal et al., 2012; Swann et al., 2012). Coherent low frequency activity has been shown between frontal midline structures and the STN (Herz et al., 2017) and beta oscillatory coupling is reported to be most prominent between STN and motor cortical structures (Accolla et al., 2016).

There are two major theoretical mechanisms discussed for response inhibition: proactive and reactive inhibitory control (Martínez-Selva et al., 2006). In the reactive model established by Frank et al. (Frank, 2006), response inhibition is implemented as response selection processes evolve. The global inhibitory signal is described as reactive in nature and is triggered by the stimulus conflict (Aron et al., 2007). In contrast, the “proactive inhibition” theory assumes that inhibition is the default mode of an executive control network responsible for basic preparatory processes, which prevents automatic responses to irrelevant signals by maintaining tonic inhibition over response processes until uncertainty is resolved (Jaffard et al., 2008).

Both theories assume a global modulatory signal suppressing all responses, rather than modulating the execution of any particular response and postulate attenuation of thalamocortical activity, with different cortical structures involved. The reactive model claims specific changes in primary motor cortex (PMC), pre-supplementary motor area (pre-SMA), the anterior cingulate cortex (ACC), and the inferior frontal gyrus (IFG) (Frank, 2006). The “proactive inhibition” hypothesis is linked to possible activation changes in medial prefrontal cortex (mPFC), Pre-cuneus, posterior cingulate cortex (PCC), and inferior parietal cortex (IPC) (Ballanger et al., 2009; Boulinguez et al., 2009; Jaffard et al., 2008). Hence, while both models claim frontal structures to be involved, only the proactive model invokes posterior structures, which have been shown to be important for movement initiation and planning (Mattingley et al., 1998; Scherberger et al., 2005).

To elucidate the functional role of the STN in cognitive control, we collected subthalamic local field potentials (LFP) from a fully implanted sensing neurostimulator and parallel EEG recordings in patients with Parkinson's disease (PD) during a modified version of an Eriksen Flanker task inducing different levels of conflict (Van Veen and Carter, 2005). We measured whether the STN oscillatory signal reflects reaction times and stimulus conflict, whether STN DBS influences conflict processing, and explored the timecourse and topography of oscillatory connectivity between cortex and STN. Electrophysiological results are presented only for recordings without DBS.

Material and methods

Patients, surgery, electrode localization and recordings

Six participants with a mean age of 66 years ($SEM \pm 1.5$), including 5 male and one female patient with Parkinson's disease (PD) took part in this study and gave their written informed consent. The protocol was approved by the ethics committee of the medical faculty of the Ludwig Maximilian University of Munich. Clinical details of all participants are provided in Table 1. All patients underwent implantation of DBS leads (model 3389; Medtronic Neurological Division, MN, USA) with 4 ring electrodes in the left and right STN for the treatment of advanced Parkinsonism at the Department of Neurosurgery at the hospital of the LMU Munich. Initial stereotactic coordinates were 12 mm lateral, 3 mm

Table 1

Clinical details. Six patients with Parkinson's disease (1 female, mean age 66.1 ± 1.5 years; disease duration 10.5 ± 1.4 years) were studied 1 month–1 year after DBS surgery.

Case	Age	Gender	Disease duration	Main symptoms	UPDRS-III ON/OFF
1	54	f	9	Equivalent	10/27
2	71	m	12	Equivalent	22/38
3	53	m	12	Equivalent	4/27
4	70	m	8	Akinetic-rigid	23/40
5	55	m	7	Equivalent	15/33
6	57	m	10	Akinetic-rigid	30/53

*Evaluation was performed OFF medication after overnight withdrawal from dopaminergic medication in random order (ON/OFF Stimulation).

posterior and 4 mm below the midpoint of the AC-PC line. Coordinates were adjusted by direct visualization of the STN on individual preoperative T2-weighted MRI scans. Intraoperative single cell recordings and macrostimulation guided the final placement of the electrode leads. The exact position of the DBS electrodes in relation to the subthalamic target structures were determined based on the preoperative T2-weighted MRI and postoperative CT scans, using the Lead DBS toolbox (Horn and Kühn, 2015) and 3DSlicer software (www.slicer.org). MRT and CT were aligned manually using 3DSlicer software, co-registered using a two-stage linear registration (rigid followed by affine) as implemented in Advanced Normalization Tools (Avants et al., 2008) and normalized to MNI space (MNI ICBM Nonlinear 2009b template, (Fonov et al., 2011)). To visualize the STN, we used an atlas to outline the STN and its putative subdivisions, the motor, the associative and the limbic area (Accolla et al., 2014). This allowed us to confirm stimulation and recording sites of all patients (Fig. 2 A). All but one stimulation contacts were considered to be placed within the motor STN (with distances between each contact center and nearest atlas voxel center below 0.5 mm). One came close with 0.6 mm and overall, a mean distance of 0.15 mm ($SEM \pm 0.05$) between each stimulation contact center and nearest atlas voxel center in the motor STN was found. In all patients, the leads were connected to the implanted sensing neurostimulator (Activa PC + S, Medtronic) to record LFP bipolarly from the electrode contact above and below the single negative stimulation contact, colored in light red in Fig. 2 A. All LFP data were sampled at 422 Hz. Scalp EEG data were recorded with a 64-electrode active cap (actiCAP) with active shielding and amplified (BrainAmp DC amplifiers) using the BrainVision Recorder software (Brain Products, Munich, Germany). Two additional electrodes were placed on the superior orbit and on the outer canthus of the right eye to detect vertical and horizontal eye movements. EEG was referenced to the FCz electrode, grounded at AFz and sampled at 1000 Hz. Impedances were kept below 5 k Ω . The data was resampled to 422 Hz to match the sampling frequency of the implanted sensing neurostimulator and re-referenced to the average across all electrodes. Data traces from the sensing neurostimulator and scalp EEG recordings were synchronized using a transcutaneous electric nerve stimulator, delivering single pulses emitted via two electrodes at the scalp, producing a marked jump in the LFP and EEG signal. Experiments were recorded following overnight withdrawal of dopaminergic medication. Participants completed the decision-making task with and without DBS. Stimulation amplitudes were chosen according to the best clinical outcome (mean constant voltage: 2.71 ± 0.15 mV), stimulation frequency was 140 Hz and pulse duration was 60 μ s for all recordings. The experiments were performed at least 2 months after initial programming on the same or on consecutive days within the first year after implantation.

Task design

Participants were seated comfortable in a dimly lit, experimental room 60 cm in front of a 21-inch TFT computer screen. The Python-based toolbox PsychoPy (Peirce, 2007) was used for instructions and presentation of visual stimuli and for recording reaction times (RT). Participants

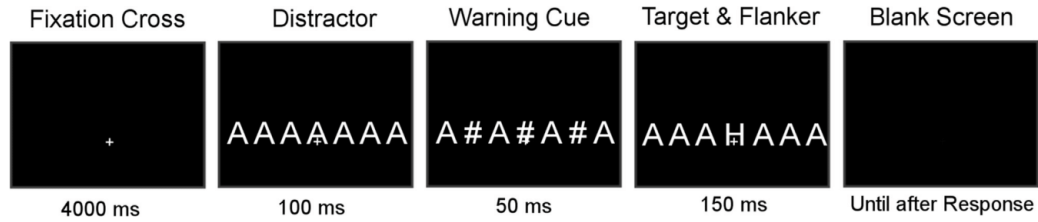


Fig. 1. Schematic illustration of a trial. Participants had to respond to the central target letter within an array of seven letters.

had to complete a letter variant of the Eriksen Flanker decision making task that provokes conflict dissociably at the perceptual and at the response selection level (Van Veen and Carter, 2005). Participants were asked to maintain fixation throughout the experiment and to respond as fast and as accurately as possible. Each trial began with a black screen containing a fixation cross for 4 s, followed by a display with 7 identical letters (either all “A”, “E”, “H” or “N”), which were presented for 100 ms, serving as initial distractors to introduce conflict. This array was followed by a brief warning cue, presented for 50 ms, in which 3 of the letters were replaced by a hash to signal the upcoming target presentation. Then the target and additional flankers were presented (150 ms) at the previously hashed locations and the subject had to decide if the central target stimulus was a vowel (“A” or “E”) or a consonant (“H” or “N”) and answer with the left or right index finger respectively by manual button press using “D” and “K” on a modified keyboard containing only task relevant keys (see Fig. 1).

The central target letter, was either congruent (SC) with the distractors (i.e. “AAA A AAA” followed by “AAA A AAA”), stimulus incongruent (SI) but requiring the same response (i.e. “AAA A AAA” followed by “AAA E AAA”) or response incongruent (RI) (i.e. “AAA A AAA” followed by “AAA H AAA”). After offset, the display stayed blank until 1000 ms after the response and then, the next trial started. In congruent trials distractors, flanker and target were the same inducing no conflict. In SI trials, distractors, flanker and target letters were different but linked to the same response alternative, supposedly resulting in conflict at the perceptual processing level. In RI trials, target, distractors and flankers were additionally associated with different response alternatives, provoking conflicts at the perceptual and the response level (Van Veen and Carter, 2005). Blocks consisted of 84 trials divided into equal numbers of SC, SI, and RI trials and trial order was randomized. All but one participant completed 7 blocks with and without deep brain stimulation while one participant completed 7 blocks without and 6 with DBS yielding on average ~580 trials per DBS condition. Blocks with and without DBS

were randomized in order and the starting block was randomized across subjects. Completion of one block took on average 7 min yielding an average time on the task of 97 min. The time between blocks (approximately 10 min) was used for changing stimulation and then downloading data from the internal pulse generator. Subjects were familiarized with the task before the main experiment by completing a test block and were only allowed to proceed if they clearly understood the task.

Analysis

EEG and LFP recordings were analyzed in Matlab (The Mathworks, Lowell, MA, USA) using custom written scripts and functions included in the Fieldtrip (Oostenveld et al., 2011) and EEGLab (Delorme and Makeig, 2004) toolboxes. At first, we inspected all raw data visually to identify and manually remove non-stereotypical noise. LFP data were then cleaned by setting a subject- and STN- specific voltage threshold to reject all trials exceeding that threshold. Next, for the EEG data, we rejected all channels exhibiting excessive artifacts, defined as any channels with kurtosis more than 5 SDs from the mean kurtosis across all channels. The EEG data were then high-pass filtered (cutoff 0.5 Hz, order 4) and decomposed into temporally maximally independent source processes using adaptive mixture independent component analysis (AMICA) (Delorme et al., 2012; Palmer et al., 2006). We then subtracted all components resembling eye-movements and non-brain sources from the data, based on ERPs, scalp topographies and single-equivalent current dipole modelling of the ICs (Oostenveld and Oostendorp, 2002).

EEG and LFP power

Event-related spectral power (ERSP) was computed using EEGLab ((Delorme and Makeig, 2004); newtimef function). Stimulus-locked as well as response-locked epochs from –6000 to 6000 ms were decomposed using Morlet wavelets, to avoid edge effects. For further analysis,

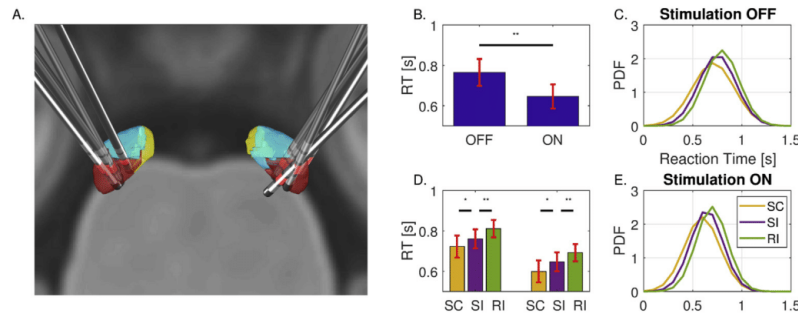


Fig. 2. Imaging and behavioral results. Stimulation and conflict affected RTs and did not interact. A. Electrode localizations. Posterior dorsal view of DBS-electrode localizations in left and right STN. The motor region of the STN is depicted in dark red, the associative subregion in light blue and limbic subregion in yellow. The contact used for stimulation is colored in light red (see text for details). B. DBS sped RTs. C. DBS sped RTs. D. RTs were modulated by conflict both without (left) and with DBS (right). Error bars indicating SEM. Black solid lines indicate significance. C and E. Probability density functions (PDF) of RTs for SC, SI and RI trials in the OFF and ON stimulation state showing similar differences between conditions with and without stimulation.

we focused on the time period from just before stimulus onset until after the response. The number of cycles for Morlet wavelets was appropriately selected for the frequency being analyzed (3 cycles at 1 Hz to 10 cycles at 60 Hz). We decomposed the signal in the frequency range from 1 to 60 Hz with a frequency resolution of 1 Hz. ERSP is a measure of induced changes in power at a given time–frequency point, and as the ERSP is sensitive to signal amplitude (which is known to differ between subjects), an individual baseline correction [−3000 ms to −1000ms before stimulus onset] was applied to the data and the difference was log scaled resulting in decibel units (dB). For each subject, we then computed the mean ERSP time-course across trials for the 3 different conflict conditions and for trials with slow and fast reaction times using an individual median split. We further focused on the average activity across two ranges, within each of which previous studies have shown homogenous task-related modulations: combined delta/theta synchronization (low frequency oscillations, LFO) (2–6 Hz), and combined alpha/beta desynchronization (10–30 Hz) (Herz et al., 2017; Zavala et al., 2017).

To visualize the variability of stimulus and response-related oscillatory activity in the LFP, we computed a spectrographic image showing trial dynamics of the power timecourse relative to baseline for both chosen frequency bands. ((Delorme and Makeig, 2004); timefreq and erpimage function). The single trial power time-courses were averaged across left and right STN for each subject, as we found no indication of lateralized activity and expressed as % change relative to the baseline (see above). All trials from each subject were then pooled, sorted in order of increasing reaction time or grouped into the three different conflict conditions, and were then smoothed with a 200-trial moving average, to attenuate interindividual differences in event-related modulations. This was done for visualization only (Figs. 4 and 5, A, D), for statistical evaluation, see below.

Connectivity: inter-site phase clustering and amplitude correlations

Inter-site phase time frequency clustering as well as amplitude-amplitude correlations were computed between the STN and all EEG electrodes (Cohen and Gulbinaite, 2014; Delorme and Makeig, 2004); newcrossf function, window size 1 s, otherwise same parameters as ERSP analysis). For phase connectivity analysis, we focused on the LFO as no other frequencies showed pronounced inter-site phase clustering. Inter-site phase coherence reflects the consistency of phase values between two recording sites over time and across trials. Inter-site phase clustering is independent of amplitude changes and a value of 0 represents the absence of EEG phase synchronization across trials between sites and a value of 1 indicates their perfect synchronization (Delorme and Makeig, 2004). For amplitude-amplitude correlations, we computed Pearson's correlation coefficients (R) (Arnulfo et al., 2015) between both STNs and each EEG electrode for the amplitude in the alpha/beta

frequency range over trials and across time. The correlation coefficient ranges from −1 to 1, with 0 indexing absence of correlation to 1 for perfect linear relationship and −1 for perfect anticorrelation. Both measures were computed separately for each subject for trials with fast and slow reaction times as well as the three different conflict conditions. Topographic representations for phase and amplitude connectivity were computed for three windows with a width of 500 ms and represent the average connectivity between both STN nuclei and each cortical electrode across subjects. Window center were chosen at 1000 ms before stimulus presentation, at the peak/through of the average power modulation and 1000 ms after response.

Statistical assessment of group differences

We excluded all error trials as well as trials with very fast (<0.25 s) and very slow (>1.5 s) RTs from further analysis. Overall, we included 3500 trials, on average 580 trials per subject and stimulation condition. To model and visualize the distribution of reaction times across subjects, we used an equal number (first 450 included trials) of trials from each subject and each condition to compute a probability distribution (Matlab function *pdf*). For group level statistical assessment of reaction time data, we used the individual mean RT from each conflict condition. As group level behavioral and neural data were not normally distributed (Kolmogorov Smirnov test, Matlab function *kstest*), we compared RTs from conflict and stimulation conditions from every subject using the non-parametric Friedman test of differences among repeated measures and conducted post Wilcoxon's signed rank tests (sample size 6) to confirm results. For assessing the impact on DBS on conflict processing, we compared the RT differences between conflict conditions with stimulation OFF and ON. For each subject, we computed the mean difference between SC and SI (“stimulus conflict”) and SI and RI trials (“response conflict”) in both stimulation conditions and compared these differences on a group level using Wilcoxon signed rank tests (Table 2). Although our data was found to be non-normally distributed with the Kolmogorov Smirnov test, Lilliefors test (matlab function *lillietest*) did not yield a significant violation of the normal distribution hypothesis for the RT data. Therefore, we also evaluated reaction times using a two-way repeated measures ANOVA with within subject factors: conflict (SC, SI, RI) and DBS (ON/OFF) (Scherberger et al., 2005). To statistically assess differences in RT between RT subgroups (median split), we used the individual mean RT from each subgroup for group level analysis.

To assess differences in spectral power and connectivity measures between different conflict conditions and reaction time bins across participants for statistical significance, we used the subject averages of the different measures in the two frequency intervals across time. To compare differences on the group level, for the ERSP analysis, we used the mean ERSP time-course in dB from the different conditions from each

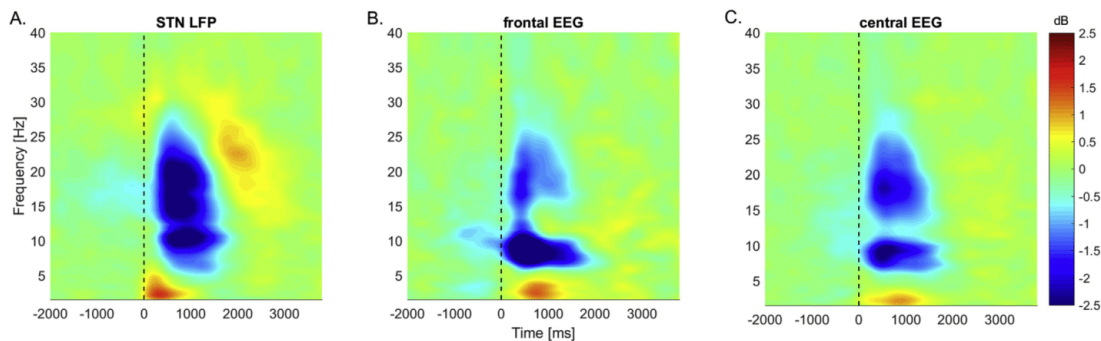


Fig. 3. A, B, C. Average STN LFP across left and right STN, frontal (Fz) and central (C3/C4) EEG ERSP (dB units) without stimulation locked to the target onset. Both subthalamic and cortical recordings show a delta/theta increase (red) and an alpha/beta decrease (blue).

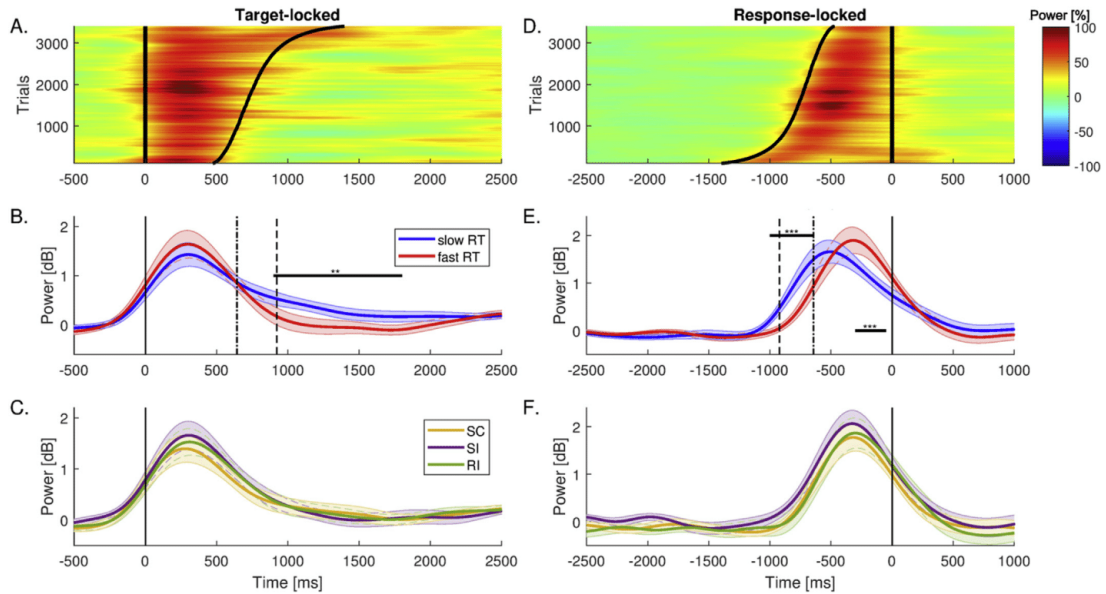


Fig. 4. Target and response-locked spectrographic images and average LFO power time-course A. and D. Spectrographic images for all trials averaged across all subthalamic nuclei (STN) and sorted by reaction times for LFO frequency range. A clear stimulus locked onset pattern is visible, while the duration of the LFO increase reflects reaction times. The vertical black line represents target stimulus presentation (A) and response execution (D) respectively. The dotted lines represent mean RT of fast and slow trial subgroups. The curved black line represents response execution in the stimulus-locked trials and stimulus presentation in the response-locked representations. B. and E. Stimulus- and response-locked average LFO time-course for slow and fast RTs and for all three different conflict scenarios (C. & F.). Shaded areas indicate SEM. Horizontal black solid lines represent significant timeperiods.

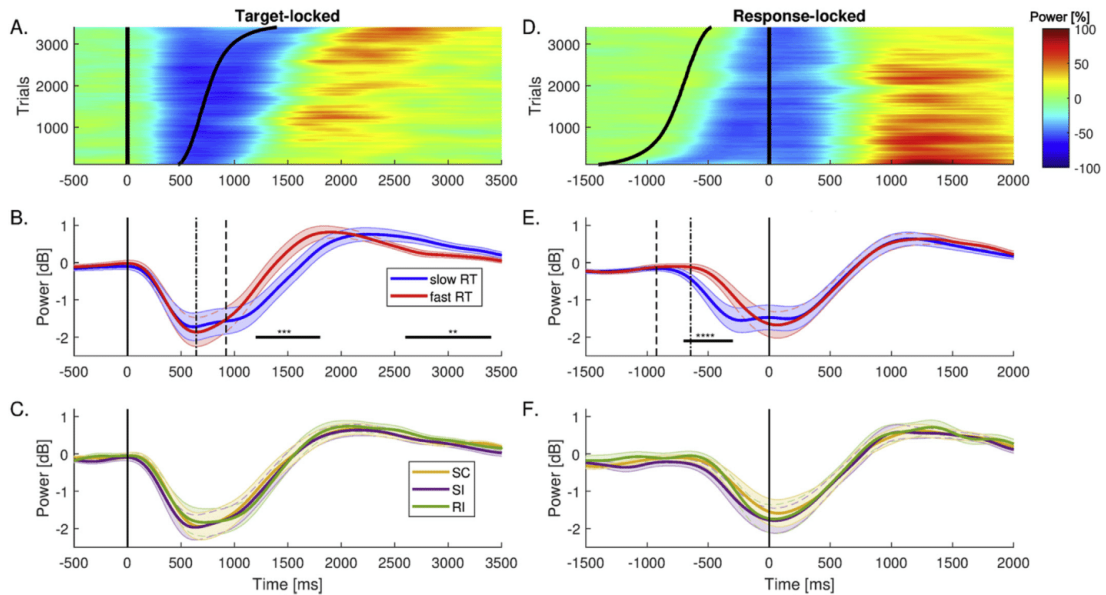


Fig. 5. Stimulus & Response locked spectrographic images and average alpha/beta power time-course A. and D. Spectrographic images for all trials averaged across all subthalamic nuclei (STN) and sorted by reaction times for beta frequency range. A stimulus locked onset pattern is visible, while the duration of the beta decrease and the latency of the following rebound reflect reaction times. B. and E. Stimulus- and response-locked average beta time-course for slow and fast RTs and for all three different conflict scenarios (C. & F.).

Table 2
Mean, SEM and p-values of Wilcoxon signed rank test for all comparisons of behavioral reaction times.

Reaction times in milliseconds	MEAN (SEM) 1st data	MEAN (SEM) 2nd data	p-value
	ms		
SC vs SI OFF Stim	722 (50)	760 (56)	.04*
SI vs RI OFF Stim	760 (56)	810 (42)	.01*
SC vs SI ON Stim	600 (48)	646 (40)	.04*
SI vs RI ON Stim	646 (40)	691 (39)	.01**
OFF vs ON Stim	764 (47)	646 (42)	.01**
slow vs fast (median split)	643 (25)	922 (44)	.0001***
OFF(SC-SI) vs ON (SC-SI)	−38 (16)	−47 (19)	.54
OFF(SI-RI) vs ON (SI-RI)	−50 (10)	−45 (8)	1

*,**,... indicate significance at $p < .05, .01, .001, .0001, .00001$ respectively. Sample size for all tests: 6.

subject and STN yielding a sample size of 12.

For the connectivity measures we used the time-course of the inter-site-phase-clustering (ISPC) and amplitude-amplitude Pearson correlation coefficient (R) from each subject and between both STNs and selected recording sites. For the analysis of the inter-site-phase-clustering, we used left STN-Fz and right STN-Fz inter-site-phase-clustering timecourses from each subject and condition for statistical evaluation, yielding a sample size of 12. For amplitude-amplitude correlation analysis we used left STN-C3 and right STN-C4 correlation coefficient timecourses from each subject and condition for visualization and statistical evaluation, yielding a sample size of 12.

We then compared conditions pairwise using the values computed separately for the different conditions across participants for each timepoint, comparing trials with slow against trials with fast reaction times to investigate the influence of RTs on the electrophysiological measures. Moreover we contrasted SC with SI trials and SI trials with RI trials, to investigate perceptual and response conflict respectively (Van Veen and Carter, 2005). To find timeperiods of statistical differences between conditions, for each timepoint and for each comparison we computed a Wilcoxon's signed rank, as data could not be assumed to be normally distributed for several timepoints and frames we tested (Kolmogorov Smirnov test). We corrected the resulting p-values with False Discovery Rate (FDR) correction for multiple comparisons (Benjamini and Yekutieli, 2005; Groppe et al., 2011) and used a significance level of $p < .05$. We then applied a cluster correction approach and used only timeperiods with at least 40 ms consecutive significant timepoints for further evaluation (Maris et al., 2007; Maris and Oostenveld, 2007), as the average difference in RT between conflict conditions was about 45 ms. To report and confirm significance and descriptive parameters, we entered the average values for each subject and time-period into a post-hoc Wilcoxon's signed rank test and corrected the p-values with Bonferroni correction for multiple timewindows. We report results for the so determined timewindows including mean and standard error of measurement (\pm SEM) and the p-value of the Wilcoxon signed rank tests (Table 3). Timeperiods of potential interest that did not survive initial correction approaches were also used for later evaluation and a clearly marked in Table 3. We increased sample size by taking into account each nucleus for statistical analysis. This has been a common approach in the field when dealing with small sample sizes (Ray et al., 2008; Zavala et al., 2017). We complemented our initial approach by taking the average across left and right STN for each subject, timewindow and condition to confirm results, yielding a sample size of 6 for the ERSP analysis.

Results

Behavioral task

Overall, DBS sped up RTs ($\chi^2(2) = 8, p < .01$). Error rates were not affected by stimulation and were low (1.5% without and 1.6% with

Table 3
Mean, SEM and p-values of Wilcoxon signed rank test for all comparisons of electrophysiological data.

Conditions:	Timeframe	MEAN (SEM) 1st data	MEAN (SEM) 2nd data	p-value
STN LFO Power (dB)				
		dB		
SC vs SI	300-500 AT	1.26 (0.30)	1.43 (0.31)	.07 ¹ (.15)
SC vs RI	300-500 AT	1.26 (0.30)	1.54 (0.34)	.13 ^{1,2} (.21)
SI vs RI	300-500 AT	1.54 (0.34)	1.43 (0.31)	.17 ^{1,2} (.31)
slow vs fast	150-350 AT	1.39 (0.32)	1.60 (0.38)	.15 ¹ (.20)
slow vs fast	900-1800 AT	0.29 (0.14)	−0.02 (0.18)	.001** (.01*)
SC vs SI	600-300 BR	0.96 (0.18)	1.08 (0.21)	.17 ¹ (.21)
SC vs RI	600-300 BR	0.96 (0.18)	1.03 (0.20)	.39 ^{1,2} (.55)
SI vs RI	600-300 BR	1.08 (0.21)	1.03 (0.20)	.66 ^{1,2} (.73)
slow vs fast	1200-700 BR	0.43 (0.06)	0.11 (0.06)	.0001*** (.02*)
slow vs fast	350-50 BR	0.41 (0.14)	1.05 (0.19)	.0001*** (.02*)
STN Alpha & Beta Power (dB)				
		dB		
slow vs fast	650-850 AT	−1.98 (0.52)	−1.75 (0.48)	.052 ¹ (.06)
slow vs fast	1200-1800 AT	0.09 (0.33)	−0.57 (0.34)	.00003*** (.003**)
slow vs fast	2600-3400 AT	0.18 (0.08)	0.45 (0.13)	.01** (.06)
slow vs fast	700-300 BR	−0.34 (0.19)	−0.92 (0.30)	.00001**** (.0005****)
STN - Fz LFO Inter-site phase coherence (ISPC)				
		ISPC		
SC vs SI	300-600 ms AT	0.17 (0.02)	0.20 (0.03)	.055 ^{1,2}
SC vs RI	300-600 ms AT	0.17 (0.02)	0.20 (0.03)	.052 ¹
SI vs RI	300-600 ms AT	0.20 (0.03)	0.20 (0.03)	.73 ^{1,2}
slow vs fast	900-1150 ms AT	0.06 (0.01)	0.11 (0.01)	.009**
SC vs SI	650-400 BR	0.19 (0.02)	0.20 (0.03)	.52 ^{1,2}
SC vs RI	650-400 BR	0.19 (0.02)	0.24 (0.03)	.052 ¹
SI vs RI	650-400 BR	0.20 (0.03)	0.24 (0.03)	.055 ^{1,2}
slow vs fast	1100-900 ms BR	0.07 (0.01)	0.11 (0.02)	.02*
slow vs fast	250-50 ms BR	0.20 (0.03)	0.13 (0.01)	.02*
STN - C3 & C4 Alpha/Beta Amplitude Correlation (R)				
		R		
slow vs fast	980-1120 AT	0.09 (0.01)	0.07 (0.01)	.01**
slow vs fast	500-250 BR	0.11 (0.01)	0.08 (0.01)	.01**

¹ did not survive FDR correction; ² did not survive cluster correction; Sample size for tests with p-values not in brackets: 12; Sample size for all tests with p-values in brackets: 6.

stimulation). RTs were robustly modulated by conflict both without DBS ($\chi^2(2) = 10.75, p < .01$) and with DBS ($\chi^2(2) = 10.75, p < .01$, Fig. 2). RTs increased with increasing conflict (Table 2). Stimulation did not affect conflict-related RT differences (Table 2). A two-way repeated measures ANOVA with factors conflict (SC, SI, RI) and DBS (ON/OFF) on RT data confirmed these findings. We found significant main effects of conflict ($F(1, 36) = 15.2, p = .0003$), DBS ($F(1, 36) = 57.5, p = .0001$) but no significant interaction between conflict and DBS ($F(1, 36) = 0.5,$

$p = .62$). Effects were consistent across participants (Inline Supplementary Fig. S2). We have performed Drift Diffusion Modelling to formally investigate decision making parameters such as the drift rate and decision threshold in our task (see Supplementary Methods). In our winning model (Inline Supplementary Fig. S1), we see a main effect of conflict on the drift rate, with higher drift rates for lower levels of conflict and a main effect of DBS on decision thresholds, with lower thresholds during DBS, confirming results from the literature (Cavanagh et al., 2011; Krypotos et al., 2015; Pote et al., 2016).

Task induced LFP and EEG power changes

The time-frequency composition of the subthalamic LFP and EEG recordings during our decision making task replicated the classical modulation pattern, where target onset is followed by an increase in LFO (2–6Hz) power, decreases in alpha/beta power, and a rebound. The latency, duration and exact frequency range of the induced activation/deactivation is slightly different between subthalamic and scalp electrodes but resemble a common pattern (Fig. 3).

Onset of modulation of oscillatory activity reflects stimulus presentation, duration reflects reaction time

The spectrographic images (Fig. 4) show a tight link between the amplitudes and the time-course of single trial ERSPs and RTs. The oscillatory amplitude on individual trials is shown as color-coded horizontal lines, sorted by RT. The target and response locked images sorted by RT (across all trials from all subjects) suggest that the onset of the LFO increase (Fig. 4) as well as the combined alpha/beta decrease (Fig. 5) is induced by target presentation and lasts until shortly after the response.

The spectrographic images show that the duration of the increase of the LFO amplitude as well as the duration of the decrease of the alpha/beta band amplitude and the onset of the beta band rebound reflect reaction times (Figs. 4 and 5). Only RT but not conflict-sorted spectrographic images showed a distinct pattern. For further evaluation of the effect of conflict and reaction time on the oscillatory changes we compared the temporal evolution of LFO and alpha/beta band power for all three conflict scenarios and for slow and fast reaction times separately.

Trials with slow RTs were associated with a significant longer increase in post-stimulus LFO power (Fig. 4) than trials with fast RTs. For the stimulus-locked LFO analysis, one time-window survived FDR and cluster correction. There was a main effect of RT for the timeframe between 900 ms and 1800 ms. The timewindow between 150 ms and 300 ms after target presentation survived cluster but not FDR correction and was found not significant (Mean, SEM and p-values for all timeframes tested and comparisons, see Table 3). For the response-locked LFO analysis, we found 2 timewindows with a main effect of RT. The window from 1200 ms before to 700 ms before the response showed significantly higher amplitudes for slow trials, while the timewindow from 350 ms to 50 ms showed significant lower amplitudes for slow trials (Fig. 4 and Table 3).

We found no significant differences for the pairwise comparison between conflict conditions. Visual assessment of time-courses might hint at lower initial amplitude increases in SC trials compared to SI and RI trials between 300 and 500 ms after target presentation. Statistical assessment of this timewindow did reveal no significant difference between SC and SI trials (with no other pairwise comparisons reaching significance), but survived cluster and not FDR correction (Fig. 4, Table 3). Statistical analysis across subjects confirmed results (Table 3).

A similar pattern, although associated with a different latency, duration and deactivation and activation profile is evident when comparing alpha/beta oscillatory activity for slow and fast reaction times (Fig. 5). Trials with slower reaction times showed relatively similar initial decreases in amplitude followed by a significant longer desynchronization period and later rebound. For the stimulus-locked analysis of alpha/

beta power differences between slow and fast RT trials, three timewindows survived cluster correction, but only two timewindows survived FDR correction and were ultimately found significant. At first, from 650 ms to 850 ms after the target stimulus onset there was less of initial amplitude decreases for slow trials, this epoch survived cluster, but not FDR correction. Then from 1200 ms to 1800 ms this was reversed, with significantly lower amplitudes in slow trials. From 2600 ms to 3400 ms then there was a higher positivity for slow trials, reflecting a longer period of deactivation followed by a later rebound. For the response-locked analysis, we found one timewindow with a main effect of RT between 700 ms and 300 ms before response with significantly lower amplitudes for slow trials (Fig. 4 and Table 3).

When we analyzed the same frequency bands for differences between different conflict conditions, we did not find any timeperiod with a statistical significant effect of condition. The timecourse and the completely overlapping SEM intervals across the whole time period did not suggest any timewindow of further interest (Fig. 5). Statistical analysis across subjects confirmed results (Table 3), except for the difference between slow and fast trials from 2600 ms to 3400 after target onset.

Subthalamic-cortical phase and amplitude connectivity reflects reaction time

Subcortical-cortical connectivity analysis using phase and amplitude relationships revealed differences in STN LFP and scalp EEG LFO and alpha/beta connectivity most likely related to reaction times, partly matching those timeframes found in the power analysis.

For LFO connectivity time-course analysis we focused on the Fz electrode to evaluate phase locking, as frontal midline delta/theta is known to be implicated in conflict processing (Cavanagh and Frank, 2014; Herz et al., 2017; Töllner et al., 2017). For the stimulus-locked LFO inter-site phase clustering analysis between STN and Fz, we found one timewindow with a significant main effect of RT. The timeframe from 900 ms to 1150 ms after the target stimulus onset showed a significantly higher mean ISPC for slow trials, partly overlapping with the second window we found to be significant in the amplitude analysis (Table 3, Fig. 6). Similar to the amplitude analysis, we could not determine any significant differences between the three conflict conditions that survived both correction methods, but the comparison between SC and RI trials survived cluster but not FDR correction in the timewindow from 300 ms till 600 ms, but was not significant as a whole (Fig. 6, Table 3).

For the response-locked LFO connectivity analysis, two timewindows showed a main effect of RT and survived correction. The timeframe from 1100 ms until 900 ms and the window from 250 ms to 50 ms before the response showed significant effect of RT: in the earlier timeframe, the ISPC of the slow trials was higher and in the second timeframe, the ISPC of the fast trials was higher (Fig. 6, Table 3). The statistical assessment of differences over time did not show any consistent significant difference for the pairwise comparison between conflict conditions. Visual assessment of time-courses might hint at an effect of conflict in the timeframe from 650 ms until 400 ms before response but these comparisons were not statistically significant after correction (Table 3).

Mapping the scalp topography of the LFO connectivity time-course using all trials independently of condition revealed that before any stimulus was presented and long after the response was submitted, the largest inter-site phase clustering was consistently visible between the STN and frontal-central electrodes Fz and FCz. From stimulus onset until shortly after response, induced inter-site phase clustering was most pronounced between subthalamic recordings and these frontal-central as well as at parietal and occipital electrodes (Fig. 6).

For statistical tests we focused on the amplitude connectivity time-courses between STN and C3 and C4 electrodes (Herz et al., 2017). Assessing the subthalamic-cortical alpha/beta band amplitude correlations, we also found main effects of RT but not other factors. Similar to the STN results, for slow reaction time trials, the duration of the amplitude-amplitude correlation decreases upon stimulus presentation

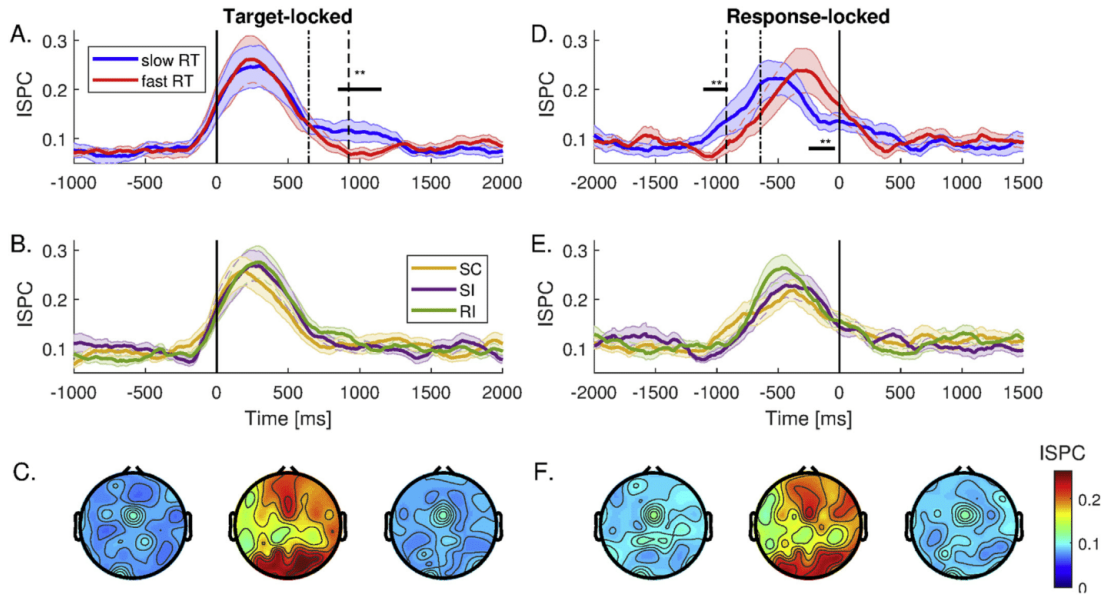


Fig. 6. STN-Cortical LFO inter-site phase clustering (ISPC) time-course A. and B. Stimulus-locked ISPC across time and topographical representation (C) at different timepoints calculated for fast and slow reaction times and for the different conflict conditions. D. and E. Response-locked ISPC across time and topographical representation (F).

was longer than in trials with fast reaction times, with significant differences in the timewindow from 980 ms to 1120 ms after the target onset. A main effect of RT was also present in the response locked analysis, with decreases in connectivity starting earlier in the slow

reaction time subgroup and significant differences in the timeframe 500 ms–250 ms before the response (Fig. 7). In contrast to the LFO phase connectivity analysis, the amplitude-amplitude correlation in the alpha/beta range was most pronounced between the subthalamic and

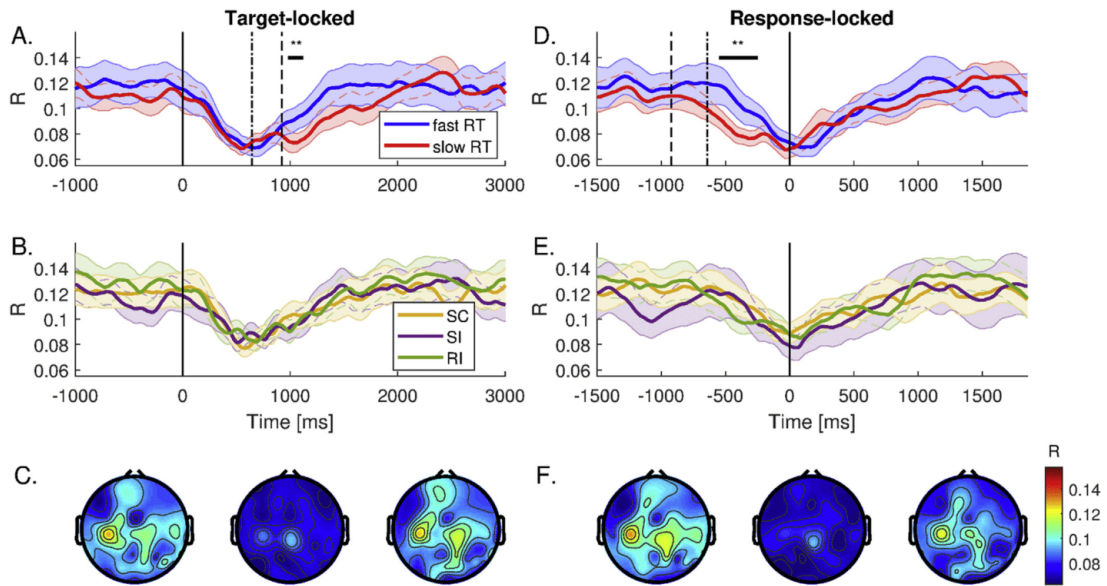


Fig. 7. STN-Cortical average alpha/beta amplitude-amplitude correlation. A. and B. Stimulus-locked amplitude correlations averaged for alpha and beta frequencies across time at different timepoints calculated for fast and slow reaction times. D., E. Response-locked amplitude correlations across time. C., F. Topographical representation of subthalamic cortical alpha/beta coherence.

motor cortical areas around electrodes C3 and C4 during the prestimulus and postresponse period, confirming earlier reports (Accolla et al., 2016). There was a topographically global decrease in cortico-subthalamic amplitude-amplitude correlation from target presentation until after response (Table 3).

Discussion

STN DBS generally decreased reaction times but did not alter conflict related processing in our task. The STN could help implement a task-specific dynamic decision threshold and not a stimulus conflict related inhibitory signal. Indeed, drift diffusion modelling hints that the decision threshold is altered by stimulation while drift rates are modulated by stimulus conflict. Between stimulus presentation and response, the STN LFO activity was most strongly coherent with frontal midline electrodes (Fz/FCz), likely reflecting a tonic (not conflict-related) inhibitory signal. Oscillations in the alpha/beta range were coherent with those in motor cortical structures during that same period, consistent with tonic hyperdirect pathway connectivity (Accolla et al., 2016). Behaviorally relevant induced LFO STN-cortical coherence changes between target and response included not only frontal but also parietal and occipital areas, possibly reflecting a reactive mechanism. Alpha/beta oscillations were reduced in amplitude and decorrelated globally, consistent with functionally relevant motor processing. With these results we suggest that a tonically active executive control and a motor network with complementary oscillatory mechanisms and structures help implement dynamical, task-related inhibitory signals and responses to behaviorally important stimuli. These results extend previous findings concerning the roles of subcortical and cortical LFO and alpha/beta oscillations and their functional importance during responding under conflict (Cavanagh et al., 2011; Herz et al., 2017; Zavala et al., 2013) and provide new insights on the putative mechanisms involved in inhibitory control.

Behavioral effects of stimulation

While previous studies have shown that PD patients are faster on the Stroop task during STN DBS, they also make more errors during stimulation (Jahanshahi, 2013; Volkmann et al., 2010). We were able to reproduce the response slowing without DBS but did not find any significant differences between error rates between stimulation conditions, probably because subjects made very few errors overall (1.5%). Replicating the classical conflict task literature, RTs were robustly modulated by cue/flanker-target compatibility. Previous work in patients has shown decreases in RT under high-conflict conditions when DBS was turned on (Frank et al., 2007), particularly when associated with high reward. In our task, STN DBS did not seem to change conflict-related differences in reaction times, as similar differences between conditions and probability distribution patterns were visible regardless of stimulation. Indeed it was striking that both types of conflict processing (perceptual and response-related) were intact in this population of Parkinsonian patients with and without DBS. Overall, we suggest that in our task the STN does not implement a stimulus conflict related inhibitory signal but rather a task-related and dynamic decision threshold that is altered during DBS. Drift diffusion modelling hints that DBS interacts with decision thresholds while drift rates seem to be related to the stimulus conflict (see Supplementary Material and Supplementary Discussion).

Task induced LFP power changes

Oscillatory activity in low and alpha/beta frequencies reflect reaction time

Our LFO findings partly resembles the pattern of conflict-related differences found in spiking as well as in low delta and theta frequency LFP activity in the STN (Zavala et al., 2015b, 2013). It is difficult to entangle conflict from reaction times, as trials with higher conflict generally show slower reaction times (Cohen and Nigbur, 2013; Nachev et al., 2007; Scherbaum and Dshemuchadse, 2013; Yeung et al., 2011).

Indeed, Zavala and colleagues found no power differences between the fast-incongruent trials and congruent trials with similar RTs (Zavala et al., 2013). Various reports (Espenhahn et al., 2017; Gross et al., 2005; Meirovitch et al., 2015; Pfurtscheller et al., 1996) show that cortical beta-band desynchronization precedes motor output and that suppression of beta oscillatory activity during movement is followed by a rebound after movement execution. It has been suggested that beta-band de/resynchronization go hand in hand with motor processing (Chung et al., 2017). There are also several reports (Alegre et al., 2013; Bastin et al., 2014; Benis et al., 2014; Joundi et al., 2013; Kühn et al., 2004; Leventhal et al., 2012; Zavala et al., 2017) of subthalamic beta oscillations in response inhibition during conflict. The interpretation of the functional role of alpha and beta band activity is complicated. A few studies compare „Go“ and „No-Go“ trials, which implement either the execution or the inhibition of a response (Kühn et al., 2004). A study by Williams et al. (2005), did show a significant relationship between oscillatory activity in the beta band and reaction times in the parkinsonian STN after „Go“ cues. Other studies using variations of the Stroop task have reported interpretation problems disentangling genuine conflict effects from influences of reaction times (Zavala et al., 2015a). We here report only main effects of RT with initially lower decreases and a significant longer period of alpha/beta band deactivation followed by a later rebound for trials with slower reaction times, confirming earlier reports but with a more fine-grained description of the time-course. We argue that these alpha/beta band dynamics reflect response preparation/execution and the time on task.

Subthalamic-cortical phase and amplitude coherence reflects reaction time

Previous studies reported stimulus as well as response locked low frequency connectivity between electrodes placed at frontal midline and the STN to be correlated with conflict (Zavala et al., 2016, 2013, 2014). Increases in EEG LFO power during cognitive motor tasks have been mainly observed at frontal midline areas that mediate response inhibition (Cavanagh et al., 2011; Cavanagh and Frank, 2014), for example over the PFC and the IFG, which are connected to the STN via the hyperdirect and indirect pathway (Alexander et al., 1986; Forstmann et al., 2010; Monakow et al., 1978; Swann et al., 2012). Herz and colleagues (Herz et al., 2017) report that STN LFO are coupled to activity at prefrontal electrode Fz and are related to decision thresholds. Fronto-parietal dynamics then are important for accurate motor performance (Chung et al., 2017; Cohen and Ridderinkhof, 2013). Previous studies neglected the posterior sensorimotor network that is involved in the initiation of motor programs and which supports proactive inhibitory control (Booth et al., 2005; Boulinguez et al., 2009; Jaffard et al., 2008; Lavalée et al., 2014; Menon et al., 2001). Neglect patients with right inferior parietal lobe (IPL) lesions show specific difficulties in initiating leftward movements towards visual targets on the left side of space, while this motor impairment was not found in neglect patients with frontal lesions (Mattingley et al., 1998), suggesting that the IPL operates as a sensorimotor interface (Fransson and Marrelec, 2008), rather than subserving only perceptual functions.

We show that subthalamic activity in the low frequency range is phase-locked to activity at electrodes over frontal structures as well as parietal and occipital electrodes. Phase-locking analysis between Fz and STN does show significant differences between slow and fast reaction times, while the duration of the increased connectivity takes longer for trials with slower reaction times resembling LFO amplitude differences in the STN for the same comparison. In the period between stimulus presentation and response, the STN LFO activity is mostly coherent with frontal midline electrodes, while during the task connectivity includes not only frontal midline but also right frontal, parietal and occipital areas. In the light of the proactive and reactive mechanisms and structures discussed to be involved in inhibitory control (Martínez-Selva et al., 2006), these observations suggest a tonically, possibly proactive inhibitory control network with a reactive mechanism, that returns to its default mode when uncertainty has been resolved and a response is

executed.

Suppression of beta activity at cortical areas during movement followed by a rebound after movement has been reported by a number of studies, especially over motor cortical areas (Espenhahn et al., 2017; Gross et al., 2005; Pfurtscheller et al., 1996) but also other areas, e. g. parietal cortex (Chung et al., 2017). Reports about beta frequency modulation during cognitive motor tasks are also abundant for the subthalamic nucleus (Alegre et al., 2013; Brittain et al., 2012; Kühn et al., 2004; Leventhal et al., 2012; Ray et al., 2012). Recently it has been described that the dorsal motor area in the STN showing the highest beta activity projected predominantly to motor and premotor cortical regions (Accolla et al., 2016) and that STN beta activity (13–30 Hz) is coupled to electrodes C3/C4 close to motor cortex (Herz et al., 2017). Tan and colleagues (Tan et al., 2014) reported movement-related modulation in STN-motor cortex inter-site-phase-clustering. We found no prominent inter-site-phase-clustering for the alpha/beta band, possibly due to our sampling rate of 422 Hz that does not allow for a proper estimation of the beta phase.

We report that cortical as well as subthalamic beta oscillations are attenuated shortly after stimulus until after the response and are followed by a rebound and that their time-course correlates with reaction times. In the timeperiod between the stimulus and response, the amplitude correlations are most pronounced between STN and motor cortical areas, possibly reflecting default oscillatory connectivity between these highly connected areas. During the task, amplitudes between all cortical areas and the STN are decorrelated, possibly reflecting motor processing.

Study limitations

This study was conducted in patients with Parkinson's disease which are known to show aberrant oscillatory activity within and connectivity between subcortical and cortical networks (Hammond et al., 2007). Patients were investigated after overnight withdrawal of medication, but they were able to perform the task with low error rates. Dopamine levels are reported to influence resting and movement related oscillatory activity in the STN and are associated with a lack of gamma frequency modulations and decreases of beta in the off medication state (Foffani et al., 2005; Hanrahan et al., 2016; Kühn et al., 2004). However, reported average group-level dynamics in LFO and alpha/beta activity seem to show a paradigmatic reactivity pattern, overlapping with earlier studies (Zavala et al., 2015a, 2014). The lack of induced gamma activity could also be due to the noise floor of the used devices, which was reached between 60 and 100Hz. The investigation of DBS-induced cortical changes is challenged of the high amplitude artifacts related to ferromagnetic extension wires from the DBS electrodes to the recording equipment or internal pulse generator. Artifacts from ferromagnetic wires are likely to be reduced in patients with internalized electrode cables (Oswal et al., 2016). It is conceivable that putative stimulation of the motor subregion could have a different effect on conflict-related behavior than stimulating the associative part, as the STN is thought to be grouped into limbic, associative and motor areas, with each subregion showing distinct connections to other subcortical and cortical areas (Jahanshahi et al., 2015; Lambert et al., 2012; Lanciego et al., 2012). It is also possible that genuine conflict related processing is characteristic for other subregions in the STN. Although we included a large number of trials per participant, we may have missed smaller effects due to the limited group sample size. The results might also depend on the characteristics of our task design (Jahfari et al., 2011; Lavallee et al., 2014), since the patients may have used high levels of proactive inhibition in our task. The low error rates that indicate an accuracy speed trade off that is shifted towards perfect task performance support this speculation. In other words, our Flanker task may tonically inhibit and drive proactive inhibition rather than reactive inhibition. Conflict related changes of the STN-frontal network have previously been shown using tasks that assess larger overall decision conflicts of about 100 ms (Zavala et al., 2013). However, conflict related changes in our task of about 45 ms for each

conflict level in both stimulation conditions resemble findings with similar tasks in the literature (Soutschek et al., 2013; Van Veen and Carter, 2005) and together yield a comparable conflict effect of about 90 ms between SC and RI trials that cannot be solely explained by proactive inhibition. As suggested by our DDM modelling results, the STN may help implement a decision threshold that is specific to our task, while the rate of evidence accumulation is influenced by the stimulus conflict, resulting in the observed differences in reaction times. Future studies are needed to confirm the functional subthalamic-cortical activity and connectivity patterns as well as the behavioral results.

Conclusion

Our findings suggest that the STN in our task does not implement a stimulus-conflict related inhibitory signal but rather a dynamic decision threshold. We suggest that subthalamic activity as well as subthalamic-cortical oscillatory connectivity reflect an inhibitory control and motor network with different oscillatory mechanisms and propose that proactive as well as reactive mechanisms and putative neural structures are involved in implementing a dynamic executive control signal. Functionally relevant and coherent low frequency oscillations could reflect the communication within an executive control network with subcortical, frontal and posterior nodes and alpha/beta oscillations might reflect the coordination of a motor network with subcortical and motor cortical structures. These networks may be tonically and coherently active, are reactive to stimulus presentation, functionally linked to response preparation and execution and return to their default and possibly proactive state afterwards.

Conflict of interest

The authors declare no competing financial interests.

Acknowledgements

We thank the patients for participating in this study. We also thank Ms. S. Irving and Ms. Ayse Bovet for their help in carefully proofreading the manuscript. F.H. was supported by the Lüneburg heritage, and P.T. by the DFG (TA 857/2-1), and BMBF (801210010-20).

Appendix A. Supplementary data

Supplementary data related to this article can be found at <https://doi.org/10.1016/j.neuroimage.2018.01.001>.

References

- Accolla, E.A., Dukart, J., Helms, G., Weiskopf, N., Kherif, F., Lutti, A., Chowdhury, R., Hetzer, S., Haynes, J.-D., Kühn, A.A., Draganski, B., 2014. Brain tissue properties differentiate between motor and limbic basal ganglia circuits. *Hum. Brain Mapp.* 35, 5083–5092. <https://doi.org/10.1002/hbm.22533>.
- Accolla, E.A., Herrojo Ruiz, M., Horn, A., Schneider, G.-H., Schmitz-Hübsch, T., Draganski, B., Kühn, A.A., 2016. Brain networks modulated by subthalamic nucleus deep brain stimulation. *Brain* 139, 2503–2515. <https://doi.org/10.1093/brain/aww182>.
- Alegre, M., Lopez-Azcarate, J., Obeso, I., Wilkinson, L., Rodriguez-Oroz, M.C., Valencia, M., Garcia-Garcia, D., Guridi, J., Artieda, J., Jahanshahi, M., Obeso, J.A., 2013. The subthalamic nucleus is involved in successful inhibition in the stop-signal task: a local field potential study in Parkinson's disease. *Exp. Neurol.* 239, 1–12. <https://doi.org/10.1016/j.expneurol.2012.08.027>.
- Alexander, G.E., DeLong, M.R., Strick, P.L., 1986. Parallel organization of functionally segregated circuits linking basal ganglia and cortex. *Annu. Rev. Neurosci.* 9, 357–381. <https://doi.org/10.1146/annurev.ne.09.030186.002041>.
- Antonelli, F., Ray, N., Strafella, A.P., 2011. Impulsivity and Parkinson's disease: more than just disinhibition. *J. Neurosci.* 31, 202–207. <https://doi.org/10.1016/j.jns.2011.06.006>.
- Arnulfo, G., Hirvonen, J., Nobili, L., Palva, S., Palva, J.M., 2015. Phase and amplitude correlations in resting-state activity in human stereotactical EEG recordings. *NeuroImage* 112, 114–127. <https://doi.org/10.1016/j.neuroimage.2015.02.031>.
- Aron, A.R., Behrens, T.E., Smith, S., Frank, M.J., Poldrack, R.A., 2007. Triangulating a cognitive control network using diffusion-weighted magnetic resonance imaging (MRI) and functional MRI. *J. Neurosci.* 27.

- Avants, B.B., Epstein, C.L., Grossman, M., Gee, J.C., 2008. Symmetric diffeomorphic image registration with cross-correlation: evaluating automated labeling of elderly and neurodegenerative brain. *Med. Image Anal.* 12, 26–41. <https://doi.org/10.1016/j.media.2007.06.004>.
- Ballanger, B., Van Eimeren, T., Moro, E., Lozano, A.M., Hamani, C., Boulinguez, P., Pellecchia, G., Houle, S., Poon, Y.Y., Lang, A.E., Strafella, A.P., 2009. Stimulation of the subthalamic nucleus and impulsivity: release your horses. *Ann. Neurol.* 66, 817–824. <https://doi.org/10.1002/ana.21795>.
- Bastin, J., Polosan, M., Benis, D., Goetz, L., Bhattacharjee, M., Piat, B., Krainik, A., Bougerol, T., Chabardès, S., David, O., 2014. Inhibitory control and error monitoring by human subthalamic neurons. *Transl. Psychiatry* 4, e439. <https://doi.org/10.1038/tp.2014.73>.
- Benis, D., David, O., Lachaux, J.-P., Seigneuret, E., Krack, P., Fraix, V., Chabardès, S., Bastin, J., 2014. Subthalamic nucleus activity dissociates proactive and reactive inhibition in patients with Parkinson's disease. *Neuroimage* 91, 273–281. <https://doi.org/10.1016/j.neuroimage.2013.10.070>.
- Benjamini, Y., Yekutieli, D., 2005. False Discovery rate-adjusted multiple confidence intervals for selected parameters. *J. Am. Stat. Assoc.* 100, 71–81. <https://doi.org/10.1198/01621450400001907>.
- Bogacz, R., Gurney, K., 2007. The basal ganglia and cortex implement optimal decision making between alternative actions. *Neural Comput.* 19, 442–477. <https://doi.org/10.1162/neco.2007.19.2.442>.
- Booth, J.R., Burman, D.D., Meyer, J.R., Lei, Z., Trommer, B.L., Davenport, N.D., Li, W., Parrish, T.B., Gitelman, D.R., Marsel Mesulam, M., 2005. Larger deficits in brain networks for response inhibition than for visual selective attention in attention deficit hyperactivity disorder (ADHD). *J. Child Psychol. Psychiatry* 46, 94–111. <https://doi.org/10.1111/j.1469-7610.2004.00337.x>.
- Botvinick, M.M., Cohen, J.D., Carter, C.S., 2004. Conflict monitoring and anterior cingulate cortex: an update. *Trends Cognit. Sci.* 8, 539–546. <https://doi.org/10.1016/j.tics.2004.10.003>.
- Boulinguez, P., Ballanger, B., Granjon, L., Benraiss, A., 2009. The paradoxical effect of warning on reaction time: demonstrating proactive response inhibition with event-related potentials. *Clin. Neurophysiol.* 120, 730–737. <https://doi.org/10.1016/j.clinph.2009.02.167>.
- Brittain, J.-S., Watkins, K.E., Joundi, R.A., Ray, N.J., Holland, P., Green, A.L., Aziz, T.Z., Jenkinson, N., 2012. A role for the subthalamic nucleus in response inhibition during conflict. *J. Neurosci.* 32, 13396–13401. <https://doi.org/10.1523/JNEUROSCI.2259-12.2012>.
- Cavanagh, J.F., Frank, M.J., 2014. Frontal theta as a mechanism for cognitive control. *Trends Cognit. Sci.* 18, 414–421. <https://doi.org/10.1016/j.tics.2014.04.012>.
- Cavanagh, J.F., Wiecki, T.V., Cohen, M.X., Figueroa, C.M., Samanta, J., Sherman, S.J., Frank, M.J., 2011. Subthalamic nucleus stimulation reverses mediofrontal influence over decision threshold. *Nat. Neurosci.* 14, 1462–1467. <https://doi.org/10.1038/nn.2925>.
- Chung, J.W., Ofori, E., Misra, G., Hess, C.W., Vaillancourt, D.E., 2017. Beta-band activity and connectivity in sensorimotor and parietal cortex are important for accurate motor performance. *Neuroimage* 144, 164–173. <https://doi.org/10.1016/j.neuroimage.2016.10.008>.
- Cohen, M.X., Gulbinaitis, R., 2014. Five methodological challenges in cognitive electrophysiology. *Neuroimage* 85, 702–710. <https://doi.org/10.1016/j.neuroimage.2013.08.010>.
- Cohen, M.X., Nigbur, R., 2013. Reply to “Higher response time increases theta energy, conflict increases response time.” *Clin. Neurophysiol.* 124, 1479–1481. <https://doi.org/10.1016/j.clinph.2013.03.013>.
- Cohen, M.X., Ridderinkhof, K.R., 2013. EEG source reconstruction reveals frontal-parietal dynamics of spatial conflict processing. *PLoS One* 8, e57293. <https://doi.org/10.1371/journal.pone.0057293>.
- Delorme, A., Makeig, S., 2004. EEGLAB: an open source toolbox for analysis of single-trial EEG dynamics including independent component analysis. *J. Neurosci. Meth.* 134, 9–21.
- Delorme, A., Palmer, J., Onton, J., Oostenveld, R., Makeig, S., 2012. Independent EEG sources are dipolar. *PLoS One* 7, e30135. <https://doi.org/10.1371/journal.pone.0030135>.
- Espenhahn, S., de Berker, A.O., van Wijk, B.C.M., Rositter, H.E., Ward, N.S., 2017. Movement-related beta oscillations show high intra-individual reliability. *Neuroimage* 147, 175–185. <https://doi.org/10.1016/j.neuroimage.2016.12.025>.
- Foffani, G., Bianchi, A.M., Baselli, G., Priori, A., 2005. Movement-related frequency modulation of beta oscillatory activity in the human subthalamic nucleus. *J. Physiol.* 568, 699–711. <https://doi.org/10.1113/jphysiol.2005.089722>.
- Fonov, V., Evans, A.C., Botteron, K., Almli, C.R., McKinstry, R.C., Collins, D.L., 2011. Unbiased average age-appropriate atlases for pediatric studies. *Neuroimage* 54, 313–327. <https://doi.org/10.1016/j.neuroimage.2010.07.033>.
- Forstmann, B.U., Anwander, A., Schafer, A., Neumann, J., Brown, S., Wagenmakers, E.-J., Bogacz, R., Turner, R., 2010. Cortico-striatal connections predict control over speed and accuracy in perceptual decision making. *Proc. Natl. Acad. Sci. Unit. States Am.* 107, 15916–15920. <https://doi.org/10.1073/pnas.1004932107>.
- Frank, M.J., 2006. Hold your horses: a dynamic computational role for the subthalamic nucleus in decision making. *Neural Network* 19, 1120–1136. <https://doi.org/10.1016/j.neunet.2006.03.006>.
- Frank, M.J., Samanta, J., Moustafa, A.A., Sherman, S.J., 2007. Hold your horses: impulsivity, deep brain stimulation, and medication in parkinsonism. *Science* (80-.) 318, 1309–1312. <https://doi.org/10.1126/science.1146157>.
- Fransson, P., Marrelec, G., 2008. The precuneus/posterior cingulate cortex plays a pivotal role in the default mode network: evidence from a partial correlation network analysis. *Neuroimage* 42, 1178–1184. <https://doi.org/10.1016/j.neuroimage.2008.05.059>.
- Groppe, D.M., Urbach, T.P., Kutas, M., 2011. Mass univariate analysis of event-related brain potentials/fields I: a critical tutorial review. *Psychophysiology* 48, 1711–1725. <https://doi.org/10.1111/j.1469-8986.2011.01273.x>.
- Gross, J., Pollok, B., Dirks, M., Timmermann, L., Butz, M., Schnitzler, A., 2005. Task-dependent oscillations during unimanual and bimanual movements in the human primary motor cortex and SMA studied with magnetoencephalography. *Neuroimage* 26, 91–98. <https://doi.org/10.1016/j.neuroimage.2005.01.025>.
- Hammond, C., Bergman, H., Brown, P., 2007. Pathological synchronization in Parkinson's disease: networks, models and treatments. *Trends Neurosci.* <https://doi.org/10.1016/j.tics.2007.05.004>.
- Hanrahan, S.J., Nedrud, J.J., Davidson, B.S., Farris, S., Giroux, M., Haug, A., Mahoor, M.H., Silverman, A.K., Zhang, J.J., Hebb, A.O., 2016. Long-term task- and dopamine-dependent dynamics of subthalamic local field potentials in Parkinson's disease. *Brain Sci.* 6. <https://doi.org/10.3390/brainsci6040057>.
- Herz, D.M., Tan, H., Brittain, J.-S., Fischer, P., Cheeran, B., Green, A.L., FitzGerald, J., Aziz, T.Z., Ashkan, K., Little, S., Foltynie, T., Limousin, P., Zrinzo, L., Bogacz, R., Brown, P., 2017. Distinct mechanisms mediate speed-accuracy adjustments in cortico-subthalamic networks. *Elife* 6. <https://doi.org/10.7554/eLife.21481>.
- Horn, A., Kühn, A.A., 2015. Lead-DBS: a toolbox for deep brain stimulation electrode localizations and visualizations. *Neuroimage* 107, 127–135. <https://doi.org/10.1016/j.neuroimage.2014.12.002>.
- Jaffard, M., Longcamp, M., Velay, J.L., Anton, J.L., Roth, M., Nazarian, B., Boulinguez, P., 2008. Proactive inhibitory control of movement assessed by event-related fMRI. *Neuroimage* 42, 1196–1206. <https://doi.org/10.1016/j.neuroimage.2008.05.041>.
- Jahanshahi, M., 2013. Effects of deep brain stimulation of the subthalamic nucleus on inhibitory and executive control over prepotent responses in Parkinson's disease. *Front. Syst. Neurosci.* 7. <https://doi.org/10.3389/fnsys.2013.00118>.
- Jahanshahi, M., Obeso, I., Rothwell, J.C., Obeso, J.A., 2015. A fronto-striato-subthalamic-pallidal network for goal-directed and habitual inhibition. *Nat. Rev. Neurosci.* 16, 719–732. <https://doi.org/10.1038/nrn4038>.
- Jahfari, S., Waldorp, L., van den Wildenberg, W.P.M., Scholte, H.S., Ridderinkhof, K.R., Forstmann, B.U., 2011. Effective connectivity reveals important roles for both the hyperdirect (fronto-subthalamic) and the indirect (fronto-striato-pallidal) fronto-basal ganglia pathways during response inhibition. *J. Neurosci.* 31, 6891–6899. <https://doi.org/10.1523/JNEUROSCI.5253-10.2011>.
- Joundi, R.A., Brittain, J.S., Green, A.L., Aziz, T.Z., Brown, P., Jenkinson, N., 2013. Persistent suppression of subthalamic beta-band activity during rhythmic finger tapping in Parkinson's disease. *Clin. Neurophysiol.* 124, 565–573. <https://doi.org/10.1016/j.clinph.2012.07.029>.
- Krypotos, A.-M., Beckers, T., Kindt, M., Wagenmakers, E.-J., 2015. A Bayesian hierarchical diffusion model decomposition of performance in Approach-Avoidance Tasks. *Cognit. Emot.* 29, 1424–1444. <https://doi.org/10.1080/02699931.2014.985635>.
- Kühn, A.A., Williams, D., Kupsch, A., Limousin, P., Hariz, M., Schneider, G.H., Yarrow, K., Brown, P., 2004. Event-related beta desynchronization in human subthalamic nucleus correlates with motor performance. *Brain* 127, 735–746. <https://doi.org/10.1093/brain/awh106>.
- Lambert, C., Zrinzo, L., Nagy, Z., Lutti, A., Hariz, M., Foltynie, T., Draganski, B., Ashburner, J., Frackowiak, R., 2012. Confirmation of functional zones within the human subthalamic nucleus: patterns of connectivity and sub-parcellation using diffusion weighted imaging. *Neuroimage* 60, 83–94. <https://doi.org/10.1016/j.neuroimage.2011.11.082>.
- Lanciego, J.L., Luquin, N., Obeso, J.A., 2012. Functional neuroanatomy of the basal ganglia. *Cold Spring Harb. Perspect. Med.* 2, a009621. <https://doi.org/10.1101/cshperspect.a009621>.
- Lavallee, C.F., Meemken, M.T., Herrmann, C.S., Huster, R.J., 2014. When holding your horses meets the deer in the headlights: time-frequency characteristics of global and selective stopping under conditions of proactive and reactive control. *Front. Hum. Neurosci.* 8, 994. <https://doi.org/10.3389/fnhum.2014.00994>.
- Leventhal, D.K., Gage, G.J., Schmidt, R., Pettibone, J.R., Case, A.C., Berke, J.D., 2012. Basal ganglia beta oscillations accompany cue utilization. *Neuron* 73, 523–536. <https://doi.org/10.1016/j.neuron.2011.11.032>.
- Lipszyc, J., Schachar, R., 2010. Inhibitory control and psychopathology: a meta-analysis of studies using the stop signal task. *J. Int. Neuropsychol. Soc.* 16, 1064–1076. <https://doi.org/10.1017/S1355617710000895>.
- Liston, C., Matalon, S., Hare, T.A., Davidson, M.C., Casey, B.J., 2006. Anterior cingulate and posterior parietal cortices are sensitive to dissociable forms of conflict in a task-switching paradigm. *Neuron* 50, 643–653. <https://doi.org/10.1016/j.neuron.2006.04.015>.
- Maris, E., Oostenveld, R., 2007. Nonparametric statistical testing of EEG- and MEG-data. *J. Neurosci. Meth.* 164, 177–190. <https://doi.org/10.1016/j.jneumeth.2007.03.024>.
- Maris, E., Schoffelen, J.M., Fries, P., 2007. Nonparametric statistical testing of coherence differences. *J. Neurosci. Meth.* 163, 161–175. <https://doi.org/10.1016/j.jneumeth.2007.02.011>.
- Martínez-Selva, J.M., Sánchez-Navarro, J.P., Bechara, A., Román, F., 2006. Mecanismos cerebrales de la toma de decisiones. *Rev. Neurol.* 42, 411–418. <https://doi.org/10.1016/j.biopsych.2010.07.024>.
- Mattingsley, J.B., Husain, M., Rorden, C., Kennard, C., Driver, J., 1998. Motor role of human inferior parietal lobe revealed in unilateral neglect patients. *Nature* 392, 179–182. <https://doi.org/10.1038/32413>.
- Meirovitch, Y., Harris, H., Dayan, E., Arieli, A., Flash, T., 2015. Alpha and beta band event-related desynchronization reflects kinematic regularities. *J. Neurosci.* 35, 1627–1637. <https://doi.org/10.1523/JNEUROSCI.5371-13.2015>.
- Menon, V., Adelman, N.E., White, C.D., Glover, G.H., Reiss, A.L., 2001. Error-related brain activation during a Go/NoGo response inhibition task. *Hum. Brain Mapp.* 12, 131–143.

- Monakow, K.H. von, Akert, K., Künzle, H., 1978. Projections of the precentral motor cortex and other cortical areas of the frontal lobe to the subthalamic nucleus in the monkey. *Exp. Brain Res.* 33, 395–403. <https://doi.org/10.1007/BF00235561>.
- Nachev, P., Wydell, H., O'Neill, K., Husain, M., Kennard, C., 2007. The role of the pre-supplementary motor area in the control of action. *Neuroimage* 36 (Suppl. 2), T155–T163. <https://doi.org/10.1016/j.neuroimage.2007.03.034>.
- Oostenveld, R., Fries, P., Maris, E., Schoffelen, J.M., 2011. FieldTrip: open source software for advanced analysis of MEG, EEG, and invasive electrophysiological data. *Comput. Intell. Neurosci.* 2011, 156869. <https://doi.org/10.1155/2011/156869>.
- Oostenveld, R., Oostendorp, T.F., 2002. Validating the boundary element method for forward and inverse EEG computations in the presence of a hole in the skull. *Hum. Brain Mapp.* 17, 179–192. <https://doi.org/10.1002/hbm.10061>.
- Oswal, A., Jha, A., Neal, S., Reid, A., Bradbury, D., Aston, P., Limousin, P., Foltynie, T., Zrinzo, L., Brown, P., Litvak, V., 2016. Analysis of simultaneous MEG and intracranial LFP recordings during Deep Brain Stimulation: a protocol and experimental validation. *J. Neurosci. Meth.* 261, 29–46. <https://doi.org/10.1016/j.jneumeth.2015.11.029>.
- Palmer, J.A., Kreutz-Delgado, K., Makeig, S., 2006. Super-gaussian Mixture Source Model for ICA, in: *Lecture Notes in Computer Science (Including Subseries Lecture Notes in Artificial Intelligence and Lecture Notes in Bioinformatics)*. Springer, Berlin, Heidelberg, pp. 854–861. https://doi.org/10.1007/11679363_106.
- Petirce, J.W., 2007. PsychoPy—psychophysics software in Python. *J. Neurosci. Meth.* 162, 8–13. <https://doi.org/10.1016/j.jneumeth.2006.11.017>.
- Pfurtscheller, G., Stancák, A., Neuper, C., 1996. Post-movement beta synchronization. A correlate of an idling motor area? *Electroencephalogr. Clin. Neurophysiol.* 98, 281–293. [https://doi.org/10.1016/0013-4694\(95\)00258-8](https://doi.org/10.1016/0013-4694(95)00258-8).
- Pote, I., Torkamani, M., Kefalopoulou, Z.-M., Zrinzo, L., Limousin-Dowsey, P., Foltynie, T., Speekenbrink, M., Jahanshahi, M., 2016. Subthalamic nucleus deep brain stimulation induces impulsive action when patients with Parkinson's disease act under speed pressure. *Exp. Brain Res.* 234, 1837–1848. <https://doi.org/10.1007/s00221-016-4577-9>.
- Ray, N.J., Brittain, J.S., Holland, P., Joundi, R.A., Stein, J.F., Aziz, T.Z., Jenkinson, N., 2012. The role of the subthalamic nucleus in response inhibition: evidence from local field potential recordings in the human subthalamic nucleus. *Neuroimage* 60, 271–278. <https://doi.org/10.1016/j.neuroimage.2011.12.035>.
- Ray, N.J., Jenkinson, N., Wang, S., Holland, P., Brittain, J.S., Joint, C., Stein, J.F., Aziz, T., 2008. Local field potential beta activity in the subthalamic nucleus of patients with Parkinson's disease is associated with improvements in bradykinesia after dopamine and deep brain stimulation. *Exp. Neurol.* 213, 108–113. <https://doi.org/10.1016/j.expneurol.2008.05.008>.
- Richardson, T.H., 2008. Inhibitory control in psychiatric disorders — a review of neuropsychological and neuroimaging research. *Undergrad. Res. J. Hum. Sci.* 7.
- Scherbaum, S., Dshemuchadse, M., 2013. Higher response time increases theta energy, conflict increases response time. *Clin. Neurophysiol.* 124, 1477–1479. <https://doi.org/10.1016/j.clinph.2012.12.007>.
- Scherberger, H., Jarvis, M.R., Andersen, R.A., 2005. Cortical local field potential encodes movement intentions in the posterior parietal cortex. *Neuron* 46, 347–354. <https://doi.org/10.1016/j.neuron.2005.03.004>.
- Soutschek, A., Taylor, P.C.J., Muller, H.J., Schubert, T., 2013. Dissociable networks control conflict during perception and response selection: a transcranial magnetic stimulation study. *J. Neurosci.* 33, 5647–5654. <https://doi.org/10.1523/JNEUROSCI.4768-12.2013>.
- Swann, N.C., Cai, W., Conner, C.R., Pieters, T.A., Claffey, M.P., George, J.S., Aron, A.R., Tandon, N., 2012. Roles for the pre-supplementary motor area and the right inferior frontal gyrus in stopping action: electrophysiological responses and functional and structural connectivity. *Neuroimage* 59, 2860–2870. <https://doi.org/10.1016/j.neuroimage.2011.09.049>.
- Tan, H., Jenkinson, N., Brown, P., 2014. Dynamic neural correlates of motor error monitoring and adaptation during trial-to-trial learning. *J. Neurosci.* 34, 5678–5688. <https://doi.org/10.1523/JNEUROSCI.4739-13.2014>.
- Töllner, T., Wang, Y., Makeig, S., Müller, H.J., Jung, T.-P., Gramann, K., 2017. Two independent frontal midline theta oscillations during conflict detection and adaptation in a Simon-type manual reaching task. *J. Neurosci.* 37, 2504–2515. <https://doi.org/10.1523/JNEUROSCI.1752-16.2017>.
- Van Veen, V., Carter, C.S., 2005. Separating semantic conflict and response conflict in the Stroop task: a functional MRI study. *Neuroimage* 27, 497–504. <https://doi.org/10.1016/j.neuroimage.2005.04.042>.
- Volkmann, J., Daniels, C., Witt, K., 2010. Neuropsychiatric effects of subthalamic neurostimulation in Parkinson disease. *Nat. Rev. Neurol.* 6, 487–498. <https://doi.org/10.1038/nrneurol.2010.111>.
- Williams, D., Kühn, A., Kupsch, A., Tijssen, M., Van Bruggen, G., Speelman, H., Hotton, G., Loukas, C., Brown, P., 2005. The relationship between oscillatory activity and motor reaction time in the parkinsonian subthalamic nucleus. *Eur. J. Neurosci.* 21, 249–258. <https://doi.org/10.1111/j.1460-9568.2004.03817.x>.
- Yeung, N., Cohen, J.D., Botvinick, M.M., 2011. Errors of interpretation and modeling: a reply to Grinband et al. *Neuroimage* 57, 316–319. <https://doi.org/10.1016/j.neuroimage.2011.04.029>.
- Zaghloul, K.A., Weidemann, C.T., Lega, B.C., Jaggi, J.L., Baltuch, G.H., Kahana, M.J., 2012. Neuronal activity in the human subthalamic nucleus encodes decision conflict during action selection. *J. Neurosci.* 32, 2453–2460. <https://doi.org/10.1523/JNEUROSCI.5815-11.2012>.
- Zamboni, G., Huey, E.D., Krueger, F., Nichelli, P.F., Grafman, J., 2008. Apathy and disinhibition in frontotemporal dementia: insights into their neural correlates. *Neurology* 71, 736–742. <https://doi.org/10.1212/01.wnl.0000324920.96835.95>.
- Zavala, B.A., Tan, H., Little, S., Ashkan, K., Hariz, M., Foltynie, T., Zrinzo, L., Zaghloul, K.A., Brown, P., 2014. Midline frontal cortex low-frequency activity drives subthalamic nucleus oscillations during conflict. *J. Neurosci.* 34, 7322–7333. <https://doi.org/10.1523/JNEUROSCI.1169-14.2014>.
- Zavala, B., Brittain, J.-S., Jenkinson, N., Ashkan, K., Foltynie, T., Limousin, P., Zrinzo, L., Green, A.L., Aziz, T., Zaghloul, K., Brown, P., 2013. Subthalamic nucleus local field potential activity during the Eriksen flanker task reveals a novel role for theta phase during conflict monitoring. *J. Neurosci.* 33, 14758–14766. <https://doi.org/10.1523/JNEUROSCI.1036-13.2013>.
- Zavala, B., Damera, S., Dong, J.W., Lungu, C., Brown, P., Zaghloul, K.A., 2017. Human subthalamic nucleus theta and beta oscillations entrain neuronal firing during sensorimotor conflict. *Cerebr. Cortex* 27, 496–508. <https://doi.org/10.1093/cercor/bhv244>.
- Zavala, B., Damera, S., Dong, J.W., Lungu, C., Brown, P., Zaghloul, K.A., 2015a. Human subthalamic nucleus theta and beta oscillations entrain neuronal firing during sensorimotor conflict. *Cerebr. Cortex* 27, 496–508. <https://doi.org/10.1093/cercor/bhv244>.
- Zavala, B., Zaghloul, K., Brown, P., 2015b. The subthalamic nucleus, oscillations, and conflict. *Mov. Disord.* 30, 328–338. <https://doi.org/10.1002/mds.26072>.
- Zavala, B., Tan, H., Ashkan, K., Foltynie, T., Limousin, P., Zrinzo, L., Zaghloul, K., Brown, P., 2016. Human subthalamic nucleus-medial frontal cortex theta phase coherence is involved in conflict and error related cortical monitoring. *Neuroimage* 137, 178–187. <https://doi.org/10.1016/j.neuroimage.2016.05.031>.

Supplementary Methods and Figures

Subthalamic stimulation, oscillatory activity and connectivity reveal functional role of STN and network mechanisms during decision making under conflict

Franz Hell^{1,3}, Paul C. J. Taylor^{1,3,4}, Jan H. Mehrkens², MD, Kai Bötzel^{1,3}, MD

¹ Department of Neurology, Ludwig-Maximilians-Universität München, Marchioninstr. 15, D-81377 Munich, Germany

² Department of Neurosurgery, Ludwig-Maximilians-Universität München, Marchioninstr. 15, D-81377 Munich, Germany

³ Graduate School of Systemic Neurosciences, GSN, Ludwig-Maximilians-Universität München, Grosshadernerstr. 2, D-82152 Martinsried, Germany

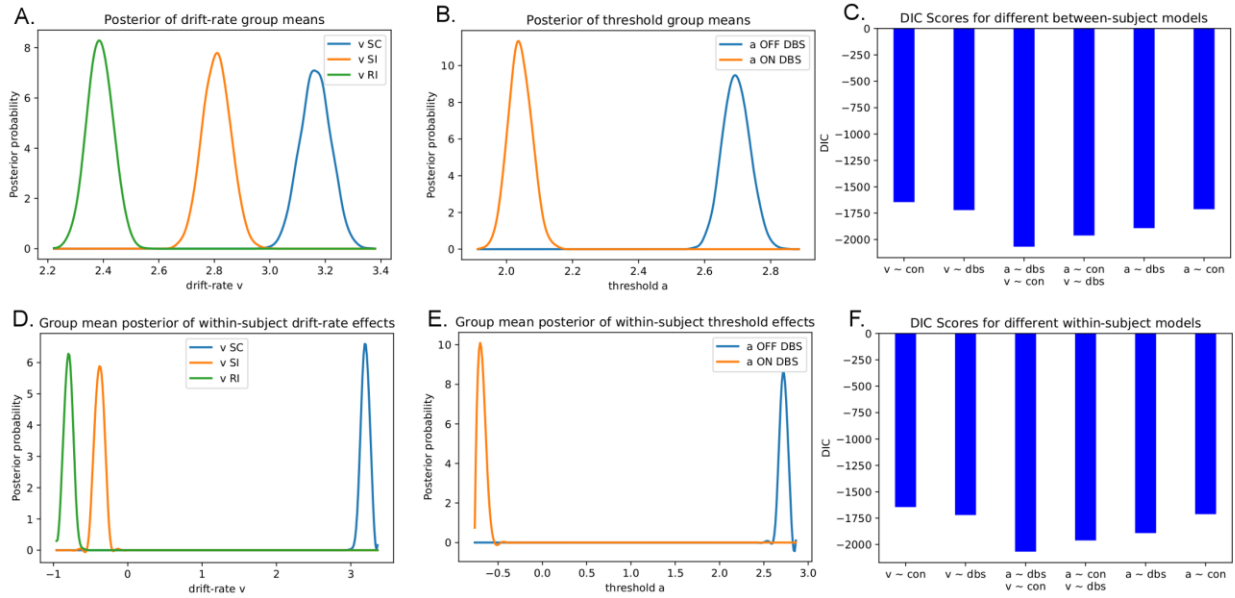
⁴ German Center for Vertigo and Balance Disorders, Ludwig-Maximilians-Universität München, Marchioninstr. 15, D-81377 Munich, Germany

Corresponding author: Franz Hell

Department of Neurology,

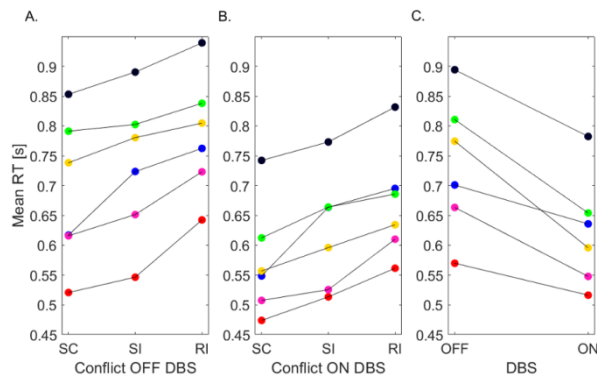
Ludwig-Maximilians-University of Munich, Marchioninstrasse 15, D-81377 Munich / Germany

E-Mail: Franz.Hell@med.uni-muenchen.de



Supplementary Figure 1: HDDM modeling results. (A) Main effects on drift rates between-subject model. A. shows the posterior probability distribution of coefficients for the effects of conflict on drift rates. Posterior probabilities are significantly different between all conditions, with $P(v \text{ SI} < v \text{ SC}) = 1.0$ and $P(v \text{ SI} < v \text{ SC}) = 1.0$. (B) Main effects on threshold between-subject model. B. shows the posterior distribution of the regression coefficient for the effects on the decision thresholds. Posterior probabilities are significantly different between all conditions, with $P(a \text{ DBS OFF} > a \text{ DBS ON}) = 1.0$. (D) and (E) show the main effects on drift rate and threshold as in (A) and (B) for the within-subject models. Note that within-subject posterior distributions do not overlap with 0 and that posterior probabilities match with the between-subject results. (C) and (F). The six between-subject and within-subject models evaluated with different parameters allowed to vary (as described in Supplementary methods) and their respective DIC scores (con = conflict). The parameters from the best model are shown in (A), (B) and (D), (E).

Drift-diffusion models (DDMs) are commonly used to investigate two-alternative choice decision making tasks such as the Eriksen Flanker Task and have been successfully used to model decision-making related parameters and their possible relation to human STN activity and stimulation (Cavanagh et al., 2011; Herz et al., 2017, 2016; Ratcliff and McKoon, 2008; Wagenmakers, 2009). We used drift diffusion modeling (DDM) to investigate how trial-by-trial fluctuations in reaction times are possibly related to decision-making processes like decision threshold (boundary) and drift rate and how they were modulated by stimulus conflict and DBS.



Supplementary Figure 2: Data from individual participants. (A) Mean RT from each subject for each 3 conflict conditions off DBS. (B) with DBS. (C) Mean RT from each subject collapsed across conflict condition. Each subject is represented by a different color.

Supplementary Methods

Drift diffusion modeling

DDM modelling normally includes four parameters: the decision threshold/boundary a , the drift rate v , the decision bias z and non-decision time t . Decision making is modelled as accumulation of information over time and is reflected by the drift rate. The accumulation of information continues until a decision threshold is reached. Fast and accurate decisions often show high drift rates, whereas lower drift rates reflect slow decisions (Kryptos et al., 2015). The decision bias parameter incorporates a task inherent bias toward one or another response. The non-decision time reflects processes like stimulus encoding and response execution (Ratcliff et al., 2016).

Here we applied a hierarchical DDM model (Python package HDDM, http://ski.clps.brown.edu/hddm_docs/) (Wiecki et al., 2013) to fit the reaction time data from our modified Eriksen Flanker task. Due to the low error rate, we could not assume that errors were equally distributed across conditions in different subjects. Therefore, we also applied our winning model to RT data without errors to confirm results. Hierarchical Bayesian models are especially suited to estimate parameters of individual subjects and groups of subjects, while individual parameter estimates are constrained by group-level distributions (Nilsson et al., 2011; Shiffrin et al., 2008).

A between-subject models implicitly assumes that the different conditions are completely independent of each other, but it is possible that there are individual differences in overall performance, and it could be that someone who is better in one conflict condition (e.g. SC) would also be better in another conflict (e.g. RI) condition. A within-subject model is able to capture these inter-individual differences in performance, by capturing overall performance in one condition (e.g. SC) as a baseline, and then expressing the other conflict conditions to SC (Wiecki et al., 2013). The same logic applies for DBS conditions.

We tested 6 between-subject models and confirmed results with within-subject models with matching parameters. We assumed an unbiased starting point z , given that left/right responses and different conflicts were counterbalanced, and assumed that non-decision time t would not be expected to vary as a function of condition, as the stimulus encoding and motor responses required across conditions were comparable. The other two parameters, the drift rate v and the decision threshold a were free to vary with DBS condition and stimulus conflict. The drift rate has previously been shown to be modulated by levels of conflict (Cavanagh et al., 2011; Herz et al., 2016; Kryptos et al., 2015) and the decision threshold is reported to interact with DBS (Cavanagh et al., 2011; Plummer, 2008). The initial analysis of our behavioral RT data revealed main effects of DBS and of conflict with no interaction. To confirm our initial hypothesis, we tested both between as well as within-subject models with different combinations of the two parameters varying with different conditions. Model specifications were as follows: in the first model, only drift rate v was permitted to vary by conflict condition, and decision threshold a was held constant; in a second model, v could vary across DBS conditions and a was held constant; in a third model, v varied with conflict and a with DBS, while in the fourth model v varied with DBS and a with conflict. In the fifth and sixth model v was held constant and in the fifth model a varied with DBS and in model six, a varied with conflict only. In the within-subject models, we used v from the SC condition and a from DBS OFF as the intercepts.

Markov Chain Monte Carlo simulations were used to generate 25,000 samples from the posterior parameter distributions in all models. We discarded the first 5000 samples as burn-in. We assessed convergence by visually inspecting the Markov chains and computed R-hat Gelman-Rubin statistics. All values were below 1.1, indicating successful convergence (Kryptos et al., 2015; O'Callaghan et al., 2017). The winning model was determined by comparing the deviance information criterion (DIC) from each model, with lower DIC values suggesting better model fit (Spiegelhalter et al., 2002). A difference in DIC of 10 is usually considered significant (Zhang and Rowe, 2014). We used Bayesian hypothesis testing to determine the extent of overlap between the parameters posterior density distributions and considered posterior

probabilities to be significantly different if less than 5% of the distributions overlapped (Herz et al., 2016; Wiecki et al., 2013).

Supplementary Results

Drift diffusion modeling

From the analysis of reaction times we expected a main effect of DBS and a main effect of conflict but no interaction. Literature suggests that modulations of drift rate are influenced by the level of conflict and higher drift rates are associated with lower conflict levels, and that the threshold varies with DBS, with a decreased threshold during DBS as compared to without DBS. To test our assumptions, we compared the model evidence of our favored model with other models that incorporated different parameter and condition combinations, using DIC (Figure 1 E.). DIC values for all between-subject models were: model 1 ($v \sim \text{conflict}$) DIC: -1645, model 2 ($v \sim \text{dbs}$) DIC: -1721, model 3 ($a \sim \text{dbs}, v \sim \text{conflict}$) DIC: -2067, model 4 ($v \sim \text{dbs}, a \sim \text{conflict}$) DIC: -1961, model 5 ($a \sim \text{dbs}$) DIC: -1891, model 6 ($a \sim \text{conflict}$) DIC: -1712., with the best model beating the second best model by 115 points. DIC values for all within-subject models were similar to between-subject models: model 1 ($v \sim \text{conflict}$) DIC: -1645, model 2 ($v \sim \text{dbs}$) DIC: -1721, model 3 ($a \sim \text{dbs}, v \sim \text{conflict}$) DIC: -2068, model 4 ($v \sim \text{dbs}, a \sim \text{conflict}$) DIC: -1961, model 5 ($a \sim \text{dbs}$) DIC: -1891, model 6 ($a \sim \text{conflict}$) DIC: -1712, with the best model beating the second best model by 116 points. The winning model posterior probabilities in the winning between-subject as well as in the within-subject model are significantly different between all conditions for all parameters, with $P(v_{SI} < v_{SC}) = 1.0$ and with $P(v_{SI} < v_{SC}) = 1.0$ and $P(a_{DBS\ OFF} > a_{DBS\ ON}) = 1.0$ (Figure 1 A.,B.). Applying our winning model to RT data without errors, we can confirm the results from our winning model. Posterior probabilities patterns for both parameters and differences between conditions matched the one found in the models with errors (data not shown).

Supplementary Discussion

Drift diffusion modeling

While we found a main effect of conflict and DBS on RTs and no interaction between them with our conventional analysis, in our winning models, we see a main effect of conflict on the drift rate and a main effect of DBS on decision thresholds. With the results from our winning models, we can confirm reaction time patterns we found with conventional analysis as well as earlier observations in the literature. A main effect of STN DBS on decision thresholds has been previously reported for example in a moving dot task when PD patients were instructed to speed up their decision as compared to accuracy instructions and in a reinforcement learning and choice conflict task (Cavanagh et al., 2011; Pote et al., 2016). We can confirm these findings as we report lower threshold levels during DBS. Fast decisions often show high drift rates, whereas lower drift rates reflect slow decisions and lower levels of conflict (Herz et al., 2016; Kryptos et al., 2015). We found that low conflict trials do show the highest drift rates and high conflict trials show significantly lower drift rates reflecting the hierarchical pattern we found in the RT analysis.

We have not investigated more complex models with additional free parameters like non-decision time, which includes response execution time or an interaction between conflict and DBS for parameters like drift-rate or decision threshold and cannot exclude the possibility of interactions. It is conceivable for example that DBS leads to general motor improvement resulting in shorter motor execution and hence reduced non-decision time. Additional parameters however increase the possible parameter combinations that could be used for modeling drastically and makes the interpretation of the results and comparison of the models increasingly challenging. Here we used DIC for model comparison and literature considers this measure too generous to over-complex models, as DIC under-penalizes more complex models (Plummer, 2008).

Supplementary References

- Cavanagh, J.F., Wiecki, T. V, Cohen, M.X., Figueroa, C.M., Samanta, J., Sherman, S.J., Frank, M.J., 2011. Subthalamic nucleus stimulation reverses mediofrontal influence over decision threshold. *Nat. Neurosci.* 14, 1462–1467. doi:10.1038/nn.2925
- Herz, D.M., Tan, H., Brittain, J.-S., Fischer, P., Cheeran, B., Green, A.L., FitzGerald, J., Aziz, T.Z., Ashkan, K., Little, S., Foltynie, T., Limousin, P., Zrinzo, L., Bogacz, R., Brown, P., 2017. Distinct mechanisms mediate speed-accuracy adjustments in cortico-subthalamic networks. *Elife* 6. doi:10.7554/eLife.21481
- Herz, D.M., Zavala, B.A., Bogacz, R., Brown, P., 2016. Neural Correlates of Decision Thresholds in the Human Subthalamic Nucleus. *Curr. Biol.* 26, 916–920. doi:10.1016/j.cub.2016.01.051
- Kryptos, A.-M., Beckers, T., Kindt, M., Wagenmakers, E.-J., 2015. A Bayesian hierarchical diffusion model decomposition of performance in Approach–Avoidance Tasks. *Cogn. Emot.* 29, 1424–1444. doi:10.1080/02699931.2014.985635
- Nilsson, H., Rieskamp, J., Wagenmakers, E.J., 2011. Hierarchical Bayesian parameter estimation for cumulative prospect theory. *J. Math. Psychol.* 55, 84–93. doi:10.1016/j.jmp.2010.08.006
- O’Callaghan, C., Hall, J., Tomassini, A., Muller, A., Walpola, I., Moustafa, A., Shine, J., Lewis, S., 2017. Accumulation of sensory evidence is impaired in Parkinson’s disease with visual hallucinations. doi.org 111278. doi:10.1101/111278
- Plummer, M., 2008. Penalized loss functions for Bayesian model comparison. *Biostatistics* 9, 523–539. doi:10.1093/biostatistics/kxm049
- Pote, I., Torkamani, M., Kefalopoulou, Z.-M., Zrinzo, L., Limousin-Dowsey, P., Foltynie, T., Speekenbrink, M., Jahansahi, M., 2016. Subthalamic nucleus deep brain stimulation induces impulsive action when patients with Parkinson’s disease act under speed pressure. *Exp. brain Res.* 234, 1837–48. doi:10.1007/s00221-016-4577-9
- Ratcliff, R., McKoon, G., 2008. The diffusion decision model: theory and data for two-choice decision tasks. *Neural Comput.* 20, 873–922. doi:10.1162/neco.2008.12-06-420
- Ratcliff, R., Smith, P.L., Brown, S.D., McKoon, G., 2016. Diffusion Decision Model: Current Issues and History. *Trends Cogn. Sci.* 20, 260–281. doi:10.1016/j.tics.2016.01.007
- Shiffrin, R.M., Lee, M.D., Kim, W., Wagenmakers, E.-J., 2008. A survey of model evaluation

approaches with a tutorial on hierarchical bayesian methods. *Cogn. Sci.* 32, 1248–84.
doi:10.1080/03640210802414826

Spiegelhalter, D.J., Best, N.G., Carlin, B.P., van der Linde, A., 2002. Bayesian measures of model complexity and fit. *J. R. Stat. Soc. Ser. B (Statistical Methodol.* 64, 583–639.
doi:10.1111/1467-9868.00353

Wagenmakers, E.-J., 2009. Methodological and empirical developments for the Ratcliff diffusion model of response times and accuracy. *Eur. J. Cogn. Psychol.* 21, 641–671.
doi:10.1080/09541440802205067

Wiecki, T. V., Sofer, I., Frank, M.J., 2013. HDDM: Hierarchical Bayesian estimation of the Drift-Diffusion Model in Python. *Front. Neuroinform.* 7, 14. doi:10.3389/fninf.2013.00014

Zhang, J., Rowe, J.B., 2014. Dissociable mechanisms of speed-accuracy tradeoff during visual perceptual learning are revealed by a hierarchical drift-diffusion model. *Front. Neurosci.* 8.
doi:10.3389/fnins.2014.00069

Affidavit

I hereby confirm that the dissertation '**Neural oscillations underlying gait and decision making**' is the result of my own work and that I have only used sources or materials listed and specified in the dissertation. Copyright to all adapted figures has been obtained by the author.

Munich, 28.11.2018

Franz Hell

Author contributions

The author contributed to the first study titled '**Subthalamic stimulation, oscillatory activity and connectivity reveal functional role of STN and network mechanisms during decision making under conflict**' by devising the research question, designing and programming the experiment, setting up the recording and experimental equipment, running the experiment and recording EEG, LFP and behavioral data, programming the analysis, analyzing the data and writing the manuscript.

The author contributed to the study titled '**Subthalamic oscillatory activity and connectivity during gait in Parkinson's disease**' by running the experiment, recording LFP and kinematic measurements, programming the analysis, analyzing the data and writing the manuscript.

Munich, 28.11.2018

Franz Hell

Acknowledgments

I want to thank everybody who helped me through these sometimes tough times and contributed to my Ph.D.. First, I want to thank my first supervisor Prof. Dr. Kai Bötzel for giving me the possibility to work on such an intriguing project and for all his support during the past years.

Second, a big thank you goes to Prof. Dr. Paul Taylor for being an inspiration and guiding me to my first major paper and Dr. Virginia Flanagin, who always had kind and inspiring words.

Also, I want to acknowledge all the support my graduate school, the GSN, has provided. It was an honor to complete my PhD in such an inspiring and caring environment.

Last but not least I want to thank all the colleagues, friends and family that are not named here. Thank you for supporting me during these years.

Thank you!

Publications

- Hell, F., Taylor, P., Mehrkens, J., Bötzel, K. (2018). Subthalamic stimulation, oscillatory activity and connectivity reveal functional role of STN and network mechanisms during decision making under conflict. *NeuroImage*. <https://doi.org/10.1016/j.neuroimage.2018.01.001>
- Hell, F., Plate, A., Mehrkens, J., Bötzel, K. (2018). Subthalamic oscillatory activity and connectivity during gait in Parkinson's disease. *NeuroImage: Clinical*. <https://doi.org/10.1016/j.nicl.2018.05.001>
- Hell, F., Köglsperger, T., Bötzel, K. (2018). Feedback signals for adaptive DBS. Current perspectives and future directions. *Neurophysiologie-Labor*. <https://doi.org/10.1016/j.neulab.2018.02.001>
- Hell, F., Köglsperger, T., Mehrkens, J., Bötzel, K. (2018). Improving the standard for deep brain stimulation therapy: Target structures and feedback signals for adaptive stimulation. Current perspectives and future directions. *Cureus* 10(4): e2468. <https://doi:10.7759/cureus.2468>
- Hell, F., Singh, A., Plate, A., Mehrkens, J., Bötzel, K. (2016). Gait specific modulation of local field potentials in the STN of patients with Parkinson's disease. *Clinical Neurophysiology*. <https://doi.org/10.1016/j.clinph.2016.05.148>
- Hell, F., Mehrkens, J., Kammermeier, S., Plate, A., Hathway, P., Boetzel, K. (2015). Gait cycle related modulation of electrophysiological activity in the human subthalamic nucleus of patients with Parkinson's disease. *Movement Disorders*. <https://doi.org/10.1002/mds.26295>
- Hell, F., Hathway, P., Plate, A., Kammermeier, S., Mehrkens, J., Ilmenberger, j., Bötzel, K. (2015). Patterns of gait-related electrophysiological activity in the human subthalamic nucleus of patients with Parkinson's disease. *Clinical Neurophysiology*. <https://doi.org/10.1016/j.clinph.2015.04.278>
- Hell, F., Hathway, P., Palacios, D., Mehrkens, J., Bötzel, K. (in submission). Subthalamic oscillatory activity during normal and impaired speech and the impact of deep brain stimulation on verbal fluency. *Clinical Neurophysiology*
- Schönecker, S., Hell, F., Bötzel, K., Wlasich E., Otto, M., German FTLD consortium, Huppertz, H.J., Anderl-Straub, S., Ludolph, A., Kassubek, J., Ackl, N., Süßmair, C., Levin, J., Danek, A. (in submission). The applause sign in frontotemporal lobar degeneration and related conditions.